

Techno-economic and Environmental Analysis of Bio-oil Production from Forest Residues via Non-catalytic and Catalytic Pyrolysis Processes

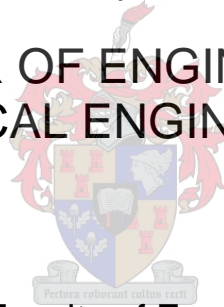
by

Dominique Lisa van Schalkwyk

Thesis presented in partial fulfilment
of the requirements for the Degree

of

MASTER OF ENGINEERING
(CHEMICAL ENGINEERING)



in the Faculty of Engineering
at Stellenbosch University

The financial assistance of the National Research Foundation (NRF) towards this research is hereby acknowledged. Opinions expressed and conclusions arrived at, are those of the author and are not necessarily to be attributed to the NRF.

Supervisor

Prof. Johann F. Görgens

Co-Supervisor

Dr. Mohsen Mandegari

December 2019

Declaration

By submitting this thesis electronically, I declare that the entirety of the work contained therein is my own, original work, that I am the sole author thereof (save to the extent explicitly otherwise stated), that reproduction and publication thereof by Stellenbosch University will not infringe any third party rights and that I have not previously in its entirety or in part submitted it for obtaining any qualification.

Date: *December 2019*

Plagiarism Declaration

1. Plagiarism is the use of ideas, material and other intellectual property of another's work and to present is as my own.
2. I agree that plagiarism is a punishable offence because it constitutes theft.
3. I also understand that direct translations are plagiarism.
4. Accordingly all quotations and contributions from any source whatsoever (including the internet) have been cited fully. I understand that the reproduction of text without quotation marks (even when the source is cited) is plagiarism.
5. I declare that the work contained in this assignment, except where otherwise stated, is my original work and that I have not previously (in its entirety or in part) submitted it for grading in this module/assignment or another module/assignment.

Student number:

Initials and surname: DL van Schalkwyk

Signature:

Date: 14 November 2019

Abstract

Forest residues are a high fire risk and often disposed of by burning or sold as firewood; both contribute to air pollution, and the latter has low economic value. The 1.5 million dry metric tonnes of forest residues available in South Africa every year can instead be converted into liquid bio-oil and solid biochar through intermediate pyrolysis. However, bio-oil is acidic and has a low energy value as a result of its high oxygen content. Bio-oil can be upgraded to improve its oxygen content by introducing a CaO catalyst *in situ* to the pyrolysis process. Upgraded bio-oil can then be co-processed in a crude-oil refinery to produce bio-derived fuels. Therefore, the aim of this project was to determine whether or not the production of crude and upgraded bio-oils via non-catalytic and catalytic pyrolysis of forest residues for co-processing in an oil refinery is economically and environmentally feasible.

Process simulations were developed in Aspen Plus™ based on pilot plant data for non-catalytic and catalytic pyrolysis processes. All of the non-condensable gas and 21.5 wt. % of the char (for non-catalytic pyrolysis biorefinery scenarios only) were combusted to meet the energy demands of the biorefinery scenarios. The net yield of non-catalytic pyrolysis products from *Eucalyptus grandis* forest residues (8.28 wt. % moisture) was 22.6 wt. % biochar and 19.8 wt. % crude bio-oil, while the net yield of catalytic pyrolysis products was 16.5 wt. % biochar and 18.4 wt. % upgraded bio-oil.

There was a clear economy-of-scale benefit for non-catalytic and catalytic pyrolysis biorefinery scenarios as the biomass collection distance increased from a 100 to 300 km radius of the biorefinery. The Minimum Selling Price (MSP) of upgraded bio-oil (\$1.35/L) was significantly higher than the MSP of crude bio-oil (\$0.75/L) for a desired 22 % Internal Rate of Return (IRR) at a 300 km radius of the biorefinery. However, the quality of upgraded bio-oil was superior to crude bio-oil for co-processing in an oil refinery. Co-processing crude bio-oil will likely produce bio-derived fuels with a significantly lower renewable carbon content and higher yield of undesirable CO, CO₂ and H₂O gases.

The price premium for crude and upgraded bio-oils was substantiated by a significant environmental benefit. A Life Cycle Impact Assessment (LCIA) was conducted using the CML-IA baseline method in SimaPro™ to assess the environmental impact of producing 1 MJ of crude or upgraded bio-oil, instead of crude-oil or diesel. The net Global Warming Potentials (GWPs) for crude bio-oil, upgraded bio-oil, crude-oil and diesel were -0.30, -0.14, 0.0052 and 0.013 kg CO₂ eq/MJ of fuel, respectively. Biochar application to soils had a substantial influence on the GWP of bio-oil production through associated carbon sequestration.

Co-processing crude and upgraded bio-oils at pilot-scale was recommended to evaluate the relationship between blending ratio, distribution of oil refinery products and extent of deoxygenation reactions. Furthermore, the scope of this project should be expanded to include a techno-economic analysis for co-processing crude and upgraded bio-oils to further evaluate the economic feasibility of crude and upgraded bio-oil production.

Opsomming

Bosbou residu is 'n hoë brandrisiko en word dikwels weggemaak deur verbranding of te verkoop as vuurmaakhout; al twee dra by tot lugbesoedeling, en die laasgenoemde het lae ekonomiese waarde. Die 1.5 miljoen droë metrieke ton bosbou residu beskikbaar in Suid-Afrika elke jaar kan eerder omgeskakel word in vloeistof bio-olie en vastestof bioverkoonsel deur intermediêre pirolise. Bio-olie is egter suurvormend en het 'n lae energiewaarde as gevolg van sy hoë suurstofinhoud. Bio-olie kan opgegradeer word om sy suurstofinhoud te verbeter deur 'n CaO-katalisator *in situ* in die pirolise proses bekend te stel. Opgegradeerde bio-olie kan dan gekoprosesseer word in 'n ru-olieraffinadery om bio-afgeleide brandstowwe te produseer. Daarom is die doel van hierdie projek om vas te stel of die produksie van ru- en opgegradeerde bio-olies via nie-katalitiese en katalitiese pirolise van bosbou residu vir koprosessering in 'n olieraffinadery uitvoerbaar is vir die ekonomie en omgewing, of nie.

Prosessimulasies is ontwikkel in Aspen PlusTM gebaseer op loodsaanlegdata vir nie-katalitiese en katalitiese pirolise prosesse. Al die nie-kondenseerbare gasse en 21.5 wt. % van die verkoonsel (slegs vir nie-katalitiese pirolise bioraffinadery scenario's) is verbrand om aan die energievereistes van die bioraffinadery scenario's te voldoen. Die netto waarde van nie-katalitiese piroliese produkte uit *Eucalyptus grandis* bosbou residu (8.28 wt. % vog) was 22.6 wt. % bioverkoonsel en 19.8 wt. % ru bio-olie, terwyl die netto opbrengs van katalitiese piroliese produkte 16.5 wt. % bioverkoonsel en 18.4 wt. % opgegradeerde bio-olie was.

Daar was 'n duidelike ekonomie-van-skaal-voordeel vir nie-katalitiese en katalitiese pirolise bioraffinadery scenario's soos wat die afstand van die biomassa versameling vergroot het van 100 tot 300 km radius van die bioraffinadery. Die Minimum Verkoopsprys (MSP) van opgegradeerde olie (\$1.35/L) was beduidend hoër as die MSP van ru bio-olie (\$0.75/L) vir 'n verlangde 22% Interne Opbrengskoers (IRR) by 'n 300 km radius van die bioraffinadery. Die kwaliteit van opgegradeerde bio-olie was egter superieur teenoor ru bio-olie vir koprosessering in 'n olieraffinadery. Koprosessering van ru bio-olie sal waarskynlik bio-afgeleide brandstowwe met 'n beduidende laer hernubare koolstofinhoud en hoër opbrengs van ongewenste CO, CO₂ en H₂O produseer.

Die prys premie vir ru en opgegradeerde bio-olies is bevestig deur beduidende omgewingsvoordeel. 'n Lewensiklusimpakassessering is gedoen deur die CML-IA basislyn metode in SimaProTM te gebruik om die omgewingsimpak van die produsering van 1 MJ van ru of opgegradeerde bio-olie, in plaas van ru-olie of diesel, te assesser. Die netto Globale Verwarmingspotensiaal vir ru bio-olie, opgegradeerde bio-olie, ru-olie en diesel was -0.30, -0.14, 0.0052 en 0.013 kg CO₂ eq/MJ van brandstof, onderskeidelik. Toepassing van bioverkoonsel op grond het 'n substansiële invloed op die Globale Verwarmingspotensiaal van bio-olie produksie deur verwante koolstof sekwestrasie.

Koprosessering van ru en opgegradeerde bio-olies op loodsskaal is aanbeveel om die verhouding tussen vermengverhouding, distribusie van olieraffinadery produkte en omvang van

reaksies van deoksigenering te evalueer. Verder moet die omvang van hierdie projek verbreed word om 'n tegno-ekonomiese analise vir koprosessering van ru en opgegradeerde bio-olies in te sluit om die ekonomiese uitvoerbaarheid van ru en opgegradeerde bio-olie produksie te evalueer.

Acknowledgements

I acknowledge and am grateful to the Paper Manufacturers Association of South Africa (PAMSA), the Department of Science and Technology (DST) and the National Research Foundation (NRF) for financially supporting this project.

To my supervisor, Prof Görgens. Thank you for giving me the opportunity to be a part of this project and a leading Bioresource Technology research group; for your guidance throughout the project; and for your meaningful feedback on this thesis.

To my co-supervisor, Dr Mandegari. Thank you, Mohsen, for your patience, guidance and encouragement; for reading, reviewing and commenting on my work throughout the project; and for sparking ideas that helped me deepen the discussions in this thesis.

I also wish to acknowledge and thank, Dr Farzad for offering her time and expertise to help me develop the Life-Cycle Assessments for this project.

Thank you to my friends and colleagues at the department for their many words of encouragement and advice. I wish to specially thank Farai Chireshe for his perseverance in generating the pilot plant data for this thesis.

I wish to acknowledge and thank, Rachel for kindly driving me to and from the department every day.

Thank you, Irma and Iain for welcoming me into your home; for your support and encouragement; and for the many “kospakkies” that sustained me during this project.

I am forever grateful to have parents that never let me use my vision impairment as an excuse not to set ambitious goals and achieve them. Thank you from the bottom of my heart, Mom (Enid) and Dad (Raymond) for the many sacrifices you both have made to build the foundations that brought me to this point.

To my dear husband, Helgard. I cannot thank you enough for being on this journey with me; for listening to me endlessly talk about pyrolysis and never complaining; for staying up with me while I worked until late at night; for your unfailing belief in me; and for your love. Your support in so many ways has carried me through this project.

List of Acronyms and Abbreviations

ADP:	Abiotic Depletion
AP:	Acidification
BFP:	Basic Fuel Price
BFW:	Boiler Feed Water
bpd:	barrels per day
C-10:	catalytic pyrolysis scenario - capacity required to co-process 10 wt. % bio-oil
C-100:	catalytic pyrolysis scenario - biomass collection within 100 km radius
C-200:	catalytic pyrolysis scenario - biomass collection within 200 km radius
C-300:	catalytic pyrolysis scenario - biomass collection within 300 km radius
C1-C4:	Condensers 1 to 4 in condenser train
C2A:	Aqueous fraction of bio-oil produced from C2
C2O:	Organic fraction of bio-oil produced from C2
CEPCI:	Chemical Engineering Plant Cost Index
COD:	Chemical Oxygen Demand
COP:	Coefficient of Performance
CPO:	Catalytic Pyrolysis Oil
db:	dry basis
DCFROR:	Discounted Cash Flow Rate of Return
<i>E. grandis</i> :	<i>Eucalyptus grandis</i>
EP:	Eutrophication
ESP:	Electrostatic Precipitator
FCC:	Fluid Catalytic Cracking
FCI:	Fixed Capital Investment
FPO:	Fast Pyrolysis Oil
GC/MS:	Gas Chromatography-Mass Spectroscopy
GGE:	Gasoline Gallon Equivalent
GHG:	Greenhouse Gases
GWP ₁₀₀ :	Global Warming Potential over 100 years
HCO:	Heavy Cycle Oil
HDO:	Hydrodeoxygenation
HHV:	Higher Heating Value
h_p :	Specific enthalpy of the pyrolysis reaction
HPO:	Hydrotreated Pyrolysis Oil

IEA:	International Energy Agency
INDC:	Intended Nationally Determined Contribution
IRR:	Internal Rate of Return
ISBL:	Inside-Battery-Limits
LHV:	Lower Heating Value
Lignin A:	lignin-derived oligomeric compounds with β -O-4 bond
Lignin B:	lignin-derived phenylcoumaran compounds
KZN:	KwaZulu-Natal
LCA:	Life Cycle Assessment
LCI:	Life Cycle Inventory
LCIA:	Life Cycle Impact Assessment
LCO:	Light Cycle Oil
LGE:	Litre Gasoline Equivalent
LPG:	Liquefied Petroleum Gas
MAT:	Micro Activity Test
MSP:	Minimum Selling Price
MW:	Molecular Weight
NC-10:	non-catalytic pyrolysis scenario - required capacity to co-process 5 wt. % bio-oil
NC-100:	non-catalytic pyrolysis scenario - biomass collection within 100 km radius
NC-200:	non-catalytic pyrolysis scenario - biomass collection within 200 km radius
NC-300:	non-catalytic pyrolysis scenario - biomass collection within 300 km radius
NPV:	Net Present Value
ODP:	Ozone Layer Depletion
PAH:	Polycyclic Aromatic Hydrocarbon
PAMSA:	Paper Manufacturers Association of South Africa
PV:	Photovoltaic
RSR:	Riser Simulator Reactor
T:	Temperature
TCI:	Total Capital Investment
TDC:	Total Direct Cost
TEA:	Techno-economic Analysis
TOC:	Total Operating Cost
UNFCCC:	United Nations Framework Convention on Climate Change
VGO:	Vacuum Gas Oil

Table of Contents

1	Introduction.....	1
2	Literature Review	3
2.1	Lignocellulosic biomass	3
2.2	Forest residue.....	6
2.3	Pyrolysis.....	8
2.3.1	Mechanisms.....	8
2.3.2	Types of pyrolysis	9
2.3.3	Effect of operating parameters	10
2.3.4	Products.....	11
2.3.5	Pyrolysis of forest residue	16
2.4	Bio-oil upgrading	17
2.4.1	Physical upgrading.....	17
2.4.2	Catalytic upgrading.....	18
2.4.3	Catalyst configuration	20
2.4.4	Catalyst to feed ratio	21
2.4.5	Catalyst selection.....	22
2.4.6	Catalytic pyrolysis challenges	25
2.5	Bio-oil co-processing in a crude-oil refinery.....	25
2.6	Techno-economic analysis	30
2.7	Environmental impact	32
2.8	Conclusion	34
3	Project Scope.....	35
3.1	Objectives	35
3.2	Research questions	35
3.3	Limitations	35
4	Methodology	36
4.1	Estimation of forest residues available in South Africa.....	38
4.2	Biorefinery scenarios.....	42
4.3	Process description	44
4.4	Process simulation data input	45
4.4.1	Mass balance reconciliation	45
4.4.2	Bio-oil composition.....	48
4.5	Process simulation development	51
4.5.1	Component selection	51
4.5.2	Thermodynamic model selection	51

4.5.3	Non-catalytic and catalytic pyrolysis design basis.....	51
4.6	Economic analysis methodology	59
4.6.1	Capital cost estimation	59
4.6.2	Operating cost estimation	61
4.6.3	Profitability analysis	63
4.6.4	Economic sensitivity analysis.....	65
4.6.5	Process sensitivity analysis	65
4.7	Environmental impact methodology.....	65
4.7.1	Goal and scope definition.....	66
4.7.2	Life cycle inventory analysis	68
4.7.3	Life cycle impact assessment	69
5	Results and Discussions	70
5.1	Process simulation results	70
5.1.1	Overall mass and energy balances	70
5.1.2	Water balance	76
5.2	Economic analysis results	77
5.2.1	Capital cost estimation	77
5.2.2	Operating cost estimation	81
5.2.3	Profitability analysis	83
5.2.4	Economic sensitivity analysis.....	89
5.2.5	Process sensitivity analysis	93
5.3	Environmental impact results	94
6	Conclusions and Recommendations	101
6.1	Addressing the objectives	101
6.1.1	Develop process simulations in Aspen Plus™ for non-catalytic and catalytic pyrolysis biorefinery scenarios based on pilot plant data.....	101
6.1.2	Develop economic analyses for non-catalytic and catalytic pyrolysis biorefinery scenarios based on process simulations	101
6.1.3	Measure and compare the environmental impact of producing crude and upgraded bio-oils to crude-oil and diesel using SimaPro™	103
6.2	Recommendations for further research.....	104
7	References.....	106
8	Appendices	118
8.1	Appendix A	118
8.2	Appendix B.....	120
8.3	Appendix C.....	130
8.4	Appendix D	135

CHAPTER 1

1 Introduction

The main sources of global anthropogenic greenhouse gas (GHG) emissions are carbon dioxide emissions from fossil fuel combustion and industrial processes. These GHG emissions have been correlated with an increase in global mean temperature since the start of the industrial revolution (Shemfe, Gu & Fidalgo, 2017). The current supply and use of energy is economically, environmentally and socially unsustainable, and if critical action is not taken, GHG emissions will be more than double by 2050 (IEA Renewable Energy Division, 2011).

There is an urgency to implement emission regulations and policies that will motivate the deployment of sustainable alternatives to fossil fuels, which is further motivated by depleting fossil fuel resources, and expected rises in global population and energy demand (Shemfe *et al.*, 2017). Policies should incentivise and promote the production and use of bioenergy and biofuels, while ensuring that food security, biodiversity and social welfare are not compromised. This is achieved by including measures that promote low risk feedstocks, sustainable land use management and efficient processing technologies (IEA Renewable Energy Division, 2011).

The Paris Agreement was adopted at the 21st United Nations Framework Convention on Climate Change (UNFCCC), and is a call for all countries to urgently address the negative impact of climate change by implementing policies to reduce GHG emissions. The goal of the Paris Agreement is to limit the increase in global mean temperature for this century to well below 2 °C, with only a 1.5 °C increase in global mean temperature as the target. South Africa is currently experiencing a severe drought brought on by the worst El Nino event in decades. Increased temperatures and reduced rainfall as a result of climate change in many parts of the world prompted South Africa and 195 other countries to sign the agreement (Department of Environmental Affairs, 2016). South Africa aims to honour the Paris Agreement and limit emissions through measures included in its Intended Nationally Determined Contribution (INDC), such as further investment into renewable power produced by the private sector, carbon taxing, carbon capture and storage, 20 % hybrid-electric vehicles by 2030, electric vehicles by 2050 and decarbonised electricity by 2050 (Department of Environmental Affairs, 2015).

Biofuels are important for reducing GHG emissions in the transport sector by limiting dependence on fossil fuels (IEA Renewable Energy Division, 2011). Today, biofuels only contribute to 2 % of transportation fuels globally but ongoing technological developments suggest considerable potential for growth in the coming years. The International Energy Agency (IEA) proposes that bioenergy has the potential to supply up to 10 % of the primary energy demand by 2035, and biofuels

have the potential to replace up to 27 % of fossil fuels in the transport sector by 2050 (Wang, Dai, Yang & Luo, 2017).

Forest residues are the woody biomass left behind in forests after felling and thinning trees, and as a high fire risk are often disposed of by burning or sold as firewood. Both of these contribute to air pollution and the latter has little economic value (Mitchell, Parker, Sharma & Kaffka, 2015). Paper and pulp industries in South Africa are already using waste products such as bark, black liquor and paper sludge to generate at least 45 % of the electricity and steam needed for the papermaking process (PAMSA, 2019), but the industry is looking for further bioenergy production by utilising forest residues to produce bio-derived transportation fuels, in an effort to reduce CO₂ emissions produced by the combustion of fossil fuels during forest operations (Melendez, LeBel & Stuart, 2013). Bioenergy and biofuel production from forest residue is considered an almost carbon neutral process (save for anthropogenic carbon emissions related to biomass transport and collection) since the biomass takes up CO₂ from the atmosphere for photosynthesis, and releases CO₂ again during combustion (Mohan, Pittman & Steele, 2006).

Biomass such as forest residue can be converted into bioenergy and biofuel by biochemical, thermochemical or hybrid processes (Farzad, Mandegari, Guo, Haigh, Shah & Görgens, 2017). The main biochemical processes are alcoholic fermentation and anaerobic digestion, and the main thermochemical processes are pyrolysis, gasification and combustion (Demirbas & Balat, 2006). Pyrolysis is the conversion of biomass at elevated temperatures and in the absence of oxygen into solid char, liquid bio-oil and non-condensable gases (Collard & Blin, 2014). Pyrolysis is one of the most suitable thermochemical processes, because it has the potential to produce high liquid yields that are more convenient for handling, storage and transport than gas (Wang, Dai, *et al.*, 2017). However, the physiochemical properties of bio-oil are unlike fossil fuels, mostly due to its high oxygen and water content, though bio-oil can be upgraded to improve its quality for the purpose of co-processing in a crude-oil refinery to produce bio-derived transportation fuels (Czernik & Bridgwater, 2004).

The aim of this project is to determine whether or not the production of crude and upgraded bio-oils via the pyrolysis of forest residues is economically and environmentally feasible for the purpose of co-processing in an oil refinery. This will be achieved through the development of process simulations in Aspen Plus™ that will generate the mass and energy balances needed to size and subsequently cost process equipment for the economic analyses. The environmental impact of producing crude and upgraded bio-oils will also be measured in SimaPro™ and compared to fossil fuels.

CHAPTER 2

2 Literature Review

This chapter reviews and discusses literature that is relevant to the project. Section 2.1 and Section 2.2 focus on lignocellulosic biomass and forest residues, respectively. The mechanisms, operating conditions and products of pyrolysis processes are then described in Section 2.3. A review of bio-oil upgrading methods is given in Section 2.4. Section 2.5 outlines the advantages and limitations of co-processing crude and upgraded bio-oils. Previous techno-economic analyses are discussed in Section 2.6 and finally, the environmental impact of the pyrolysis process is considered in Section 2.7.

2.1 Lignocellulosic biomass

Biomass includes all organic (living) matter that is renewable (Van de Velden, Baeyens, Brems, Janssens & Dewil, 2010), and can be classified as woody, agricultural, aquatic, human and animal waste or industrial waste. Woody and agricultural biomasses are the most abundant type of biomass. Woody biomass includes the stems, branches, bark, leaves and off-cuts of trees, while agricultural biomass includes the stalks, straws, shells and other non-edible parts of agricultural crops. Aquatic biomass includes plants, microalgae and other microorganisms found in water. Human and animal waste biomass includes animal manure, food, paper and plastics. Industrial waste, such as black liquor produced by the paper industry, is separate from human and animal waste as it may contain toxic chemicals and harmful additives (Tripathi, Sahu & Ganesan, 2016). The estimated distribution of biomass available in South Africa is shown in Figure 1.

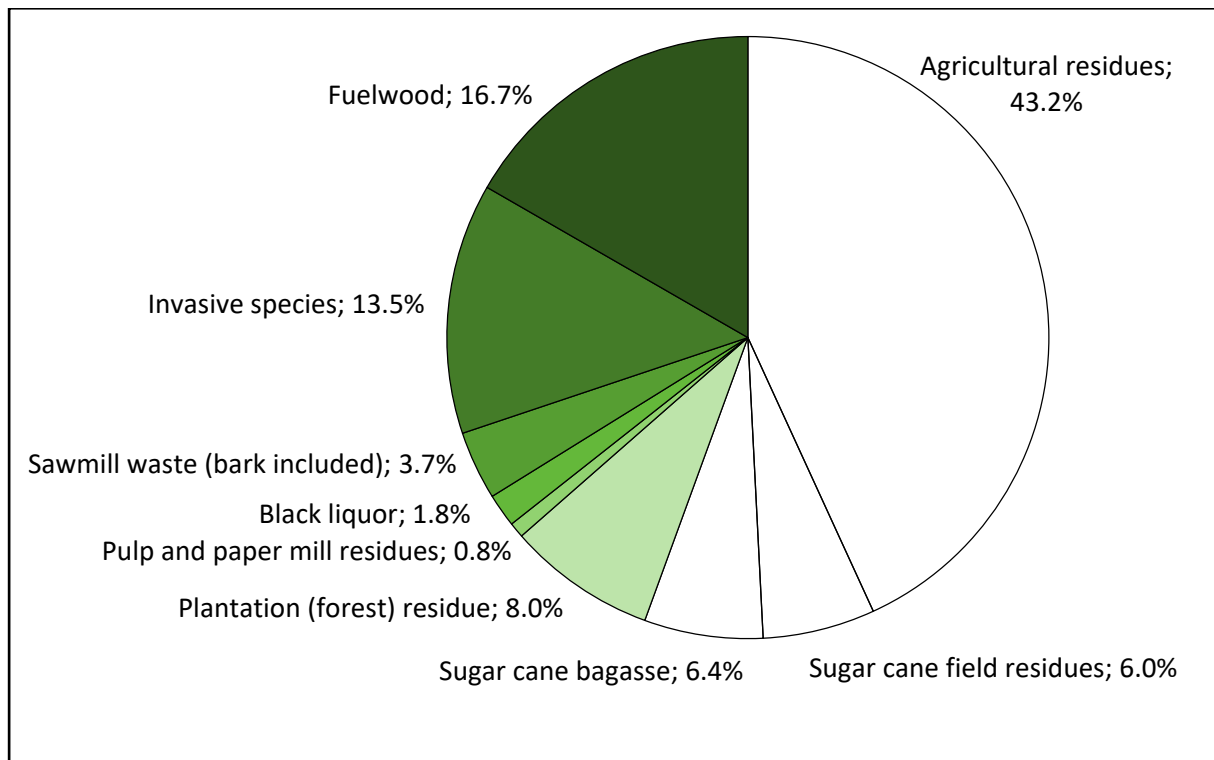


Figure 1: Estimated mass distribution of biomass available in South Africa (Hugo, 2016)

Woody and agricultural biomasses are classified as lignocellulosic biomasses. Lignocellulose is a three dimensional biopolymer largely composed of cellulose, hemicellulose and lignin, with small amounts of extractives and ash (Wang, Dai, *et al.*, 2017). Typical biochemical compositions of lignocellulosic biomasses are given in Table 1.

Table 1: Biochemical composition of lignocellulosic biomasses (wt. %)

Biomass	Cellulose	Hemicellulose	Lignin	Extractives	Ash	Reference
Pine (softwood)	46.9	20.3	27.3	5.1	0.3	(Wang, Dai, <i>et al.</i> , 2017)
Beech (hardwood)	45	33	20	2	0.2	
Corn stover	26.9-42.7	13.3-23.2	15.2-18.2	9.8-22.0	3.5-11.0	(Wang, Dai, <i>et al.</i> , 2017)
Sugarcane bagasse	40.6	22.8	25.5	7.5	3.6	(Demirbas, 2016)
Rice straw	37	16.5	13.6	13.1	19.8	(Qu, Guo, Shen, Xiao & Zhao, 2011)

Trees can be classified as softwood or hardwood: softwoods originate from gymnosperm (seeding) trees and hardwoods originate from angiosperms (flowering) trees. Softwoods generally grow faster but hardwoods are more dense (Wang, Dai, *et al.*, 2017). Hardwoods are usually made up

of more cellulose and hemicelluloses than softwoods, while softwoods contain more lignin. Hardwoods are made up of approximately 43-47 wt. % cellulose, 25-35 wt. % hemicelluloses, 16-24 wt. % lignin and 2-8 wt. % extractives, while softwoods contain approximately 40-44 wt. % cellulose, 25-29 wt. % hemicellulose, 25-31 wt. % lignin and 1-5 wt. % extractives (Balat, Balat, Kirtay & Balat, 2009). The proportion of cellulose, hemicellulose and lignin biopolymers has a significant effect on the conversion of the biomass as a whole during the pyrolysis process (Wang, Dai, *et al.*, 2017).

Cellulose is a linear polymer made up of glucose units connected by β -1,4-glycoside bonds. Its linear structure allows strong hydrogen bonds to form between the long polymer chains, which gives cellulose its high crystallinity, high stability, strong chemical resistance and small surface area (Serrano-Ruiz & Dumesic, 2012). Hemicellulose is made up of a heterogeneous mixture of glucose, galactose, mannose, xylose, arabinose and glucuronic acid. It surrounds cellulose and forms a link between cellulose and lignin polymers. Unlike cellulose, hemicellulose is amorphous, has a low molecular weight and poor physical strength (Dhyani & Bhaskar, 2018; Mohan *et al.*, 2006). Lignin is a three-dimensional, highly branched, cross-linked phenol polymer consisting of hydroxy- and methoxy- substituted phenyl-propane monomers. These monomers can be classified as guaiacyl, syringyl and p-hydroxyl phenyl units. Lignin provides structural rigidity to the biomass by holding cellulose and hemicellulose polymers together, and also protects the biomass against microbial and fungal attack (Dhyani & Bhaskar, 2018; Mohan *et al.*, 2006; Serrano-Ruiz & Dumesic, 2012). The arrangement of cellulose, hemicellulose and lignin in the lignocellulose biomass is shown simply in Figure 2.

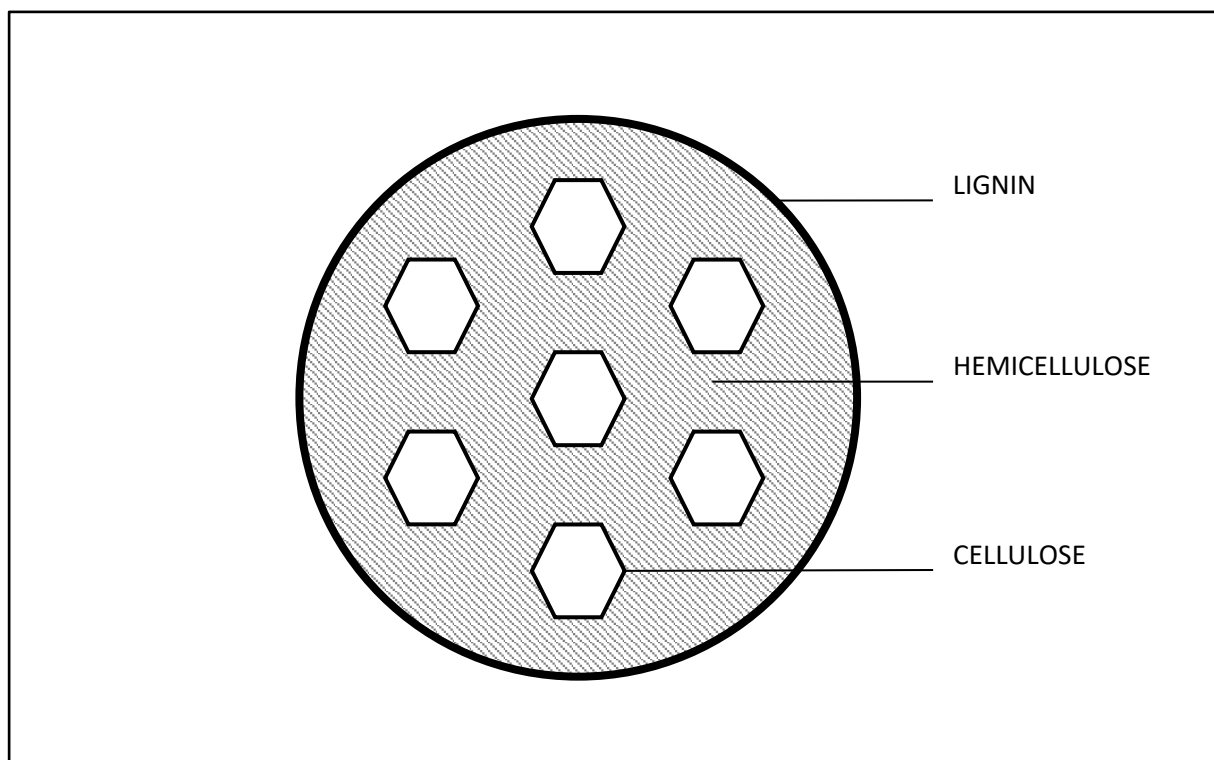


Figure 2: Arrangement of cellulose, hemicellulose and lignin in the lignocellulose biomass

Extractives are non-structural components of the lignocellulosic biomass (Wang, Dai, *et al.*, 2017) that can be extracted using solvents (Rowell, Pettersen, Han, Rowell & Tshabalala, 2005). Extractives can be present as fats, waxes, proteins, simple sugars, pectin, essential oils and many other minor organic compounds (Dhyani & Bhaskar, 2018; Mohan *et al.*, 2006). Forest residues, specifically bark and needles, are high in extractives but the proportion and composition of the extractives are highly dependent on the wood species. Oasmaa and colleagues (2003) found that the extractives in forest residue can range from 5.4 to 10.5 wt. % of the dry biomass (Oasmaa, Kuoppala, Gust & Solantausta, 2003).

The inorganic content of wood is made up of a wide range of elements derived from mineral salts absorbed through the roots of trees, and is often referred to as ash. Ash is retained as a solid residue after biomass combustion. About 80 wt. % of ash is made up of calcium, magnesium and potassium elements (Rowell *et al.*, 2005; Wang, Dai, *et al.*, 2017).

2.2 Forest residue

In 2016, 50 % of the commercial timber plantation area in South Africa was made up of softwoods and the other 50 % was made up of hardwoods. Pulpwood, sawlogs and mining timber production comprised of 57, 38 and 2 % of the plantation area, respectively with the remaining 3 % of the plantation area allocated for other purposes (Forestry Economics Services, 2017). The distribution of pulpwood, sawlogs and mining timber products for softwoods and hardwoods is given in Table 2.

Table 2: Distribution (% area) of Softwoods and Hardwoods (Forestry Economics Services, 2017)

Product	Softwood	Hardwood
Sawlogs	73.5	2.9
Pulpwood	26.1	87.2
Mining Timber	-	4.6
Other	0.4	5.4

Softwoods are mainly grown for sawlogs and hardwoods are mainly grown for pulpwood. *Pinus patula* (*P. patula*) is the main softwood species planted in South Africa and comprises of 50.4 % of the total softwood area, while *Eucalyptus grandis* (*E. grandis*) is the main hardwood species planted in South Africa and comprises of 42.4 % of the total hardwood area (Forestry Economics Services, 2017).

Forest residue is the woody biomass left behind in forests after felling or thinning operation, and typically includes treetops, small trees, stumps, branches, bark, twigs and leaves (Melendez *et al.*, 2013). There are approximately 1.5 million dry tonnes of forest residues available in South Africa every year (Hugo, 2016). The paper and pulp industry has the largest share in South Africa's forest

plantations, and inevitably produces the majority of these forest residues. Forest residues left behind in forests, however, are a high fire risk and often disposed of by burning or sold as firewood. Both of these contribute to air pollution and the latter has little economic value, therefore there is an opportunity for the paper and pulp industry to utilise the energy potential of forest residues in an environmentally friendly and profitable way (Mitchell *et al.*, 2015).

Conversely, the removal of all forest residues has a negative effect on soil fertility. A 30 % reduction in stem wood production was observed in the following harvest period when all forest residues were removed from *E. grandis* plantation areas (Gonçalves, Wichert, Gava, Masetto, Junior, Serrano & Mello, 2007). The soil was left deficient of the important calcium and potassium nutrients.

The paper and pulp industry relies on soil productivity to maintain stem wood production therefore, forest litter (leaves and small twigs), stumps, root systems and a portion of branches should not be removed from plantations to preserve nutrients, prevent soil erosion and protect against compaction by heavy machinery (Wright, Eaton, Perlack & Stokes, 2012; Yang, Li & Zhang, 2016). Soil productivity in response to plantation management is highly site-specific (Nambiar & Kallio, 2008), however, in the KwaZulu-Natal and Mpumalanga provinces of South Africa, where pulpwood production is concentrated (Forestry Economics Services, 2017), typically 80 wt. % of branches are safe to remove for biofuel production¹.

Forest residues are collected from forests either by one-pass or two-pass systems. The former occurs when round wood and forest residues are harvested simultaneously and forwarded to the primary landing, whereas the latter occurs when forest residues are recovered after the round wood is harvested. Two-pass systems are implemented when round wood is harvested by cut-to-length extraction and not full-tree extraction (Ackerman, Ham, Dovey, Toit, Wet, Kunneke & Seifert, 2013; Röser, 2008).

Several factors influence the cost of harvesting forest residues for one and two-pass systems such as terrain and terrain accessibility, rate of recovery, chip quality and chip storage. Terrain accessibility is crucial for two-pass systems, and often determines the forwarding distance to landings and roadside due to the limited movability of harvesting and extraction equipment. In some cases, it will even be necessary to use the biomass as a brush mat to protect soft and sensitive soils against compaction and damage caused by heavy machinery, and as a result, the biomass will become contaminated. In two-pass systems, the biomass is allowed to dry in field, which decreases its recoverable volume per area but increases its energy value and allows time for nutrient transfer from the biomass back into the soil to take place. Chip quality is also improved when the biomass is allowed to dry in field. The moisture content of the biomass will decrease by 30-40 % within the first two weeks

¹ Communication with Prof Ben du Toit, Department of Forest and Wood Science at Stellenbosch University

after felling. The proper storage of chips is costly but also crucial to avoid physical and microbial degradation, and spontaneous combustion (Ackerman *et al.*, 2013; Röser, 2008).

2.3 Pyrolysis

Pyrolysis is the thermochemical conversion of biomass at elevated temperatures and in the absence of oxygen into solid char, liquid bio-oil and non-condensable gas products (Collard & Blin, 2014; Collard, Blin, Bensakhria & Valette, 2012).

2.3.1 Mechanisms

The chemical bonds within the cellulose, hemicellulose and lignin biopolymers are broken as the biomass is heated. Volatile compounds are released and interact by means of rearrangement reactions (primary mechanisms) to form the primary pyrolysis products. Simultaneously, unstable volatile compounds undergo further conversion (secondary mechanisms) to form the secondary pyrolysis products (Collard & Blin, 2014).

2.3.1.1. Primary mechanisms

The primary mechanisms of biomass conversion can be described by three pathways (i.e. char formation, depolymerisation and fragmentation) that are defined by the conditions under which the chemical bonds are broken (Collard & Blin, 2014).

a. *Char formation*

The formation and combination of benzene rings in a polycyclic structure produces a solid residue known as char. Water vapour and non-condensable gases are typically released during these rearrangement reactions (Collard & Blin, 2014; Pisupati & Tchapda, 2015).

b. *Depolymerisation*

Depolymerisation occurs when covalent bonds between monomer units break, followed by stabilisation of the two new chain ends. Further depolymerisation results in shorter polymer chains, until volatile compounds are produced. These compounds are condensable at ambient temperature (Collard & Blin, 2014). Lignin and hemicellulose have amorphous structures that depolymerise at lower temperatures than the crystalline structure of cellulose (Pisupati & Tchapda, 2015).

c. *Fragmentation*

Fragmentation occurs when covalent bonds within monomer units break to form non-condensable gases and a range of volatile, low molecular weight compounds that are condensable at ambient temperature (Collard & Blin, 2014; Collard *et al.*, 2012).

2.3.1.2. Secondary mechanism

Unstable volatile compounds can undergo cracking or recombination reactions. Cracking occurs when the intramolecular bonds within volatile compounds are broken to form lower molecular weight compounds. The products of the fragmentation and cracking pathways are often indistinguishable, making it difficult to determine which pathway is responsible. Recombination occurs when volatile compounds are recombined to form higher molecular weight compounds that can either be volatile or solid (secondary char) depending on the reaction conditions. Cracking and recombination reactions can be catalysed at the surface of the char, reactor or intentionally added catalyst. Catalyst deactivation during recombination reactions is also possible as secondary char can block pores on the catalytic surface (Collard & Blin, 2014).

2.3.2 Types of pyrolysis

2.3.2.1. Slow pyrolysis

Slow pyrolysis is characterised by low heating rates and long vapour residence times. Slow pyrolysis of biomass occurs at temperatures ranging between 400 and 500 °C under heating rates from 0.1 to 1 °C/s for vapour residence times between 300 and 550 s. These long vapour residence times are optimal for secondary reactions to reach completion (Tripathi *et al.*, 2016). The main product of slow pyrolysis is char, but typically 30 wt. % bio-oil and 35 wt. % non-condensable gas are also produced (Bridgwater, 2012a).

2.3.2.2. Fast pyrolysis

Fast pyrolysis is characterised by high heating rates and short vapour residence times. Fast pyrolysis of biomass occurs at temperatures ranging between 450 and 650 °C (Kan, Strezov & Evans, 2016) under heating rates from 10 to 200 °C/s for vapour residence times between 1 and 10 s. These operating conditions are aimed at minimising char formation and secondary reactions therefore, fast pyrolysis typically produces 60 to 75 wt. % bio-oil (Tripathi *et al.*, 2016).

2.3.2.3. Intermediate pyrolysis

Intermediate pyrolysis takes place between slow and fast pyrolysis operating conditions. Intermediate pyrolysis occurs at temperatures ranging between 500 and 650 °C under heating rates from 1 to 10 °C/s for vapour residence times between 0.5 and 20 s. This type of pyrolysis with biomass typically produces 15 to 25 wt. % char, 40 to 60 wt. % bio-oil and 20 to 30 wt. % non-condensable gas (Tripathi *et al.*, 2016).

2.3.2.4. Vacuum pyrolysis

Vacuum pyrolysis is operated at very low or vacuum pressures, unlike slow, fast and intermediate pyrolysis processes that are operated at atmospheric pressure. Vacuum pyrolysis occurs at temperatures ranging between 450 and 600 °C and pressures from 0.01 to 0.02 MPa. The heating rate is comparable to slow pyrolysis, but the vapour residence time is shorter than 1 s. The low pressure/vacuum atmosphere results in the rapid removal of vapours, which considerably minimises secondary reactions to produce a high quality bio-oil. Vacuum pyrolysis typically produces 35 to 50 wt. % bio-oil (Tripathi *et al.*, 2016).

2.3.3 Effect of operating parameters

2.3.3.1. Temperature

Pyrolysis reaction temperature and heating rate have the most significant effect on product distribution (Isahak, Hisham, Yarmo & Yun Hin, 2012). The biomass undergoes dehydration reactions below 300 °C to produce mostly char, however, as temperature increases, depolymerisation takes over to produce condensable volatiles. Bio-oil production is maximised between 450 and 550 °C before fragmentation and secondary reactions take over. Meanwhile, char yield decreases from 300 to 600 °C but remains relatively stable as temperature increases above 600 °C. Finally, non-condensable gases are predominantly produced above 800 °C (Neves, Thunman, Matos, Tarelho & Gómez-Barea, 2011).

2.3.3.2. Heating rate

Heating rate determines the type of pyrolysis (i.e. slow, fast or intermediate), and the composition and nature of the pyrolysis products (Kan *et al.*, 2016). Higher char yields are produced under lower heating rates, where secondary cracking reactions are reduced, whereas lower char yields are produced under higher heating rates, where primary fragmentation reactions are promoted and bio-oil and non-condensable gas yields are enhanced (Tripathi *et al.*, 2016). Bio-oil oxygen content also decreases at higher heating rates, while oxygen containing non-condensable gas (CO₂ and CO) yield increases (Akhtar & Amin, 2012).

2.3.3.3. Vapour residence time

Vapour residence time is the amount of time volatiles spend in the reactor before separation into bio-oil and non-condensable gas. Higher char yields are associated with longer vapour residence times as sufficient time is allowed for secondary recombination reactions to reach completion. Conversely, higher bio-oil yields are associated with shorter vapour residence times. Vapour residence time not only effects the char yield but also the char composition, by stimulating the development of micro and macro pores (Tripathi *et al.*, 2016). The effect of temperature and vapour residence time on the quality

of pyrolysis products is still not completely understood (Akhtar & Amin, 2012). Nevertheless, the effect of vapour residence time on pyrolysis products is overshadowed by the effects of temperature and heating rate (Tripathi *et al.*, 2016).

2.3.3.4. Particle size

The primary and secondary mechanisms of pyrolysis are influenced by biomass particle size because biomass is a poor conductor of heat. The temperature gradient across the particle naturally increases with particle size, thereby impeding the rate of heat transfer and enhancing secondary reactions to produce char. Smaller particle sizes of <1 mm are preferred for fast pyrolysis and bio-oil production but particle size reduction can be expensive and significantly impact the economics of biomass pyrolysis (Kan *et al.*, 2016). Slow pyrolysis requires particle sizes ranging from 5 to 50 mm, while intermediate pyrolysis requires particle sizes between 1 and 5 mm (Tripathi *et al.*, 2016).

2.3.4 Products

The biochemical composition of the lignocellulosic biomass influences the distribution and quality of pyrolysis products. At lower pyrolysis temperatures, cellulose degrades into stable anhydrocellulose to produce char, while at higher pyrolysis temperatures, cellulose decomposes into volatile compounds to produce bio-oil and non-condensable gas. Hemicellulose also decomposes into volatiles, while lignin more readily yields char due to the fragmentation of its relatively weak bonds (Kan *et al.*, 2016; Tripathi *et al.*, 2016). Further detail about the pyrolysis products is provided in this section.

2.3.4.1. Char

Char (also referred to as biochar) is a solid product made up of unconverted organic solids, carbonaceous residues and inorganics (Kan *et al.*, 2016). The proximate analysis, elemental analysis and higher heating value (HHV) for biochar produced from hardwood stem and hardwood bark under slow pyrolysis conditions at 500 °C are given in Table 3. The HHV was calculated using the empirical correlations given in Equation 2-1.

$$HHV = 0.3491C + 1.1783H + 0.1005S - 0.1034O - 0.0151N - 0.0211A \quad \text{Equation 2-1}$$

Where, *C*, *H*, *O*, *N*, *S* and *A* represent carbon, hydrogen, oxygen, nitrogen, sulphur and ash, respectively, and are expressed in mass percentages on a dry basis (Channiwala & Parikh, 2002).

Table 3: Proximate and elemental analyses for biochar produced from hardwood (Lee, Park, Ryu, Gang, Yang, Park, Jung & Hyun, 2013)

Analysis		Hardwood Stem	Hardwood Bark
Proximate (wt. %, db)	Moisture	1.46	0.36
	Volatile Matter	12.79	18.14
	Fixed Carbon	83.47	68.66
	Ash	2.28	12.84
Elemental (wt. %, db)	Carbon	89.31	84.84
	Hydrogen	2.57	3.13
	Oxygen	7.34	10.20
	Nitrogen	0.78	1.83
	Sulphur	-	-
HHV (MJ/kg, db)	-	32.63	27.82

Lignocellulosic biomass, pyrolysis temperature and heating rate determines the physiochemical properties that makes biochar suitable for a wide range of applications. Biochar produced under low-temperature pyrolysis conditions is high in volatile matter that is made up of easily decomposable nutrient-rich substrates, which are suitable for soil applications. Alternatively, biochar produced under high-temperature pyrolysis conditions yields a large microscopic surface area and aromatic carbon content that is suitable for adsorption and carbon sequestration applications, respectively (Jindo, Mizumoto, Sawada, Sanchez-Monedero & Sonoki, 2014). The applications of biochar related to its economic value are discussed in more detail below.

a. *Carbon sequestration*

Biochar can store carbon for thousands of years due to its strong resistance to biological decay (Lee *et al.*, 2013). The economic value of biochar intended for carbon sequestration is dependent on its carbon content and the carbon tax rate set by government. Biochar with a carbon content of 89.31 wt. % (given in Table 3) stores an equivalent 2.62 metric tonnes of carbon dioxide per metric tonne of biochar, assuming that 80 wt. % of the carbon will be sequestered over a significant period of time (Han, Elgowainy, Dunn & Wang, 2013). The carbon tax rate set by the South African government is R120/MT CO₂ eq (Republic of South Africa, 2019) therefore, biochar with a carbon content of 89.31 wt. % is worth R314.66/MT (~\$23/MT).

b. *Charcoal*

Biochar with an HHV of 32.63 MJ/kg (included in Table 3) is similar to bituminous coal with an HHV of 31.00 MJ/kg therefore, it is traditionally used as fuel (charcoal) to produce heat for cooking

(Channiwala & Parikh, 2002; Lee *et al.*, 2013). The economic value of charcoal in South Africa can range from R3 400/MT (~\$243/MT) to R4 800/MT (~\$343/MT) including VAT (Burger, 2018; Konz, Cohen & van der Merwe, 2015; Wattle Wood Farm, 2019).

c. *Soil application*

Biochar increases the capacity for soil to hold water and nutrients, which reduces the need for fertilizers, and decreases the emission of greenhouse gases such as nitrous oxide and methane (Lee *et al.*, 2013). Biochar also has the potential to increase crop productivity since inorganic minerals such as potassium, phosphorous, calcium and magnesium are present in high concentrations in the biochar, and are important for plant growth (Kim, Kim, Lee, Choi, Yeo, Choi & Choi, 2013).

The capacity for biochar to replace fertilizer is not fully established because of the many parameters that influence its properties and application to the soil, such as: feedstock properties, pyrolysis conditions, soil properties and plant growth mechanisms (Lee *et al.*, 2013). Based on the review by Agegnehu and colleagues (2017), a conservative assumption is to replace fertilizer with biochar in a 1:1 ratio (Agegnehu, Srivastava & Bird, 2017). Biochar is comparable to Limestone Ammonium Nitrate (LAN) fertilizers, which were sold for between R5 000/MT (~\$357/MT) and R5 800/MT (~\$414/MT) in 2017 (Grain SA, 2019). Furthermore, biochar produced in South Africa by *C Fert* and *Biogrow* for soil application is sold for between R5 000/MT and R6 111/MT (~\$437/MT).

d. *Activated carbon*

Biochar is similar to commercial activated carbon in activity but different in feedstock type, production and physiochemical properties. The surface of cellulose and hemicellulose biopolymers is made up of a wide range of functional groups that can be physically activated during pyrolysis or by further treatment with either steam or carbon dioxide. The resultant biochar has a high-degree of porosity, large microscopic surface area and strong affinity for non-polar substances, which makes it possible, for example, to adsorb organic and inorganic pollutants found in wastewater. Biochar was found to be more effective than commercial activated carbon in lead adsorption (Cao, Ma, Gao & Harris, 2009; Lu, Zhang, Yang, Huang, Wang & Qiu, 2012), and has shown to effectively adsorb other heavy metals such as cadmium, copper and nickel found in heavy metal contaminated soils (Kan *et al.*, 2016; Lee *et al.*, 2013; Qambrani, Rahman, Won, Shim & Ra, 2017). Jindo and colleagues (2014) studied the effect of temperature on the volatile matter, surface area and carbon content of biochars produced via the pyrolysis of apple tree and oak tree wood chips. The authors found that biochars produced at higher temperatures (600 to 800 °C) had lower volatile matter, larger surface area and higher carbon content than biochars produced at lower temperatures (400 to 500 °C) as shown in Table 4 (Jindo *et al.*, 2014).

Table 4: Volatile matter, surface area and carbon content of biochars produced at a range of temperatures (Jindo et al., 2014)

Feedstock	Temperature (°C)	Volatile Matter (wt. %)	Surface Area (m ² /g)	Carbon Content (wt. %)
Apple tree wood chips	400	32.4	11.9	70.2
	500	18.3	58.6	79.1
	600	11.1	208.7	81.5
	700	7.7	418.7	82.3
	800	6.8	545.4	84.8
Oak tree wood chips	400	32.1	5.6	70.5
	500	19.4	103.2	77.6
	600	12.3	288.6	81.2
	700	8.3	335.6	83.2
	800	7.9	398.2	82.9

The economic value of biochar intended for activated carbon applications falls within a wide range. *Seal Water Tech* sells activated carbon produced from coconut shells for R9 200/MT (~\$657/MT) including VAT (*Seal Water Tech*, 2019). *Activated Carbon Innovations* produces activated carbon (ranging from large granules to a fine powder) from macadamia nut shells that is sold for between R39 500/MT (~\$2 821/MT) and R49 500/MT (~\$3 536/MT) excluding VAT (*Activated Carbon Innovations*, 2019). *Rotocarb* also produces activated carbon from macadamia nut shells, which is sold for R36 480/MT (~\$2 606/MT) including VAT (*Burger*, 2018).

2.3.4.2. Gas

The main non-condensable gases produced from biomass pyrolysis are carbon dioxide (CO₂), carbon monoxide (CO), hydrogen (H₂), methane (CH₄), ethane (C₂H₆) and ethylene (C₂H₄) (*Kan et al.*, 2016). The amount of CO₂ and CO produced is dependent on the thermal decomposition of hemicellulose and cellulose, respectively. The amount of H₂ and CH₄ is dependent on the thermal decomposition of lignin (*Dhyani & Bhaskar*, 2018). Non-condensable gases can be combusted to generate heat for the process or recycled to the pyrolysis reactor as a fluidising gas (*Dhyani & Bhaskar*, 2018; *Kan et al.*, 2016).

2.3.4.3. Bio-oil

Bio-oil is a dark brown, free-flowing liquid composed of a complex mixture of oxygenated hydrocarbons, water and traces of char (*Bridgwater*, 2012b). It is produced by rapidly cooling the vapours leaving the pyrolysis reactor. Two phases are present in bio-oil due to its high water content, specifically the organic phase (also referred to as the organic fraction) and the aqueous phase (aqueous

fraction). The organic phase has similar properties to a low-grade fuel and can be upgraded (as discussed in Section 2.4 below) to a high-grade fuel or useful chemicals, while the aqueous phase mostly consists of low-grade, oxygen-rich compounds such as acetic acid that cannot be used for fuel (Mirkouei, Haapala, Sessions & Murthy, 2017; Zhang, Yan, Li & Ren, 2005).

The organic compounds found in bio-oil can be categorised into chemical families such as acids, aldehydes, ketones, phenols, and sugars (García-Pérez, Chaala, Pakdel, Kretschmer & Roy, 2007). Azeez and colleagues (2010) carried out fast pyrolysis experiments at approximately 470 °C with beech and spruce wood feedstocks to identify and quantify the major chemical families found in the produced bio-oils. The gas chromatography-mass spectroscopy (GC/MS) analysis results for the bio-oils are given in Table 5. Acetic acid, hydroxyacetaldehyde and hydroxypropanone were present in the highest concentrations for both bio-oils. Furthermore, a portion of each bio-oil consisted of carbohydrate and lignin-derived compounds that are undetectable by GC/MS (Azeez, Meier, Odermatt & Willner, 2010).

Table 5: Major chemical families (wt. %, db) identified and quantified in beech and spruce wood bio-oils (Azeez et al., 2010)

Chemical Families	Beech (Hardwood)	Spruce (Softwood)
Acids	8.2	2.6
Aldehydes	10.3	11.3
Ketones	5.1	4.2
Sugars	3.3	5.4
Furans	2.5	2.6
Pyrans	1.9	1.8
Aromatics	0.1	0.1
Lignin-derived phenols	0.3	0.5
Guaiacols	1.5	4.1
Syringols	3.1	<0.0
Undetectable by GC/MS	63.7	67.3

The properties of bio-oils are significantly different from conventional hydrocarbon fuels. Bio-oil has a high oxygen and water content, is highly acidic, mostly viscous, and undergoes undesirable secondary reactions during storage (aging). Table 6 summarises the typical properties of bio-oil produced from wood pyrolysis compared to heavy fuel oil.

Table 6: Properties of bio-oil produced from wood and heavy fuel oil (Czernik & Bridgwater, 2004)

Physical Property	Bio-oil	Heavy Fuel Oil
Moisture content (wt. %)	15–30	0.1
pH	2.5	-
Elemental composition (wt. %, db)		
C	54–58	85
H	5.5–7.0	11
O	35–40	1
N	0–0.2	0.3
Ash	0–0.2	0.1
HHV	16–19	40
Viscosity at 50 °C (cP)	40–100	180

Oxygen (in the form of oxygenated hydrocarbons) lowers the heating value of bio-oil and gives bio-oil its polar nature, making it immiscible with conventional hydrocarbon fuels (Dhyani & Bhaskar, 2018). Bio-oil contains about 35 to 40 wt. % oxygen, which is distributed over 300 compounds (Czernik & Bridgwater, 2004). Most of these compounds are present as carboxylic acids, hydroxyaldehydes, hydroxyketones, sugars and phenolics (Meier, Oasmaa & Peacocke, 1997).

Water is derived from moisture in the feedstock and the dehydration reactions taking place during pyrolysis. Bio-oil contains about 15 to 30 wt. % water, depending on the feedstock and its moisture content. Water affects the heating value, stability, aging and viscosity of bio-oil (Bridgwater, 2012b; Dhyani & Bhaskar, 2018).

High quantities of organic acids (such as acetic and formic acids) lowers the pH of bio-oil to range between 2 and 3. High acidity and moisture content at high operating temperatures makes bio-oil corrosive to process equipment, specifically process equipment in existing oil-refineries, where the bio-oil will eventually be co-processed with conventional hydrocarbon fuels (Bridgwater, 2012b).

The viscosity of bio-oil at 40 °C can vary between 35 and 1000 cP depending on the nature of the feedstock, pyrolysis reaction conditions, separation efficiency of char, water content and storage time or aging. However, the viscosity of bio-oil produced from wood typically ranges from 40 to 100 cP (Czernik & Bridgwater, 2004). The viscosity of bio-oil tends to increase during storage as secondary reactions between bio-oil compounds take place, which sometimes results in phase separation (Bridgwater, 2012b).

2.3.5 Pyrolysis of forest residue

Oasmaa and colleagues (2010) conducted fast pyrolysis with green forest residue (86 wt. % spruce, 9 wt. % pine and 5 wt. % birch) and brown forest residue (80 wt. % spruce, 10 wt. % pine and 10 wt. %

birch) in a fluidising bed reactor operating between 480 and 520 °C. The bio-oil yields were 63.7 and 57.9 wt. % for the green forest residue (8.1 wt. % moisture) and brown forest residue (4.9 wt. % moisture), respectively (Oasmaa, Solantausta, Arpiainen, Kuoppala & Sipilä, 2010). The green forest residue (initially 55 wt. % moisture) included about 63 wt. % branches (37 wt. % bark) and 37 wt. % needles, whereas the brown forest residue (initially 35 wt. % moisture) consisted of about 90 wt. % branches (33 wt. % bark) and 10 wt. % needles (Oasmaa *et al.*, 2003).

Puy and colleagues (2011) carried out pyrolysis in an auger reactor with softwood (pine) forest residues (6.21 wt. % moisture) at a range of temperatures (500 to 800 °C) and solid residence times (1.5 to 5 min). The highest bio-oil yield was 58.7 wt. % at a temperature of 500 °C and a solids residence time of 5 min. The main compounds found in bio-oil (as identified by GC/MS) were oxygen-containing carboxylic acids, ketones, aldehydes, phenols and aromatics (Puy, Murillo, Navarro, López, Rieradevall, Fowler, Aranguren, García, Bartrolí & Mastral, 2011).

Luo and colleagues (2017) conducted fast pyrolysis in an ablative reactor operating between 500 and 550 °C with softwood (pine) forest residues (7.3 wt. % moisture). The bio-oil yield was 60 wt. % with an oxygen content of 54.05 wt. % (Luo, Chandler, Anjos, Eng, Jia & Resende, 2017).

Torri and colleagues (2016) investigated intermediate pyrolysis at 550 °C and fast pyrolysis at 500 °C with hardwood (gum) and softwood (spruce) forest residues. The bio-oil yields were 49 and 69 wt. % for intermediate and fast pyrolysis of hardwood forest residues (4.5 wt. % moisture), and 50 and 70 wt. % for intermediate and fast pyrolysis of softwood forest residues (6.3 wt. % moisture), respectively. The authors then conducted catalytic pyrolysis experiments with softwood forest residues and a zeolite catalyst at 500 °C for a weight hourly space velocity of 4.3 h⁻¹. The yield of bio-oil decreased from 70 to 62 wt. %, while the quality of bio-oil in terms of oxygen content improved from 36.6 to 32.6 wt. % (Torri, Paasikallio, Faccini, Huff, Caramão, Sacon, Oasmaa & Zini, 2016).

Many researchers have found that forest residues are a suitable feedstock to produce bio-oil via pyrolysis, however, the high oxygen content of the produced bio-oil significantly limits its application as a fuel. Alternatively, bio-oil can be upgraded to improve its quality as discussed in Section 2.4 below.

2.4 Bio-oil upgrading

Bio-oil can be upgraded to improve its oxygen content, water content, and other physiochemical properties that make it unlike conventional hydrocarbon fuels. Several upgradation techniques have been studied, and can be classified as either physical or catalytic.

2.4.1 Physical upgrading

Bio-oil can be physically upgraded by filtration, solvent addition or emulsification. In the case of filtration, hot vapours leaving the pyrolysis reactor are filtered before condensation to reduce ash

content in the bio-oil (Dhyani & Bhaskar, 2018). Hot vapour filtration has been reported to reduce ash content in the bio-oil to 100 ppm and alkali content to less than 10 ppm, which is a considerable improvement from conventional cyclone separation. Liquid filtration to remove ash content with low particle sizes (less than 5 μm) from the condensed bio-oil is challenging and requires high pressure drops and self-cleaning filters. Bio-oil mixed with polar solvents such as methanol has been reported to homogenise, reduce viscosity and improve aging. Finally, surfactant emulsifiers can improve the miscibility of bio-oil with conventional hydrocarbon fuels, however, this process is costly and energy intensive (Bridgwater, 2012a).

2.4.2 Catalytic upgrading

Bio-oil can be catalytically upgraded by ash, hydrodeoxygenation or catalyst vapour cracking. Active alkali metals such as potassium and sodium are naturally present in the biomass as ash, and through secondary vapour cracking can reduce bio-oil yield and quality. Ash vapour cracking can sometimes be more severe than char vapour cracking depending on the concentration of ash present in the biomass. Ash can be removed by washing the biomass in water or dilute acid but this method is not always viable as the cellulose and hemicellulose biopolymers can be hydrolysed, which reduces the bio-oil yield and quality inevitably, and the wet biomass still has to be dried before pyrolysis (Bridgwater, 2012a).

Hydrodeoxygenation (HDO) or hydrotreating involves the removal of oxygen from bio-oil by catalytic reaction with hydrogen to form water as shown in Figure 3. This process occurs separately from pyrolysis. HDO requires a high pressure of about 20 MPa, a moderate temperature of about 400 $^{\circ}\text{C}$ and a source of hydrogen (Bridgwater, 2012a; Dhyani & Bhaskar, 2018). Catalysts that have been extensively studied are cobalt-molybdenum disulphide, nickel-molybdenum disulphide and transition metals such as platinum, palladium and ruthenium (Bu, Lei, Zacher, Wang, Ren, Liang, Wei, Liu, Tang, Zhang & Ruan, 2012; Dhyani & Bhaskar, 2018). This process upgrades the bio-oil to an energy dense, non-corrosive, naphtha-like product. The disadvantage is the high cost associated with hydrogen supply from a renewable resource and operating at intensive pressures (Dickerson & Soria, 2013).

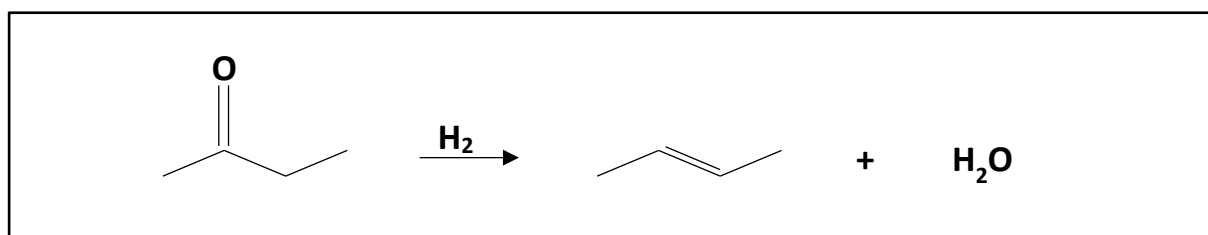


Figure 3: Hydrodeoxygenation reaction (Nolte & Shanks, 2017)

Hydrogen generation is a limitation of HDO. One of the methods to generate hydrogen involves bio-oil reforming, and another method involves biochar steam gasification. However, both of these methods are unfavourable for process economics as some of the product yield and inevitably revenue are expended. A third method involves natural gas steam reforming, which is favourable for process economics as natural gas is cheap, however, natural gas is produced from fossil fuel, which negatively impacts the environment. Moreover, the energy content of the natural gas can be as high as 20 % of the energy content of the upgraded bio-oil. Hydrogen can also be generated through biomass steam gasification, however, diverting biomass to hydrogen production reduces the scale of bio-oil and biochar production. Finally, hydrogen produced from water electrolysis with renewable electricity (solar photovoltaic (PV) panels) is a clean and sustainable method that is better suited for processes where upgraded bio-oil and biochar are both revenue generating products. The downside of this method is the high capital cost and overall low efficiency (Carrasco, Gunukula, Boateng, Mullen, DeSisto & Wheeler, 2017; Nikolaidis & Poullikkas, 2017).

Catalytic cracking is an alternative method that deoxygenates bio-oil without using hydrogen. Bio-oil is usually processed over acidic zeolite catalysts at atmospheric pressure and moderate temperatures. The mechanism involves cracking pyrolysis vapours (breaking C-C bonds), hydrogen transfer, isomerisation, aromatic side chain scission, and deoxygenation reactions (Liu, Wang, Karim, Sun & Wang, 2014). Oxygen is removed in the form of water, carbon dioxide and carbon monoxide via simultaneous dehydration, decarboxylation and decarbonylation reactions (Gollakota, Reddy, Subramanyam & Kishore, 2016; Serrano-Ruiz & Dumesic, 2012) as shown in Figure 4.

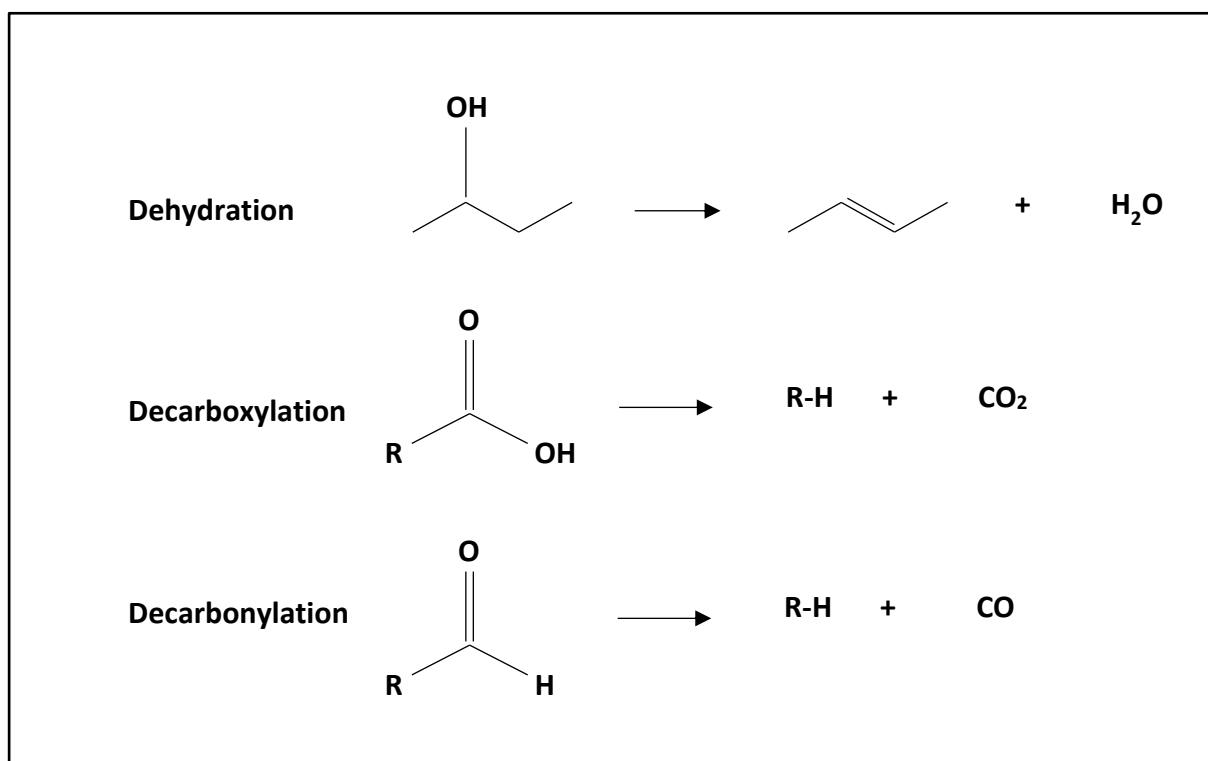


Figure 4: Catalytic cracking reactions (Nolte & Shanks, 2017)

Catalytic cracking has significant technical and economic advantages over HDO. In catalyst cracking, hydrogen is not required and reactions take place at similar conditions to pyrolysis (atmospheric pressure and moderate temperatures), which allows both processes to be carried out in a single reactor (Serrano-Ruiz & Dumesic, 2012).

2.4.3 Catalyst configuration

Upgrading bio-oil can be achieved via *ex situ* or *in situ* catalytic pyrolysis. For *ex situ* catalytic pyrolysis, the biomass is first pyrolysed, then the resulting vapours are passed over the catalyst in a second reactor, where deoxygenation takes place (Nolte & Shanks, 2017). Pyrolysis and catalysis occur in separate reactors therefore, the operating conditions of both reactions can be optimised. Additionally, char can easily be separated from pyrolysis vapours prior to catalytic conversion to reduce catalyst deactivation (Wang, Dai, *et al.*, 2017). The disadvantages are that the vapour residence time increases as the vapour stream travels to the *ex situ* reactor and eventually the condenser, and the second reactor adds to the capital cost of the process (Yildiz, Ronsse, Duren & Prins, 2016).

For *in situ* catalytic pyrolysis, the biomass and catalyst are added to the pyrolysis reactor simultaneously, allowing the pyrolysis vapours to be deoxygenated as they are produced (Nolte & Shanks, 2017), and reducing unfavourable recombination reactions. The disadvantages are that both pyrolysis and catalysis occur at the same temperature, which limits the opportunity to optimise both reactions, and char and ash may accumulate on the catalyst's surface, poisoning the catalyst (Wang,

Dai, *et al.*, 2017). Moreover, the catalyst is invariably entrained with the char, and is either discarded or recycled by combusting the char and separating the ash (Dayton, Carpenter, Kataria, Peters, Barbee, Mante & Gupta, 2015). Both are unfavourable for process economics. Furthermore, higher catalyst loading is required for the *in situ* configuration to achieve the same quality of bio-oil produced from the *ex situ* configuration (Yildiz *et al.*, 2016).

Li and colleagues (Li, Ou, Dang, Meyer, Jones, Brown & Wright, 2015) compared *ex situ* and *in situ* catalytic pyrolysis processes, and found that the capital cost of the *ex situ* configuration is higher than the *in situ* configuration; the catalyst life span for the *ex situ* configuration is longer than the *in situ* configuration due to the reduced risk of deactivation, which also suggests that the *ex situ* configuration requires less maintenance; the catalyst in the *ex situ* configuration can be recycled more readily than the *in situ* configuration; and both configurations produce similar organic fraction yields but the *in situ* configuration produces significantly more aromatics and phenols (Li *et al.*, 2015).

2.4.3.1. Catalyst mixing

The biomass and catalyst are combined for *in situ* catalytic pyrolysis by impregnation or dry mixing (Collard *et al.*, 2012). Impregnation involves combining the biomass, catalyst and water to form a well-mixed slurry followed by drying to remove the water (Couhert, Commandre & Salvador, 2009; Richardson, Blin, Volle, Motuzas & Julbe, 2010). Uniform dispersion of the catalyst and intimate contact between the biomass and catalyst are achieved. Therefore, reactions taking place between volatiles and reactions taking place in the biomass matrix are both catalysed, which has a significant effect on the yield and composition of char and other products (Collard *et al.*, 2012). Impregnation simultaneously washes the biomass particles and removes some of the inorganic content that would have formed part of the ash (Bru, Blin, Julbe & Volle, 2007). Dry mixing involves mechanically combining the biomass and catalyst. This method does not achieve the same intimate contact between the biomass and catalyst as impregnation but it does not require additional energy for drying, which makes it a lot cheaper.

2.4.4 Catalyst to feed ratio

A high catalyst to feed ratio results in a lower bio-oil yield but a better bio-oil quality in terms of lower oxygen content and higher HHV (Dhyani & Bhaskar, 2018; Paasikallio, Kalogiannis, Lappas, Lehto & Lehtonen, 2017). The optimal catalyst to feed ratio is not only dependent on the type of catalyst and biomass but also on process specific factors such as reactor design and pyrolysis temperature. In general, high catalyst to feed ratios will enhance catalyst cracking (increasing bio-oil quality), and produce water, non-condensable gases and coke (decreasing bio-oil yield) (Paasikallio *et al.*, 2017). Conversely, low catalyst to feed ratios (1:6 to 1:8) will not necessarily be sufficient enough to significantly deoxygenate bio-oil because some vapours could leave the pyrolysis reactor without

contacting the catalyst (Veses, Aznar, López, Callén, Murillo & García, 2015; Yildiz *et al.*, 2016) therefore, finding a balance is essential to producing the desired bio-oil quality. Veses and colleagues (2014) found that the optimal catalyst to feed ratio was 1:3 for CaO catalytic pyrolysis of pine wood chips at 450 °C since higher catalyst to feed ratios of 3:1, 1:1 and even 1:2 produced lower bio-oil yields (Veses, Aznar, Martinez, Martinez, Lopez, Navarro, Callen, Murillo & Garcia, 2014).

Lin and colleagues (2010) conducted *in situ* catalytic pyrolysis at 520 °C with dry mixed white pine powder and CaO catalyst. The catalyst to feed ratio was 5:1 and silica sand was used as a heat carrier. CaO decreased oxygen content in the organic fraction from 39 wt. % to 31 wt. %. The researchers found that high catalyst to feed ratios were required to sufficiently deoxygenate the bio-oil as a result of the low contact achieved between the catalyst and biomass (Lin, Zhang, Zhang & Zhang, 2010).

2.4.5 Catalyst selection

The ideal catalyst is highly active, selective towards specific compounds, resistant to deactivation, readily recyclable and effective at low catalyst to feed ratios (Veses *et al.*, 2014). A catalyst is designed to make bio-oil less viscous by increasing cracking reactions and less corrosive by decreasing the formation of carboxylic acids. A catalyst is also designed to increase the heating value of bio-oil by enhancing the production of valuable hydrocarbons (Balat *et al.*, 2009).

It is important to choose a catalyst that will select for desirable compounds. The following oxygen-containing functional groups (Oasmaa *et al.*, 2003) are considered undesirable in bio-oil intended for co-processing in an existing oil refinery (Stefanidis, Kalogiannis, Iliopoulou, Lappas & Pilavachi, 2011; Stefanidis, Karakoulia, Kalogiannis, Iliopoulou, Delimitis, Yiannoulakis, Zampetakis, Lappas & Triantafyllidis, 2016):

- Ketones and aldehydes enhance aging reactions.
- Acids make bio-oil corrosive to materials of construction commonly found in an oil refinery. Acids also catalyse polymerisation reactions and reduce the stability of bio-oil.
- Esters and ethers reduce the heating value of bio-oil.
- Polycyclic aromatic hydrocarbons do not contain oxygen but are considered undesirable because of their carcinogenic properties that are hazardous for the environment, and polycyclic aromatic hydrocarbons also act as precursors for coke formation that can lead to catalyst deactivation.

The desired functional groups in bio-oil are aromatic and aliphatic hydrocarbons, and alcohols. Aliphatic and aromatic hydrocarbons have low oxygen and high energy content, which makes bio-oil more compatible with conventional hydrocarbon fuels (Wang, Dayton, Peters & Mante, 2017). In addition, phenols and furans are high value-added chemicals that can make bio-oil production economically attractive (Stefanidis *et al.*, 2011).

Basic metal oxide catalysts such as CaO and MgO are covered in more detail as this type of catalyst was chosen for the pilot plant experiments conducted by Chireshe (2019) for this project. A review of traditional and promising catalysts for the catalytic pyrolysis of biomass is given below.

2.4.5.1. Zeolites

Zeolites are made up of alumina and silica units, linked by oxygen anions in a crystalline tetrahedral structure (Morris, 2011). Zeolites can have a variety of crystalline structures with open cavities that influence their selectivity. Naturally occurring zeolites such as chabazite and mordenite are not as vastly employed in industry as their synthetic counterparts (Galadima & Muraza, 2015).

H-ZSM-5 is the most common zeolite catalyst employed in industry (Dickerson & Soria, 2013). Zhang and colleagues (2014) reported that H-ZSM-5 catalytic pyrolysis of Aspen wood lignin (3:1 catalyst to feed ratio) reduced the oxygen content of the bio-oil from 28 to 4 wt. %, increased the HHV from 30 to 46 MJ/kg, and increased the yield of toluene (Zhang, Resende & Moutsoglou, 2014). Unfortunately, zeolite catalysts undergo irreversible deactivation (de-aluminate) in the presence of bio-oil with a high water content (Serrano-Ruiz & Dumesic, 2012).

2.4.5.2. Acidic metal oxides

Metal oxides have acid, base or combined properties due to lattice imperfections, such as electron holes and dislocations. Acid and base sites on the surface of metal oxides alter the composition of the bio-oil produced by promoting or preventing the formation of certain products (Wang, Dai, *et al.*, 2017).

Acidic metal oxides such as Al₂O₃ and SiO₂ deoxygenate bio-oil via cracking, dehydration and decarbonylation reactions (Wang, Dai, *et al.*, 2017). Catalytic pyrolysis with Al₂O₃ produces more aromatic hydrocarbons and polycyclic aromatic hydrocarbons. Silicon dioxide catalysts with weak acidity and medium porosity are effective at removing acids, ketones and aldehydes and preventing coke and polycyclic aromatic hydrocarbon formation. Stefanidis and colleagues (2011) conducted *in situ* catalytic pyrolysis of beech wood at 500 °C with Al₂O₃ and SiO₂-Al₂O₃ catalysts at a catalyst to feed ratio of 1:2. Al₂O₃ and SiO₂-Al₂O₃ both decreased oxygen content in the organic fraction of the bio-oil from 41.68 wt. % to 24.00 and 30.45 wt. %, respectively (Stefanidis *et al.*, 2011).

2.4.5.3. Basic metal oxides

Basic metal oxides such as MgO and CaO deoxygenate pyrolysis vapours via ketonisation and aldol condensation of carboxylic acid and carbonyl compounds (Liu *et al.*, 2014; Wang, Dai, *et al.*, 2017). MgO decreases the bio-oil yield but improves its quality in terms of heating value, oxygen content and hydrocarbon distribution. CaO decreases selectivity towards phenols and sugars, removes acids and increases selectivity towards ketones. Catalytic pyrolysis with CaO also reacts with CO₂-like compounds

at temperatures above 400 °C to form CaCO₃, which reduces CO₂ emissions during pyrolysis (Carpenter, Westover, Czernik & Jablonski, 2014; Shadangi & Mohanty, 2014a; Veses *et al.*, 2014).

Stefanidis and colleagues (2011) found that catalytic pyrolysis with MgO produced the lowest oxygen content and consequently the lowest organic fraction yield out of all the catalysts tested (such as Al₂O₃, H-ZSM-5, SiO₂-Al₂O₃ and NiO). MgO also produced relatively low amounts of aromatic hydrocarbons and polycyclic aromatic hydrocarbons, and relatively high amounts of phenols and ketones (Stefanidis *et al.*, 2011).

A summary of catalytic pyrolysis results reported in literature is presented in Table 7. In each case (where data was available), the addition of a basic metal oxide catalyst decreased the oxygen content and increased the HHV of the organic fraction. The organic fraction yield generally decreased under catalytic pyrolysis conditions but Veses and colleagues (2014) observed an increase because better separation between the organic and aqueous fractions could be achieved due to an increase from 50 to 60 wt. % in the water content of the aqueous fraction (Veses *et al.*, 2014). Lin and colleagues (2010) reported that a high catalyst to feed ratio (5:1) was required to overcome the relatively low contact efficiency achieved in the fluidised bed reactor operating at a high superficial gas velocity (Lin *et al.*, 2010).

Table 7: Effect of pyrolysis temperature (T) and catalyst to feed ratio (C:F) on organic fraction yield, oxygen content and HHV

Feed	Catalyst	T (°C)	C:F	Yield (wt. %)		Oxygen (wt. %)		HHV (MJ/kg)		Reference
				Crude	Upgraded	Crude	Upgraded	Crude	Upgraded	
Pine	CaO	520	5:1	39.4	34.1	39.0	31.0	-	-	(Lin et al., 2010)
Beech	Al ₂ O ₃	500	1:2	37.4	16.6	41.7	24.0	-	-	(Stefanidis et al., 2011)
	MgO				15.0		21.9	-	-	
Pine	CaO-MgO	450	1:3	27.0	31.0	31.5	25.4	22.4	30.2	(Veses et al., 2014)
	CaO				34.0		24.2	29.6		
Karanja seed	CaO	550	1:8	33.0	31.3	-	-	22.5	23.0	(Shadangi & Mohanty, 2014b)

2.4.5.4. Low cost materials

Low cost materials such as clay minerals (attapulgite, bentonite and sepiolite) and an industrial aluminium oxide residue known as red mud have shown promising results for catalytic pyrolysis. The

advantage of selecting a low cost material such as CaO or MgO for the catalyst is that for *in situ* configurations, the catalyst does not have to be recovered or recycled at the end of the process (Veses *et al.*, 2015). Thus, the cost associated with either separating the essential nutrients (Ca or Mg) from the char or combusting the char to recover the catalyst is avoided; instead the biochar and essential nutrients can be sold as a soil additive (Carpenter *et al.*, 2014).

Natural MgO, derived via thermal decomposition of magnesium carbonate (MgCO_3), is a promising cost effective and more environmentally friendly alternative to acidic synthetic zeolites. Basic oxide catalysts also have a greater tolerance against deactivation induced by alkali metals present in the ash than zeolites (Stefanidis *et al.*, 2016).

2.4.6 Catalytic pyrolysis challenges

Coke is a product of catalysis, while char is a product of pyrolysis. Coke formation occurs when small biomass particles undergo catalytic polymerisation inside catalyst pores, whereas primary and secondary pyrolysis mechanisms contribute to char formation. Coke formation shortens the lifespan of the catalyst through catalyst deactivation, which can negatively impact process economics (Du, Valla & Bollas, 2013). Carlson and colleagues (2009) reported that coke formation, however, can be reduced by applying high heating rates, maintaining high catalyst to feed ratios and selecting optimal catalysts (Carlson, Tompsett, Conner & Huber, 2009). A thorough understanding of the mechanisms at play in the catalytic pyrolysis of biomass to produce upgraded bio-oil still remains a major research challenge (Lappas, Kalogiannis, Iliopoulou, Triantafyllidis & Stefanidis, 2012).

2.5 Bio-oil co-processing in a crude-oil refinery

The highly oxygenated composition, physiochemical properties and instability under storage prevents bio-oil from being directly blended with petroleum fractions in crude-oil refineries. This is problematic for successful co-processing (blending) via hydrotreating but less so for co-processing via fluid catalytic cracking (FCC), which can be accomplished without physically mixing the bio-oil and petroleum fractions (Bezergianni, Dimitriadis, Kikhtyanin & Kubička, 2018). Fluid catalytic cracking is one of the main processes used in crude-oil refineries around the world to convert vacuum gas oil (VGO) or other heavy petroleum fractions into high-value products such as gasoline, liquefied petroleum gas (LPG), diesel-range light cycle oil (LCO) and heavy cycle oil (HCO) (Pinho, de Almeida, Mendes, Casavechia, Talmadge, Kinchin & Chum, 2017). A possible route for co-processing bio-oil in an oil refinery is shown using a block flow diagram in Figure 5. Heavy petroleum fractions such as VGO are typically hydrotreated before conversion in the FCC unit to improve hydrogen-to-carbon ratios (Talmadge, Baldwin, Biddy, McCormick, Beckham, Ferguson, Czernik, Magrini-bair, Foust, Metelski, Hetrick & Nimlos, 2014). However, at a much lower concentration to VGO, crude or upgraded bio-oil can be

directly injected into the FCC unit without prior hydrotreating. The FCC gasoline and LCO products are then hydrotreated to remove sulphur in compliance with fuel specifications (Pinho *et al.*, 2017).

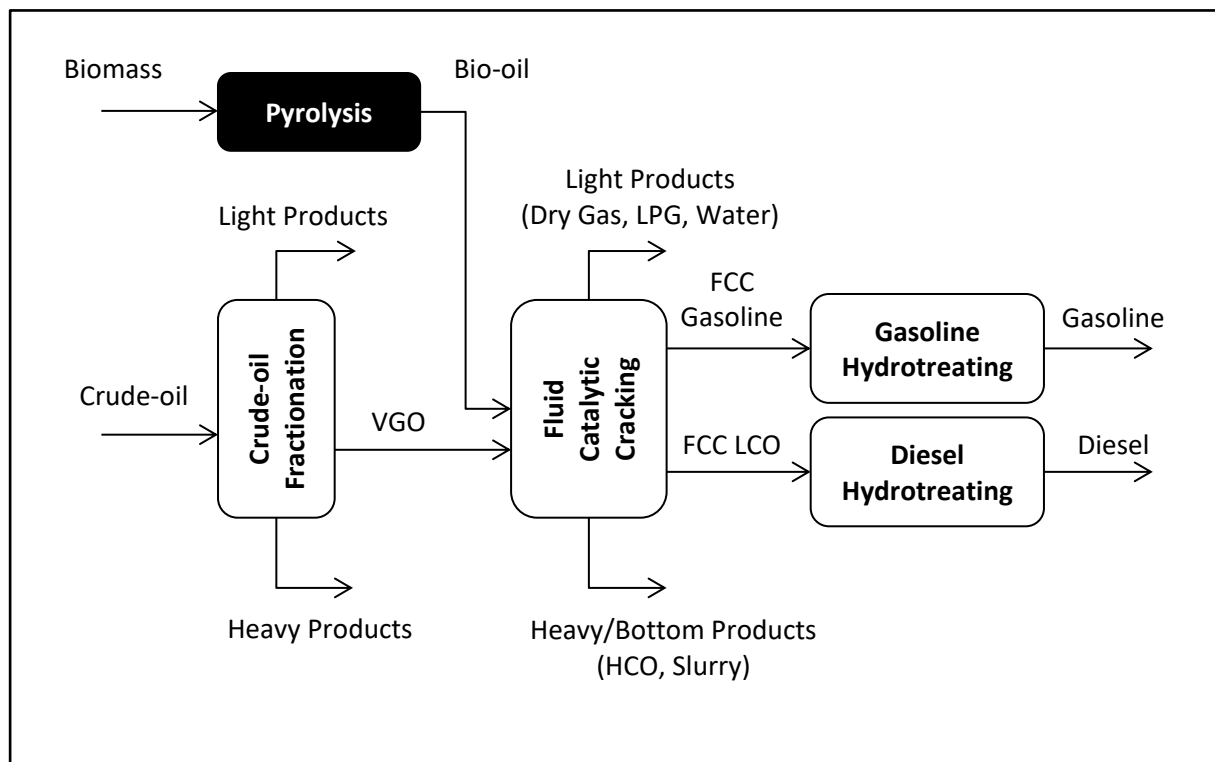


Figure 5: Co-processing bio-oil and VGO in an oil refinery (redrawn from Pinho *et al.* (2017))

A review of studies previously conducted on co-processing bio-oil with VGO is given below. Crude bio-oil refers to bio-oil produced via pyrolysis without further upgrading, and upgraded bio-oil refers to bio-oil produced via catalytic pyrolysis or pyrolysis with further upgrading (for example, hydrotreating). The blending ratio is defined as the mass percent of bio-oil present in the FCC feed.

Pinho and colleagues (2015) co-processed crude bio-oil produced via fast pyrolysis of pine wood chips with commercial VGO in a 150 kg/h FCC demonstration-scale unit. Blends of 10 and 20 wt. % fast pyrolysis oil (FPO) were co-processed with VGO to produce high-value gasoline and diesel range products. An 8.2 wt. % decrease in gasoline yield was observed when 20 wt. % FPO was co-processed due to the dilution effect caused by the large amount of water present in the FPO. There was also a significant 19.6 wt. % increase in coke yield with 20 wt. % FPO but an insignificant increase with 10 wt. % FPO. The first of its kind co-processing FCC demonstration-scale unit overcame the challenges experienced with blending FPO and VGO at lab-scale. Co-processing 20 wt. % FPO was achieved with separate feed injection points into the FCC reactor. The authors concluded that up to 20 wt. % FPO could be directly co-processed with VGO in an FCC unit without prior upgrading (Pinho, De Almeida, Mendes, Ximenes & Casavechia, 2015).

The same research group then co-processed blends of 5 and 10 wt. % FPO with VGO in a 200 kg/h FCC demonstration-scale unit. The researchers suggested that even though co-processing 20 wt. % crude bio-oil is technically feasible, co-processing 5 wt. % bio-oil is a reasonable starting point for the current commercial supply of bio-oil relative to VGO. Approximately 84 and 89 wt. % of the 50.7 wt. % oxygen present in the crude bio-oil was converted into CO, H₂O and some CO₂ when VGO was co-processed with 5 and 10 wt. % FPO, respectively. Furthermore, the successful demonstration of co-processing crude bio-oil suggests that it would also be feasible to co-process upgraded bio-oil (Pinho *et al.*, 2017).

Lindfors and colleagues (2015) investigated the effect of upgrading crude bio-oil prior to co-processing on coke and liquid product yields. Co-processing was conducted with dry thermal bio-oil (6.6 wt. % moisture), catalytic pyrolysis oil (CPO) and hydrotreated pyrolysis oil (HPO) in a 20 kg/h pilot-scale micro activity test (MAT) reactor. Co-processing 20 wt. % bio-component resulted in higher liquid yields for the upgraded bio-oils compared to crude bio-oil, however, liquid yields were lower than catalytic cracking of pure VGO overall. Co-processing 20 wt. % bio-component also produced more coke than catalytic cracking of pure VGO overall (Lindfors, Paasikallio, Kuoppala, Reinikainen, Oasmaa & Solantausta, 2015).

Thegarid and colleagues (2014) are of the view that crude bio-oil cannot be co-processed without upgrading the bio-oil first, either by HDO or catalytic pyrolysis. The researchers compared co-processing 10 wt. % CPO with VGO to co-processing 10 wt. % HDO-oil with VGO, and found that both blends produced similar liquid products in terms of distribution and quality therefore, bio-oil can be upgraded in a single step with a suitable catalyst instead of the additional and costly hydrogenation step after pyrolysis (Thegarid, Fogassy, Schuurman, Mirodatos, Stefanidis, Iliopoulou, Kalogiannis & Lappas, 2014).

Ibarra, Veloso and colleagues (2016) studied two coke deposition pathways by co-processing 20 wt. % FPO and VGO in a riser simulator reactor (RSR). Cracking FPO tends to form soluble and insoluble coke with high concentrations of hydrogen and oxygen, whereas cracking VGO results in the formation of coke with high concentrations of aromatics. The authors found that when these coke formation pathways interact (i.e. in co-processing), the result was a decrease in coke formation. The high water content from the FPO formed steam and inhibited the VGO coke deposition pathway, while the hydrocarbons from the VGO act as hydrogen donors for the FPO oxygenates and inhibited the FPO coke deactivation pathway (Ibarra, Veloso, Bilbao, Arandes & Castaño, 2016).

Wang, Venderbosch and Fang (2018) investigated the co-processing of 10 wt. % crude (Crude-PL), mildly hydrotreated (SPO-1) and severely hydrotreated (SPO-2) bio-oils with VGO in a pilot-scale FCC unit operated at four different catalyst to oil (C/O) ratios (5.1, 6.3, 7.2 and 8.7). The conversion of co-processed crude and upgraded bio-oils with VGO and pure VGO increased as the C/O ratio increased. The results for dry gas, gasoline, coke, and CO and CO₂ yields for increasing conversion are

given in Figure 6. For all co-processing tests, the dry gas yield decreased by approximately half compared to pure VGO catalytic cracking as a result of a decrease in hydrogen donors from the VGO needed for hydrogen transfer reactions to take place. Co-processing of upgraded bio-oils produced comparable or slightly higher gasoline yields than pure VGO catalytic cracking, while co-processing crude bio-oil produced significantly lower gasoline yields due to lower carbon and higher oxygen contents. Co-processing of upgraded bio-oils could effectively transform more carbon into gasoline than pure VGO catalytic cracking by suppressing over-cracking reactions and lowering LPG yields. In addition, significant amounts of CO and CO₂ were produced via decarbonylation and decarboxylation reactions in co-processing tests due to the presence of oxygenated compounds in the bio-oils (Wang, Venderbosch & Fang, 2018). Co-processing crude and (less so) upgraded bio-oils in existing FCC units at oil refineries may require modifications to account for pressure build-up and increased capacity (van Dyk, Su, McMillan & Saddler, 2019). Bio-oils with high water contents may also damage FCC catalysts and effect downstream processes (Talmadge *et al.*, 2014).

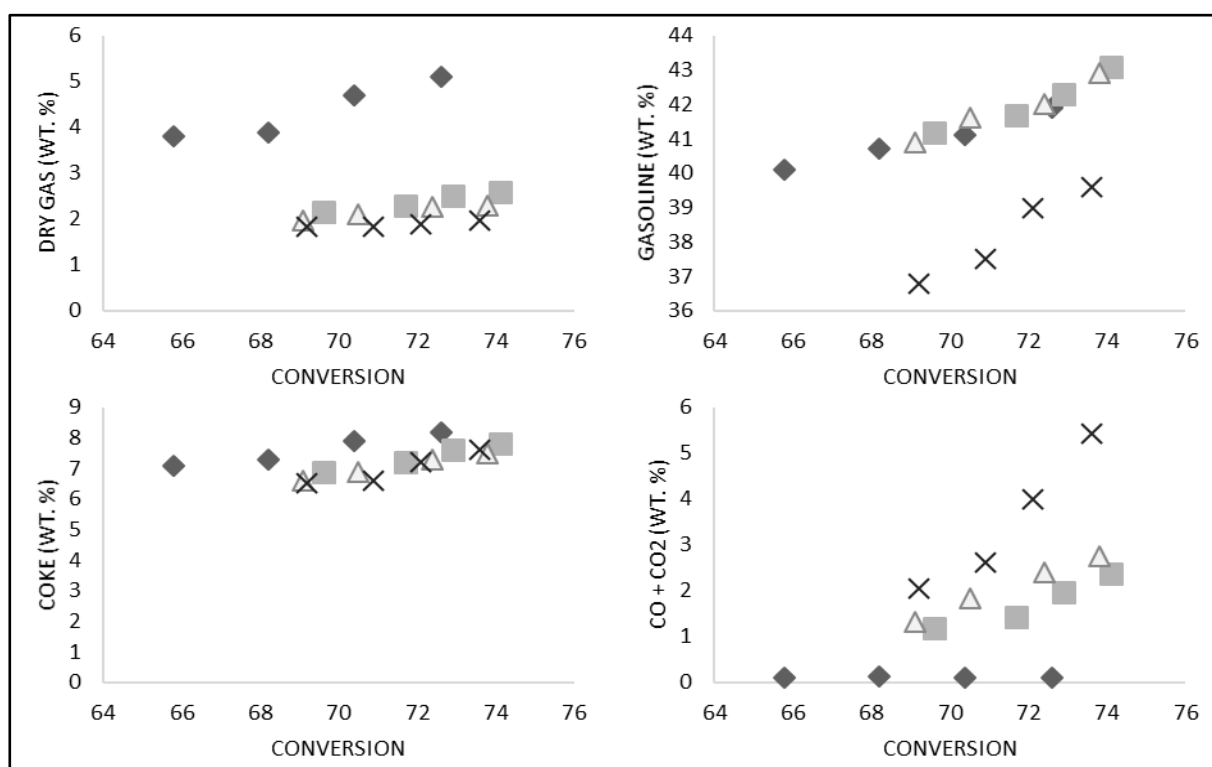


Figure 6: Dry gas, gasoline, coke, and CO and CO₂ yields for increasing conversion of pure VGO catalytic cracking and co-processing crude and upgraded bio-oils (redrawn from Wang *et al.* (2018))
 – ◆ VGO, ■ SPO-2, △ SPO-1 and X Crude-PL

Previous studies on co-processing crude and upgraded bio-oils with VGO are presented in Table 8. Co-processing 20 wt. % crude and upgraded bio-oils generally increased coke yield. The interaction of the coke deposition pathways as described by Ibarra, Veloso and colleagues (2016) due

to co-processing crude bio-oil with a high water content was the only exception (Ibarra *et al.*, 2016). Co-processing 10 wt. % crude and upgraded bio-oils resulted in a negligible change in coke yield at pilot and demonstration-scale, however, co-processing 10 wt. % upgraded bio-oil produced more coke at lab-scale (de Miguel Mercader, Groeneveld, Kersten, Way, Schaverien & Hogendoorn, 2010). Pinho and colleagues (2015) pointed out that co-processing on a larger scale can improve feed dispersion and catalyst contact that is problematic at lab-scale (Pinho *et al.*, 2015). Co-processing 10 wt. % upgraded bio-oil had negligible effect on total liquid yield (gasoline, LPG, LCO and bottoms), however, co-processing the same amount of crude bio-oil decreased total liquid yield. Co-processing 10 wt. % upgraded bio-oil containing up to 28.8 wt. % water at pilot-scale also had negligible effect on coke and total liquid yield (Wang, Li & Fang, 2016). Furthermore, co-processing 5 wt. % crude bio-oil decreased coke yield and had negligible effect on total liquid yield. Therefore, a maximum of 5 wt. % crude bio-oil and a maximum of 10 wt. % upgraded bio-oil will be considered for co-processing in this project.

Table 8: Co-processing crude and upgraded bio-oils with VGO in FCC units

Blend (wt. %)	Oxygen (wt. %, db)			Water (wt. %)	HHV (MJ/kg)	Coke	Total Liquid	Scale	Reference
	Crude	CPO	HDO-oil						
5	50.7	-	-	31.9	-	↓	N/A	Demo	(Pinho <i>et al.</i> , 2017)
10						N/A	↓		
10	51.15	-	-	25.5	21.46	N/A	↓	Demo	(Pinho <i>et al.</i> , 2015)
20						↑	↓		
20	37.8	-	-	46.5	-	↓	↓	Lab	(Ibarra <i>et al.</i> , 2016)
10	-	19.5	-	28.8	-	N/A	N/A	Pilot	(Wang <i>et al.</i> , 2016)
10	-	27	-	11	-	↑	N/A	Lab	(Thegarid <i>et al.</i> , 2014)
		-	21	3	-	↑	N/A		
20	36.5	-	-	6.7	22.1	↑	↓	Pilot	(Lindfors <i>et al.</i> , 2015)
	-	22	-	8.3	27.7	↑	↓		
20	-	-	28	15.9	25.2	↑	N/A	Lab	(de Miguel Mercader <i>et al.</i> , 2010)
10	50.97	-	-	24.5	-	N/A	↓	Pilot	(Wang <i>et al.</i> , 2018)
	-	-	39.25	12.5	-	N/A	N/A		
	-	-	27.43	12.7	-	N/A	N/A		

The feasibility of co-processing crude and upgraded bio-oils with VGO in an FCC unit is not only evaluated by reaction conditions and product yields but also by the amount of renewable carbon that is present in the total liquid product (Bezergianni *et al.*, 2018). Wang, Venderbosch and Fang (2018) reported that co-processing upgraded bio-oils with VGO produced more than double the amount of renewable carbon in the total liquid product than co-processing crude bio-oil (Wang *et al.*, 2018). Pinho and colleagues (2015) reported 2 and 5 wt. % renewable carbon in the total liquid produced via co-processing 10 and 20 wt. % crude bio-oil with VGO, respectively. The carbon content in bio-oil was reduced from 42.35 wt. % to approximately 30 wt. % in the FCC unit primarily because of decarbonylation reactions taking place (Pinho *et al.*, 2015). The same research group later co-processed 5 wt. % crude bio-oil with VGO and reported 1 wt. % renewable carbon in the total liquid product (Pinho *et al.*, 2017). Two more studies that both co-processed 10 wt. % upgraded bio-oil with VGO reported 7 wt. % (Wang *et al.*, 2016) and 7.5 wt. % (Fogassy, Thegarid, Schuurman & Mirodatos, 2012) renewable carbon in the total liquid product. A summary of the renewable carbon content in the total liquid produced via co-processing crude and upgraded bio-oils with VGO is given in Table 9.

Table 9: Renewable carbon content of total liquid produced from co-processing crude and upgraded bio-oils with VGO

Blend (wt. %)	Renewable Carbon (wt. %)		Reference
	Crude	Upgraded	
10	2.3	5.6 (SPO-1) 6.4 (SPO-2)	(Wang <i>et al.</i> , 2018)
5	1.0	-	(Pinho <i>et al.</i> , 2017)
10	2.0	-	(Pinho <i>et al.</i> , 2015)
20	5.0	-	
10	-	7.0	(Wang <i>et al.</i> , 2016)
10	-	7.5	(Fogassy <i>et al.</i> , 2012)

2.6 Techno-economic analysis

A techno-economic analysis (TEA) is used to evaluate the technical and economic performances of a new and innovative product design or to make existing product designs more competitive (Brown & Brown, 2013; Do & Lim, 2016). Ringer and colleagues (2006) conducted a TEA on the production of crude bio-oil via fast pyrolysis of wood chips at a production rate of 550 dry MT/day. The internal rate of return (IRR) for the process and minimum selling price (MSP) of the bio-oil was 10 % and \$7.62/GJ on a lower heating value (LHV) basis (\$0.16/L for an assumed 17 MJ/kg LHV and 1200 kg/m³ density), respectively. The Total Capital Investment (TCI) for the process was \$48.3 million (Ringer, Putsche & Scahill, 2006).

Wang and Jan (2018) conducted a TEA on the production of crude bio-oil via fast pyrolysis of rice husks at a biomass throughput (9 wt. % moisture) of 1000 dry MT/day. The biochar co-product yield and carbon content were 27 and 20.4 wt. %, respectively, and the biochar selling price was \$100/MT. The MSP of bio-oil for a 10 % IRR was \$0.55/L, and the TCI for the process was \$42.3 million. The biochar contained almost 50 wt. % silica sand, which hindered its value as a fertilizer therefore, biochar (as a credit) only represented \$0.02/L of bio-oil (Wang & Jan, 2018).

There are several techno-economic analyses available in literature on upgraded bio-oils produced via fast pyrolysis or catalytic pyrolysis with zeolite catalysts, followed by hydrotreating (Anex, Aden, Kazi, Fortman, Swanson, Wright, Satrio, Brown, Daugaard, Platon, Kothandaraman, Hsu & Dutta, 2010; Dutta, Sahir, Tan, Humbird, Snowden-swan, Meyer, Ross, Sexton, Yap & Lukas, 2015; Jones, Meyer, Snowden-Swan, Asanga, Eric, Abhijit, Jacob & Cafferty, 2013; Li *et al.*, 2015; Thilakaratne, Brown, Li, Hu & Brown, 2014; Wright, Satrio, Brown, Daugaard & Hsu, 2010). Hydrogen is either produced onsite (usually biogenic) or purchased from an external source (usually anthropogenic). The latter is often cheaper but has a negative impact on the environment (Patel, Zhang & Kumar, 2016). A summary of MSP and TCI for these studies is given in Table 10.

The MSP and TCI for the studies reported in Table 10 range from \$0.53/L to \$1.65/L and \$200 million to \$700 million, respectively. Feedstock cost is effected by feedstock production, collection, pre-treatment (e.g. chipping) and transportation distance (Roy & Dias, 2017). The feedstock cost has a substantial impact (21.3 %) on MSP as reported by Carrasco and colleagues (2017). Onsite hydrogen production versus offsite procurement also has a significant impact on MSP. Hydrogen purchased from an external source gave the lowest MSP of \$0.53/L, while hydrogen produced onsite from purchased natural gas gave a high MSP of \$1.11/L. Wright and colleagues (2010) showed that hydrogen production onsite from a portion of the bio-oil gave a higher MSP of \$0.82/L than hydrogen purchased from an external source as the bio-oil yield in the former case decreased by ~40 vol. % (Wright *et al.*, 2010). The TCI estimate of \$700 million by Jones and colleagues (2013) is considerably higher than the other estimates as the authors estimated a total capital cost of \$174 million for the pyrolysis reactor (Jones *et al.*, 2013), whereas Dutta and colleagues (2015) assumed a substantially lower total capital cost of \$92.5 million (Dutta *et al.*, 2015).

Table 10: MSP and TCI of upgraded bio-oil production via pyrolysis followed by hydrotreating (2000 dry MT/day capacity, 10% IRR, FR: forest residue, CS: corn stover, NG: natural gas)

Feedstock	Feedstock		Hydrogen	MSP (\$/L)	TCI (\$m)	Cost Year	Reference
	Cost (\$/MT)	Pyrolysis					
CS	75	Fast	Onsite	0.79	280	2010	(Anex <i>et al.</i> , 2010)
			Offsite	0.53	200		
CS	83	Fast	Onsite	0.82	287	2010	(Wright <i>et al.</i> , 2010)
			Offsite	0.56	200		
Pine	80	<i>In situ</i>	Onsite (NG)	1.11	-	2011	(Li <i>et al.</i> , 2015)
		<i>Ex situ</i>	-	1.13	-		
Poplar	97	<i>In situ</i>	Onsite	0.98	457	2011	(Thilakarathne <i>et al.</i> , 2014)
Woody	80	<i>In situ</i>	Onsite (NG)	0.91	546	2011	(Dutta <i>et al.</i> , 2015)
		<i>Ex situ</i>		0.88	590		
Woody (incl. FR)	80	Fast	Onsite (NG)	0.90	700	2011	(Jones <i>et al.</i> , 2013)
FR	69	Fast	Onsite	1.65*	427	2015	(Carrasco <i>et al.</i> , 2017)

*15.3 % IRR

Techno-economic analyses on upgraded bio-oil production via catalytic pyrolysis with basic metal oxide catalysts such as CaO and MgO, on the other hand, are scarce in literature. Moreover, to the best of the author's knowledge, there is currently no literature available in this regard that evaluates forest residues as a feedstock.

2.7 Environmental impact

Bio-oil production via pyrolysis produces air emissions, wastewater and solid waste during operations such as biomass harvesting, biomass transportation and bio-oil combustion. Therefore, it is important to consider the environmental impact of the process. The Life Cycle Assessment (LCA) is a comprehensive method that assesses environmental impact at each step of a product life cycle, from raw materials to product disposal or end use. This is termed the "cradle-to-grave" approach. In some cases, however, the end use of the product is excluded from the LCA, and termed the "cradle-to-gate" approach (Sharifzadeh, Sadeqzadeh, Guo, Borhani, Murthy, Cortada, Wang, Hallett & Shah, 2019).

An environmental advantage of bio-oil production from sustainable forest products such as forest residue is the positive impact in mitigating long-term climate change. Trees take up CO₂ from the atmosphere and store carbon in wood. The harvested wood then releases the carbon back into the atmosphere as CO₂ during decomposition or combustion, completing the cycle. Therefore, with the

exception of CO₂ emissions related to forestry operations, forest residues are considered a carbon neutral source of energy. Fossil fuel, on the other hand, is not a carbon neutral source of energy as CO₂ is released into the atmosphere during combustion but not taken up during formation (Mohan *et al.*, 2006; Steele, Puettmann, Penmetsa & Cooper, 2012). Furthermore, biochar production from forest residues has the potential to make a near carbon neutral process carbon negative through carbon sequestration (Lee *et al.*, 2013).

One of the ways that the LCA quantifies environmental impact is through the Global Warming Potential (GWP) metric. The GWP metric relates the amount of heat a greenhouse gas (GHG) traps in the atmosphere to an equivalent amount of heat CO₂ traps in the atmosphere, over a fixed period of time, commonly 20, 100 or 500 years. For example, the GWP of methane over 20 years is 56, which means that methane will trap 56 times more heat than an equivalent amount of CO₂ over 20 years (Steele *et al.*, 2012).

Steele and colleagues (2012) compared the environmental impact of producing crude bio-oil via fast pyrolysis of southern pine forest residue to residual fuel oil (RFO), a by-product of transportation fuel production in an oil refinery, using the “cradle-to-grave” approach. The GWP for bio-oil and RFO was 0.032 kg CO₂/MJ and 0.107 kg CO₂/MJ, respectively, therefore substituting bio-oil for RFO resulted in a 69.8 % reduction in GWP (Steele *et al.*, 2012).

Iribarren, Peters and Dufour (2012) conducted an LCA on upgraded bio-oil gasoline and diesel fractions produced via fast pyrolysis of Poplar followed by hydrotreating using the “cradle-to-gate” approach. The GWP was -0.053 and -0.048 kg CO₂eq/MJ for gasoline and diesel, respectively (Iribarren, Peters & Dufour, 2012). The GWP reported for gasoline and diesel is negative because the end use (combustion) of the products was excluded.

Han and colleagues (2013) conducted an LCA using the “cradle-to-grave” approach to investigate the GWP of upgraded bio-oils produced via three pathways involving fast pyrolysis followed by hydrotreating: 1) hydrogen was produced via onsite natural gas reforming, 2) hydrogen was produced via onsite bio-oil reforming and electricity was produced via biochar combustion, and 3) hydrogen was produced via onsite bio-oil reforming and biochar was applied to the soil. The feedstock for the first pathway was forest residues, and the feedstock for the second and third pathways was corn stover. The GWPs for pathways 1, 2 and 3 were 0.037, 0.011 and -0.012 kg CO₂eq/MJ, respectively (Han *et al.*, 2013). The environmental benefit was significant when biochar was applied to the soil instead of combusted for electricity production, even though biochar was produced as a by-product with unsurprisingly low yield (14.7 wt. %) and carbon content (51.0 wt. %) under fast pyrolysis conditions. In a recent state-of-the-art review, Sharifzadeh and colleagues (2019) pointed out the gap in research on the environmental benefit of biochar as a co-product of pyrolysis (Sharifzadeh *et al.*, 2019).

2.8 Conclusion

Forest residues are a high fire risk and are often disposed of by burning or sold as firewood, both of which eventually contribute to air pollution. There are approximately 1.5 million dry metric tonnes of forest residues available in South Africa every year therefore, there is an opportunity for the paper and pulp industry to utilise these forest residues in a more environmentally friendly and profitable way. Moreover, CO₂ emissions associated with forestry operations can be reduced by replacing fossil fuels with bio-derived fuels.

Fast pyrolysis is associated with high bio-oil yields, whereas intermediate pyrolysis produces both bio-oil and biochar as primary products. Biochar has a wide range of applications, from carbon sequestration to wastewater treatment hence, biochar has the potential to contribute significantly to improving the profitability and reducing the environmental impact of the pyrolysis process.

Bio-oil can be upgraded to improve its oxygen and water content, and physiochemical properties that make it unlike conventional hydrocarbon fuel. Basic metal oxide catalysts such as CaO and MgO are both suitable for upgrading bio-oil via catalytic pyrolysis. There are several techno-economic analyses available in literature on upgraded bio-oil production via fast pyrolysis or catalytic pyrolysis with zeolite catalysts followed by hydrotreating. On the other hand, techno-economic analyses on upgraded bio-oil production via catalytic pyrolysis with basic metal oxide catalysts such as CaO and MgO catalysts are scarce.

Co-processing a maximum of 5 wt. % crude bio-oil and 10 wt. % upgraded bio-oil at an oil refinery will be the benchmark for techno-economic analysis development of non-catalytic and catalyst pyrolysis biorefineries, respectively.

Bio-oil production from forest residues has a positive environmental impact since forest residues are considered a close to carbon neutral source of energy. Furthermore, biochar production from forest residues has the potential to make a near carbon neutral process carbon negative through carbon sequestration, however, there is a gap in research on the environmental benefit of biochar as a co-product of pyrolysis.

CHAPTER 3

3 Project Scope

3.1 Objectives

The overall aim of this project is to determine whether or not the production of crude and upgraded bio-oils via non-catalytic and catalytic pyrolysis of forest residues for co-processing in an oil refinery is economically and environmentally feasible. This will be achieved through the following objectives:

1. Develop process simulations in Aspen Plus™ for non-catalytic and catalytic pyrolysis biorefinery scenarios based on pilot plant data.
2. Develop economic analyses for non-catalytic and catalytic pyrolysis biorefinery scenarios based on process simulations.
3. Measure and compare the environmental impact of producing crude and upgraded bio-oils to crude-oil and diesel using SimaPro™.

3.2 Research questions

The following research questions need to be answered to accomplish these objectives:

1. What is the energy demand for non-catalytic and catalytic pyrolysis processes, and how is it achieved?
2. Which pyrolysis process produces the lowest MSP of bio-oil?
3. How does the MSP of crude and upgraded bio-oils compare in terms of energy value?
4. How does the biorefinery capacity effect the MSP of crude and upgraded bio-oils?
5. Which economic parameters will be most sensitive to the MSP of crude and upgraded bio-oils?
6. Which pyrolysis process has the lowest environmental impact?
7. What is the estimated reduction in GWP of the FCC feed when crude or upgraded bio-oil is co-processed with VGO instead of pure VGO catalytic cracking?

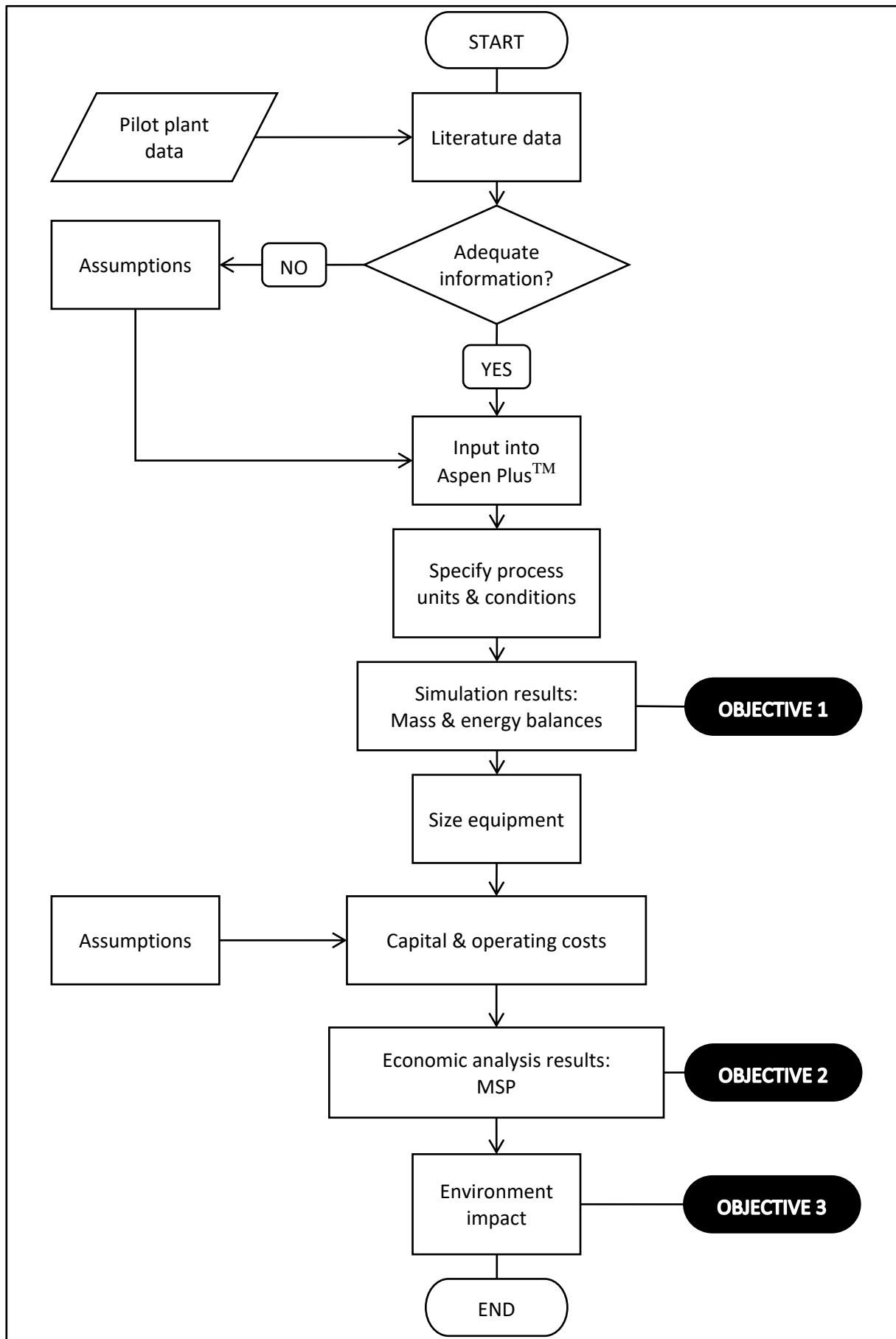
3.3 Limitations

1. This project is based on the results of non-catalytic and catalytic pyrolysis pilot plant experiments conducted by Farai Chireshe (Chireshe, 2019), but some assumptions were made from literature, where experimental data was not available.
2. Process simulation for bio-oil co-processing in an FCC unit was not considered in this project.
3. Environmental impact for bio-oil co-processing in an FCC unit was also not considered in this project. However, the environmental burden of crude-oil and diesel production was taken from the SimaPro™ inventory for comparison.

CHAPTER 4

4 Methodology

The overall research approach for this project is shown graphically in Figure 7. Non-catalytic and catalytic pyrolysis processes were simulated in Aspen Plus™ using literature and available pilot plant data, and sound technical assumptions to specify process units. The process simulations provided the mass and energy balances needed to size process equipment in preparation for the economic analyses. Profitability was measured by MSP, and the sensitivity thereof was evaluated against economic variables and model assumptions such as biomass cost and working capital. Finally, the environmental impact of crude and upgraded bio-oil production was measured in SimaPro™ and compared to fossil fuel production.

**Figure 7: Research approach**

4.1 Estimation of forest residues available in South Africa

The amount of forest residues available in South Africa was estimated based on a method developed by Dovey (2009), where plantation timber volumes are converted into stem, bark and branch dry masses by experimentally determined multipliers (Dovey, 2009). The timber products sold from plantations around South Africa in 2016 was recently reported by the Forestry Economics Services, a division of the Department of Agriculture, Forestry and Fisheries (Forestry Economics Services, 2017). The total products sold from plantations according to species are provided in Table 11. The timber products published in units of mass were converted to units of volume using the multipliers in Table 12. The multipliers reported by Dovey (2009) and given in Table 13 were then used to convert timber volumes into the stem, bark and branch dry masses that are reported in Table 14. The following assumptions were made: 1) all 'softwoods' were taken as *P. patula*, 2) 'wattle' and 'other hardwoods' were taken as *A. mearnsii*, and 3) 'other gum' was taken as an average of *E. dunnii*, *E. macarthurii*, *E. nitens* and *E. smithii*. Finally, the total amount of forest residues (considering branches only) available in South Africa in 2016 was estimated to be just over 1.5 million dry metric tonnes.

Table 11: Timber products sold from plantations in 2016 (Forestry Economics Services, 2017)

	Sawlogs & Veneer Logs (m ³)	Poles & Droppers (m ³)	Mining Timber (MT)	Pulpwood (MT)	Charcoal & Firewood (MT)	Other Products (MT)
Total softwoods	4 227 050	55 877	0	2 292 485	27 359	33 889
Total <i>E. grandis</i>	176 632	216 867	268 061	3 024 702	66 044	22 025
Total other gum	43 661	28 664	31 127	2 711 823	12 560	6 851
Total wattle	0	312	0	607 220	91 191	22 077
Total other hardwoods	0	25 800	0	23 922	231	2 462

Table 12: Multipliers to convert between volume and mass (Forestry Economics Services, 2017)

Product	Species	Conversion (m ³ /MT)
Sawlogs	Softwood	0.94
	<i>Eucalyptus grandis</i>	0.94
	Other eucalyptus species	0.78
Mining timber	<i>Eucalyptus grandis</i>	1.47
	Other eucalyptus species	1.25
	Wattle	1.19
Pulpwood	Softwood	1.00
	<i>Eucalyptus grandis</i>	1.47
	Other eucalyptus species	1.25
	Wattle	1.19
	Other hardwood species	1.25
Matchwood	-	1.03
Firewood	-	1.25
Poles, laths, droppers etc.	-	1.56
Transmission poles	-	1.25
Cross arms	-	1.25

Table 13: Multipliers to convert timber volume to dry mass, timber dry mass to bark and timber dry mass to branches (Dovey, 2009)

Species	Timber Dry Mass (MT/m ³)	Bark (MT/ha)	Branches (MT/ha)
<i>A. mearnsii</i>	0.654	0.130	0.260
<i>P. patula</i>	0.387	0.090	0.260
<i>E. dunnii</i>	0.536	0.160	0.120
<i>E. grandis</i>	0.450	0.120	0.120
<i>E. macarthurii</i>	0.551	0.150	0.210
<i>E. nitens</i>	0.526	0.120	0.340
<i>E. smithii</i>	0.581	0.100	0.210

Table 14: Total forest residue available in South Africa

	Total (m³)	Stem (dry MT)	Bark (dry MT)	Branches (dry MT)
Total softwoods	6 651 972	2 574 313	231 688	669 321
Total <i>E. grandis</i>	5 343 947	2 404 776	288 573	288 573
Total other gum	3 525 276	1 933 614	256 204	425 395
Total wattle	864 489	565 376	73 499	146 998
Total other hardwoods	59 069	38 631	5 022	10 044

Collection and transport costs of forest residues are high because forest residues are often spread over extensive areas and transported over long distances to biorefineries (Brown, Rowe & Wild, 2013). Polagye, Hodgson and Malte (2007) compared the cost of biofuel production via fast pyrolysis of forest thinnings at mobile and centralised (stationary) facilities to biomass transport distance. The authors found that industrial-scale and long-term biofuel production at a mobile facility was significantly more expensive than at a centralised facility. Biofuel production at a centralised facility was also increasingly more attractive for transport distances below 300 km (Polagye, Hodgson & Malte, 2007). Similarly, Brown, Rowe and Wild (2016) reported that biomass transport to a centralised facility was more cost effective than to a mobile facility when transport distance was below 300 km (Brown *et al.*, 2013).

The distribution of forest residues (considering branches only) available in South Africa in 2016 according to region is given in Table 15. The regions with the most forest residues were KwaZulu-Natal (KZN) Midlands (19.6 wt. %), Mpumalanga South (18.4 wt. %) and KZN South (13.5 wt. %). The location of the centralised biorefinery is approximately 40 km west of Dundee (KZN Midlands), which was determined by drawing a circle with a 300 km radius around the regions with the most forest residues as shown in Figure 8. The total amount of forest residues available for collection and transportation from Mpumalanga South, KZN North, KZN Midlands, Zululand and KZN South to the biorefinery was then 1 067 210 dry metric tonnes. However, not all forest residues should be removed from the forest floor. Forest litter (leaves and small twigs), stumps, root systems and a portion of branches should be retained to maintain soil productivity by preserving nutrients, preventing soil erosion and protecting against compaction (Wright *et al.*, 2012; Yang *et al.*, 2016) therefore, only 853 768 dry metric tonnes (equivalent to 80 wt. %) of forest residues were available for collection.

Table 15: Distribution of forest residues (branches) available in South Africa according to region

Region	Branches (wt. %)
Limpopo	3.58
Mpumalanga North	10.59
Central Districts	3.36
Mpumalanga South	18.39
Maputaland	0.00
Zululand	11.18
KZN Midlands	19.55
KZN North	6.65
KZN South	13.51
Eastern Cape	7.98
Southern Cape	4.17
Western Cape	1.04

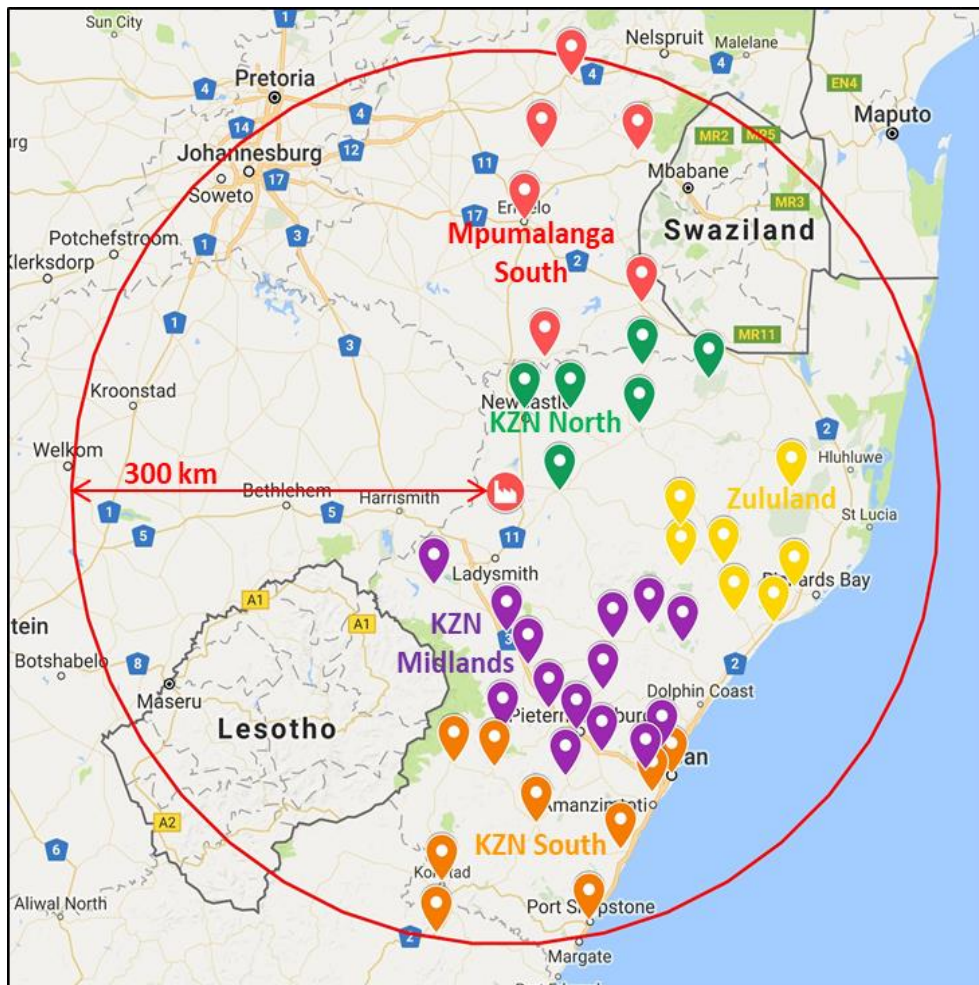


Figure 8: Location of the forest residue pyrolysis plant (biorefinery) - ● Mpumalanga South ● KZN North ● Zululand ● KZN Midlands ● KZN South


4.2 Biorefinery scenarios

South Africa has four crude-oil refineries, one coal-to-liquid refinery and one gas-to-liquid refinery. The location of the refinery, distance from the biorefinery, capacity (barrels per day or bpd) and production of VGO are summarised in Table 16.

Table 16: Locations and Capacities of refineries in South Africa

Refinery	Location	Distance (km) ^b	Type	Capacity (bpd) ^a	VGO (m ³ /day) ^c
Chevref	Cape Town	1 247	Crude-oil	100 000	3 609
Enref	Durban	224	Crude-oil	120 000	4 331
Natref	Sasolburg	249	Crude-oil	108 000	3 898
Sapref	Durban	228	Crude-oil	180 000	6 496
Sasol	Secunda	196	CTL	150 000	5 413
PetroSA	Mossel Bay	999	GTL	45 000	1 624

- (South African Petroleum Industry Association, 2017)
- Straight-line distance measured from the refinery to the biorefinery
- The conversion of crude-oil to VGO was taken as 22.7 vol. % (Hill, 2011). The density of VGO was taken as 947.2 kg/m³ (Pinho *et al.*, 2015)

The total amount of forest residues available for bio-oil production within a 300 km radius of the biorefinery was assumed to stay constant at 853 768 dry MT/year. Since biomass cost is proportional to biomass collection distance, the economic feasibility of crude and upgraded bio-oil production was evaluated for biomass collection within 100, 200 and 300 km radii of the pyrolysis biorefinery as shown in Figure 9. The corresponding biorefinery capacities for biomass collection within 100, 200 and 300 km radii were 338, 1655 and 2549 dry MT/day, respectively. Considering the findings from literature, co-processing of up to 5 wt. % crude bio-oil and 10 wt. % upgraded bio-oil with VGO was investigated. *Natref* is a suitable refinery for co-processing because of its size and distance from the biorefinery, however, where the biorefinery capacity exceeds the maximum amount of bio-oil that can be co-processed at *Natref*, the remaining bio-oil can be sent to *Enref* or *Sapref*. The corresponding biorefinery capacities for co-processing 5 wt. % crude bio-oil and 10 wt. % upgraded bio-oil were 813 and 1710 dry MT/day, respectively. A summary of the biorefinery scenarios that were considered for non-catalytic (NC-100, NC-5, NC-200 and NC-300) and catalytic (C-100, C-200, C-10 and C-300) pyrolysis is presented in Table 17. The average distance reported was calculated based on a weighted average: the amount of biomass available in each zone (indicated by the  location markers in Figure 9) within the considered radius multiplied by the straight-line distance between each zone and the biorefinery,

divided by the total amount of biomass available within the considered radius. The amount of biomass available in each region was determined from the biomass distribution given in Table 15 and evenly distributed between the zones in each region (actual data for each zone is not publically available).

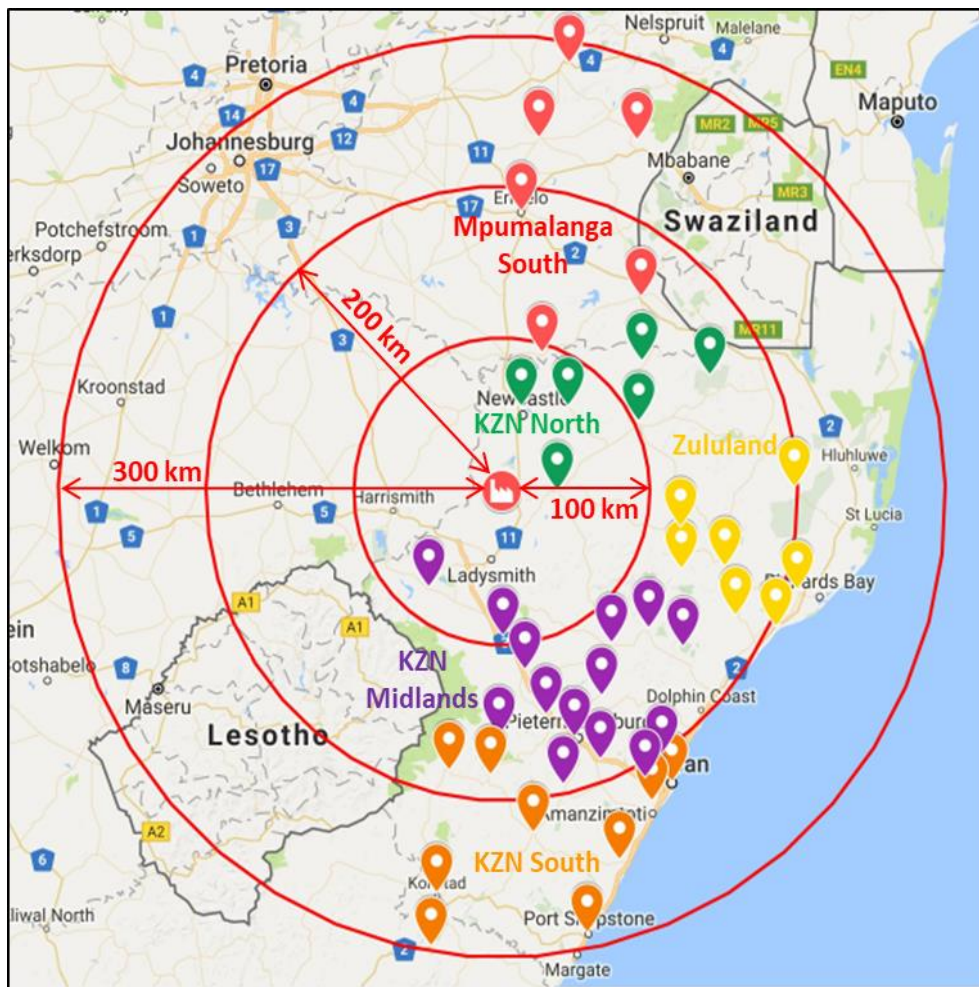


Figure 9: 100, 200 and 300 km radii from biorefinery for biomass collection - 📍 Mpumalanga South
📍 KZN North 📍 Zululand 📍 KZN Midlands 📍 KZN South

Table 17: Biorefinery scenarios for co-processing bio-oil produced via non-catalytic (NC) and catalytic (C) pyrolysis

Scenario	Radius (km)	Average Distance (km)	Biorefinery Capacity (dry MT/day) ^a	Blend	Blend	Blend
				(wt. % bio-oil) <i>Natref</i>	(wt. % bio-oil) <i>Enref</i>	(wt. % bio-oil) <i>Sapref</i>
NC-100	100	80	338	2.08	-	-
NC-5	157	113	813	5.00	-	-
NC-200	200	143	1 655	5.00	4.66	-
NC-300	300	179	2 549	5.00	5.00	3.07
C-100	100	80	338	1.98	-	-
C-200	200	143	1655	9.68	-	-
C-10	224	153	1710	10.00	-	-
C-300	300	179	2 549	10.00	4.42	-

- a. Bio-oil yield was 22.86 wt. % and 21.65 wt. % for non-catalytic and catalytic pyrolysis, respectively. Biomass moisture content was 8.28 wt. %. Biorefinery operates for 335 days per year.

4.3 Process description

An overview of the non-catalytic and catalytic pyrolysis experiments is given here. However, the detailed experimental methodology followed to generate non-catalytic and catalytic pyrolysis data for this project can be found in the corresponding thesis by Farai Chireshe (Chireshe, 2019). Non-catalytic and catalytic pyrolysis experiments were conducted with a 5 kg/h pilot plant reactor. A diagram of the pilot plant setup is given in Figure 10. A dry-mixed mixture of *E. grandis* forest residues (8.28 wt. % moisture) and CaO catalyst (in catalytic pyrolysis runs) was passed from the feed hopper to the pyrolysis reactor through the piston feeder system. The pyrolysis reactor at atmospheric pressure was heated to 500 °C and rotated at 25 Hz. Pyrolysis vapours, char, CaO and CaCO₃ (CaO captured CO₂) then progressed from the pyrolysis reactor to the char pot, where the char, CaO and CaCO₃ were separated from the vapours. The vapours continued on to the condenser train system, where four condensers separated the vapours into bio-oil and non-condensable gases. The water temperature of the condensers ranged from 80 °C (C1) to approximately 12 °C (C4). Finally, the non-condensable gases leaving C4 were sampled, collected in the gas towers and measured (by volume) before leaving the process. The non-condensable gas samples were analysed by GC/MS. The bio-oil collected in the second condenser (C2) was further separated into an aqueous fraction (C2A) and an organic fraction (C2O).

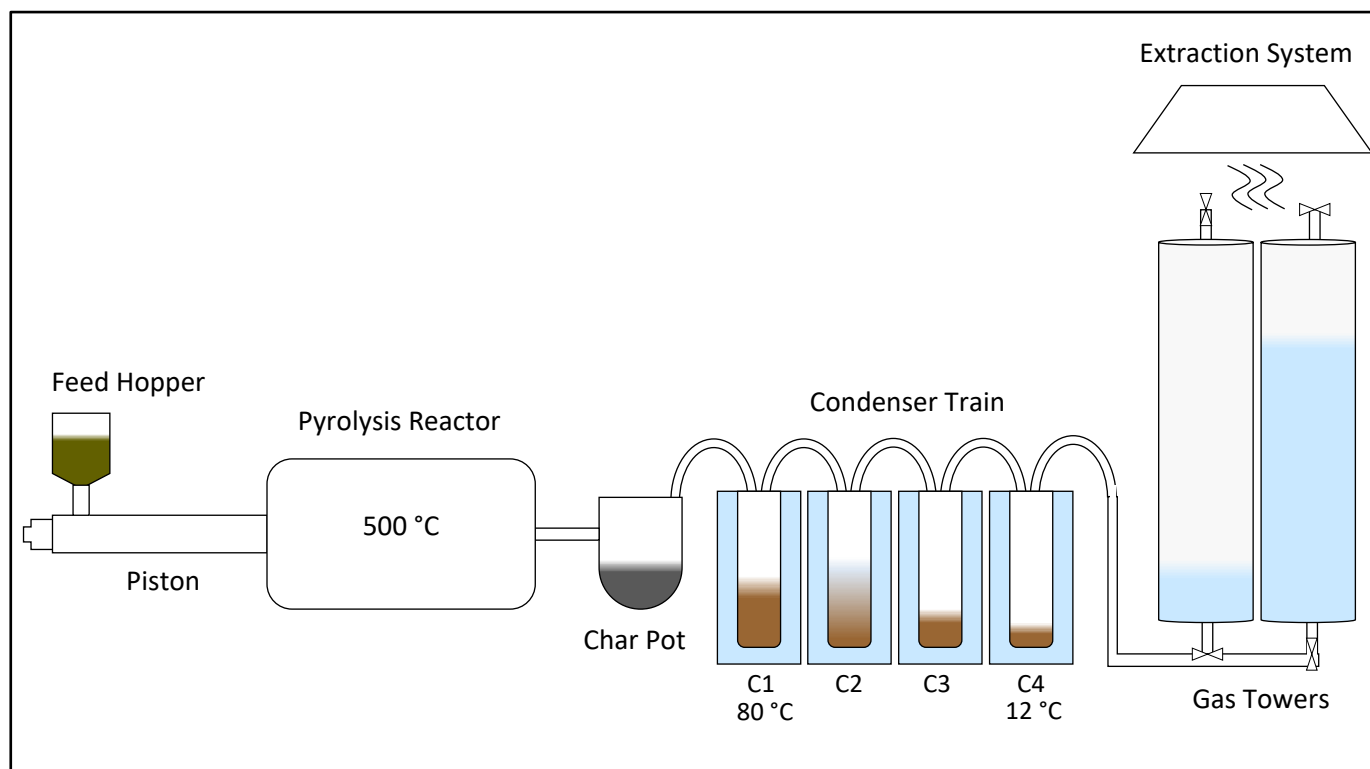


Figure 10: Pilot plant setup (redrawn from Chireshe (2019))

The biorefinery scenarios were simulated in Aspen Plus™ version 8.8 with the pilot plant data for non-catalytic and catalytic pyrolysis given in Appendix A. The simulated biorefinery scenarios include biomass pre-treatment (milling and drying), heat recovery, steam and power production and utility production (cooling and chilled water) in addition to pyrolysis and product recovery executed at the pilot plant.

4.4 Process simulation data input

4.4.1 Mass balance reconciliation

The total mass yield of non-catalytic and catalytic pyrolysis products from *E. grandis* forest residues (8.28 wt. % moisture) was 89.10 and 89.06 wt. %, respectively. The mass balance closure was agreeable with literature and considered acceptable by industrial experts for a pilot-scale pyrolysis process. Sandström and colleagues (2016) conducted fast pyrolysis of forest residues and other biomasses at pilot-scale, and reported an average mass balance closure of 90.5 wt. % (Sandström, Johansson, Wiinikka, Öhrman & Marklund, 2016). Other researchers reported mass balance closures of 81 (Mullen, Boateng, Goldberg, Lima, Laird & Hicks, 2010) and 93 wt. % (Dayton *et al.*, 2015) for pilot-scale pyrolysis processes.

The deficit in the mass balance was attributed to pyrolysis vapours (bio-oil and non-condensable gas components) escaping through the feed hopper, bio-oil components condensing between the char pot and C1, incomplete condensation of bio-oil components passing through the condenser train (Yang, Heaven, Venetsaneas, Banks & Bridgwater, 2018), and measuring the non-condensable gas yield based on the assumption that the non-condensable gas density remained constant throughout the experimental run². However, mass and elemental balances have to be closed to avoid process simulation calculation errors in Aspen Plus™ therefore, the following assumptions were made:

1. All nitrogen, sulphur and ash (Onarheim, Solantausta & Lehto, 2015) compounds found in the biomass reported to the char in both non-catalytic and catalytic pyrolysis runs. All CaO and CaCO₃ also reported to the char in catalytic pyrolysis runs (Veses *et al.*, 2014). Thereafter, the char yield and elemental composition were unchanged.
2. The missing products for non-catalytic and catalytic pyrolysis runs (after applying the first assumption) were evenly split between the bio-oil (organics and water) and non-condensable gas components. This conservative approach was chosen based on the rationale presented for the deficit in the mass balance and subsequently to minimise the uncertainty placed on either product: if the mass balance were closed with the non-condensable gas only, the yield of non-condensable gas would have significantly increased by 53 wt. % for non-catalytic pyrolysis and 62 wt. % for catalytic pyrolysis, whereas if the mass balance were closed with the bio-oil only, the yield of bio-oil would have significantly increased by 55 wt. % for non-catalytic pyrolysis and 64 wt. % for catalytic pyrolysis. The organic content and water content of the missing bio-oil was allocated as follows:
 - a. The organic content of the missing bio-oil was the same as the organic content of the measured bio-oil collected in C1. During the bench-scale experiments, where an electrostatic precipitator (ESP) was used to capture uncondensed vapours leaving the condenser train, Chireshe (2019) found that the composition of these organics closely resembled the composition of the organics collected in C1 (Chireshe, 2019).
 - b. The water content of the missing bio-oil was the same as the overall water content of the measured bio-oil.
3. The overall elemental balance for carbon, hydrogen and oxygen was finally closed for non-catalytic and catalytic pyrolysis runs by changing the chemical composition of the non-condensable gas. The HHV of the new gas composition was matched to the calculated HHV (using Equation 2-1) of the measured gas composition since the non-condensable gases were mostly combusted to generate heat for the pyrolysis reactor in the process simulation.

² Communication with Mr. Richard Bingham, Technotherm

The reconciled pilot plant data for non-catalytic and catalytic pyrolysis are given in Table 18 and Table 19, respectively.

Table 18: Reconciled pilot plant data for non-catalytic pyrolysis

		Feed	Char	C1	C2A	C2O	C3	C4	Gas
Yield (wt. %)			28.75	11.06	22.33	5.03	4.28	2.49	26.05
Elemental Analysis (wt. %, db)	C	48.01	83.02	44.31	42.51	71.97	67.46	74.24	
	H	6.36	3.39	8.02	4.98	6.69	8.74	6.91	
	O	45.46	13.01	47.67	52.51	21.34	23.79	18.85	
	N	0.12	0.39	0.00	0.00	0.00	0.00	0.00	
	S	0.06	0.19	0.00	0.00	0.00	0.00	0.00	
Proximate analysis (wt. %)	Moisture	8.28	0.00	7.48	88.54	20.01	28.63	23.62	
	Fixed carbon	15.06	77.42						
	Volatile matter	75.70	19.27						
	Ash	0.95	3.32						
HHV (MJ/kg, db)		19.33		22.10		29.08	30.17	32.63	
Density (kg/m ³ , db)				1184	1288	1041	1117	1234	
Composition (wt. %)	CO ₂								58.59
	CO								33.18
	CH ₄								5.18
	H ₂								1.47
	C ₂ H ₆								0.79
	C ₂ H ₄								0.56
	C ₃ H ₈								0.13
	C ₄ H ₆								0.13

Table 19: Reconciled pilot plant data for catalytic pyrolysis

		Feed	Char	CO ₂ (CaCO ₃)	C1	C2A	C2O	C3	C4	Gas
Yield (wt. %)			16.53	20.85	12.86	17.86	3.81	3.02	1.95	23.11
Elemental analysis (wt. %, db)	C	48.01	79.09		80.02	29.30	80.68	61.10	82.29	
	H	6.36	3.36		7.14	6.55	6.09	6.20	7.31	
	O	45.46	16.52		12.83	64.15	13.23	32.70	10.41	
	N	0.12	0.69		0.00	0.00	0.00	0.00	0.00	
	S	0.06	0.34		0.00	0.00	0.00	0.00	0.00	
Proximate analysis (wt. %)	Moisture	8.28	0.00		20.56	88.38	15.70	62.73	19.25	
	Fixed carbon	15.06	56.25							
	Volatile matter	75.70	37.98							
	Ash	0.95	5.77							
HHV (MJ/kg, db)		19.33		35.37		34.61	25.93	37.84		
Density (kg/m ³ , db)				1152	1198	1040	1031	1042		
Composition (wt. %)	CO ₂									48.07
	CO									2.23
	CH ₄									1.01
	H ₂									17.76
	C ₂ H ₆									3.50
	C ₂ H ₄									0.90
	C ₃ H ₈									25.30
	C ₄ H ₆									1.23

4.4.2 Bio-oil composition

Bio-oil is made up of water and hundreds of organic compounds, while only 25 to 40 wt. % of these compounds are detectable by GC/MS (Mullen, Strahan & Boateng, 2009). Lignin and carbohydrate derived compounds are not volatile enough to be detected, which makes it difficult to determine the chemical composition of the organic content of bio-oil.

A method employed to estimate the chemical composition of the organic content of bio-oil for the purpose of process simulation involves matching the measured elemental analysis (C, H and O), HHV and density to known organic compounds found in bio-oil. Jones and colleagues (2013) and Carrasco and colleagues (2017) both estimated the chemical composition of the organic content of

bio-oil using this method, and chose organic compounds from the main chemical families found in wood-derived bio-oils such as: acids, alcohols, aldehydes, ketones, phenols and sugars, as well as extractive and lignin-derived compounds (Carrasco *et al.*, 2017; Jones *et al.*, 2013). The organic compounds chosen by these researchers were combined to estimate the chemical composition of the organic content of crude and upgraded bio-oils in this project.

A list of the organic compounds chosen according to compound group is given in Table 20. The organic compositions of crude and upgraded bio-oils were determined by matching the corresponding elemental analysis, HHV and density results for non-catalytic and catalytic pyrolysis given in

Table 18 and Table 19 to the compounds listed in Table 20. This multi-objective-specification problem was solved using the Microsoft Excel add-in program *Solver*, and the solving method was set to the *Generalized Reduced Gradient Nonlinear* method. In some instances, a 100 wt. % match in C, H and O elements between the elemental analysis and chemical composition could not be found therefore, a balancing component (made up of elements C, H and O) was added to the composition to close the elemental balance. The share of the balancing component in the composition, however, was limited to a maximum of 2 wt. %. The subsequent chemical composition of the organic content recovered from each condenser and overall are given in Table 20 for crude and upgraded bio-oils produced via non-catalytic and catalytic pyrolysis, respectively. Furthermore, it is worth mentioning that the estimated chemical composition of the organic content of crude and upgraded bio-oils has negligible impact on the subsequent economic analysis because bio-oil as a whole was the focus of the study, and not the individual bio-chemicals.

Table 20: Composition of the organic content recovered from each condenser and overall for non-catalytic and catalytic pyrolysis

Group	Compound	Formula	Organic content composition (wt. %)											
			Non-catalytic pyrolysis						Catalytic pyrolysis					
			C1	C2A	C2O	C3	C4	Overall	C1	C2A	C2O	C3	C4	Overall
Acids	Acetic acid	C2H4O2	33.50	-	-	-	-	15.83	-	1.65	-	20.58	-	1.52
	Crotonic acid	C4H6O2	5.04	-	4.22	-	-	3.15	-	-	5.13	4.49	5.41	1.68
	Formic acid	CH2O2	1.08	39.21	-	-	-	5.26	-	83.74	-	5.78	-	9.90
Alcohols	1, 4 Benzenediol	C6H6O2	-	-	25.11	-	-	4.65	2.21	-	-	-	-	1.24
Aldehydes	3-Methoxy-4-Hydroxybenzaldehyde	C8H8O3	2.20	-	-	-	-	1.11	-	-	5.82	-	-	1.32
Aromatics	Benzene	C6H6	-	-	-	-	36.95	3.26	-	-	-	6.11	73.78	6.75
	Phenol	C6H6O	-	-	-	-	32.80	2.92	2.29	-	-	-	-	1.28
	Toluene	C7H8	-	-	1.06	5.81	-	1.01	27.42	-	22.58	-	-	19.38
Esters	Propyl benzoate	C10H12O2	-	-	3.42	4.29	-	1.23	2.70	-	-	-	-	1.51
Extractives	Dehydroabietic acid	C20H28O2	-	-	-	26.43	-	3.76	3.16	-	-	-	-	1.77
Furans	Furfural	C5H4O2	-	19.79	-	-	-	2.41	1.03	-	-	12.04	-	1.32
Guaiacols	Isoeugenol	C10H12O2	-	-	6.51	-	-	1.21	2.05	-	1.88	20.58	-	2.75
	Guaiacol	C7H8O2	-	-	-	7.02	-	1.04	2.05	-	-	-	-	1.15
Ketones	Hydroxyacetone	C3H6O2	33.60	-	-	20.45	-	18.72	-	2.67	5.21	-	-	1.47
Lignin-derived	Dibenzofuran	C12H8O	-	5.39	36.95	-	-	7.50	12.24	-	53.26	9.86	4.36	17.26
	Dimethoxy stilbene	C16H16O2	-	-	1.71	19.61	-	3.08	34.83	3.00	2.00	-	-	20.25
	Oligomeric compounds with β -O-4 bond	C20H26O8	-	-	9.11	-	-	1.68	2.22	-	-	-	-	1.25
	Phenylcoumaran compounds	C21H26O8	-	-	-	5.15	10.21	1.67	2.83	-	-	-	-	1.59
Sugars	Cellobiose	C12H22O11	17.04	6.51	-	10.25	19.18	11.96	2.34	-	-	-	4.15	1.77
	Levoglucosan	C6H10O5	6.54	27.89	-	-	-	6.43	1.06	6.14	3.12	-	11.85	2.87
Syringols	Syringol	C8H10O3	-	-	6.51	-	-	1.21	-	-	-	19.56	-	1.27

4.5 Process simulation development

4.5.1 Component selection

Biomass and char were specified as nonconventional components in Aspen Plus™. Nonconventional components are not defined by a molecular formula found in the Aspen Plus™ databanks. Instead, these components are specified by their elemental and proximate analyses to estimate through empirical models enthalpy and density properties (Onarheim *et al.*, 2015). Specifically, the HCOALGEN and the DCOALIGT models were used to estimate the enthalpy and density of biomass and char components (AspenTech, 2013). Isoeugenol, lignin-derived oligomeric compounds with β -O-4 bond ('Lignin A'), lignin-derived phenylcoumaran compounds ('Lignin B'), cellobiose and levoglucosan are user-defined compounds. Jones and colleagues (2013) provided the molecular structure and thermodynamic data for these compounds to be defined in Aspen Plus™ (Jones *et al.*, 2013). The remaining bio-oil and non-condensable gas compounds were specified as conventional components, which had thermodynamic properties readily available in the Aspen Plus™ databanks.

4.5.2 Thermodynamic model selection

An activity coefficient thermodynamic model was selected for process simulations over an equation-of-state thermodynamic model because of the non-ideal nature of the organic compounds present in the bio-oil, and the complicated component interactions taking place during pyrolysis. More specifically, the UNIQUAC thermodynamic model was selected (Onarheim *et al.*, 2015).

4.5.3 Non-catalytic and catalytic pyrolysis design basis

An overview of the mass and energy flows between the sections of the biorefinery for non-catalytic and catalytic pyrolysis scenarios is given in Figure 11.

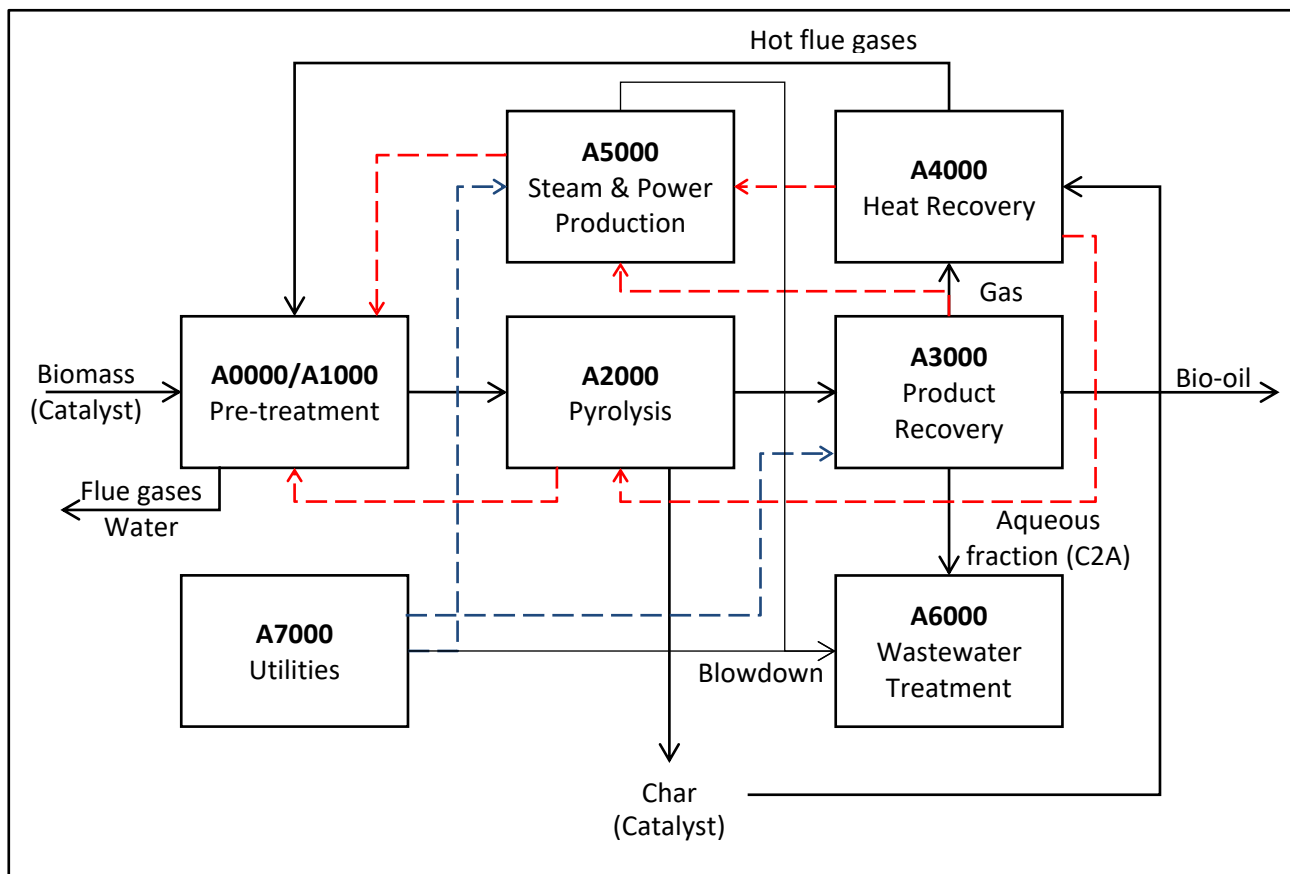


Figure 11: Overview of biorefinery mass flows (—) and energy flows (---) for non-catalytic and (catalytic) pyrolysis scenarios

4.5.3.1. Section A1000 (pre-treatment)

Pre-treatment is modelled in Sections A1000 as shown in the screenshot of the Aspen Plus™ model given in Figure 12. The biomass (1001) with 40 wt. % moisture (1002) was ground down from 2 cm to approximately 2 mm in size. The grinder (MILL) was not modelled but the power required for grinding was taken as 14 kWh/green MT (Carrasco *et al.*, 2017) and included in the process utilities.

The biomass was partially dried with the flue gases produced in Section A4000 therefore, to avoid creating a loop that would have slowed down process calculations in Aspen Plus™, the drying process shown in Figure 13 was modelled simply as a separator (S1001) and heater (H1001) to achieve the same moisture content (8.28 wt. %) and temperature of the biomass leaving the real drying process. The real drying process is shown in the screenshot of the Aspen Plus™ model given in Figure 13. It was necessary to simulate this process in order to more accurately estimate the energy demand and cost of the process units involved.

The ground biomass stream (1003) was duplicated to feed into the real drying process (0001), where it was first preheated (HX0001) up to 100 °C by indirect contact with the hot char produced in Section A2000, followed by direct contact drying (DR0001) with the flue gases (0003) leaving Section A4000 at 130 °C. The remaining moisture in the biomass was finally decreased to 8.28 wt. % by indirect

contact drying (HX0002/DR0002) at 100 °C with the steam produced in Section A5000 at 4.5 bar and 170 °C. In the catalytic pyrolysis scenarios, the dried biomass (1008) and catalyst (1009) were dry mixed (MIX1001) before entering the pyrolysis reactor in Section A2000.

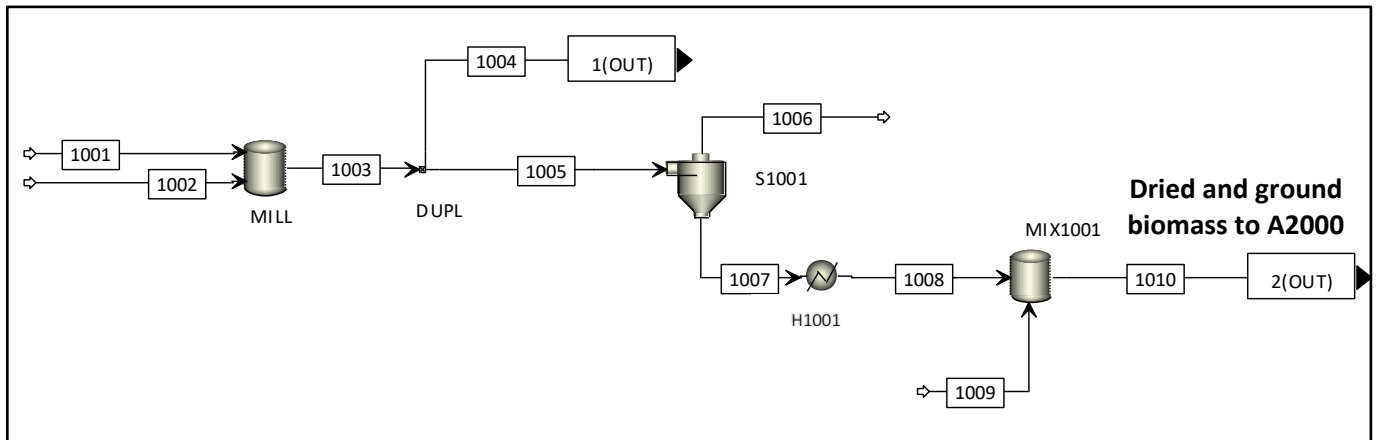


Figure 12: Pre-treatment

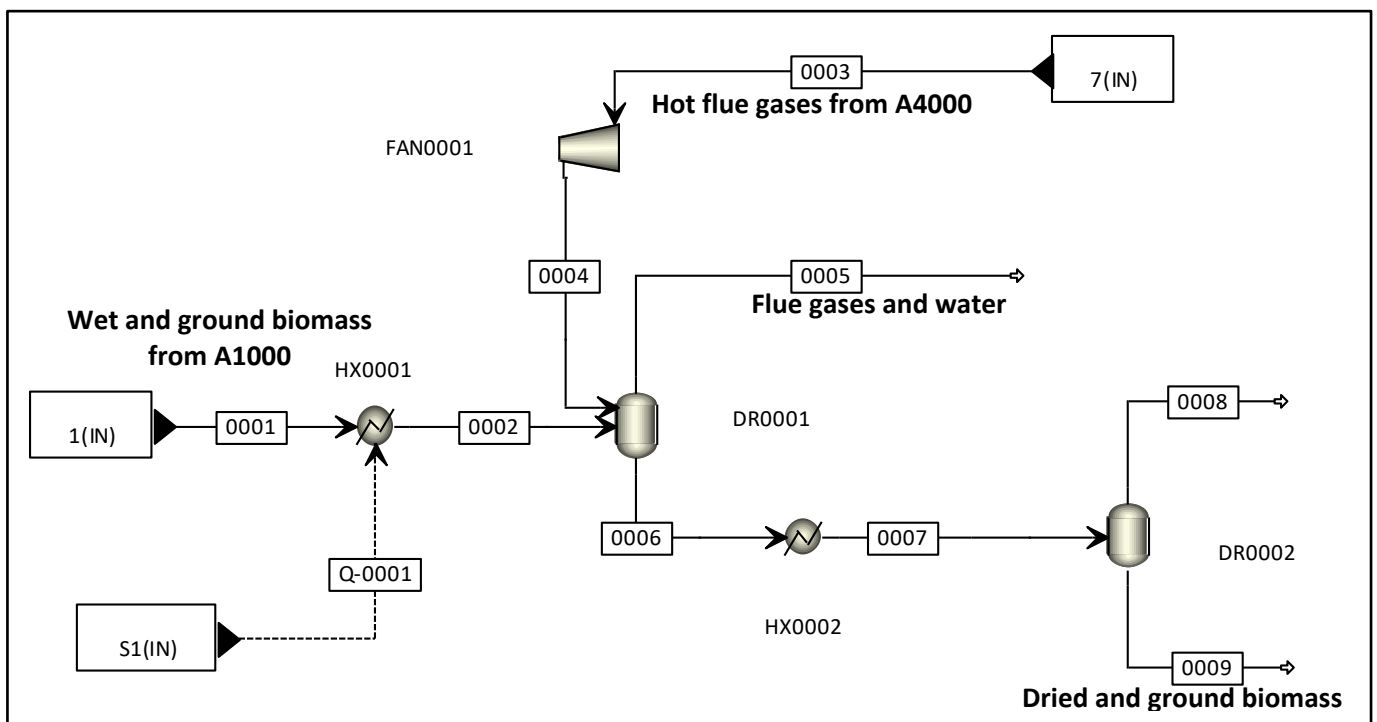


Figure 13: Pre-treatment (real drying process)

4.5.3.2. Section A2000 (pyrolysis)

Pyrolysis is modelled in Section A2000 as shown in the screenshot of the Aspen Plus™ model given in Figure 14. The dried biomass (2001) and catalyst (in catalytic pyrolysis scenarios) were sent to the pyrolysis reactor (PYRO), which was modelled using the RYield block. The yields of char, bio-oil components (determined in Section 4.4.2) and non-condensable gas components, and pyrolysis temperature (500 °C) and pressure (1.01325 bar) were the only inputs required. In catalytic pyrolysis

scenarios, the CaO catalyst reacts during pyrolysis with some of the CO₂ produced to form solid CaCO₃, which was modelled using the RStoic block (CAT). This reaction is exothermic ($\Delta H_{298K}^0 = -179$ kJ/mol (Veses *et al.*, 2014)) therefore, less heat is expected for catalytic pyrolysis than non-catalytic pyrolysis. Heat will be generated for the pyrolysis reactor (Q-2004) in Section A4000 by combusting all of the non-condensable gases produced and if necessary, some of the char produced. HX2001 represents the wall separating the pyrolysis reaction from the hot flue gases. The volatiles and char (containing CaO and CaCO₃ in catalytic pyrolysis scenarios) leaving the pyrolysis reactor were immediately separated by a cyclone (CY2001). The volatiles (2005) were sent to Section A3000 to recover bio-oil and non-condensable gases. A portion of the char (2007) was sent to Section A4000 for combustion (as described above) and the remaining char (2008) was cooled down to 150 °C in the biomass preheater in Section A0000.

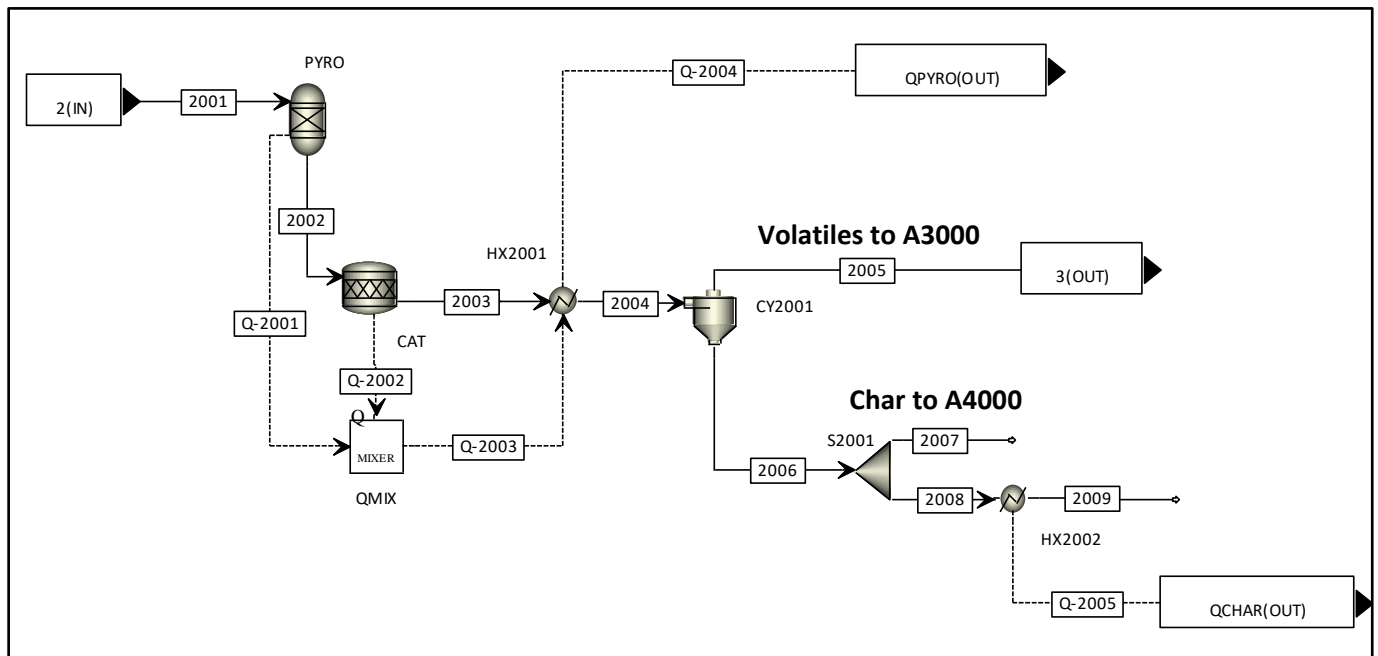


Figure 14: Pyrolysis

4.5.3.3. Section A3000 (product recovery)

Product recovery is modelled in Section A3000 as shown in the screenshot of the Aspen Plus™ model given in Figure 15. The pyrolysis vapours (3001) leaving Section A2000 at 500 °C were first cooled to 260 °C (HX3001) and then 210 °C to recover some heat for steam and power production in Section A5000 before bio-oil recovery, which was modelled based on the condenser train implemented at the pilot plant. Each condenser (C1-C4) was modelled using heat exchanger and separator blocks as specified in Table 21. The condenser train similar to the pyrolysis reactor, operated at atmospheric pressure. The bio-oil recovered from C2 was further separated (S3002B) into organic (3009) and aqueous (3010) fractions. The aqueous fraction was sent for wastewater treatment in Section A6000.

The non-condensable gases leaving C4 were sent to Section A4000 for combustion, while the recovered bio-oils and organic fraction were pumped (P3001) into a storage tank (T3001).

Table 21: Process simulation condenser train specifications

Condenser	Blocks	Temperature (°C)	Utility
C1	CON3001, S3001	80	Cooling Water
C2	CON3002, S3002A	60	Cooling Water
C3	CON3003, S3003	40	Chilled Water
C4	CON3004, S3004	20	Chilled Water

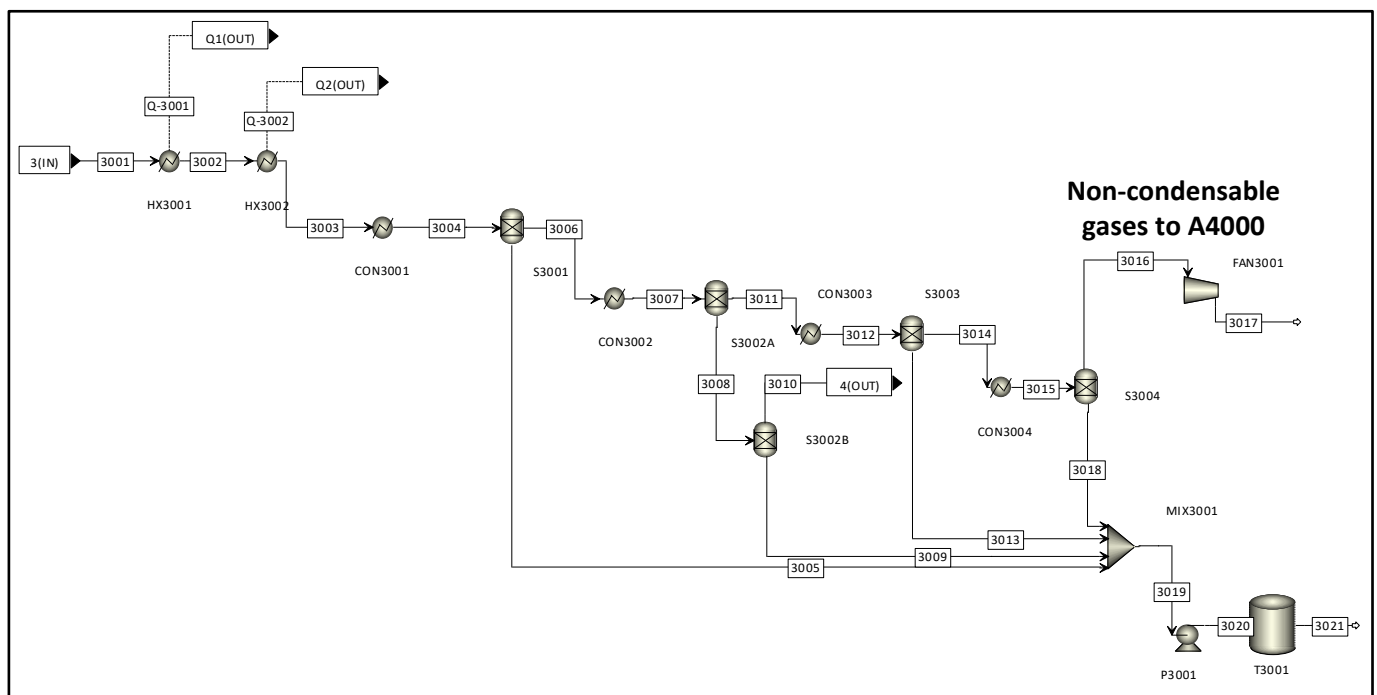


Figure 15: Product recovery

4.5.3.4. Section A4000 (heat recovery)

Heat recovery is modelled in Section A4000 as shown in the screenshot of the Aspen Plus™ model given in Figure 16. The RStoic block was used to model the combustor (H4001) that provides heat for the pyrolysis reactor and dryer. Nonconventional components such as char cannot undergo combustion in the RStoic block without first converting the elemental analysis into conventional components with known stoichiometry (AspenTech, 2013). Instead, char was represented by an equivalent amount of solid carbon (4001) in energy value. The real yield and composition of non-condensable gases (4002) was used instead of the reconciled yield and composition to avoid underestimating the amount of char required to meet the energy needs of the process because char is a high-value product. Ambient air (4003) was preheated (HX4002) by flue gases (4008) before

additional electricity production in the second turbine (C5002). The turbines operated at 85 % isentropic efficiency and 96 % mechanical efficiency (Ali Mandegari, Farzad & Görgens, 2017). Low pressure steam (5011) was discharged to saturated steam at 0.2 bar from the second turbine and condensed (CON5001) to 50 °C before joining the condensed steam at 110 °C (5015) from the indirect dryer in the condensate collection tank (S5002). The condensate was then treated in hot condensate polishing and deaerator process units not modelled in Aspen Plus™ but included in the economic analyses (Dutta *et al.*, 2015). Treated BFW makeup water (5018) was added to the treated condensate (MIX5001) and pumped (P5001) to 30 bar at the beginning of the steam cycle.

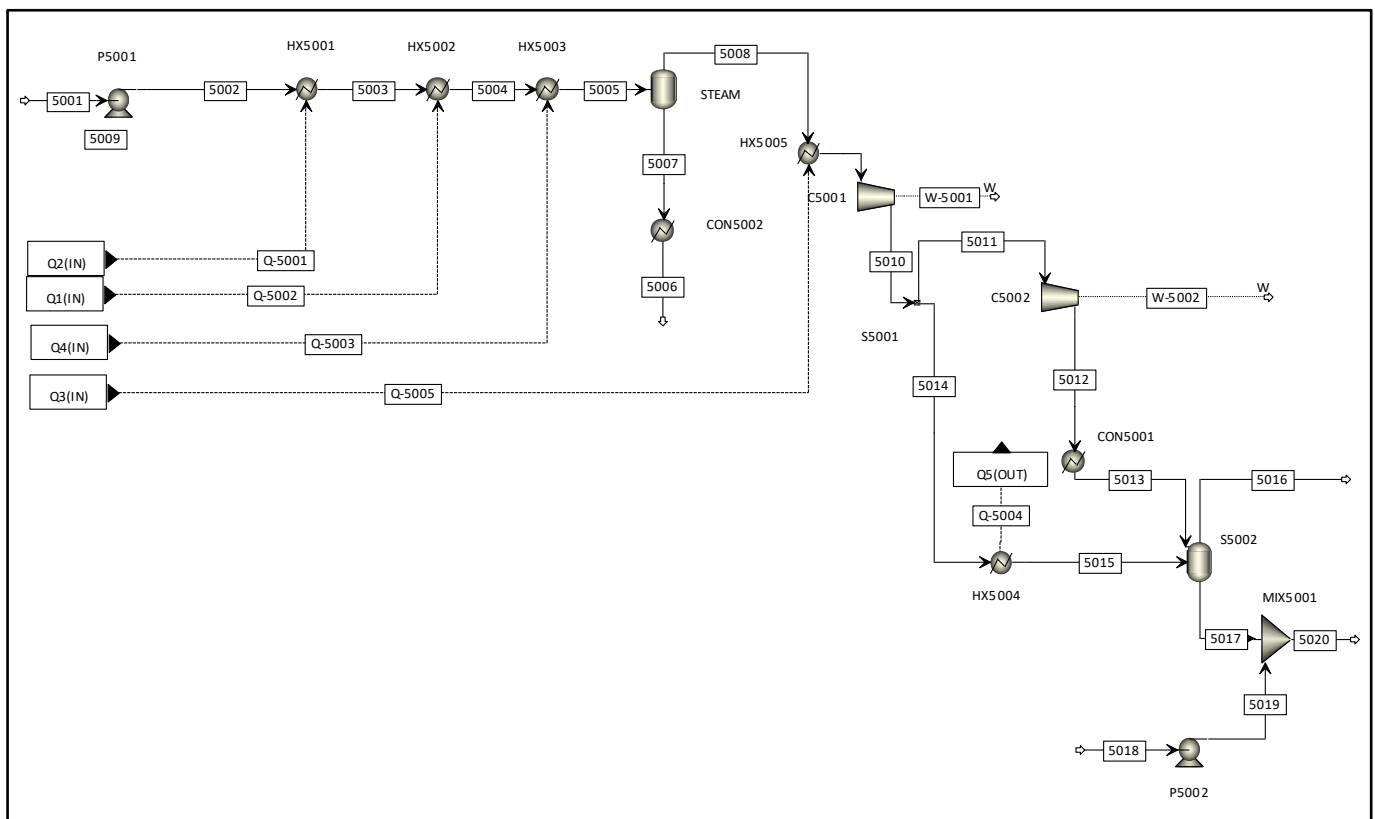


Figure 17: Steam and power production

4.5.3.6. Section A6000 (wastewater treatment)

Wastewater for both non-catalytic and catalytic pyrolysis processes was made up of the aqueous fraction of bio-oil recovered from the second condenser (3010), steam drum blowdown (5007) and cooling tower blowdown. The chemical oxygen demand (COD) of the aqueous fraction was approximately 11 g/L (estimated by Aspen Plus™), which was considered low enough (<51 g/L) to be treated by aerobic digestion followed by discharge to municipal wastewater treatment (Jones *et al.*, 2013). Aerobic digestion was not modelled in Aspen Plus™ but included in the economic analyses.

4.5.3.7. Section A7000 (utilities)

The cooling tower was modelled based on the principle of evaporative cooling. Makeup water was added to the cooling tower to account for water losses attributed to evaporation, drift and blowdown (Turton, Bailie, Whiting & Shaeiwitz, 2009), which is expressed mathematically in Equation 4-1.

$$W_M = W_E + W_D + W_B \quad \text{Equation 4-1}$$

Where, W_M [m³/h] is makeup water, and W_E , W_D and W_B are evaporation, drift and blowdown water losses [m³/h], respectively. The evaporation water loss was calculated using Equation 4-2 (Perry, Green & Maloney, 1997).

$$W_E = 0.00085 \times W_C \times (T_{in} - T_{out}) \times 1.8 \quad \text{Equation 4-2}$$

Where, W_C [m³/h] is the combined flow rate of the cooling water required by the process ($W_{CW req}$) and W_M given in Equation 4-3, T_{in} [°C] is the returned cooling water temperature and T_{out} [°C] is the supplied cooling water temperature.

$$W_C = W_M + W_{CW req} \quad \text{Equation 4-3}$$

Equation 4-1, Equation 4-2 and Equation 4-3 are then combined in Equation 4-4 and rearranged in Equation 4-5 to give an expression to calculate W_C , which was required to model the cooling tower in Aspen PlusTM. Drift and blowdown water losses were taken as 0.3 and 3 vol. % of W_C , respectively (Walas, 1990).

$$W_C = (0.00085 \times (T_{in} - T_{out}) \times 1.8 + 0.003 + 0.03) \times W_C + W_{CW req} \quad \text{Equation 4-4}$$

$$W_C = \frac{W_{CW req}}{1 - (0.00085 \times (T_{in} - T_{out}) \times 1.8 + 0.003 + 0.03)} \quad \text{Equation 4-5}$$

The cooling tower was modelled in Aspen PlusTM by specifying the outlet temperature and evaporative water loss of a flash drum. Cooling water was supplied to the process at 28 °C and returned to the cooling tower at 37 °C (Ali Mandegari *et al.*, 2017). The power P [W] required for the pumps and fans that operate the cooling tower was calculated by dividing the heat duty Q [W] of the cooling tower by its coefficient of performance (COP) as shown in Equation 4-6. The COP for the cooling tower was taken as 7 (Bergsten, 2009). Cooling water was supplied to CON3001, CON3002 and CON5001.

$$P = \frac{Q}{COP}$$

Equation 4-6

Chilled water was supplied to the process at 4 °C and 2 atm, and returned to the chilled water system at 15 °C and 1 atm (Ali Mandegari *et al.*, 2017). The power consumption for the chilled water system compressor was estimated at 0.56 kW/ton of refrigeration. The chilled water system required cooling water to condense the refrigerant. The amount of cooling water required was calculated by assuming that the amount of heat removed from the refrigerant was equal to the amount of heat removed from the process (Humbird, Davis, Tao, Kinchin, Hsu, Aden, Schoen, Lukas, Olthof, Worley, Sexton & Dudgeon, 2011). Chilled water was supplied to CON3003, CON3004 and CON5002.

4.6 Economic analysis methodology

The economic analysis followed after mass and energy balances were generated from the process simulation for each biorefinery scenario in Aspen Plus™. The mass and energy balances were used to size and cost process equipment, and calculate variable operating costs based on feedstock, chemicals, wastewater and solid waste disposal flowrates for the capital and operating cost estimates (Ali Mandegari *et al.*, 2017). The economic feasibility of each biorefinery scenario was then evaluated through a profitability analysis, and the effect of a change in economic parameter on profitability was assessed through a sensitivity analysis.

4.6.1 Capital cost estimation

Capital costs are costs incurred during the construction of the biorefinery, leading up to its operation. The Fixed Capital Investment (FCI) included capital cost estimates for purchased and installed equipment, and direct and indirect costs (Vlysidis, Binns, Webb & Theodoropoulos, 2011). The Total Capital Investment (TCI) was then calculated as the sum of the FCI, land cost and working capital (Turton *et al.*, 2009). The capital cost estimate provided is only a preliminary estimate with an accuracy range of ±30 % (Woods, 2007).

4.6.1.1. Fixed capital investment

Purchased equipment costs (C_P^0) were either found in literature (Carrasco *et al.*, 2017; Dutta *et al.*, 2015; Humbird *et al.*, 2011; Jones *et al.*, 2013; Woods, 2007), quoted by the manufacturer (i.e. the pyrolysis reactor) or estimated by Aspen Plus™. The installed equipment cost (C_P) was calculated using Equation 4-7 for the referenced capacity, and relates the purchased equipment cost to operating pressure and materials of construction by means of an installation factor (F) that can be found in

literature. However, Aspen Plus™ calculates installed equipment costs based on predefined installation factors.

$$C_P = C_P^0 F \quad \text{Equation 4-7}$$

The installed equipment cost was then adjusted using Equation 4-8 and Equation 4-9 to the required capacity and relevant year of study, respectively.

$$\frac{C_a}{C_b} = \left(\frac{A_a}{A_b}\right)^n \quad \text{Equation 4-8}$$

$$C_1 = C_2 \left(\frac{CEPCI_2}{CEPCI_1}\right) \quad \text{Equation 4-9}$$

Where A_a , A_b and n represent the capacity for the referenced installed equipment cost, the capacity for the required installed equipment cost and the scaling exponent, respectively. The adjusted installed equipment cost was then scaled to reflect the relevant year of study using the Chemical Engineering Plant Cost Index (*CEPCI*). The chosen year and *CEPCI* for this project were 2017 and 567.5, respectively.

Direct costs are costs incurred for new plant installation such as warehouse, site development and additional installation such as piping. These costs were calculated based on a percentage of the inside-battery-limits (ISBL) installed equipment cost, which is the sum of installed equipment costs for Sections A1000/A0000, A2000, A3000 and A4000 of the biorefinery. The total direct cost (TDC) was then calculated as the sum of the installed equipment costs and direct costs. Indirect costs include proratable costs, field expenses, home office and construction fees, project contingency and other costs such as start-up and commissioning costs. These costs were calculated based on a percentage of the TDC. The FCI was finally calculated as the sum of the TDC and total indirect costs (Humbird *et al.*, 2011). The guidelines for calculating direct and indirect costs are given in Table 22.

Table 22: Guidelines for calculating direct and indirect costs (Humbird et al., 2011)

Cost	Factor
Warehouse	4 % of ISBL
Site development	9 % of ISBL
Additional piping	4.5 % of ISBL
Prorateable costs	10 % of TDC
Field expenses	10 % of TDC
Home office and construction fees	20 % of TDC
Project contingency	10 % of TDC
Other costs	10 % of TDC

4.6.2 Operating cost estimation

Operating costs are incurred during the operation of the biorefinery, and can be categorised as either fixed or variable. Fixed operating costs such as employee salaries and benefits, general overheads, maintenance, taxes and insurance are not dependent on the operating capacity of the biorefinery. Variable operating costs such as forest residues and catalysts, utilities and waste treatment are dependent on the operating capacity of the biorefinery (Brown & Brown, 2013; Turton *et al.*, 2009).

Table 23 lists the expected number of employees and their salaries for a 2000 dry MT/day pyrolysis biorefinery in the United States (Jones *et al.*, 2013). Salaries for South Africa are expected to be lower (Gorgens, Mandegari, Farzad, Daful & Haigh, 2016) therefore, the effect of salaries on profitability will be explored through a sensitivity analysis. The number of employees required for each biorefinery scenario was adjusted to the scale of the biorefinery. Employee salaries were adjusted to the relevant year of study using a labour cost index of 24.29 for 2017 and 21.45 for 2011 (U.S. Bureau of Labor Statistics, 2019). Benefits and overheads (90 % of salaries) were included in the fixed operating cost estimate along with insurance and taxes (0.7 % of FCI), and general maintenance (3 % of FCI) (Jones *et al.*, 2013).

Table 23: Employee salaries (Jones et al., 2013)

Position	Amount (2011 \$)	Number of Employees	Amount (2017\$)
Plant Manager	161 400	1	182 770
Plant Engineer	76 800	1	86 968
Maintenance Supervisor	62 600	1	70 888
Lab Manager	61 500	1	69 643
Shift Supervisor	52 700	5	298 388
Lab Technician	43 900	3	149 137
Maintenance Technician	43 900	16	695 974
Shift Operators	52 700	40	2 029 036
Yard Employees	30 700	12	347 647
Clerks and Secretaries	39 500	3	134 190

Forest residues are collected after round wood harvesting (two-pass system) and forwarded to the roadside with tractor-trailers. The biomass is then chipped at the roadside directly into truck trailers. Ackerman and colleagues (2013) calculated the roadside cost of collected and chipped forest residues using the *South African Harvesting and Transport System Costing Model*. The roadside cost was adjusted from R112.25/MT (\$12.90/MT for a 2012 R8.70/\$ exchange rate) in 2012 (Ackerman *et al.*, 2013) to R146.83/MT (\$10.49/MT for a 2017 R14.00/\$ exchange rate) in 2017 using the Producer's Price Index (Statistics South Africa, 2019).

Ackerman and colleagues (2013) suggested that the best truck configuration for biomass transport from the roadside to the biorefinery is a self-unloading system with side and back tippers (Ackerman *et al.*, 2013). The estimated transport cost (including capital) for this type of vehicle with a payload of 33 metric tonnes was R17.11/km in 2017 (Department of Agriculture Forestry and Fisheries, 2018). The average one-way distance from the roadside to the biorefinery within a 300 km radius of the biorefinery is 179 km therefore, the transport cost for a round trip (assuming the transport cost of R17.11/km remains the same regardless of a full or empty load) was R185.66/MT (\$13.26/MT). The transport cost for biomass collection within a 200 and 100 km radius of the biorefinery was calculated in a similar way and reported in Table 24. The total biomass cost was calculated by adding the roadside cost and transport cost.

Table 24: Transport cost and total cost of forest residues

Radius (km)	Roadside Cost (R/MT)	Average Distance (km)	Transport Cost (R/MT)	Total Cost (R/MT)	Total Cost (\$/MT)
300	146.83	179	185.66	332.49	23.75
200	146.83	143	148.17	295.00	21.07
100	146.83	80	82.66	229.49	16.39

Other variable operating costs such as catalyst cost and wastewater treatment cost are given in Table 25. Variable operating costs were adjusted to the relevant year of study using a chemical cost index (Federal Reserve Economic Data, 2019). The total operating cost is finally the sum of the total fixed and variable operating costs.

Table 25: Variable operating costs

Variable cost	Value	Cost Year	Unit	Value (2017\$)	Reference
Catalyst (CaO)	150.00	2017	\$/MT	150.00	www.alibaba.com
Ash disposal	31.81	2007	\$/MT	41.59	(Humbird <i>et al.</i> , 2011)
Wastewater	0.73	2011	\$/100 m ³	0.75	(Jones <i>et al.</i> , 2013)
Process water	0.22	2001	\$/MT	0.41	
Cooling tower chemicals	7.70	2014	\$/year/kW	7.70	(Dutta <i>et al.</i> , 2015)
BFW chemicals	0.17	2014	\$/MT blowdown	0.17	
50 wt. % caustic	0.18	2010	\$/kg	0.20	

4.6.3 Profitability analysis

The profitability or economic feasibility of each biorefinery scenario was measured after the capital and operating cost estimates were complete. The discounted cash flow rate of return (DCFROR) analysis was used to measure the minimum selling price (MSP) profitability metric, which is defined as the lowest market price capable of yielding a net present value (NPV) of zero at a nominal or desired internal rate of return (IRR). The nominal IRR (discount rate) was 10 %, whereas the desired IRR (to attract private investors to the Greenfields project) was 22 %. The MSP profitability metric is useful for comparison between a product and its competitor (Brown & Brown, 2013). The assumptions required for the DCFROR analysis are presented in Table 26.

The bulk selling price for electricity in South Africa in 2017 was \$0.06/kWh (Motiang & Nembahe, 2017). Agri-lime is used in agricultural applications to increase soil pH and improve crop productivity. The catalytic pyrolysis biorefinery scenarios produced a mixture of approximately 25 wt. % CaO and 75 wt. % CaCO₃, which is similar to the chemical composition of agri-lime. Therefore, the

selling price of this mixture was assumed to be the same as agri-lime. Agri-lime is sold from *Kalkor* for R163.00/MT (\$11.64/MT) in South Africa (Kalkor, 2019). The conservative selling price of R5 000/MT (\$357.14/MT) for biochar as a soil additive was chosen based on the literature review given in Section 2.3.4.1. The pyrolysis temperature was too low at 500 °C to produce biochar with a large enough surface area for activated carbon applications but suitable to produce biochar with enough volatile matter for soil applications, and still gain the environmental benefit of carbon sequestration.

Table 26: Profitability analysis assumptions

Parameter	Value	Reference
Project life (years)	25	(Ali Mandegari <i>et al.</i> , 2017)
Exchange rate (R/\$)	14	-
Income tax rate (%)	28	(Ali Mandegari <i>et al.</i> , 2017)
Annual operating hours	8040	-
Loan (% of FCI)	0	(Nieder-Heitmann, Haigh & Görgens, 2018)
Working capital (% of FCI)	5	(Ali Mandegari <i>et al.</i> , 2017)
Depreciation period (years)	5	
Depreciation method	Straight Line	(Nieder-Heitmann <i>et al.</i> , 2018)
Salvage value	0	
Construction period (years)	2	
% Spent in -2	10	(Nieder-Heitmann <i>et al.</i> , 2018)
% Spent in -1	60	
% Spent in 0	30	
Start-up time (years)	0.5	
Production during start-up (%)	50	(Dutta <i>et al.</i> , 2015)
Variable costs during start up (%)	75	
Fixed costs during start-up (%)	100	
Biochar selling price (\$/MT)	357.14	-
Agri-lime selling price (\$/MT)	11.64	(Kalkor, 2019)
Electricity selling price (\$/kWh)	0.06	(Motiang & Nembahe, 2017)
Nominal IRR (%)	10	-
Desired IRR (%)	22	-
Cost year	2017	-
CEPCI	567.5	-

4.6.4 Economic sensitivity analysis

The DCFROR analyses for non-catalytic and catalytic biorefinery scenarios were based on several economic parameter assumptions that need to be evaluated against profitability. The economic sensitivity analysis quantifies the effect a change in model parameter (e.g. biomass cost price) has on the MSP profitability metric. The sensitivity of the MSP was evaluated for a 25 % change (increase and decrease) in the model parameters given in Table 27. The baseline values for total operating cost (TOC) and FCI will be determined from the capital and operating cost estimates for non-catalytic and catalytic pyrolysis biorefinery scenarios.

Table 27: Sensitivity analysis parameters

Parameter	Unit	-25%	Baseline	+25%
Electricity selling price	\$/kWh	0.04	0.06	0.07
Agri-lime selling price	\$/MT	8.73	11.64	14.55
Working capital	% FCI	3.75	5.00	6.25
Biomass cost price	\$/MT	15.80	21.07	26.34
Income tax rate	%	21.00	28.00	35.00
Biochar selling price	\$/MT	267.86	357.14	446.43
Catalyst cost price	\$/MT	112.50	150.00	187.50
TOC	\$/year	-	variable	-
FCI	\$	-	variable	-

4.6.5 Process sensitivity analysis

Approximately 89 wt. % of the biomass was recovered as pyrolysis products during pilot plant experiments therefore, several assumptions were made to close the mass balance for process simulation development as discussed in Section 4.4.1. The MSP of bio-oil was conservatively estimated based on the unreconciled bio-oil yields for non-catalytic and catalytic pyrolysis processes. However, more efficient product recovery and longer operation at industrial-scale may improve these yields: depositions on the surfaces of process equipment occur at the start of operation, while thereafter these depositions build-up at a slower rate (Sandström *et al.*, 2016). Therefore, the sensitivity of the MSP was also evaluated for a change in bio-oil yield correlated to an 89.0, 94.5 and 100.0 wt. % mass balance closure.

4.7 Environmental impact methodology

The LCA method was selected to assess the environmental impact of bio-oil production via non-catalytic and catalytic pyrolysis processes based on the developed process simulation. The four phases of the LCA are 1) goal and scope definition, 2) Life Cycle Inventory (LCI), 3) Life Cycle Impact Assessment

(LCIA) and 4) interpretation. Phase 4 takes place throughout Phases 1 to 3, as shown in Figure 18, and will be discussed in Section 5.3.

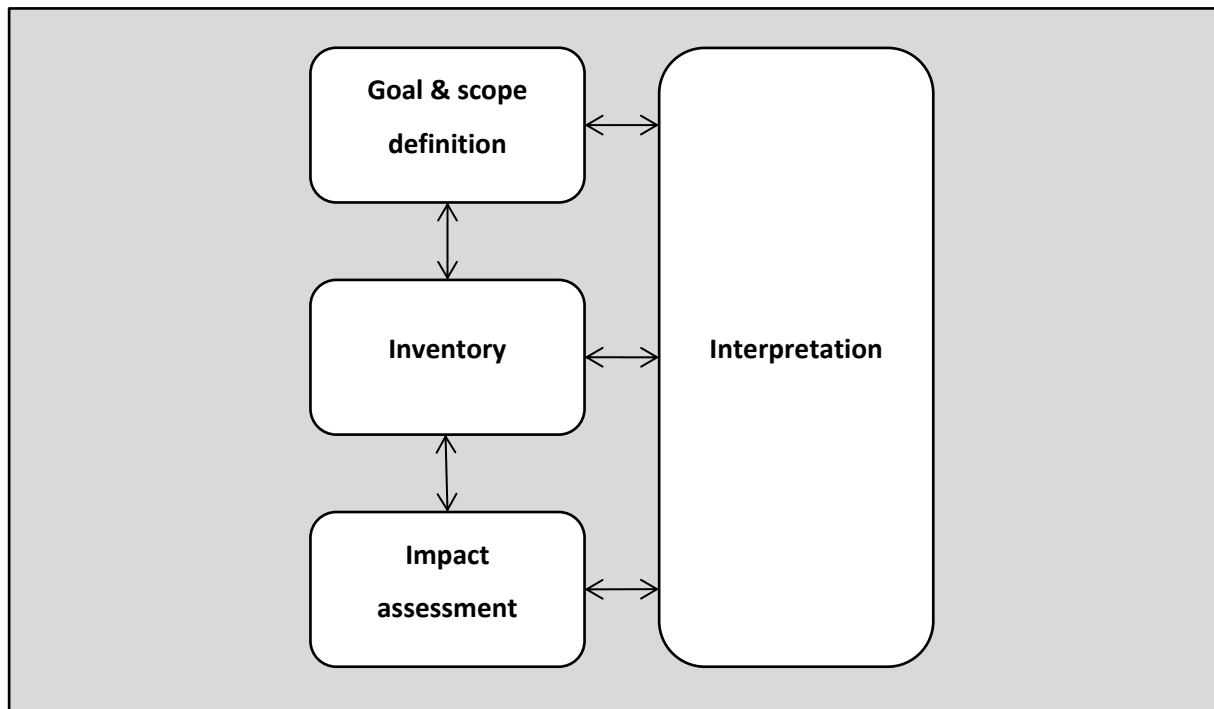


Figure 18: Interaction between the four phases of the LCA

4.7.1 Goal and scope definition

The intended application of the product, system boundary and functional unit are fundamental modelling elements of the LCA described in Phase 1 (Sharifzadeh *et al.*, 2019).

4.7.1.1. Description of LCA scenarios

Two LCA scenarios were considered for this project. The first scenario evaluated the environmental impact of valorising forest residues by producing bio-oil via non-catalytic or catalytic pyrolysis instead of disposing of forest residues by in-field burning. The second scenario evaluated the environmental impact of bio-oil production via non-catalytic or catalytic pyrolysis instead of crude-oil and diesel production.

4.7.1.2. System boundary

A “cradle-to-gate” approach for bio-oil production was employed for both scenarios. The activities related to cultivation, thinning and felling of trees to produce forest residues were not included in the LCA because these processes are essential to the production of merchantable wood products (Steele *et al.*, 2012). Therefore, the “cradle” in both scenarios was forest residue collection. The products of pyrolysis were biochar, bio-oil, agri-lime (in the case of catalytic pyrolysis) and a small amount of

electricity. In the first scenario, the end point of the LCA was the biorefinery gate therefore, the applications of bio-oil and biochar were not considered. In the second scenario, the biochar was transported to an agricultural area and applied to the soil, and the bio-oil was transported to the oil refinery gate, which was the end point of the LCA. The system boundary for bio-oil production via catalytic pyrolysis in the second scenario is given in Figure 19.

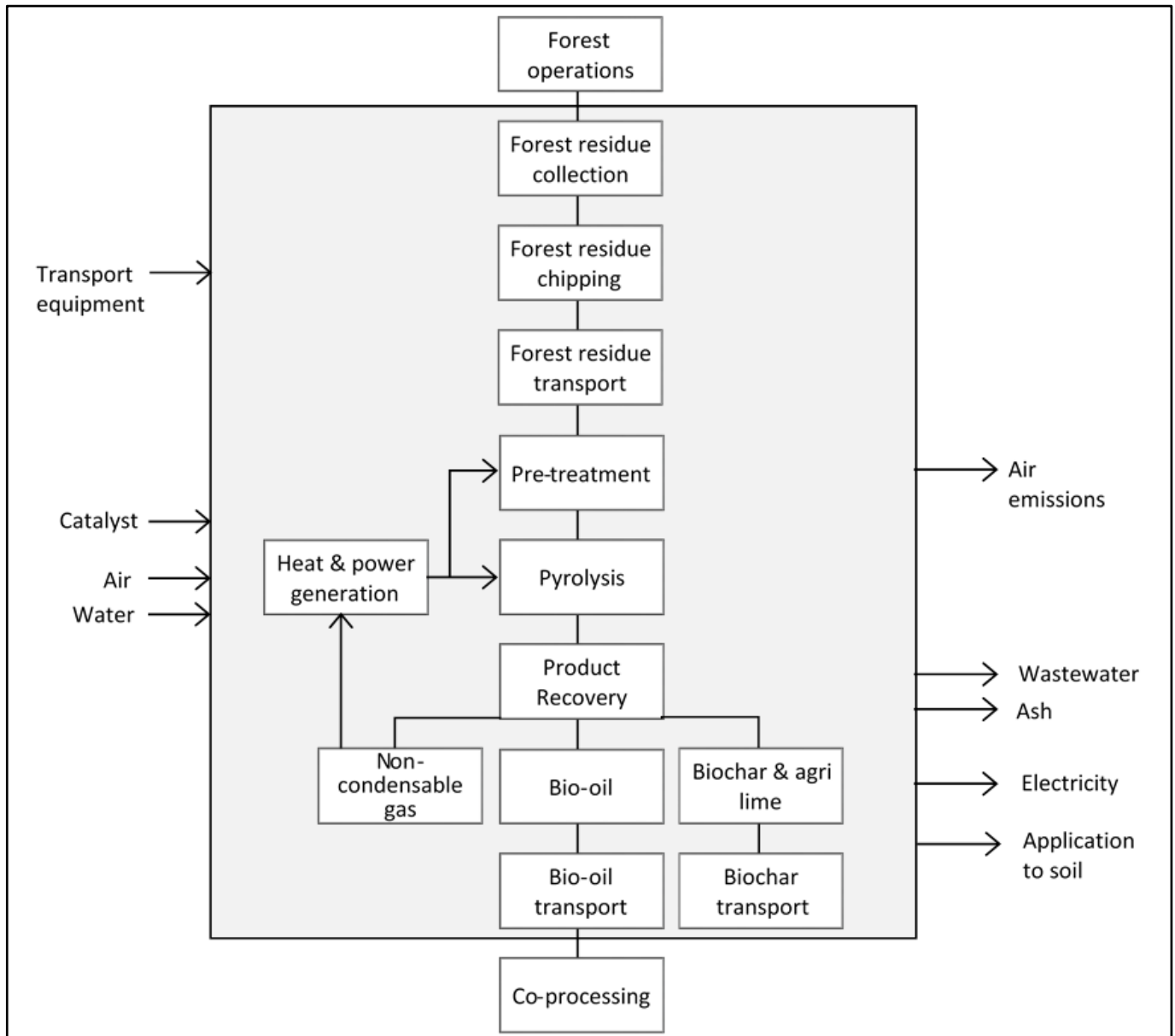


Figure 19: System boundary for bio-oil production in the second scenario via catalytic pyrolysis

4.7.1.3. Functional unit

Researchers have previously chosen functional units such as calorific value of products (Iribarren *et al.*, 2012), mass of feedstock (Roberts, Gloy, Joseph, Scott & Lehmann, 2010), distance travelled (Hsu, 2012) and area of land cultivated (Kauffman, Hayes & Brown, 2011) based on their system boundary.

However, distance travelled and area of land cultivated are less common functional units (Patel *et al.*, 2016). In this study, the functional unit for the first scenario was 1 kg of dry forest residues since the valorisation of forest residues was compared to its disposal, and the functional unit for the second scenario was 1 MJ of energy produced since bio-oil production was compared to fossil fuel production.

4.7.1.4. Allocation procedure

The main methodologies of the LCA such as allocation procedure are also defined in Phase 1. There are three main allocation procedures to divide the environmental impacts of a process between its products. The first is allocation by a physical relation such as mass or energy, the second is allocation by economic value, and the third is system boundary expansion (Sharifzadeh *et al.*, 2019). The system boundary expansion method is used when a co-product of the investigated process displaces a conventional product (i.e. the environmental impact of the conventional process is avoided and credited to the investigated process) but may not be appropriate if the yield of the co-product is comparable to the yield of the intended product as the co-product credit may disproportionately overshadow the environmental impact of the intended product (Han *et al.*, 2013).

Allocation by mass was chosen for both scenarios. Biochar has a significant economic value as a co-product, which is not suitable for allocation by economic value when bio-oil is the main product (Lu & El Hanandeh, 2019). Furthermore, the economic value of bio-oil is not fixed but determined through the profitability analysis, where several assumptions were made. Bio-oil and biochar are similar in calorific value, whereas agri-lime is not a fuel but still a significant co-product of catalytic pyrolysis therefore, neither allocation by energy value nor allocation by system boundary expansion were appropriate.

4.7.2 Life cycle inventory analysis

Inventory data related to all inputs and outputs across the system boundary are collected for each unit operation in the second phase of the LCA (Sharifzadeh *et al.*, 2019). The inventory data for both scenarios are given in Appendix D, and were entered into SimaPro™ version 8.5.0 to compare the environmental impact of each scenario in the third phase of the LCA. The following assumptions were made regarding the inventory data:

1. Carbon dioxide taken up by the biomass was included but activities directly related to stem wood production such as land use, water use, nutrient replenishment and forest operations were excluded.
2. Capital goods were included for all transport-related inventory.
3. Biochar was transported to the agricultural areas around Durban (KZN), 300 km away from the biorefinery.

4. 20 wt. % of biochar carbon content was released to the atmosphere as carbon dioxide over 100 years of carbon sequestration (Han *et al.*, 2013).
5. Biochar nitrogen content was equivalent to conventional N fertilizer (Han *et al.*, 2013).
6. The environmental impact of biochar beyond carbon sequestration and conventional N fertilizer was not considered (Han *et al.*, 2013).
7. Calcium carbonate was an avoided product since it was applied to the soil with biochar, and replaced conventional pH raising agents.
8. Carbon dioxide was released when calcium carbonate was applied to the soil with biochar.
9. Calcium oxide also replaced conventional pH raising agents when it was applied to the soil with biochar: 1 kg of calcium oxide is equivalent to 1.79 kg of calcium carbonate (Carey, Ketterings & Hunter, 2006).
10. Electricity was assigned an energy value of 29.0 MJ/kg for the purpose of mass allocation.

4.7.3 Life cycle impact assessment

There are two main methodologies for LCIA in the third phase of the LCA: the environmental problem-oriented (midpoint) approach and the damage-oriented (endpoint) approach (Farzad, Mandegari & Görgens, 2017). The Institute of Environmental Sciences (CML) at Leiden University developed a midpoint method (CML-IA baseline), which has previously been applied to characterise the environmental impact of pyrolysis processes (Iribarren *et al.*, 2012; Peters, Iribarren & Dufour, 2015). Therefore, CML-IA baseline was chosen as the default characterisation method for the LCIA in this study. Furthermore, abiotic depletion (ADP) of fossil fuels, acidification (AP), eutrophication (EP), global warming potential over 100 years (GWP₁₀₀), and ozone layer depletion (ODP) impact categories were evaluated.

CHAPTER 5

5 Results and Discussions

In this chapter, the mass and energy balance results of process simulations developed in Aspen Plus™ for non-catalytic and catalytic pyrolysis biorefinery scenarios are discussed in Section 5.1 to address Objective 1. The outcome of Objective 1 was integral to the development of economic analyses for the biorefinery scenarios. The results of capital and operating cost estimates, and subsequent profitability and sensitivity analyses are discussed in Section 5.2 to address Objective 2. Finally, the results for the LCIA developed in SimaPro™ to evaluate the environmental impact of non-catalytic and catalytic pyrolysis processes are discussed in Section 5.3 to address Objective 3.

5.1 Process simulation results

The mass and energy balance results for the non-catalytic and catalytic pyrolysis biorefinery scenarios are presented and discussed below. Stream tables for the process simulations developed in Aspen Plus™ are given in Appendix B.

5.1.1 Overall mass and energy balances

The overall mass and energy balance represents the main contributors to the material and energy flows through the process, and provides meaningful insight into the overall process performance. The overall mass and energy balances for the biorefinery scenarios are given in Table 28. The mass balance over the pilot plant was closed for process simulation development in Aspen Plus™ as discussed in Section 4.4.1, but the bio-oil and non-condensable gas masses reported in Table 28 are based on the unreconciled yields to prevent overestimating profitability for the economic analyses and energy resources available to meet the heating, cooling and power demands of the biorefinery scenarios, respectively.

Table 28: Overall mass and energy balances for the biorefinery scenarios

Scenario†		NC-100	NC-5	NC-200	NC-300	C-100	C-200	C-10	C-300
Input									
Forest residues‡	MT/day	338	813	1655	2549	338	1655	1710	2549
Catalyst	MT/day	-	-	-	-	158	773	799	1 190
Net output									
Char	MT/day	83	200	407	627	61	298	308	459
Agri-lime	MT/day	-	-	-	-	234	1 148	1 186	1 768
CO ₂ (of CaCO ₃)	MT/day	-	-	-	-	77	375	388	578
Bio-oil*	MT/day	73	176	358	551	68	332	343	511
Aqueous fraction*	MT/day	72	173	352	541	56	274	283	422
Surplus electricity	MW	0.42	1.03	2.10	3.24	1.62	7.95	8.22	12.25
Energy demand									
Heating	MW	17.1	41.2	83.8	129.0	17.0	83.3	86.0	128.2
Cooling	MW	4.14	9.95	20.24	31.17	7.72	37.79	39.03	58.18
Power	MW	0.65	1.56	3.17	4.88	0.84	4.09	4.23	6.29
Energy resources									
Char	MT/day	23	55	112	172	-	-	-	-
	MW	8	19	39	61	-	-	-	-
Non-condensable gas*	MT/day	76	183	372	573	65	318	329	490
	MW	11	26	53	82	20	96	99	147

†Non-catalytic (NC) and catalytic (C) pyrolysis for biomass collection within a 100, 200 and 300 km radius of the biorefinery, and NC and C at the required biorefinery capacity to co-process 5 and 10 wt. % bio-oil, respectively

‡Dry basis (8.28 wt. % moisture)

*Based on unreconciled mass balance yield

The total energy recovered in bio-oil and biochar products based on a mass basis of forest residues is 10.97 and 9.39 MJ/kg (61.9 and 53.0 % of biomass HHV) for non-catalytic and catalytic pyrolysis biorefinery scenarios, respectively. All of the non-condensable gases and 21.5 wt. % of the char yield (in the non-catalytic pyrolysis biorefinery scenarios) were combusted to provide heat for the pyrolysis reactor, and to produce steam for the dryer and power for the biorefinery. The total energy supplied on a mass basis of forest residues is 4.43 and 4.58 MJ/kg (25.0 and 25.9 % of biomass HHV) for non-catalytic and catalytic pyrolysis biorefinery scenarios, respectively.

The total heating demand on a mass basis of forest residues is approximately 4 MJ/kg (about 22.6 % of the biomass HHV). The total heating demand of all biorefinery scenarios is almost the same

but the heating demand distribution is significantly different for non-catalytic and catalytic pyrolysis biorefinery scenarios as shown in Figure 20.

The pyrolysis reactor is one of the key energy consumers in the biorefinery. The pyrolysis reactor heating demand is the summation of the heat required to increase the temperature of the feed to 500 °C and the heat required for the pyrolysis reaction itself. The specific enthalpy of the pyrolysis reaction (denoted as h_p) was 1.41 MJ/kg and 0.12 MJ/kg for non-catalytic and catalytic pyrolysis, respectively. The result for non-catalytic pyrolysis is in good agreement with previous studies. Daugaard and Brown (2003) estimated h_p for fast pyrolysis conducted in a pilot-scale reactor at 500 °C with oak wood chips (8 wt. % moisture) as 1.61 MJ/kg (Daugaard & Brown, 2003). Onarheim, Solantausta and Lehto (2015) reported h_p for fast pyrolysis simulated in Aspen Plus™ at 500 °C with pine wood chips (8 wt. % moisture) as 1.78 MJ/kg (Onarheim et al., 2015). Yang and colleagues (2013) investigated pyrolysis at 500 °C with cedar wood chips for variable heating rates (0.5 to 5.3 °C/s) from slow to intermediate pyrolysis conditions. The authors found that h_p (on a dry basis) increased with heating rate from 1.1 MJ/kg at 0.5 °C/s to 1.2 MJ/kg at 5.3 °C/s (Yang, Kudo, Kuo, Norinaga, Mori, Ondrej & Hayashi, 2013). On the other hand, h_p was far less for catalytic pyrolysis compared to non-catalytic pyrolysis because of the exothermic reaction taking place between the CaO catalyst and carbon dioxide inside the pyrolysis reactor (Veses *et al.*, 2014; Zhao, Zhang, Chen, Sun, Si & Chen, 2014).

In the catalytic pyrolysis biorefinery scenarios, the heating demand for the pyrolysis reactor, dryer and power for the biorefinery could have been met by only burning a portion of the non-condensable gas produced, however, this would have a negative effect on the environmental impact of the biorefinery as the non-condensable gas contained high concentrations of carbon monoxide and methane gases therefore, all of the non-condensable gas produced was combusted to produce surplus electricity that was sold to the grid. Thus, the heating demand for power generation in catalytic pyrolysis was greater than non-catalytic pyrolysis.

The biomass was dried from 40 to 8.28 wt. % moisture in two stages: the first stage involved drying the biomass by direct contact with hot flue gases, and the second stage involved drying the biomass by indirect contact with steam. The first stage of drying reduced the biomass moisture content by 28.1 wt. % for catalytic pyrolysis as opposed to 12.8 wt. % for non-catalytic pyrolysis. The significant difference in drying efficiency is directly related to the amount of flue gases produced. Catalytic pyrolysis produced more flue gases than non-catalytic pyrolysis because 85 vol. % excess air was required to keep the outlet temperature of the combustor below 1100 °C compared to 20 vol. % for non-catalytic pyrolysis. Therefore, the heating demand for the indirect dryer was higher for the non-catalytic pyrolysis biorefinery scenarios than the catalytic pyrolysis biorefinery scenarios.

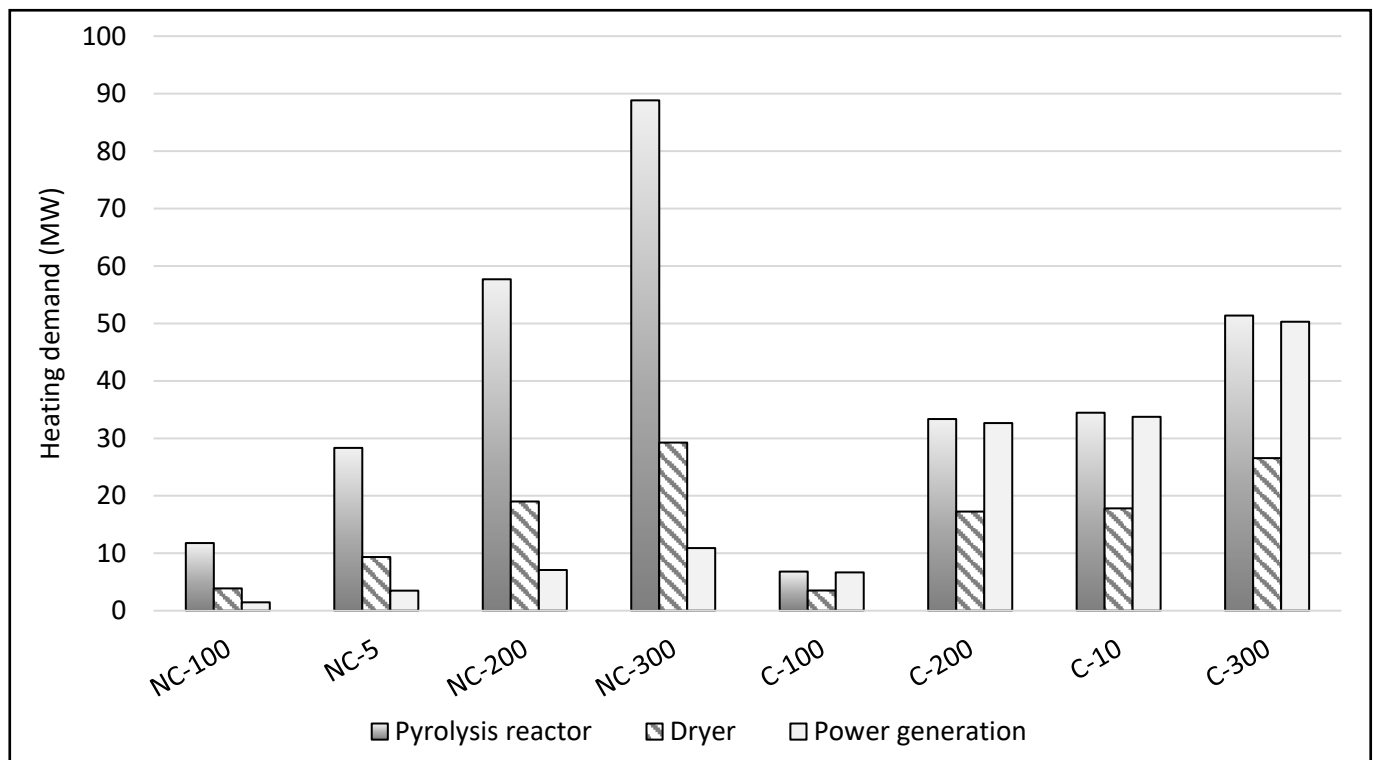


Figure 20: Heating demand distribution for each biorefinery scenario

The total cooling demand on a mass basis of forest residues is approximately 0.97 and 1.81 MJ/kg for non-catalytic and catalytic pyrolysis biorefinery scenarios, respectively. The cooling demand distribution is depicted in Figure 21. The cooling demand for the condenser train, in particular C1 and C2, was lower for catalytic than non-catalytic pyrolysis because catalytic pyrolysis produced less bio-oil than non-catalytic pyrolysis. Furthermore, the absorption of CO₂ by the CaO catalyst in the pyrolysis reactor upstream from the condenser train resulted in an even lower cooling demand for catalytic pyrolysis. Catalytic pyrolysis also produced more steam for power generation than non-catalytic pyrolysis therefore, the cooling demand to condense the low pressure steam discharged from the second turbine was higher.

The total cooling demand is met by about 95.0 and 95.8 % cooling water with the remainder chilled water for non-catalytic and catalytic pyrolysis biorefinery scenarios, respectively. A similar study by Dutta and colleagues (2015) fulfilled a small portion of the cooling demand for a catalytic pyrolysis biorefinery with cooling water (0.64 MJ/kg feedstock with 10 wt. % moisture) and chilled water (0.27 MJ/kg) but the majority of the cooling demand was met by air-cooling (5.95 MJ/kg) (Dutta *et al.*, 2015). In brief, air-coolers require more capital cost than water coolers but air-coolers reduce operating cost by eliminating water lost and wastewater generated through cooling tower evaporation and blowdown (Mandegari, Farzad & Gorgens, 2016). The total cooling demand for catalytic pyrolysis in the compared study (6.86 MJ/kg) is considerably higher than this study (1.81 MJ/kg) because almost

three times more power was produced (Dutta et al., 2015). Therefore, the cooling demand to condense the low pressure steam discharged from the second turbine was much greater.

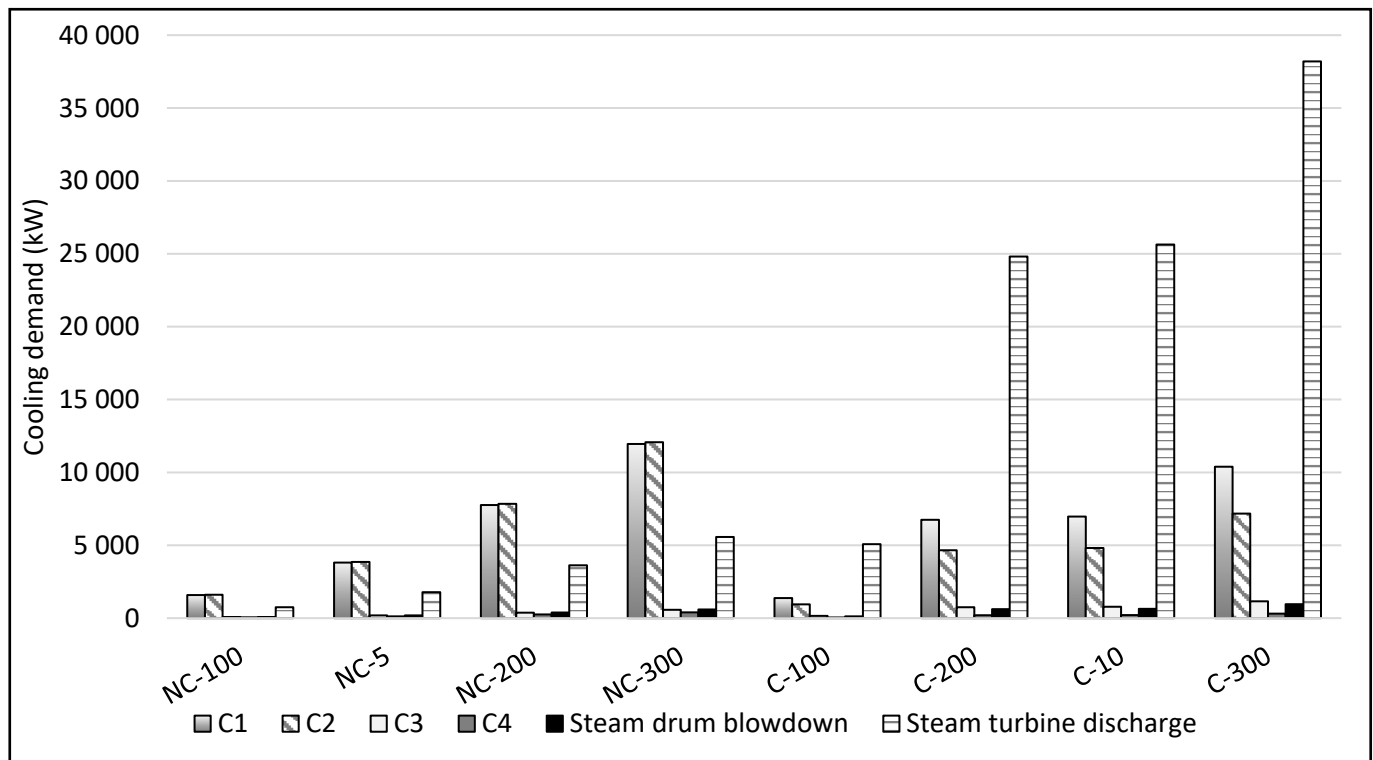


Figure 21: Cooling demand distribution for each biorefinery scenario

The total power demand on a mass basis of forest residues is approximately 0.15 and 0.20 MJ/kg for non-catalytic and catalytic pyrolysis biorefinery scenarios, respectively. The power demand distribution is given in Figure 22. The grinder consumed the most power in each biorefinery scenario, contributing to about 51 and 39 % of the total power demand for non-catalytic and catalytic pyrolysis, respectively. Grinding has previously been reported as an energy-intensive process (Bridgwater, Toft & Brammer, 2002; Wright *et al.*, 2010). The total power demand for catalytic pyrolysis was higher than non-catalytic pyrolysis because the cooling demand was greater, and 85 vol. % excess air was required to keep the outlet temperature of the combustor below 1100 °C for catalytic pyrolysis versus 20 vol. % for non-catalytic pyrolysis. Therefore, more power was consumed by the fans driving the air and flue gases through the combustor and direct dryer.

Finally, the overall heating, cooling and power demand per litre of bio-oil produced (kW/L) from non-catalytic and catalytic pyrolysis biorefinery scenarios are compared in Figure 23. Heating and power demands for non-catalytic and catalytic pyrolysis biorefinery scenarios were comparable overall, while catalytic pyrolysis required more cooling per litre of bio-oil produced than non-catalytic pyrolysis.

Process heat was recovered to satisfy the heating (steam for the indirect dryer) and power demands of the biorefinery, which characterized the process as entirely energy self-sufficient. The excess electricity produced was minimised as far as possible and sold to the grid at Eskom’s bulk electricity selling price (R0.81/kWh or \$0.06/kWh (Motiang & Nembahe, 2017)), and not at the higher renewable electricity selling price (R2.22/kWh or \$0.16/L (Eskom, 2019)) since the excess electricity produced was not a main product of the biorefinery.

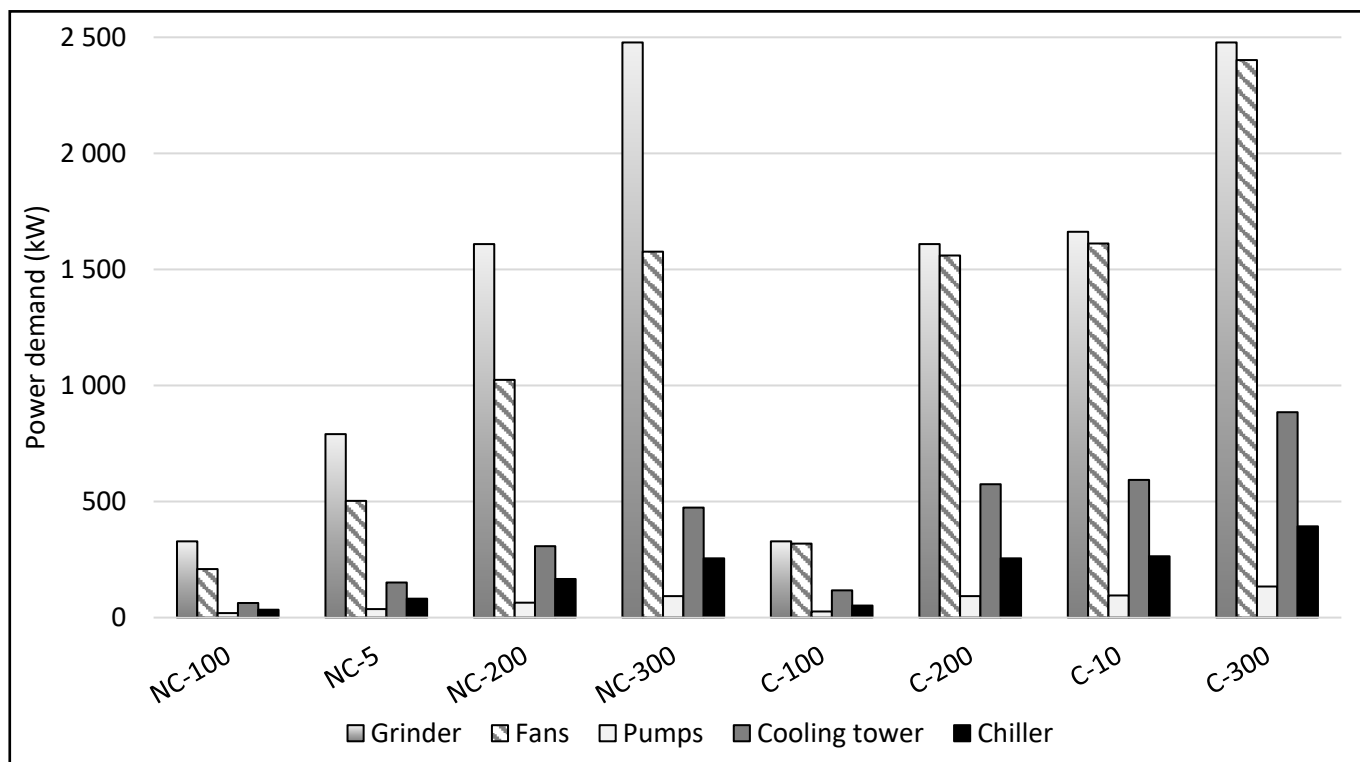


Figure 22: Power demand distribution for each biorefinery scenarios

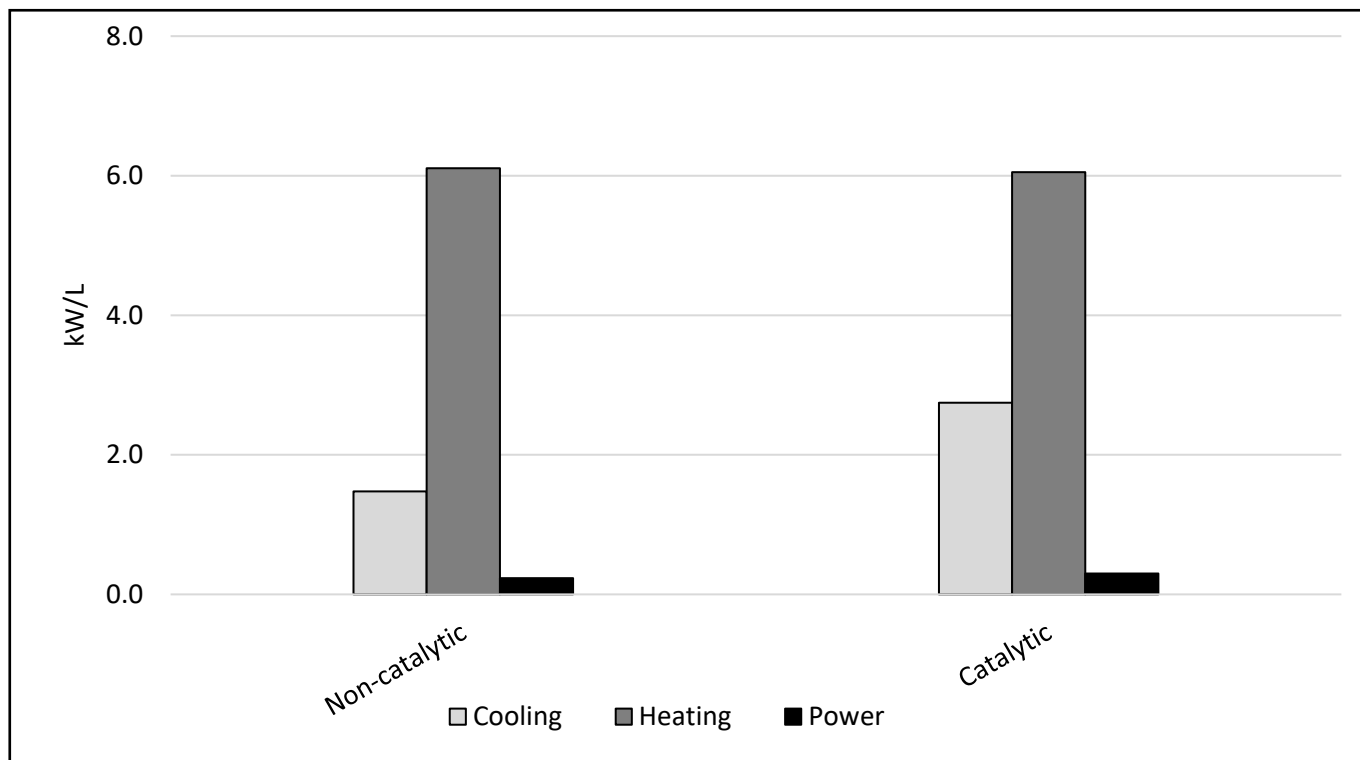


Figure 23: Overall heating, cooling and power demand per litre of bio-oil produced

5.1.2 Water balance

It is also important to consider water consumption in the overall performance evaluation of the biorefinery scenarios due to the limited water resources in South Africa. A summary of the process water and wastewater required and generated for each biorefinery scenario is given in Table 29. The total wastewater generated was 1.05 and 1.72 kg/kg forest residues (8.28 wt. % moisture) for non-catalytic and catalytic pyrolysis biorefinery scenarios, respectively, and was mostly made up of the cooling tower blowdown. The wastewater generated by the catalytic pyrolysis biorefinery in a similar study by Dutta and colleagues (2015) was predictably lower at 0.43 kg/kg feedstock (10 wt. % moisture) than the wastewater generated by the catalytic pyrolysis biorefinery scenarios in this study because the former mostly made use of air-cooling rather than water-cooling to meet the cooling demands of the biorefinery (Dutta *et al.*, 2015).

Table 29: Water balance (MT/day) for each biorefinery scenario

Scenario†		NC-100	NC-5	NC-200	NC-300	C-100	C-200	C-10	C-300
Process water	BFW makeup	7	16	33	51	11	53	55	82
	Cooling water makeup	468	1 123	2 284	3 517	871	4 263	4 404	6 564
Wastewater	Steam drum blowdown	7	16	33	51	11	53	55	82
	Cooling tower blowdown	300	720	1 465	2 256	559	2 734	2 825	4 210
	Aqueous fraction	82	198	403	620	66	321	332	495

†Non-catalytic (NC) and catalytic (C) pyrolysis for biomass collection within a 100, 200 and 300 km radius of the biorefinery, and NC and C at the required biorefinery capacity to co-process 5 and 10 wt. % bio-oil, respectively.

5.2 Economic analysis results

The economic analysis was developed based on the mass and energy balance results, and involved estimating capital and operating costs for the profitability and sensitivity analyses. The economic analysis results for non-catalytic and catalytic pyrolysis biorefinery scenarios are presented and discussed below.

5.2.1 Capital cost estimation

The mass and energy balance results were used to size and subsequently cost process equipment for each biorefinery scenario. The total installed equipment cost, direct cost, indirect cost, Fixed Capital Investment (FCI) and Total Capital Investment (TCI) for each biorefinery scenario is given in Table 30. A summary of the purchased equipment costs, installation factors and scaling factors used to determine the installed equipment costs is given Table C1 in Appendix C. Further details on the calculation of FCI and TCI for each biorefinery scenario are given in Table C2 in Appendix C. The assumed cost of land was R952 141/ha (~\$68 000/ha) based on the average cost of land in the area surrounding the biorefinery. The area of land required was calculated based on a 2000 dry MT/day biorefinery requiring approximately 463 ha of land (Dutta *et al.*, 2015).

Table 30: Summary of total installed equipment cost, direct cost, indirect cost, FCI and TCI (Million \$) for each biorefinery scenario

Scenario†	NC-100	NC-5	NC-200	NC-300	C-100	C-200	C-10	C-300
Total Installed Equipment Cost	54.7	99.2	161.8	218.5	64.3	194.5	199.0	264.3
Total direct cost	61.8	112.4	183.7	248.3	72.5	220.1	225.2	299.4
Total indirect cost	37.1	67.5	110.2	149.0	43.5	132.1	135.1	179.7
Fixed Capital Investment	98.9	179.9	294.0	397.2	116.0	352.2	360.4	479.1
Total Capital Investment	104.4	190.2	311.3	421.1	122.3	372.4	381.1	507.0

†Non-catalytic (NC) and catalytic (C) pyrolysis for biomass collection within a 100, 200 and 300 km radius of the biorefinery, and NC and C at the required biorefinery capacity to co-process 5 and 10 wt. % bio-oil, respectively.

The TCI for each biorefinery scenario in this study is compared to the TCI for similar studies against biorefinery capacity in Figure 24. The TCI for catalytic pyrolysis is higher than non-catalytic pyrolysis at the same biorefinery capacity mostly because of the extra processing capacity required for the catalyst. The TCI reported for catalytic pyrolysis in this study is significantly lower than the TCI reported for catalytic pyrolysis by Dutta and colleagues (2015) because hydrotreating process units were added after catalytic pyrolysis to further upgrade bio-oil into gasoline and diesel-quality fuels (Dutta *et al.*, 2015). Jones and colleagues (2013) conducted a techno-economic analysis (TEA) to produce gasoline and diesel-quality fuels via fast pyrolysis followed by hydrotreating (Jones *et al.*, 2013). The TCI reported was higher than both non-catalytic and catalytic pyrolysis biorefinery scenarios in this study. Co-processing crude or upgraded bio-oil in an oil refinery to produce gasoline and diesel-quality fuels instead of a costly hydrotreating step is advantageous for the economic feasibility of the biorefinery scenarios in this study.

The TCI reported for non-catalytic pyrolysis in this study is significantly higher than the TCI reported in similar studies (Nsafu, Görgens & Knoetze, 2013; Ringer *et al.*, 2006). The compared studies excluded installed equipment costs for wastewater treatment and reported lower installed equipment costs for the pyrolysis section of the biorefinery as presented in Table 31. The pyrolysis reactors were costed based on individual pieces of equipment (Ringer *et al.*, 2006) and literature (Nsafu *et al.*, 2013), whereas the pyrolysis reactor in this study was costed based on a vendor quote. The installed equipment cost of the catalytic pyrolysis reactor in this study is agreeable with the study by Dutta and colleagues (2015), which also costed the catalytic pyrolysis reactor based on a vendor quote (Dutta *et al.*, 2015). Furthermore, the only difference between the installed equipment cost of the non-catalytic and catalytic pyrolysis reactors in this study is the capacity required for the catalyst therefore, the TCI for non-catalytic pyrolysis is reasonable.

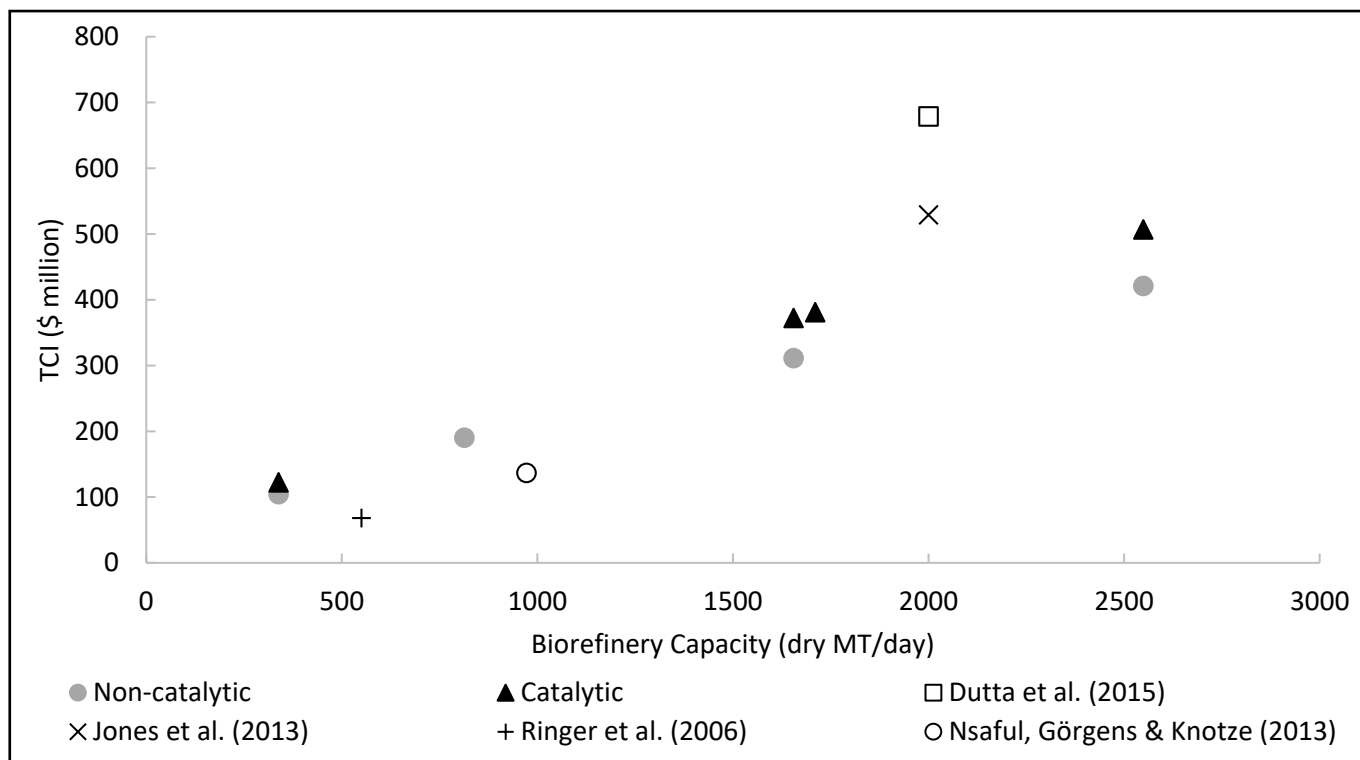


Figure 24: Comparison between TCI for non-catalytic and catalytic biorefinery scenarios in this study and similar studies (adjusted to 2017\$)

Table 31: Installed equipment cost for the pyrolysis section of the biorefinery

Reference	Biorefinery Capacity (dry MT/day)	Installed Cost (2017\$)
(Ringer <i>et al.</i> , 2006)	550	5 533 831
(Nsaful <i>et al.</i> , 2013)	972	7 106 087
(Dutta <i>et al.</i> , 2015)	2000	89 625 662
This study (non-catalytic)	2549	90 457 375
This study (catalytic)	2549	116 364 134

The installed equipment costs per section of the catalytic pyrolysis biorefinery in this study were compared and verified with the study by Dutta and colleagues (2015) as shown in Table 32. Less electricity was produced in this study (12.0 and 18.5 MW for 1655 and 2549 dry MT/day biorefinery capacities, respectively) than in the compared study (43.2 MW) therefore, the installed equipment cost for steam and power production was significantly more for the latter. The installed equipment cost for wastewater treatment in the compared study was also higher, due to the additional wastewater produced during hydrotreating. Hydrotreating contributed to 34.7 % of the overall TCI for the compared study, which is a significant saving for the biorefinery scenarios in this study as bio-oil can be co-processed in an existing oil refinery without a dedicated hydrotreating unit.

Table 32: Installed equipment costs (Million 2017\$) per section of the catalytic pyrolysis biorefinery

Reference	(Dutta <i>et al.</i> , 2015)	This study	
Biorefinery capacity (dry MT/day)	2 000	1 655	2 549
TCI (Million 2017\$)	678.8	372.4	507.0
Pre-treatment	0.5*	38.0	56.0
<i>In situ</i> catalytic pyrolysis	89.6	86.0	116.0
Product recovery	21.7	18.0	22.0
Hydrotreating	31.5	-	-
Hydrogen plant	68.4	-	-
Heat recovery	-	4.0	6.0
Steam and power production	50.8	14.0	19.0
Wastewater treatment	16.7	8.0	11.0
Utilities	9.1	5.0	7.0
Storage	-	20.0	27.0

*Installed equipment costs were mostly included in biomass cost price

The total installed equipment cost per section of the biorefinery based on the total volume of bio-oil produced per year for non-catalytic and catalytic pyrolysis biorefinery scenarios are compared in Figure 25 to demonstrate the significant economy-of-scale benefit, and predict hotspots that will influence the economic feasibility of the biorefinery scenarios. Section A2000 (pyrolysis) contributed the most to the total installed equipment cost of all biorefinery scenarios. Catalytic pyrolysis resulted in higher installed equipment costs for Section A2000 than non-catalytic pyrolysis because of the increased pyrolysis reactor capacity required for the catalyst. Section A1000 (pre-treatment) also contributed significantly to the total installed equipment cost of all biorefinery scenarios. Similarly, catalytic pyrolysis produced higher installed equipment costs for Section A1000 than non-catalytic pyrolysis because of the additional biomass/catalyst mixer and the increased biomass preheater capacity required to remove heat from the CaO and CaCO₃ present in the char. On the other hand, non-catalytic pyrolysis generated higher installed equipment costs for Section A3000 (product recovery) than catalytic pyrolysis since non-catalytic pyrolysis produced more bio-oil and non-condensable gas (19.8 and 20.6 wt. %) than catalytic pyrolysis (18.4 and 17.6 wt. %). Finally, catalytic pyrolysis resulted in higher installed equipment costs for Section A5000 (steam and power production) than non-catalytic pyrolysis as catalytic pyrolysis produced more electricity than non-catalytic pyrolysis.

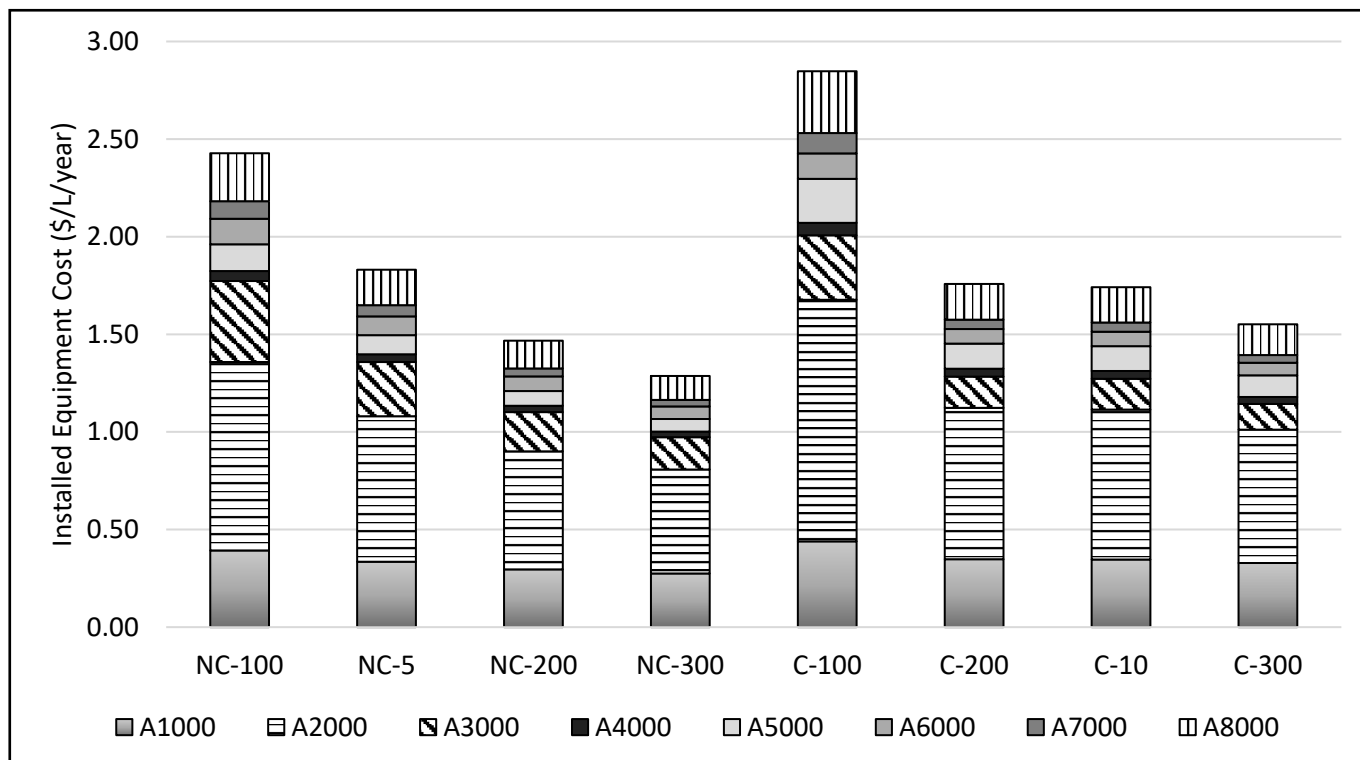


Figure 25: Breakdown of installed equipment costs per section for each biorefinery scenario - Sections A1000 (pre-treatment), A2000 (pyrolysis), A3000 (product recovery), A4000 (heat recovery), A5000 (steam and power production), A6000 (wastewater treatment), A7000 (utilities) and A8000 (storage) - Non-catalytic (NC) and catalytic (C) pyrolysis for biomass collection within a 100, 200 and 300 km radius of the biorefinery, and NC and C at the required biorefinery capacity to co-process 5 and 10 wt. % bio-oil, respectively

5.2.2 Operating cost estimation

Operating costs are estimated on a per annum basis and categorised as either fixed or variable operating costs. The total fixed operating cost for each biorefinery scenario consists of employee salaries, benefits and overheads, maintenance, and insurance and taxes. The total variable operating cost for each biorefinery scenario is made up of feedstock, process water, auxiliary chemicals, wastewater and ash disposal costs. In addition, catalytic pyrolysis biorefinery scenarios also have the catalyst as a variable operating cost. The total fixed and variable operating costs for each biorefinery scenario are given in Table 33. Details for the calculation of total fixed and variable operating costs for each biorefinery scenario are given in Table C3 in Appendix C.

The \$20.20 million/year total operating cost for the 813 dry MT/day biorefinery capacity (Scenario NC-5) in this study was significantly lower than the \$47.27 million/year total operating cost for a 1000 dry MT/day biorefinery capacity in a similar study (Wang & Jan, 2018) because natural gas (for heating) and electricity were bought in, and the rice husk biomass was more expensive at \$30/MT. The total fixed operating cost for the catalytic pyrolysis biorefinery scenarios in this study was agreeable with a similar study (Dutta et al., 2015), but the total variable operating cost for this study

was once again lower than the compared study due to a higher biomass cost of \$80/MT (including \$24.67/MT for grinding and drying (Jacobson, Roni, Lamers & Cafferty, 2014)). Biomass cost in South Africa and other developing countries is considerably lower than the United States and Europe (IEA Renewable Energy Division, 2010). This will have a significant impact on the economic feasibility of the biorefinery scenarios in this study, and possibly attract foreign investors to the country.

Table 33: Fixed, variable and total operating costs (Million \$) for each biorefinery scenario

Scenario†	NC-100	NC-5	NC-200	NC-300	C-100	C-200	C-10	C-300
Total fixed operating costs	6.0	11.1	18.6	26.6	6.6	20.8	21.2	29.6
Total variable operating costs	3.3	9.2	20.7	35.7	11.4	60.2	62.9	96.6
Total operating costs	9.4	20.2	39.3	62.3	18.1	81.0	84.2	126.2

†Non-catalytic (NC) and catalytic (C) pyrolysis for biomass collection within a 100, 200 and 300 km radius of the biorefinery, and NC and C at the required biorefinery capacity to co-process 5 and 10 wt. % bio-oil, respectively.

The total fixed operating cost for catalytic pyrolysis biorefinery scenarios is slightly higher than non-catalytic pyrolysis biorefinery scenarios because maintenance, and insurance and taxes were costed based on the FCI. The total variable operating cost for catalytic pyrolysis, on the other hand, is significantly higher than non-catalytic pyrolysis due to the added cost of the catalyst. The contribution of fixed and variable operating costs to the total operating cost based on the total volume of bio-oil produced per year is shown in Figure 26. The individual contributions of process water, auxiliary chemicals, wastewater and ash disposal costs to the total operating cost of each biorefinery scenario were minor therefore, these costs were combined under the legend *other variable costs*. Feedstock, catalyst (in catalytic pyrolysis biorefinery scenarios) and maintenance costs contributed the most to the total operating cost for each biorefinery scenario. Feedstock cost increased with biomass transport distance from the biorefinery, which cancelled out the economy-of-scale benefit for the total operating cost beyond a 200 km radius of the biorefinery. However, the economy-of-scale benefit is far greater for the capital cost estimate up to a 300 km radius of the biorefinery, which will influence the economic feasibility of the biorefinery scenarios more significantly than the operating cost estimate.

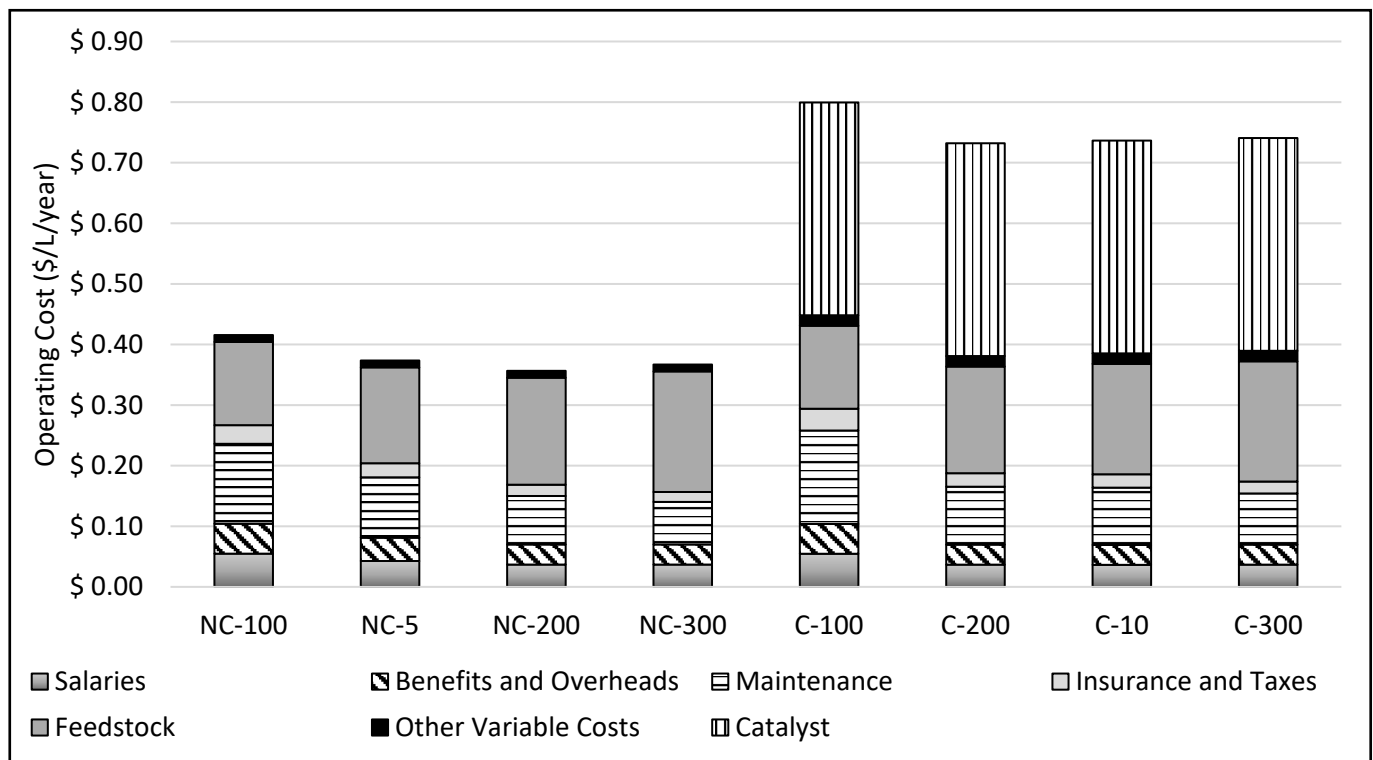


Figure 26: Fixed and variable operating costs contribution to total operating cost for each biorefinery scenario – Sections A1000 (pre-treatment), A2000 (pyrolysis), A3000 (product recovery), A4000 (heat recovery), A5000 (steam and power production), A6000 (wastewater treatment), A7000 (utilities) and A8000 (storage) - Non-catalytic (NC) and catalytic (C) pyrolysis for biomass collection within a 100, 200 and 300 km radius of the biorefinery, and NC and C at the required biorefinery capacity to co-process 5 and 10 wt. % bio-oil, respectively

5.2.3 Profitability analysis

The capital and operating cost estimates were used to perform a Discounted Cash Flow Rate of Return (DCFROR) analysis to determine the profitability of the biorefinery scenarios. The Minimum Selling Price (MSP) of bio-oil for each biorefinery scenario is reported in Table 34 based on the unreconciled bio-oil yield previously reported in Table 28, while the MSP of bio-oil based on the reconciled bio-oil yield will be evaluated through a sensitivity analysis in Section 5.2.5. The non-catalytic and catalytic pyrolysis biorefinery capacities reported in Table 34 were chosen based on the biomass collection distance from the biorefinery, and the amount of crude and upgraded bio-oil required to co-process 5 and 10 wt. % at the *Natref* oil refinery, respectively.

Table 34: MSP (\$/L) of bio-oil for each biorefinery scenario

Scenario†	Biorefinery Capacity (dry MT/day)	MSP (\$/L)	
		IRR = 10 %	IRR = 22 %
NC-100	338	0.62	1.51
NC-5	813	0.42	1.09
NC-200	1 655	0.31	0.85
NC-300	2 549	0.27	0.75
C-100	338	1.18	2.21
C-200	1 655	0.82	1.47
C-10	1710	0.82	1.46
C-300	2 549	0.77	1.35

†Non-catalytic (NC) and catalytic (C) pyrolysis for biomass collection within a 100, 200 and 300 km radius of the biorefinery, and NC and C at the required biorefinery capacity to co-process 5 and 10 wt. % bio-oil, respectively.

Crude and upgraded bio-oils can be co-processed with vacuum gas oil (VGO) in an FCC unit to produce bio-derived transportation fuels. VGO is an intermediate product between crude-oil distillation, and gasoline and diesel production therefore, VGO does not have an available market price that can be used as a benchmark for the selling price of bio-oil. A market price can be estimated though based on the crude-oil price and the Basic Fuel Price (BFP) set by the government. Brent Crude is considered the benchmark for crude-oil prices in South Africa (Motiang & Nembahe, 2017), and sold for an average value of \$54.71/bbl in 2017 (Macrotrends, 2019). Additionally, the average value for the BFP in 2017 was \$65.19/bbl (Department of Energy, 2019). The market price of VGO lies between these two values, and is estimated based on a percentage of the total production cost for the oil refinery. Li and colleagues (2013) reported the average production cost for oil refineries in China per section of the oil refinery (Li, Fu, Ma, Liu, Li & Dai, 2013). Crude-oil distillation accounted for approximately 13.81 % of the production cost less the crude-oil price therefore, the market price of VGO in 2017 was estimated as \$56.16/bbl or \$0.35/L. The MSP of crude and upgraded bio-oils for biomass collection within a 100, 200 and 300 km radius of the biorefinery is compared to the estimated market price of VGO in Figure 27.

There is a significant decrease in MSP overall from a 100 to 200 km radius of the biorefinery relating to an increase in biorefinery capacity from 338 to 1655 dry MT/day. Thereafter, the MSP slightly decreases again from a 200 to 300 km radius of the biorefinery relating to an increase in biorefinery capacity from 1655 to 2549 dry MT/day. There is a clear economy-of-scale benefit up to a 300 km radius of the biorefinery for both non-catalytic and catalytic pyrolysis processes. However, the MSP of upgraded bio-oil (as expected from the capital and operating cost estimates) is higher than the

MSP of crude bio-oil for the same Internal Rate of Return (IRR). The MSP of crude bio-oil at a nominal 10 % IRR fell below the estimated market price of VGO at \$0.31/L and \$0.27/L corresponding to a 200 and 300 km radius of the biorefinery. However, the MSP of both crude and upgraded bio-oils at a more desirable 22 % IRR was at least \$0.39/L and \$0.99/L above the estimated market price of VGO, respectively. The price premium of crude and upgraded bio-oils though can be substantiated by their environmental benefit over fossil-derived VGO, which will be evaluated in Section 5.3.

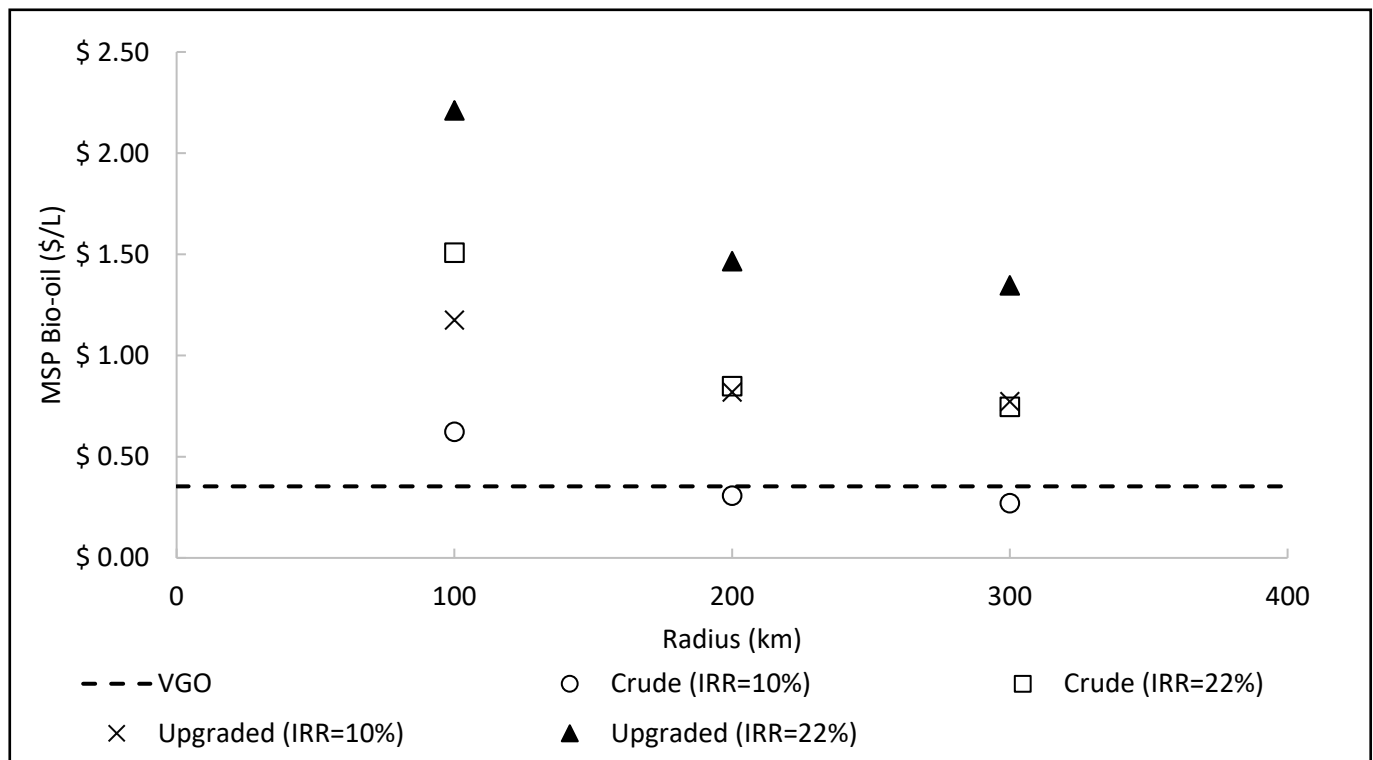


Figure 27: MSP (\$/L) of crude and upgraded bio-oils for biomass collection within a 100, 200 and 300 km radius of the biorefinery

The water content, oxygen content, LHV and HHV of crude and upgraded bio-oils produced via non-catalytic and catalytic pyrolysis compared to VGO are given in Table 35. Upgraded bio-oil more closely resembles VGO in energy value than crude bio-oil. Therefore, it is important to also compare the MSP of crude and upgraded bio-oils on a gasoline gallon equivalent (GGE) basis. The MSP was converted to a GGE basis using the LHV of crude and upgraded bio-oils. A litre of crude bio-oil is equivalent to 0.65 litres of gasoline, and a litre of upgraded bio-oil is equivalent to 0.77 litres of gasoline. The MSP of crude and upgraded bio-oils on a GGE basis for biomass collection within a 100, 200 and 300 km radius of the biorefinery is compared to the estimated market price of VGO in Figure 28. The MSP of crude bio-oil remains lower than the MSP of upgraded bio-oil overall. However, the MSP of upgraded bio-oil is slightly closer to the MSP of crude bio-oil at a desired 22 % IRR, which indicates that upgraded bio-oil is actually more competitive with crude bio-oil. Furthermore, a litre of

VGO is equivalent to 1.26 litres of gasoline therefore, the MSP of crude bio-oil at the nominal 10 % IRR rose above the market value of VGO for biomass collection within a 300 km radius of the biorefinery.

Table 35: Properties of bio-oils produced via non-catalytic and catalytic pyrolysis compared to VGO

	Non-catalytic	Catalytic	VGO
Water (wt. %)	16.1	25.6	0.6 ^a
Oxygen (wt. %, db)	35.8	14.0	0.3 ^a
LHV (MJ/kg, db)	23.0	33.2	43.0 ^b
HHV (MJ/kg, db)	24.5	34.7	45.0 ^b

a. (Lindfors *et al.*, 2015)

b. (Jechura, 2016)

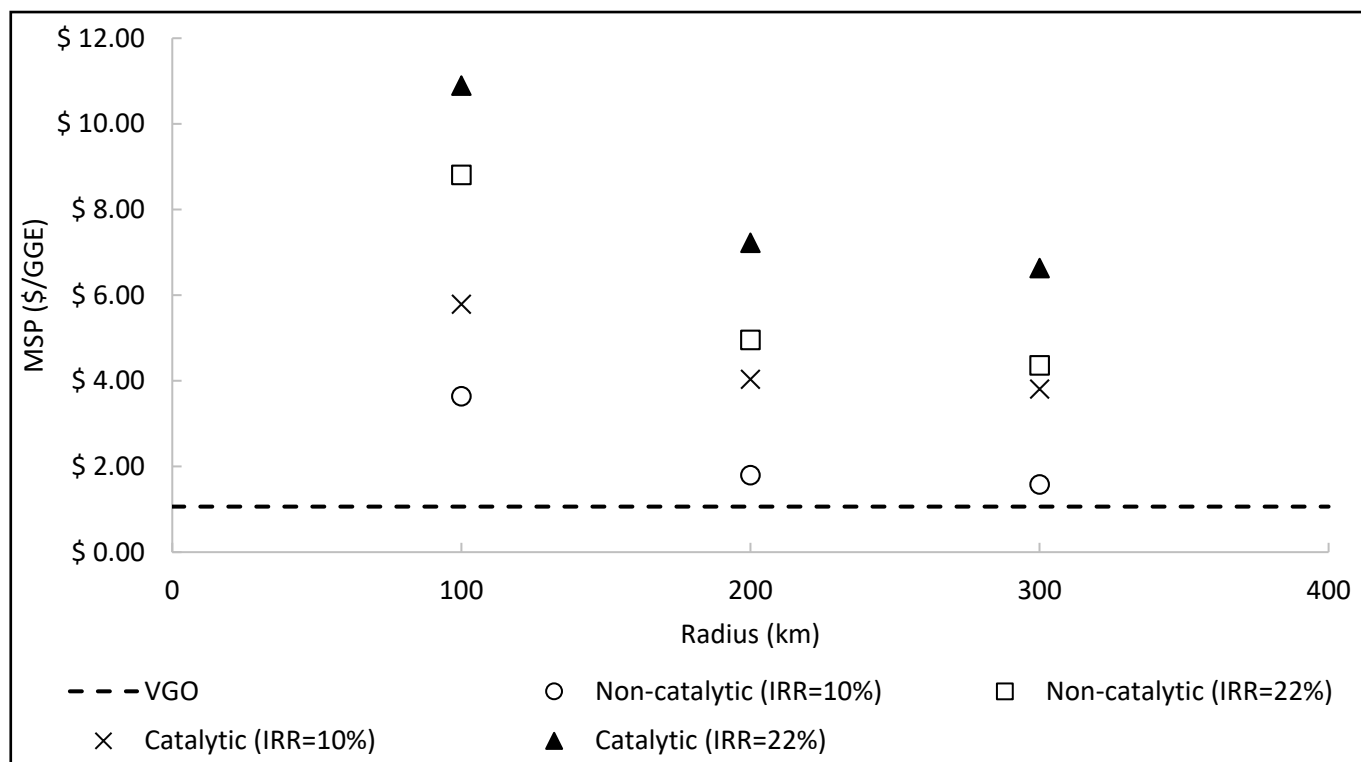


Figure 28: MSP (\$/GGE) of crude and upgraded bio-oils for biomass collection within a 100, 200 and 300 km radius of the biorefinery

The higher MSP of upgraded bio-oil can be justified over the lower MSP of crude bio-oil by its superior quality and suitability for co-processing. The impact on product yield and quality are unknown for co-processing bio-oil in an industrial-scale FCC unit but can be likened to co-processing bio-oil in a pilot-scale FCC unit. Co-processing 10 wt. % upgraded bio-oil at pilot-scale had little effect on gasoline yield, while co-processing the same amount of crude bio-oil decreased gasoline yield from 41.1 wt. % (pure VGO catalytic cracking) to 37.5 wt. % (Wang *et al.*, 2018). Co-processing 5 wt. % crude bio-oil had

negligible effect on gasoline yield but the renewable carbon content of the total liquid produced was substantially lower at 1.0 wt. % (Pinho *et al.*, 2017) than the 5.6 to 7.0 wt. % renewable carbon content achieved when 10 wt. % upgraded bio-oil was co-processed (Wang *et al.*, 2016, 2018). Oil refineries in South Africa will be looking to offset their anthropogenic carbon emissions with the implementation of the Carbon Tax Act on 1 June 2019 (Republic of South Africa, 2019), which could make co-processing upgraded bio-oil more attractive than crude bio-oil if the carbon tax saving outweighs the difference in MSP.

Co-processing crude and (to a lesser extent) upgraded bio-oils at pilot-scale produces CO₂, CO and H₂O gaseous products as a result of deoxygenation reactions (Wang *et al.*, 2018). Modifications related to pressure build-up and increased capacity for existing FCC units at oil refineries may be required to accommodate these gaseous products (van Dyk *et al.*, 2019). Bio-oil with a high water content may also damage FCC catalysts and impact downstream processing. Furthermore, the construction materials of most existing FCC units at oil refineries may be susceptible to the corrosivity of bio-oil (Talmadge *et al.*, 2014). The additional costs that the oil refinery may incur due to crude bio-oil co-processing are mostly unknown but based on the observations made by other researchers, it is reasonable to suggest that these costs will be less for upgraded bio-oil co-processing.

An oil refinery such as *Natref* could co-process 5 wt. % crude bio-oil for \$1.09/L or 10 wt. % upgraded bio-oil for \$1.46/L at the desired 22 % IRR. Alternatively, oil refineries such as *Enref* and *Sapref* could collaborate with *Natref* to benefit from economy-of-scale by co-processing crude and upgraded bio-oils at the lowest price of \$0.75/L and \$1.35/L for a desired 22 % IRR, respectively. The MSP of crude bio-oil for a nominal 10 % IRR is at best \$0.27/L, which falls below the average BFP of \$0.41/L in 2017 (Department of Energy, 2019), while the MSP of upgraded bio-oil for a nominal 10 % IRR is almost double the BFP at \$0.77/L. However, investors are looking for higher returns for innovative projects associated with high financial risk therefore, in addition to carbon tax rebates, oil refineries would require government subsidisation to make co-processing crude and upgraded bio-oils economically viable.

The MSP (\$/L) of crude and upgraded bio-oils produced via non-catalytic and catalytic pyrolysis in this study are compared to the MSP of bio-oils produced in similar studies against biorefinery capacity in Figure 29. The crude bio-oil MSP of \$0.42/L for a 813 dry MT/day biorefinery capacity (Scenario NC-5) in this study is significantly lower than the MSP of \$0.56/L for a 1000 dry MT/day biorefinery capacity in the compared study (Wang & Jan, 2018), because of the differences in biochar selling price (\$357/MT versus \$100/MT) and biomass cost price (\$19/MT versus \$30/MT). The biochar in the compared study had a low carbon content of 20.4 wt. % as a result of fast pyrolysis conditions, which limited its selling price. The production of high quality biochar in addition to bio-oil is an advantage of the intermediate pyrolysis conditions in this study. Alternatively, Ringer and colleagues (2006) reported lower installed equipment costs for a 550 dry MT/day biorefinery capacity than the

338 dry MT/day biorefinery capacity (Scenario NC-100) in this study therefore, the reported MSP of \$0.21/L for crude bio-oil was unsurprisingly lower (Ringer *et al.*, 2006).

The MSP of \$0.82/L and \$0.77/L for upgraded bio-oil production corresponding to a 1655 and 2549 dry MT/day biorefinery capacity (Scenarios C-200 and C-300) in this study falls within the range reported in literature (\$0.57/L to \$1.11/L) corresponding to a 2000 dry MT/day biorefinery capacity. However, the MSP of \$0.57/L (Anex *et al.*, 2010) and \$0.60/L (Wright *et al.*, 2010) was reported for upgraded bio-oil production via hydrotreating with hydrogen purchased (anthropogenic) instead of produced onsite (usually biogenic), which is cheaper but has a negative impact on the environment. Most of the reported studies supplemented the hydrogen produced from the pyrolysis process with a small amount of hydrogen produced from steam reforming natural gas (Dutta *et al.*, 2015; Jones *et al.*, 2013; Li *et al.*, 2015), while the remaining study (Thilakaratne *et al.*, 2014) was satisfied by the hydrogen produced from the pyrolysis process alone. Before hydrotreating bio-oil, some of the reported studies (Dutta *et al.*, 2015; Li *et al.*, 2015; Thilakaratne *et al.*, 2014) upgraded bio-oil via *in situ* catalytic pyrolysis with zeolite catalysts instead of fast pyrolysis. Zeolite catalysts are more expensive than basic metal oxide catalysts such as CaO (Stefanidis *et al.*, 2016), which (in addition to the process equipment required to produce hydrogen onsite) can explain the difference in MSP between this study and the reported studies.

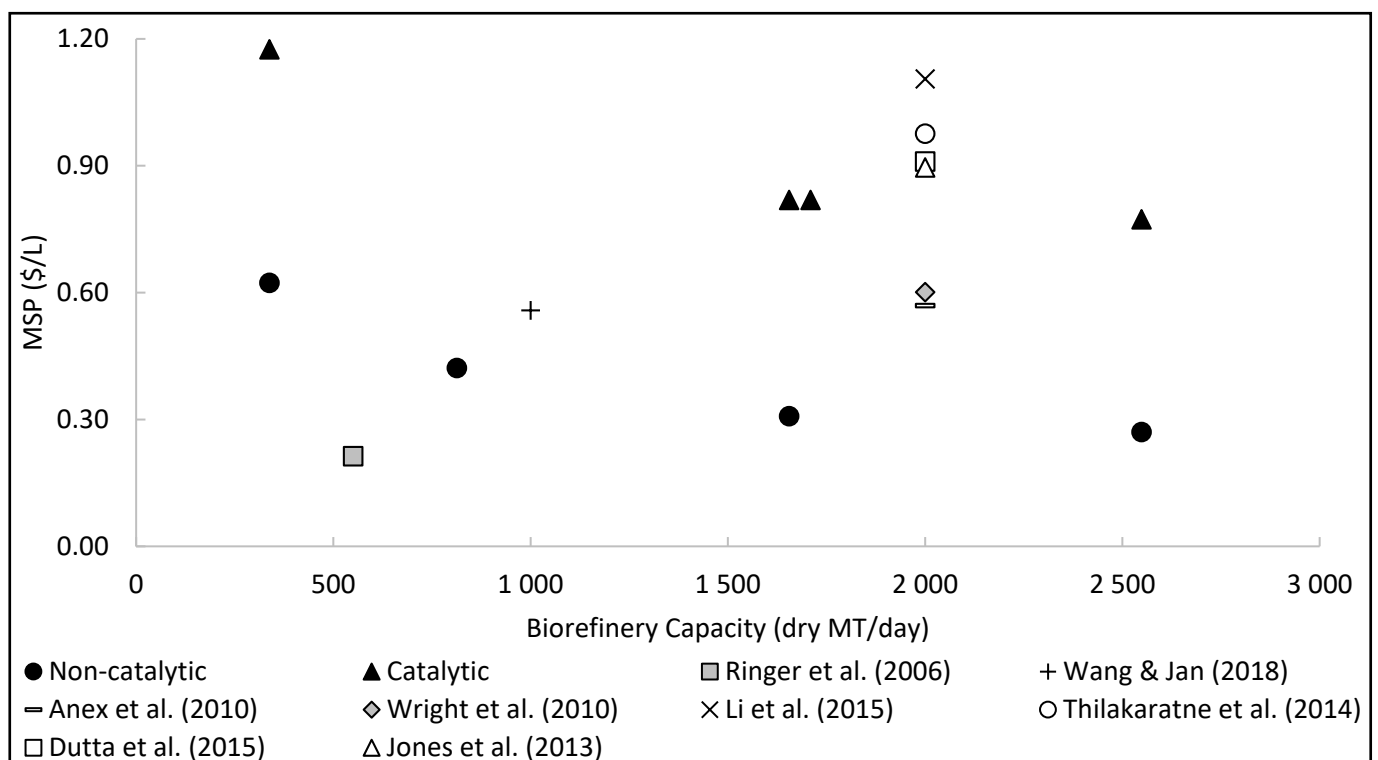


Figure 29: Comparison between the MSP (\$/L) of bio-oils produced via non-catalytic and catalytic pyrolysis in this study and similar studies (adjusted to 2017\$) for a 10 % IRR

The MSP (\$/GGE) of crude and upgraded bio-oils produced via non-catalytic and catalytic pyrolysis in this study are compared to the MSP of bio-oils produced in similar studies against biorefinery capacity in Figure 30. The MSP of upgraded bio-oils in this study compared to the MSP of upgraded bio-oils in the reported studies on an energy basis (Figure 30) is significantly different to the same comparison but on a volume basis (Figure 27). The MSP of \$4.04/GGE and \$3.81/GGE for upgraded bio-oil production corresponding to a 1655 and 2549 dry MT/day biorefinery capacity (Scenarios C-200 and C-300) in this study is greater than the MSP between \$3.52/GGE and \$3.38/GGE for upgraded bio-oil production corresponding to a 2000 dry MT/day biorefinery capacity in the reported studies (Dutta *et al.*, 2015; Jones *et al.*, 2013; Thilakaratne *et al.*, 2014). Therefore, the upgraded bio-oils in the reported studies are closer in energy value to gasoline than the upgraded bio-oils in this study. There is also an obvious trade-off between production cost and product quality, however, lower production costs are still not competitive with fossil fuels at a desirable IRR.

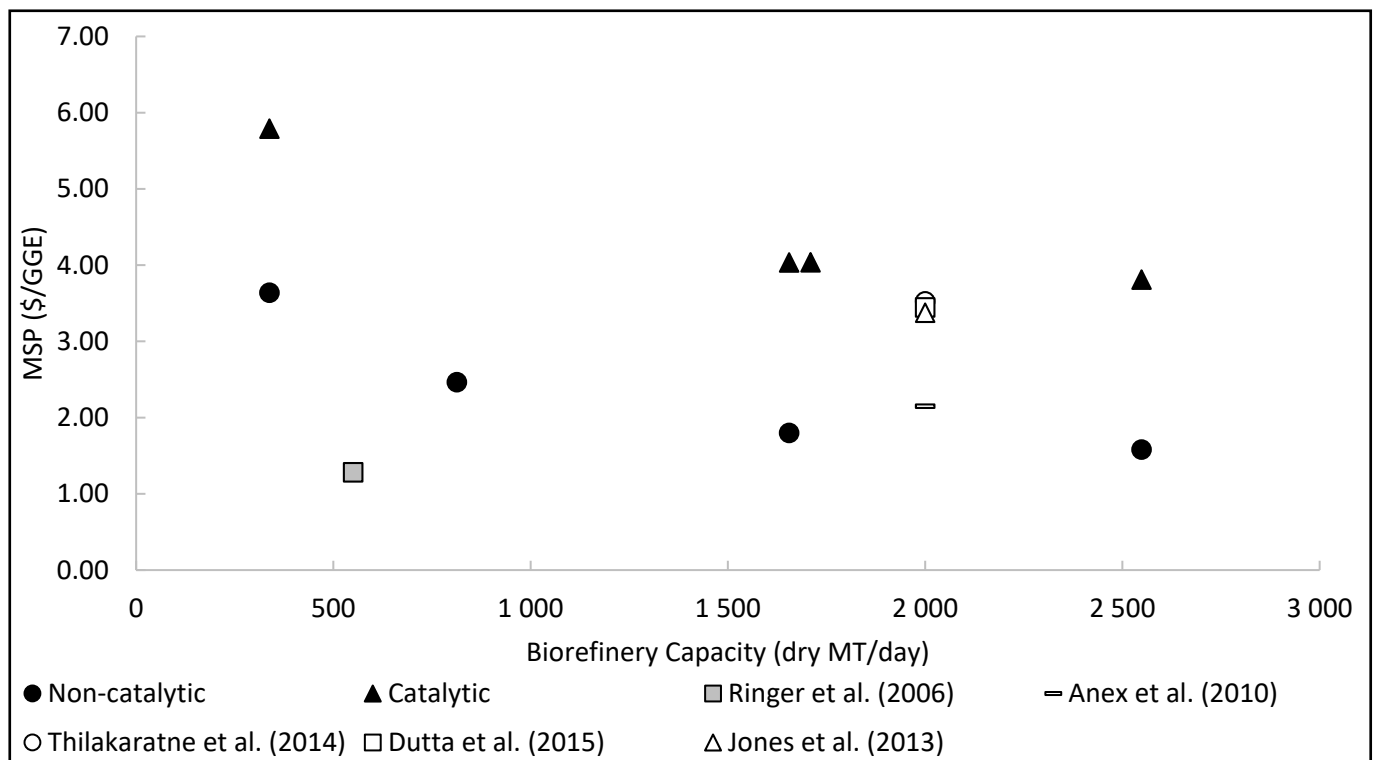


Figure 30: Comparison between the MSP (\$/GGE) of bio-oils produced via non-catalytic and catalytic pyrolysis in this study and similar studies (adjusted to 2017\$) for a 10 % IRR

5.2.4 Economic sensitivity analysis

The DCFROR analyses for non-catalytic and catalytic pyrolysis biorefinery scenarios were based on some economic parameter assumptions to estimate the MSP of bio-oil. Therefore, an economic sensitivity analysis was conducted to assess how the MSP of bio-oil reacts to a 25 % change (increase and decrease) in these parameters. The NC-200 and C-200 biorefinery scenarios at a desired 22 % IRR

were chosen for the economic sensitivity analysis over the more profitable NC-300 and C-300 biorefinery scenarios based on the economic risk associated with larger biorefineries (Yildiz *et al.*, 2016). Moreover, the MSP of bio-oil for the chosen scenarios performed average overall out of the studied range.

The sensitivity analyses for the NC-200 and C-200 biorefinery scenarios (MSP in \$/L) are given in Figure 31 and Figure 32, respectively. The MSP of crude bio-oil for the NC-200 biorefinery scenario was most sensitive to changes in FCI, biochar selling price and total operating cost, while the MSP of upgraded bio-oil for the C-200 biorefinery scenario was most sensitive to changes in FCI, total operating cost and catalyst cost (also included in the total operating cost). The MSP of crude bio-oil for the NC-200 biorefinery scenario was least sensitive to changes in electricity selling price and working capital, while the MSP of upgraded bio-oil for the C-200 biorefinery scenario was least sensitive to changes in electricity selling price, agri-lime selling price and working capital. Thilakaratne and colleagues (2014) also found that the MSP of bio-oil was least sensitivity to changes in electricity selling price (Thilakaratne *et al.*, 2014). Surplus electricity contributed to about 40 and 66 % of the total electricity produced for non-catalytic and catalytic pyrolysis, respectively. Therefore, sufficient electricity can be diverted back to the biorefinery to satisfy additional power demand without significantly impacting profitability.

A 25 % increase in biochar selling price prompted the MSP of bio-oil for the NC-200 and C-200 biorefinery scenarios to decrease by 13.0 and 5.5 %, respectively. The biochar selling price influenced the MSP of bio-oil for the NC-200 biorefinery scenario more than the C-200 biorefinery scenario because more biochar was produced and sold. Furthermore, the more optimistic MSP of bio-oil may be achieved if biochar is sold to an international market instead of in South Africa, where the biochar market is still developing and biochar selling prices are more conservative (Konz *et al.*, 2015).

For a 25 % decrease in FCI, the MSP of bio-oil for the NC-200 and C-200 biorefinery scenarios responded with a 30.1 and 20.8 % decrease, respectively. Similarly, for a 25 % decrease in total operating cost, the MSP of bio-oil for the NC-200 and C-200 biorefinery scenarios decreased by 10.9 and 12.9 %, respectively. These optimistic scenarios may be possible with further technological development of pyrolysis processes (Sharifzadeh *et al.*, 2019).

The sensitivity analyses for the NC-200 and C-200 biorefinery scenarios (MSP in \$/GGE) are given in Figure 33 and Figure 34, respectively. The MSP of bio-oil for the NC-200 and C-200 biorefinery scenarios was still sensitive to changes in FCI and total operating cost, however the MSP of bio-oil was more comparable on an energy basis than on a volume basis. The difference in MSP of bio-oil (\$/L) for the NC-200 and C-200 biorefinery scenarios for a 25 % decrease in FCI and total operating cost was 60.4 and 75.9 %, respectively. Alternatively, the difference in MSP of bio-oil (\$/GGE) for the NC-200 and C-200 biorefinery scenarios for a 25 % decrease in FCI and total operating cost was 35.3 and 48.3 %, respectively.

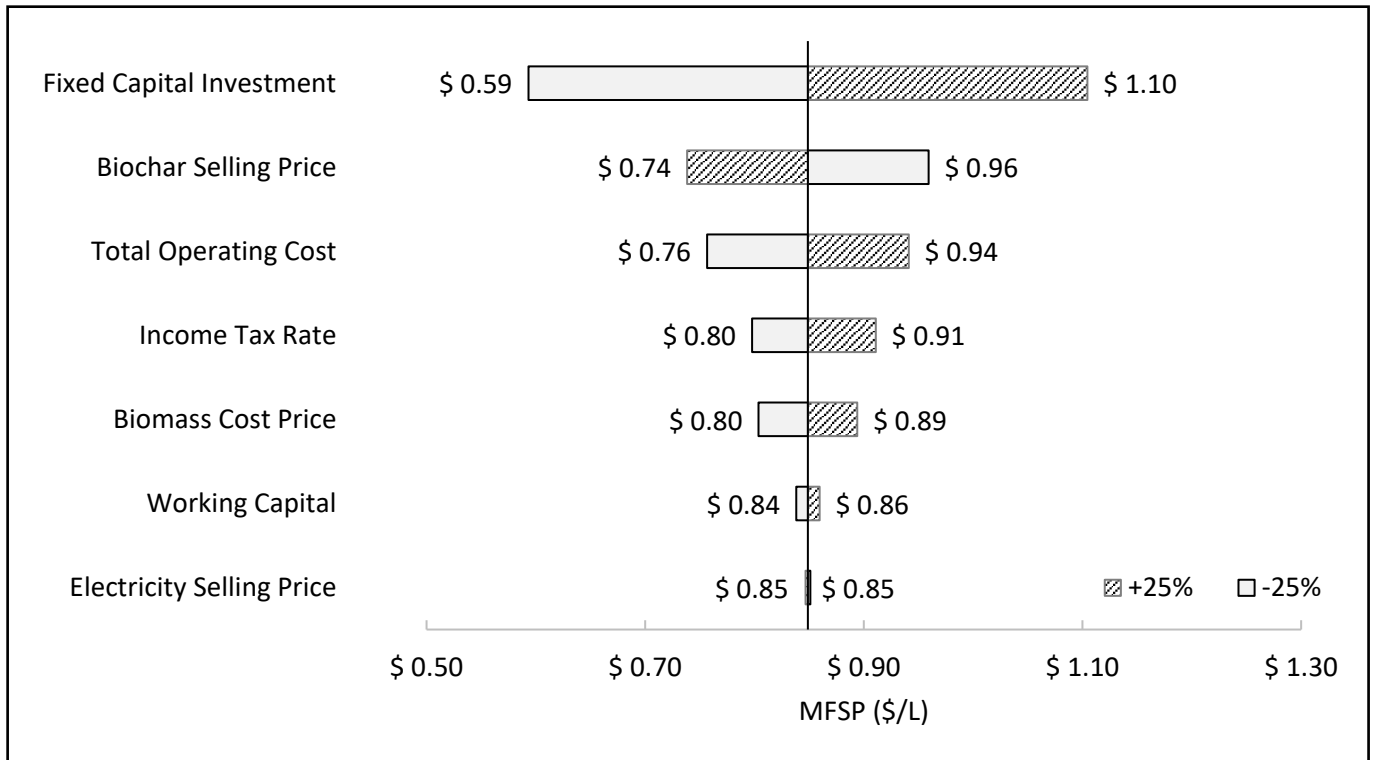


Figure 31: Sensitivity analysis (MSP in \$/L) for biorefinery scenario NC-200

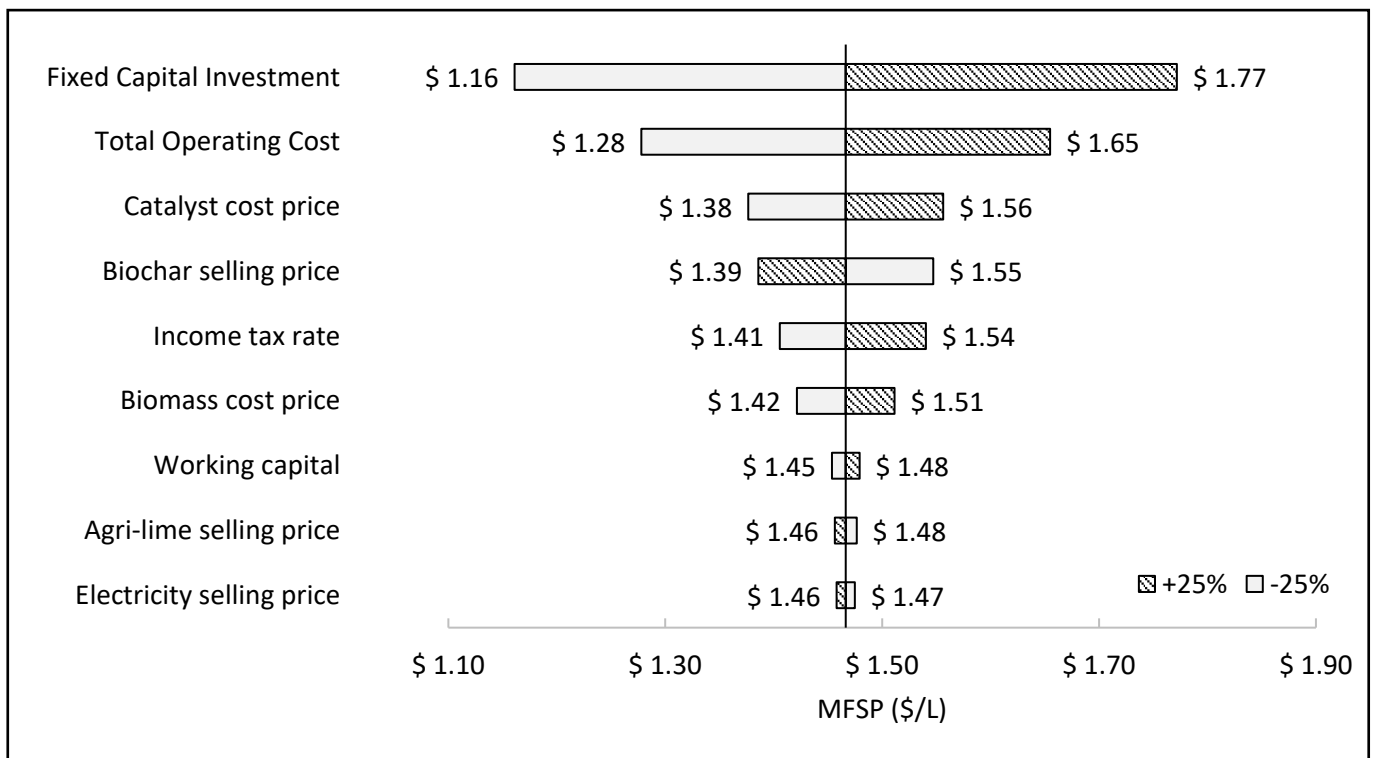


Figure 32: Sensitivity analysis (MSP in \$/L) for biorefinery scenario C-200

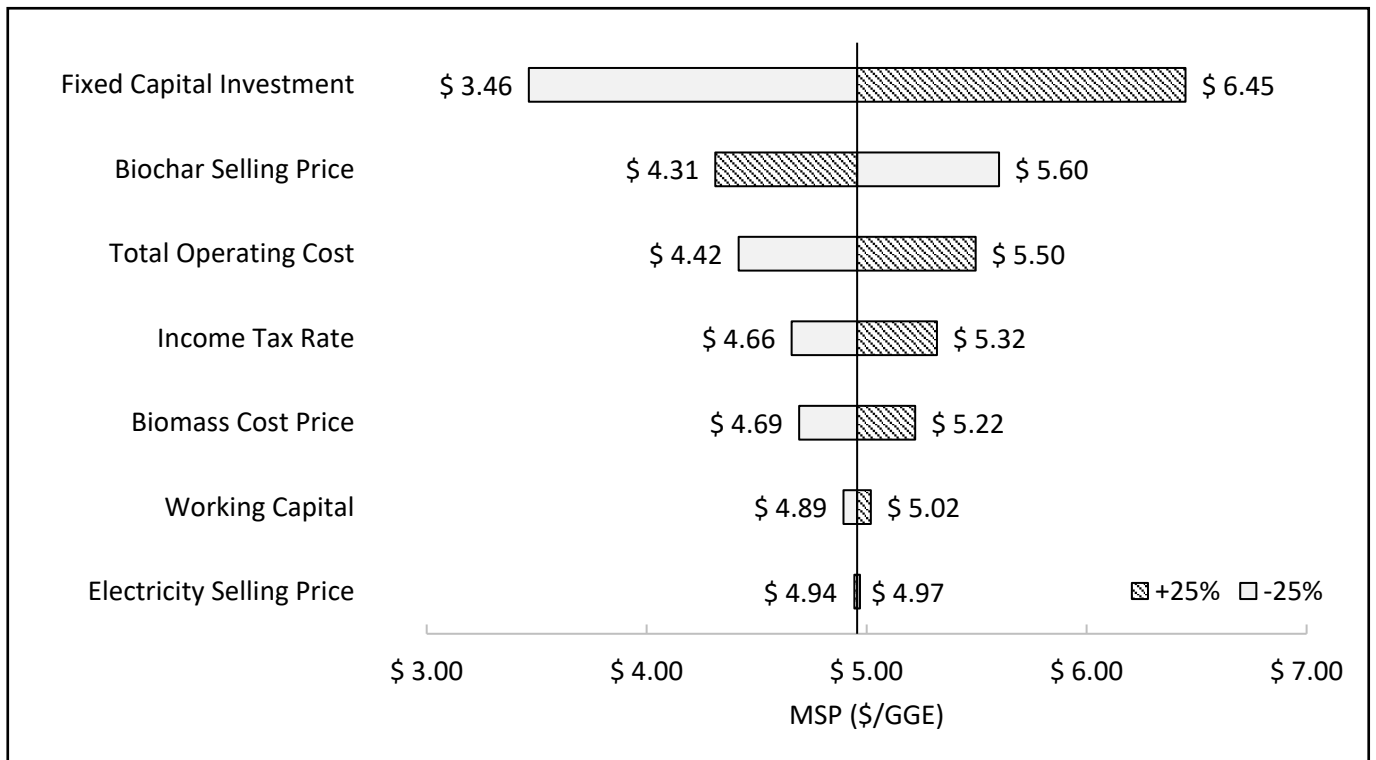


Figure 33: Sensitivity analysis (MSP in \$/GGE) for biorefinery scenario NC-200

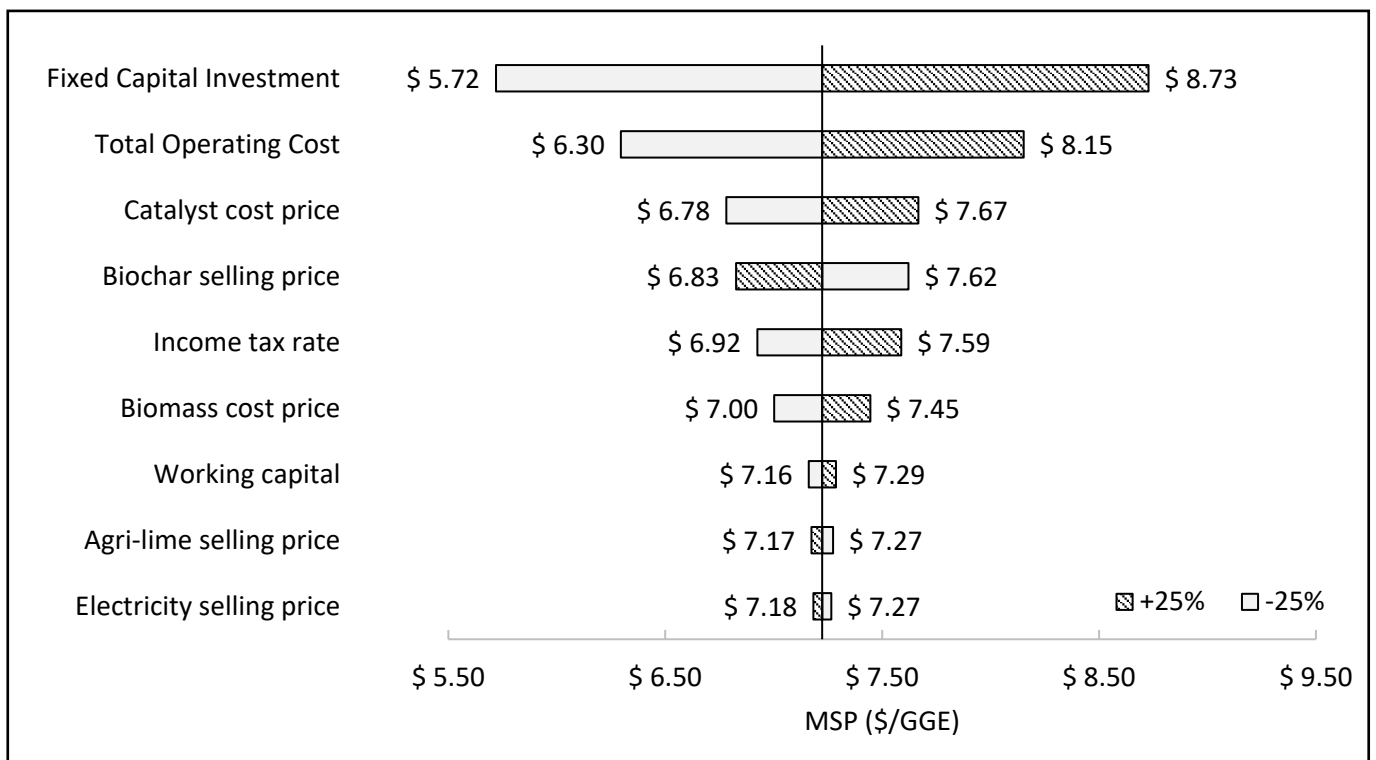


Figure 34: Sensitivity analysis (MSP in \$/GGE) for biorefinery scenario C-200

Installed equipment costs and employee salaries for the non-catalytic and catalytic pyrolysis biorefinery scenarios in this study are in-line with studies conducted for the United States and not South Africa, which may overestimate the MSP of bio-oil. Therefore, an additional economic sensitivity analysis was conducted to assess how the MSP of bio-oil reacts to a 25 % simultaneous decrease in FCI and employee salaries. For a 25 % decrease in both FCI and employee salaries, the MSP of bio-oil for the NC-200 and C-200 biorefinery scenarios was \$0.57/L (\$3.36/GGE) and \$1.14/L (\$5.63/GGE), respectively. This change in the MSP of bio-oil for the NC-200 and C-200 biorefinery scenarios corresponds to a 32.3 and 22.1 % decrease. Furthermore, employee salaries alone only slightly decreased the MSP of bio-oil for the NC-200 and C-200 biorefinery scenarios by 2.2 and 1.2 %, respectively.

5.2.5 Process sensitivity analysis

The products recovered from pilot plant experiments amounted to approximately 89 wt. % of the biomass feed therefore, several assumptions were made to close the mass balance for process simulation development as discussed in Section 4.4.1. The MSP of bio-oil for each biorefinery scenario was conservatively estimated based on unreconciled bio-oil and non-condensable gas yields for non-catalytic and catalytic pyrolysis processes as previously reported in Table 28. However, more efficient product recovery at industrial-scale may improve these yields. Therefore, a process sensitivity analysis was also conducted to assess the effect of an 89.0, 94.5 and 100.0 wt. % mass balance closure on the MSP of bio-oil at the desired 22 % IRR for the NC-200 and C-200 biorefinery scenarios. The results are presented in Table 36. The MSP (\$/L) of bio-oil for the NC-200 and C-200 biorefinery scenarios decreased by 16.3 and 14.5 % for a 100 wt. % mass balance closure, respectively. The MSP of bio-oil decreased mostly because more bio-oil is produced. In addition, the energy demand for the non-catalytic biorefinery scenarios was met by combusting 21.5 wt. % of the char and all of the unreconciled non-condensable gases produced. However, improved non-condensable gas yields reduces the amount of char required for combustion to 18.0 and 14.5 wt. % for a 94.5 and 100.0 wt. % mass balance closure, respectively. Therefore, more char is available for sale. The improved non-condensable gas yields increases the amount of surplus electricity produced in the catalytic biorefinery scenarios since the energy demand for the process was already met by only combusting the unreconciled non-condensable gases produced. The biochar selling price though exceeds the electricity selling price therefore, the MSP of crude bio-oil improved slightly more than the MSP of upgraded bio-oil as product recovery increased.

Table 36: Sensitivity analysis for mass balance reconciliation

Mass Balance Closure (%)	NC-200		C-200	
	MSP (\$/L)	MSP (\$/GGE)	MSP (\$/L)	MSP (\$/GGE)
100.0	0.71	4.15	1.25	6.17
94.5	0.77	4.53	1.34	6.62
89.0	0.85	4.96	1.47	7.22

5.3 Environmental impact results

The Life Cycle Impact Assessment (LCIA) was conducted using the CML-IA baseline method to characterise the environmental impact of bio-oil production via non-catalytic and catalytic pyrolysis processes based on the developed process simulations. Two scenarios are defined for the LCIA: Scenario 1 assesses the environmental impact of valorising 1 kg of dry forest residues by producing bio-oil via non-catalytic or catalytic pyrolysis instead of disposing of forest residues by in-field burning, and Scenario 2 evaluates the environmental impact of producing 1 MJ of bio-oil via non-catalytic or catalytic pyrolysis instead of producing 1 MJ of crude-oil or 1 MJ of diesel. Crude-oil and diesel are chosen for Scenario 2 to estimate the environmental impact of producing 1 MJ of the VGO intermediate. The LCIA results for abiotic depletion (ADP) of fossil fuels, acidification (AP), eutrophication (EP), global warming potential over 100 years (GWP), and ozone layer depletion (ODP) for Scenario 1 and Scenario 2 are given in Figure 35 and Figure 36, respectively.

In Scenario 1, the combustion of forest residues resulted in the highest environmental impact for AP and EP due to higher SO₂ and NO₂ emissions than the pyrolysis processes, where nitrogen and sulphur compounds from the biomass were stored in the biochar. Furthermore, catalytic pyrolysis produced the highest environmental impact for ADP of fossil fuels and ODP mostly because of the CaO catalyst, whereas other contributors for both non-catalytic and catalytic pyrolysis were related to biomass collection and transport.

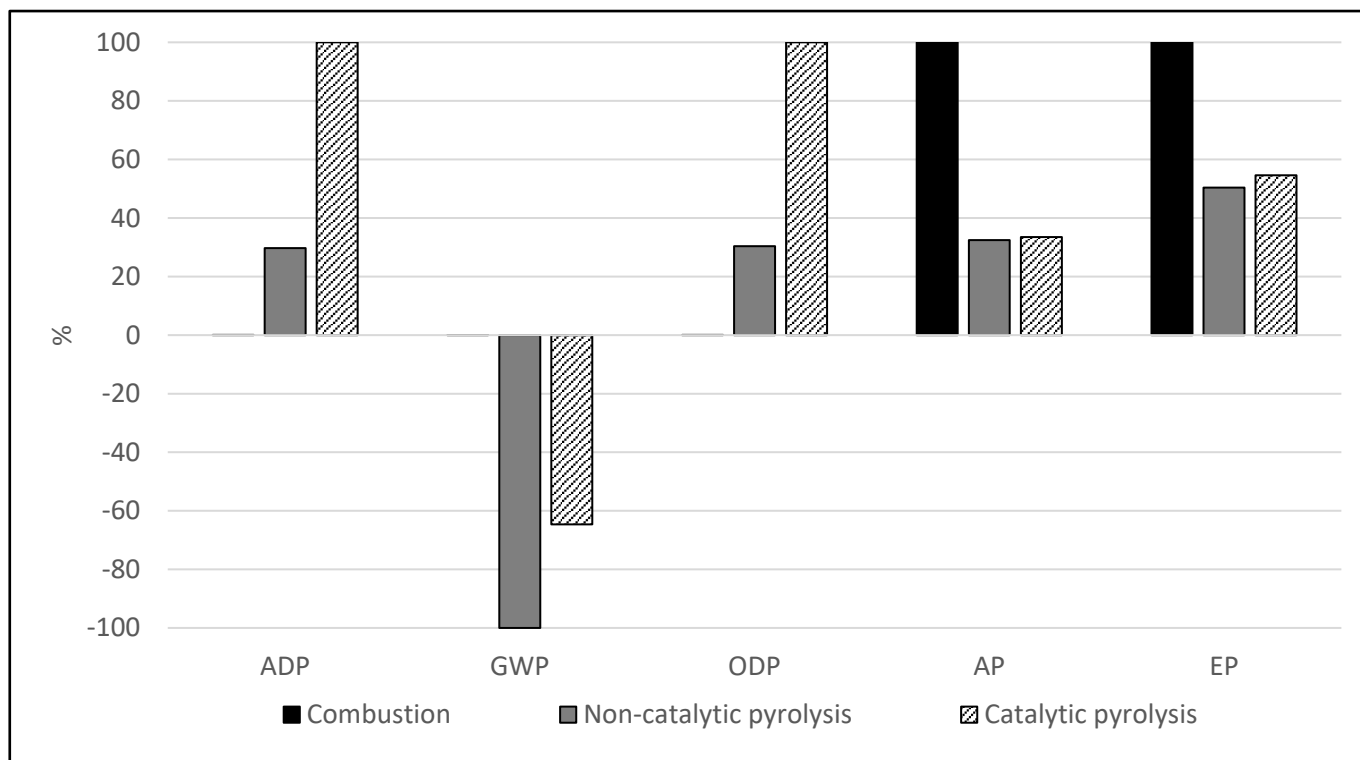


Figure 35: LCIA results for Scenario 1 (valorisation compared to in-field burning of forest residues)

In Scenario 2, crude-oil and diesel production had unsurprisingly the highest environmental impact for ADP of fossil fuels and ODP. Biomass collection and transport, biochar transport to agricultural areas and bio-oil transport to the oil refinery gate contributed to ADP of fossil fuels and ODP for both bio-oil production via non-catalytic and catalytic pyrolysis processes. Non-catalytic pyrolysis, on the other hand, had the highest environmental impact for AP and EP as a result of some biochar combustion to provide heat for the process.

The GWPs for crude and upgraded bio-oil production in both Scenario 1 and Scenario 2 are significantly negative. Non-catalytic pyrolysis also has the lowest GWP overall because more biochar was produced for carbon sequestration than catalytic pyrolysis, and no CaO catalyst was consumed in the process. The net GWPs for combustion, non-catalytic pyrolysis and catalytic pyrolysis in Scenario 1 are 0.00018, -1.13 and -0.73 kg CO₂ eq/kg of forest residues, respectively. These results indicate that valorising forest residues by producing crude and upgraded bio-oils is far better in terms of CO₂ emissions than in-field burning. Therefore, paper and pulp industries in South Africa could successfully reduce their carbon emissions through both non-catalytic and catalytic pyrolysis of the forest residues left behind after pulpwood production. The net GWPs for crude bio-oil, upgraded bio-oil, crude-oil and diesel production in Scenario 2 are -0.30, -0.14, 0.0052 and 0.013 kg CO₂ eq/MJ of fuel, respectively. The results for Scenario 2 substantiate that crude or upgraded bio-oil production has a considerably lower environmental impact in terms of CO₂ equivalent emissions than both crude-oil and diesel production.

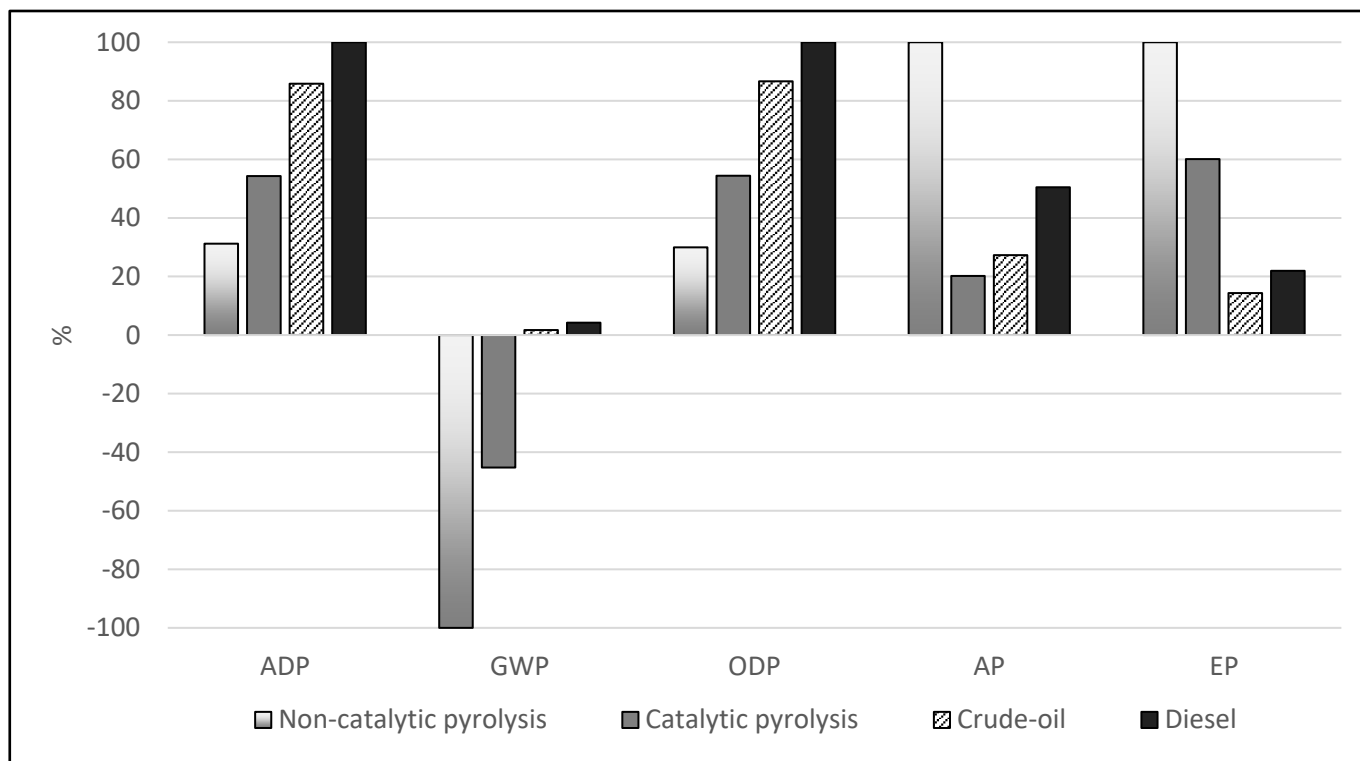


Figure 36: LCIA results for Scenario 2 (producing 1 MJ of bio-oil compared to 1 MJ of crude-oil or 1 MJ of diesel)

The contributors to the net GWP for crude and upgraded bio-oil production via non-catalytic and catalytic pyrolysis in Scenario 2 are shown in Figure 37 and Figure 38, respectively. The contributions to GWP are divided into positive and negative contributions. Positive GWP contributions for bio-oil production via non-catalytic pyrolysis come from forest residue (FR) collection, chipping and transport, pyrolysis, biochar transport and bio-oil transport. Bio-oil production via catalytic pyrolysis had the same positive GWP contributors with the addition of the CaO catalyst, agri-lime transport and agri-lime application. Total positive GWP was 0.13 and 0.20 kg CO₂ eq/MJ for non-catalytic and catalytic pyrolysis, respectively. The CaO catalyst contributed the most to the total positive GWP for catalytic pyrolysis with 0.094 kg CO₂ eq/MJ. Negative GWP contributions for bio-oil production via non-catalytic and catalytic pyrolysis came from biomass CO₂ absorption and biochar carbon sequestration. Total negative GWP was -0.43 and -0.34 kg CO₂ eq/MJ for non-catalytic and catalytic pyrolysis, respectively.

The GWP reported by Iribarren, Peters and Dufour (2012) was -0.051 kg CO₂ eq/MJ of liquid fuel produced (Iribarren *et al.*, 2012). The researchers applied a “cradle-to-gate” LCA approach for the production of gasoline and diesel-quality fuels from short-rotation poplar wood chips via fast pyrolysis and hydrotreating. The GWP for the biomass alone was -0.120 kg CO₂ eq/MJ of liquid fuel produced and included biomass cultivation, harvesting and CO₂ absorption. In comparison, the GWP for the biomass was -0.287 kg CO₂ eq/MJ of upgraded bio-oil produced in this study, which was much lower

because the environmental impact associated with biomass cultivation and harvesting were allocated to stem wood production only, and not to the forest residues. All of the char produced in the reported study was also combusted to provide sufficient heat for the pyrolysis reactor. Therefore, the overall GWP for the reported study was 62.7 % higher than the overall GWP for upgraded bio-oil production in this study. Furthermore, producing both bio-oil and biochar as main products is an environmental advantage of operating at intermediate pyrolysis conditions. Biochar clearly had a significant influence on the GWP of bio-oil production through carbon sequestration.

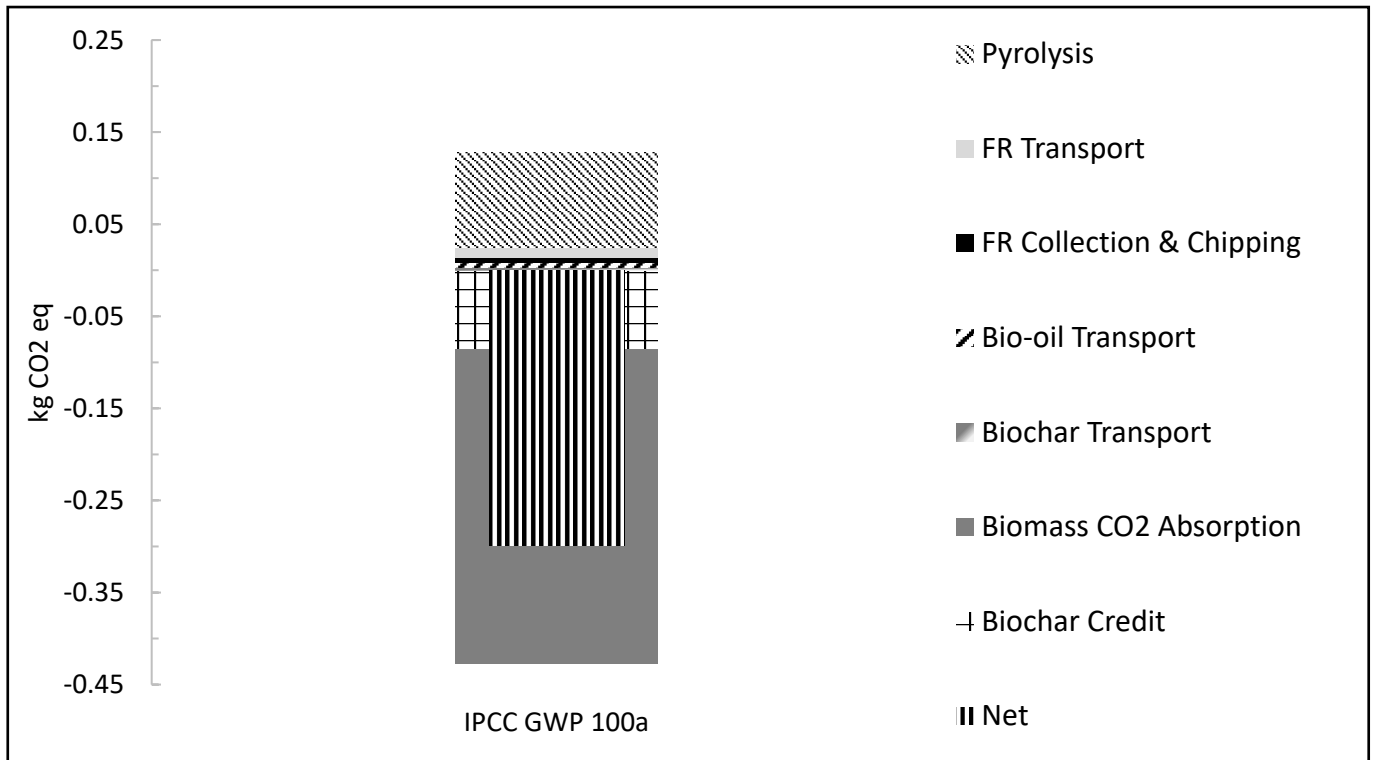


Figure 37: GWP contributions for bio-oil production via non-catalytic pyrolysis in Scenario 2

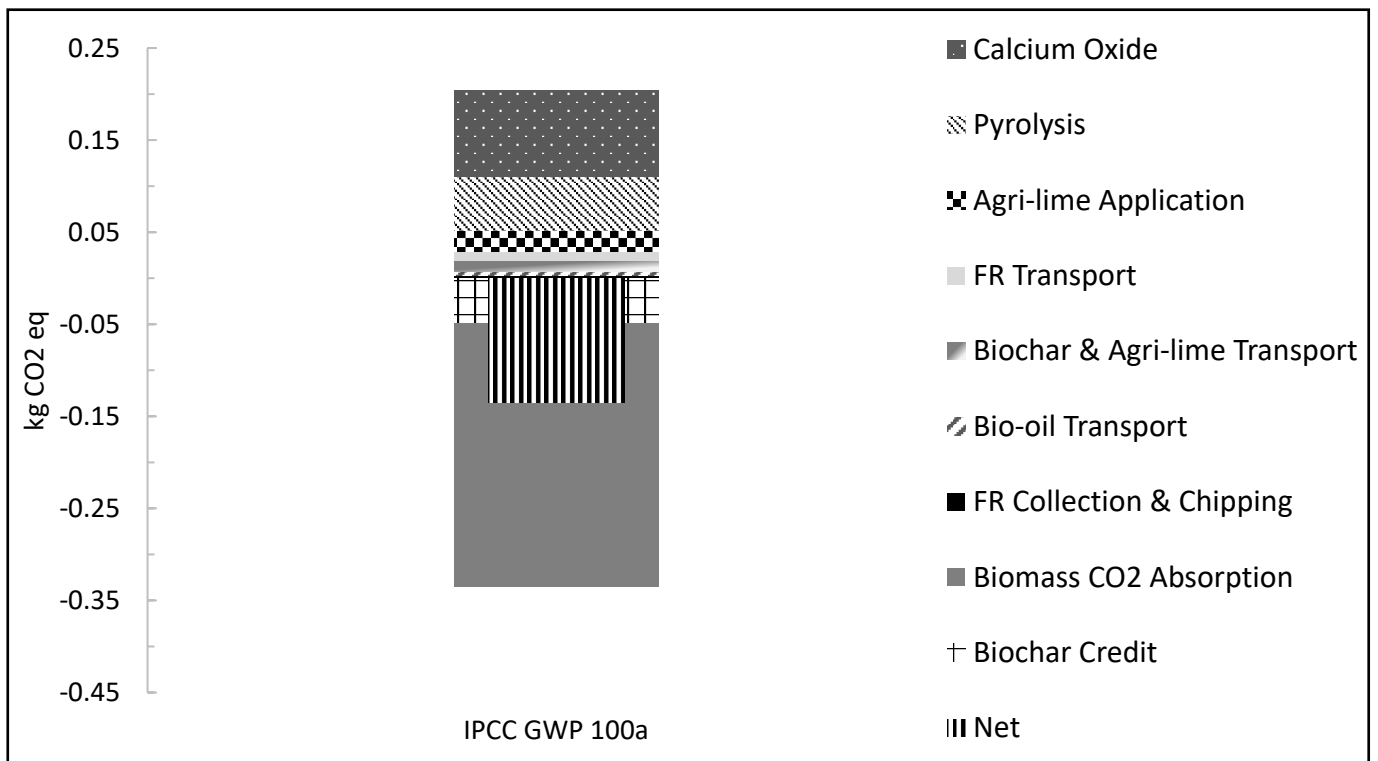


Figure 38: GWP contributions for bio-oil production via catalytic pyrolysis in Scenario 2

The net GWPs on a mass basis for crude bio-oil, upgraded bio-oil, crude-oil and diesel production in Scenario 2 are -6.15, -3.50, 0.24 and 0.57 kg CO₂ eq/kg of fuel, respectively. Consequently, co-processing crude or upgraded bio-oil has the potential to significantly decrease the GWP of the FCC feed. The blend of crude or upgraded bio-oil and VGO that can be co-processed at the *Natref*, *Enref* and *Sapref* oil refineries was previously reported in Table 17 in Section 4.2. The GWP of VGO is between the GWP of crude-oil and the GWP of diesel. The GWP of the FCC feed (crude bio-oil with crude-oil or upgraded bio-oil with crude-oil or crude bio-oil with diesel or upgraded bio-oil with diesel) is measured against the GWP of pure crude-oil or pure diesel to yield the reduction in GWP for each biorefinery scenario.

The average price of Brent Crude in 2017 was \$0.34/L (Macrotrends, 2019), and the average price (specifically, the BFP) of diesel in 2017 was \$0.41/L (Department of Energy, 2019). The MSP (22 % IRR) of crude or upgraded bio-oil presented in Table 34 is measured against these crude-oil and diesel prices to determine the price premium of either crude or upgraded bio-oil for each biorefinery scenario.

The reduction in GWP is subsequently plotted against the price premium of crude or upgraded bio-oil for each biorefinery scenario in Figure 39. The shaded areas seen in Figure 39 represent the range for the reduction in GWP and price premium of co-processing crude bio-oil and VGO (light grey) or upgraded bio-oil and VGO (dark grey). The reduction in GWP increases for co-processing crude bio-oil and crude-oil from 55.8 to 351.0 %, and for crude bio-oil and diesel from 24.4 to 153.7 % as the biomass collection distance increases up to a 300 km radius of the biorefinery. Simultaneously, the price premium decreases for co-processing crude bio-oil and crude-oil from 77.2 to 53.9 %, and for crude bio-oil and diesel from 72.7 to 44.8 % as the biomass collection distance increases up to a 300 km radius of the biorefinery. The same trend is seen for upgraded bio-oil, however, the change is less significant. The reduction in GWP increases for co-processing upgraded bio-oil and crude-oil from 31.0 to 226.3 %, and for upgraded bio-oil and diesel from 14.1 to 102.6 % as the biomass collection distance increases up to a 300 km radius of the biorefinery. At the same time, the price premium decreases for co-processing upgraded bio-oil and crude-oil from 84.4 to 74.5 %, and for upgraded bio-oil and diesel from 81.4 to 69.4 % as the biomass collection distance increases up to a 300 km radius of the biorefinery.

At a 300 km radius of the biorefinery, and overall, co-processing crude bio-oil reduces the GWP of the FCC feed far more for a lower price premium than co-processing upgraded bio-oil. However, the reduction in GWP for co-processing 5 wt. % crude bio-oil (Scenario NC-5) is between 134.3 (crude-oil) and 58.8 (diesel) %, whereas the reduction in GWP for co-processing 10 wt. % upgraded bio-oil (Scenario C-10) is between 157.0 (crude-oil) and 71.2 (diesel) %. Therefore, the potential to co-process more upgraded bio-oil than crude bio-oil significantly decreases the GWP of the FCC feed at the *Natref* oil refinery alone. The 8.0 (crude-oil) to 13.1 (diesel) % difference in price premium for co-processing

5 wt. % crude bio-oil or 10 wt. % upgraded bio-oil also has the potential to decrease if the additional costs (process equipment modifications, changes in FCC product distribution etc.) for co-processing at the *Natref* oil refinery are considered.

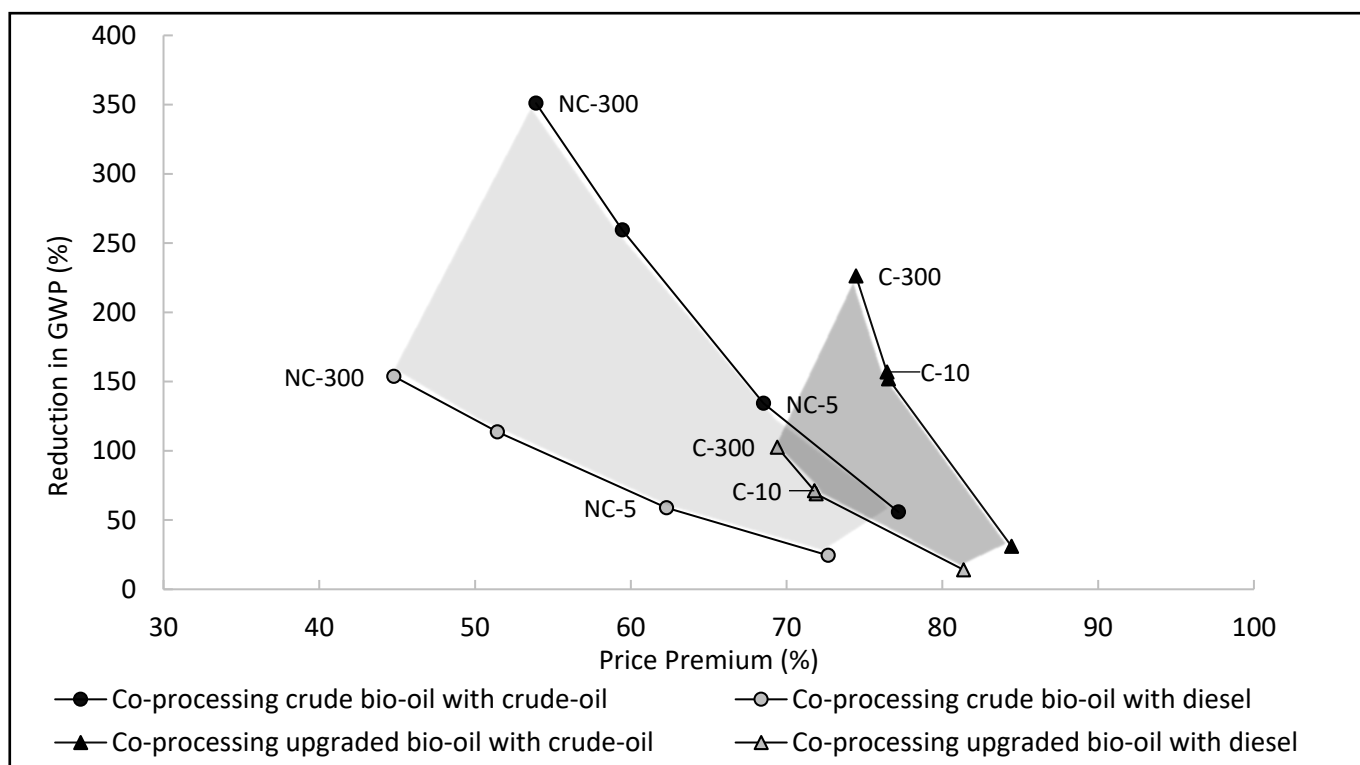


Figure 39: Reduction in GWP for price premium of crude and upgraded bio-oils - Non-catalytic (NC) and catalytic (C) pyrolysis for biomass collection within a 100, 200 and 300 km radius of the biorefinery, and NC and C at the required biorefinery capacity to co-process 5 and 10 wt. % bio-oil, respectively

CHAPTER 6

6 Conclusions and Recommendations

The overall aim of this project was to determine whether or not the production of crude and upgraded bio-oils via non-catalytic and catalytic pyrolysis of forest residues for co-processing in an oil refinery is economically and environmentally feasible. This chapter gives an overview of the objectives for the project, answers key research questions and provides recommendations for further research.

6.1 Addressing the objectives

The objectives for this project were developed to address the gaps in literature on the techno-economic analysis of upgraded bio-oil production via catalytic pyrolysis with a basic metal oxide catalyst, and the environmental benefit of biochar as a co-product of pyrolysis.

6.1.1 Develop process simulations in Aspen Plus™ for non-catalytic and catalytic pyrolysis biorefinery scenarios based on pilot plant data

Non-catalytic pyrolysis of *E. grandis* forest residues (8.28 wt. % moisture) yielded 22.6 wt. % biochar and 19.8 wt. % crude bio-oil available for sale, while catalytic pyrolysis yielded 16.5 wt. % biochar and 18.4 wt. % upgraded bio-oil available for sale.

Both non-catalytic and catalytic biorefinery scenarios were designed to be entirely energy self-sufficient by combusting the non-condensable gas and 21.5 wt. % of the char (for non-catalytic pyrolysis biorefinery scenarios only) products. Consequently, the total energy supplied to the non-catalytic and catalytic pyrolysis biorefinery scenarios for heating, cooling and power was 25.0 and 25.9 % of biomass HHV, respectively. Furthermore, the total energy recovered in bio-oil and biochar products was 61.9 and 53.0 % of the biomass HHV for non-catalytic and catalytic pyrolysis biorefinery scenarios, respectively.

6.1.2 Develop economic analyses for non-catalytic and catalytic pyrolysis biorefinery scenarios based on process simulations

The non-catalytic (NC-100, NC-200, NC-300 and NC-5) and catalytic (C-100, C-200, C-300 and C-10) pyrolysis biorefinery scenarios were chosen based on the biomass collection distance from the biorefinery (100, 200 and 300 km radius), and the amount of crude and upgraded bio-oil required to co-process 5 and 10 wt. % at the *Natref* oil refinery, respectively.

There was a clear economy-of-scale benefit for the MSP of both crude and upgraded bio-oils as the biomass collection distance increased up to a 300 km radius of the biorefinery. The MSP of upgraded bio-oil though was always higher than the MSP of crude bio-oil for the same IRR and biomass

collection distance. The most economically viable biorefinery scenario (Scenario NC-300) and the lowest MSP of crude bio-oil at a nominal 10 % IRR was \$0.27/L, which fell below the estimated VGO market price of \$0.35/L. The MSP of upgraded bio-oil at a nominal 10 % IRR for the corresponding catalytic pyrolysis biorefinery scenario (Scenario C-300) was \$0.77/L, which was considerably higher than the MSP of crude bio-oil. However, the quality of upgraded bio-oil was superior to crude bio-oil for co-processing in an oil refinery.

Co-processing up to 10 wt. % crude bio-oil with VGO compared to upgraded bio-oil with VGO in an industrial-scale FCC unit will likely decrease gasoline yields and produce more CO, CO₂ and H₂O gaseous products as a result of deoxygenation reactions. Co-processing up to 5 wt. % crude bio-oil with VGO will be more reasonable. However, a significantly lower renewable carbon content present in the bio-derived fuels produced, as well as the process equipment and FCC catalyst modifications required to accommodate co-processing crude bio-oil in an oil refinery could make co-processing upgraded bio-oil more economically feasible. Nevertheless, investors will look for higher returns on innovative projects associated with high financial risk.

An oil refinery such as *Natref* could co-process 5 wt. % crude bio-oil for \$1.09/L (Scenario NC-5) or 10 wt. % upgraded bio-oil for \$1.46/L (Scenario C-10) at the desired 22 % IRR. Alternatively, oil refineries such as *Enref* and *Sapref* could collaborate with *Natref* to benefit from economy-of-scale by co-processing crude and upgraded bio-oils at the lowest price of \$0.75/L (NC-300) and \$1.35/L (C-300) for a desired 22 % IRR, respectively. The most economically viable biorefinery scenarios was still NC-300, however, the MSP on a volume basis did not account for the difference in energy value of the crude and upgraded bio-oils.

The MSP of crude and upgraded bio-oils were compared on a gasoline gallon equivalent (GGE) basis. The MSP of crude bio-oil on a GGE basis remained lower than the MSP of upgraded bio-oil overall. However, the MSP of upgraded bio-oil (\$6.64/GGE) was slightly closer to the MSP of crude bio-oil (\$4.36/GGE) for a desired 22 % IRR at a 300 km radius of the biorefinery, which showed that upgraded bio-oil was in fact more competitive with crude bio-oil.

An economic sensitivity analysis showed that the MSP of crude bio-oil was most sensitive to a 25 % change in FCI, biochar selling price and total operating cost, while the MSP of upgraded bio-oil was most sensitive to a 25 % change in FCI, total operating cost (catalyst cost included) and catalyst cost. Therefore, the catalyst cost was a substantial contributor to the difference in MSP of crude and upgraded bio-oils.

The price premium for crude and upgraded bio-oils, however, have to be substantiated by a significant environmental benefit over VGO for oil refineries to recover costs through potential carbon tax rebates and potential government subsidisation.

6.1.3 Measure and compare the environmental impact of producing crude and upgraded bio-oils to crude-oil and diesel using SimaPro™

Scenario 1 assessed the environmental impact of valorising 1 kg of dry forest residues by producing bio-oil via non-catalytic or catalytic pyrolysis instead of disposing of forest residues by in-field burning, and Scenario 2 evaluated the environmental impact of producing 1 MJ of bio-oil via non-catalytic or catalytic pyrolysis instead of producing 1 MJ of crude-oil or 1 MJ of diesel.

The GWP for crude and upgraded bio-oil production in both Scenario 1 and Scenario 2 was significantly negative. Intermediate pyrolysis conditions had the advantage of producing both bio-oil and biochar as main products. Therefore, biochar had a substantial influence on the GWP for bio-oil production through carbon sequestration. The net GWP for combustion, non-catalytic pyrolysis and catalytic pyrolysis in Scenario 1 was 0.00018, -1.13 and -0.73 kg CO₂ eq/kg of forest residues, respectively. Forest residue valorisation into crude or upgraded bio-oil was considerably better than in-field burning. The net GWP for crude bio-oil, upgraded bio-oil, crude-oil and diesel in Scenario 2 was -0.30, -0.14, 0.0052 and 0.013 kg CO₂ eq/MJ of fuel, respectively. The GWP for VGO production was in the region between the GWP for crude-oil production and the GWP for diesel production. Crude and upgraded bio-oil production had a significantly lower GWP compared to crude-oil and diesel production. Furthermore, the GWP for crude bio-oil production was superior to upgraded bio-oil production because of the negative environmental impact associated with the CaO catalyst.

The reduction in GWP of the FCC feed for each biorefinery scenario was measured against the price premium of crude or upgraded bio-oil. At a 300 km radius of the biorefinery, co-processing crude bio-oil reduced the GWP of the FCC feed by between 153.7 (diesel) and 351.0 (crude-oil) %, while co-processing upgraded bio-oil reduced the GWP of the FCC feed by between 102.6 (diesel) and 226.3 (crude-oil) %. Simultaneously, the price premium for co-processing crude bio-oil ranged from 44.8 (diesel) to 53.9 (crude-oil) %, whereas the price premium for co-processing upgraded bio-oil ranged from 69.4 (diesel) to 74.5 (crude-oil) %.

However, the reduction in GWP for co-processing 5 wt. % crude bio-oil (Scenario NC-5) was between 58.8 (diesel) and 134.3 (crude-oil) %, whereas the reduction in GWP for co-processing 10 wt. % upgraded bio-oil (Scenario C-10) was between 71.2 (diesel) and 157.0 (crude-oil) %. Therefore, the GWP of the FCC feed for a single oil refinery decreased considerably by co-processing more upgraded bio-oil than crude bio-oil. The difference in price premium for co-processing 5 wt. % crude bio-oil or 10 wt. % upgraded bio-oil was between 13.1 (diesel) and 8.0 (crude-oil) %. Furthermore, considering the possible costs to the oil refinery for co-processing crude or (less so) upgraded bio-oil, this difference in price premium will likely decrease.

6.2 Recommendations for further research

Recommendations are made for future experimental work that will expand the scope of this project, and provide further insight into the economic feasibility of commercial bio-oil production for co-processing in an oil refinery:

- Biomass collection (currently forest residues only) could be expanded to include invasive alien plants, which are problematic for conservation throughout South Africa, but especially in KZN and Mpumalanga. A decrease in biomass transport distance to the biorefinery will also be favourable for the process economics, while maintaining bio-oil production and supply (i.e. economy-of-scale) to oil refineries as described in this study.
- The biomass grinder consumed up to 51 % of the power required by the biorefinery therefore, further pilot-plant experiments followed by an update of the techno-economic analysis developed in this study could be conducted to assess the technical and economic feasibility of processing larger biomass particles at industrial-scale. Industrial-scale pyrolysis reactors operating at intermediate pyrolysis conditions may not require grinding biomass particles down from 2 cm to 2 mm.
- The power demand of the biorefinery could be supplied from the grid (mostly coal-fired power) instead of recovering heat from the process to produce steam for the installed steam turbines. Consequently, the production of crude and upgraded bio-oils has the potential to be more economically feasible, however, the environmental impact of the biorefinery could significantly change.
- Recovery of the CaO catalyst without compromising the biochar (usually by combustion) could be investigated since the cost and GWP of the catalyst significantly influenced the MSP of upgraded bio-oil and the environmental impact of upgraded bio-oil production in this study, respectively. One potential method, depending on the biochar particle size distribution, involves entraining biochar particles using a process known as *blow through*. Another physical separation method involves sieving the biochar and catalyst particles.
- Alternative upgrading methods (to *in situ* catalytic pyrolysis with CaO catalyst) could be considered to potentially reduce the MSP of upgraded bio-oil and improve the GWP of upgraded bio-oil production; such as hydrotreating with hydrogen produced via water electrolysis powered by solar PV panels. Various hydrogen production methods (natural gas steam reforming, biomass/biochar steam gasification, bio-oil reforming etc.) could also be compared both economically and environmentally.
- Co-processing crude and upgraded bio-oils at lab and pilot-scale could be investigated to evaluate the correlation between blending ratio, distribution of FCC products (specifically coke, gasoline and LCO) and the extent of deoxygenation reactions that produce the

undesirable H₂O, CO and CO₂ gaseous product. Co-processing up to 20 wt. % crude bio-oil at demonstration-scale is technically feasible therefore, co-processing more than 20 wt. % upgraded bio-oil could be investigated. However, biomass availability and the long-term implications for an oil refinery should also be considered. Furthermore, these experiments could be used to evaluate the susceptibility of FCC construction materials to the corrosivity of bio-oil, as well as the damage caused to FCC catalysts by the high water content of bio-oil.

- The scope of this project could be expanded to include a techno-economic analysis for co-processing crude and upgraded bio-oils at an oil refinery using co-processing data (FCC product yields, reaction conditions etc.) preferably generated from lab or pilot-scale experiments or available in literature (upgraded bio-oil co-processing data is limited to upgraded bio-oil produced via hydrotreating or catalytic pyrolysis with zeolite catalysts). The additional capital and operating costs incurred by the oil refinery could then be included in the profitability analysis developed for this project to better compare the MSP of crude and upgraded bio-oils. Subsequently, the environmental impact of co-processing crude and upgraded bio-oils could be investigated to expand the GWP analysis from crude and upgraded bio-oil production to bio-derived fuel production.
- A techno-economic analysis to compare crude bio-oil deoxygenation during FCC co-processing to upgrading bio-oil followed by FCC co-processing could be investigated to determine whether or not it is necessary and economically feasible to upgrade bio-oil before FCC co-processing. Furthermore, the techno-economic analysis could compare upgrading bio-oil through catalytic pyrolysis to upgrading bio-oil through hydrotreating at the oil refinery, where hydrogen is readily available. The latter could benefit from a significant improvement in the process economics, however, the environmental benefit and renewable carbon content of the FCC products should be considered.

7 References

- Ackerman, P., Ham, C., Dovey, S., Toit, B., Wet, J. De, Kunneke, A. & Seifert, T. 2013. State of the art use of forest residues for bioenergy in southern Africa. *Institute for Commercial Forestry Research*.
- Activated Carbon Innovations. 2019. *Our Products*. [Online], Available: <http://activatedcarbon.co.za/our-products/> [2019, May 14].
- Agegnehu, G., Srivastava, A.K. & Bird, M.I. 2017. The role of biochar and biochar-compost in improving soil quality and crop performance: A review. *Applied Soil Ecology*. 119:156–170.
- Akhtar, J. & Amin, N.S. 2012. A review on operating parameters for optimum liquid oil yield in biomass pyrolysis. *Renewable and Sustainable Energy Reviews*. 16(7):5101–5109.
- Ali Mandegari, M., Farzad, S. & Görgens, J.F. 2017. Economic and environmental assessment of cellulosic ethanol production scenarios annexed to a typical sugar mill. *Bioresource Technology*. 224:314–326.
- Amos, W. a. 1998. Report on Biomass Drying Technology. *National Renewable Energy Laboratory*.
- Anex, R.P., Aden, A., Kazi, F.K., Fortman, J., Swanson, R.M., Wright, M.M., Satrio, J.A., Brown, R.C., et al. 2010. Techno-economic comparison of biomass-to-transportation fuels via pyrolysis, gasification, and biochemical pathways. *Fuel*. 89:S29–S35.
- AspenTech. 2013. *Aspen Plus - Getting Started Modeling Processes with Solids*. Aspen Technology Inc.
- Azeez, A.M., Meier, D., Odermatt, J. & Willner, T. 2010. Fast pyrolysis of African and European lignocellulosic biomasses using Py-GC/MS and fluidized bed reactor. *Energy and Fuels*. 24(3):2078–2085.
- Balat, M., Balat, M., Kirtay, E. & Balat, H. 2009. Main routes for the thermo-conversion of biomass into fuels and chemicals. Part 1: Pyrolysis systems. *Energy Conversion and Management*. 50(12):3147–3157.
- Bergsten, B. 2009. Evaporative Cooling Tower and Chilled Beams. Design Aspects for Cooling in Office Buildings in Northern Europe. Chalmers University of Technology.
- Bezergianni, S., Dimitriadis, A., Kikhtyanin, O. & Kubička, D. 2018. Refinery co-processing of renewable feeds. *Progress in Energy and Combustion Science*. 68:29–64.
- Bridgwater, A. V. 2012a. Review of fast pyrolysis of biomass and product upgrading. *Biomass and Bioenergy*. 38:68–94.
- Bridgwater, A. V. 2012b. Upgrading Biomass Fast Pyrolysis Liquids. *Environmental Progress & Sustainable Energy*. 31(2):261–268.
- Bridgwater, A. V, Toft, A.J. & Brammer, J.G. 2002. A techno-economic comparison of power production by biomass fast pyrolysis with gasification and combustion. *Renewable and Sustainable Energy Reviews*. 6:181–248.

- Brown, T.R. & Brown, R.C. 2013. Techno-economics of advanced biofuels pathways. *RSC Advances*. 3(17):5758–5764.
- Brown, D., Rowe, A. & Wild, P. 2013. A techno-economic analysis of using mobile distributed pyrolysis facilities to deliver a forest residue resource. *Bioresource Technology*. 150:367–376.
- Bru, K., Blin, J., Julbe, A. & Volle, G. 2007. Pyrolysis of metal impregnated biomass: An innovative catalytic way to produce gas fuel. *Journal of Analytical and Applied Pyrolysis*. 78(2):291–300.
- Bu, Q., Lei, H., Zacher, A.H., Wang, L., Ren, S., Liang, J., Wei, Y., Liu, Y., et al. 2012. A review of catalytic hydrodeoxygenation of lignin-derived phenols from biomass pyrolysis. *Bioresource Technology*. 124:470–477.
- Burger, M.D. 2018. Evaluating different value adding processing systems for bamboo developments. Stellenbosch University.
- Cao, X., Ma, L., Gao, B. & Harris, W. 2009. Dairy-manure derived biochar effectively sorbs lead and atrazine. *Environmental Science & Technology*. 43(9):3285–3291.
- Carey, P., Ketterings, Q. & Hunter, M. 2006. *Liming materials*. [Online], Available: <http://cceanondaga.org/resources/liming-materials> [2019, May 09].
- Carlson, T.R., Tompsett, G.A., Conner, W.C. & Huber, G.W. 2009. Aromatic production from catalytic fast pyrolysis of biomass-derived feedstocks. *Topics in Catalysis*. 52(3):241–252.
- Carpenter, D., Westover, T.L., Czernik, S. & Jablonski, W. 2014. Biomass feedstocks for renewable fuel production: a review of the impacts of feedstock and pretreatment on the yield and product distribution of fast pyrolysis bio-oils and vapors. *Green Chemistry*. 16(2):384–406.
- Carrasco, J.L., Gunukula, S., Boateng, A.A., Mullen, C.A., DeSisto, W.J. & Wheeler, M.C. 2017. Pyrolysis of forest residues: An approach to techno-economics for bio-fuel production. *Fuel*. 193:477–484.
- Channiwala, S.A. & Parikh, P.P. 2002. A unified correlation for estimating HHV of solid, liquid and gaseous fuels. *Fuel*. 81(8):1051–1063.
- Chireshe, F. 2019. Production of an upgraded bio-oil by catalytic pyrolysis of forest residues. Stellenbosch University.
- Collard, F.-X. & Blin, J. 2014. A review on pyrolysis of biomass constituents: Mechanisms and composition of the products obtained from the conversion of cellulose, hemicelluloses and lignin. *Renewable and Sustainable Energy Reviews*. 38:594–608.
- Collard, F.-X., Blin, J., Bensakhria, A. & Valette, J. 2012. Influence of impregnated metal on the pyrolysis conversion of biomass constituents. *Journal of Analytical and Applied Pyrolysis*. 95:213–226.
- Couhert, C., Commandre, J.M. & Salvador, S. 2009. Is it possible to predict gas yields of any biomass after rapid pyrolysis at high temperature from its composition in cellulose, hemicellulose and lignin? *Fuel*. 88(3):408–417.
- Czernik, S. & Bridgwater, A. V. 2004. Overview of applications of biomass fast pyrolysis oil. *Energy and Fuels*. 18(2):590–598.

- Daugaard, D.E. & Brown, R.C. 2003. Enthalpy for Pyrolysis for Several Types of Biomass. *Energy and Fuels*. 17:934–939.
- Dayton, D.C., Carpenter, J.R., Kataria, A., Peters, J.E., Barbee, D., Mante, O.D. & Gupta, R. 2015. Design and operation of a pilot-scale catalytic biomass pyrolysis unit. *Green Chemistry*. 17(9):4680–4689.
- Demirbas, A. 2016. Calculation of higher heating values of fatty acids. *Energy Sources, Part A: Recovery, Utilization and Environmental Effects*. 38(18):2693–2697.
- Demirbas, M.F. & Balat, M. 2006. Recent advances on the production and utilization trends of bio-fuels: A global perspective. *Energy Conversion and Management*. 47(15–16):2371–2381.
- Department of Agriculture Forestry and Fisheries. 2018. *Guide to Machinery Costs 2015-2016*. [Online], Available: <https://www.daff.gov.za/daffweb3/Home/Crop-Estimates/Economic> [2018, June 08].
- Department of Energy. 2019. *Petrol Price Archive*. [Online], Available: http://www.energy.gov.za/files/esources/petroleum/petroleum_arch.html [2019, May 13].
- Department of Environmental Affairs. 2015. *South Africa's Intended Nationally Determined Contribution*. [Online], Available: <https://www.environment.gov.za> [2019, September 05].
- Department of Environmental Affairs. 2016. *South Africa joins Nations of the World in ratifying the Paris Agreement on Climate Change*. [Online], Available: https://www.environment.gov.za/mediarelease/southafrica_ratifies_parisagreement [2017, November 12].
- Dhyani, V. & Bhaskar, T. 2018. A comprehensive review on the pyrolysis of lignocellulosic biomass. *Renewable Energy*. 129:695–716.
- Dickerson, T. & Soria, J. 2013. Catalytic fast pyrolysis: A review. *Energies*. 6(1):514–538.
- Do, T.X. & Lim, Y. II. 2016. Techno-economic comparison of three energy conversion pathways from empty fruit bunches. *Renewable Energy*. 90:307–318.
- Dovey, S.B. 2009. Estimating biomass and macronutrient content of some commercially important plantation species in South Africa. *Southern Forests*. 71(3):245–251.
- Du, S., Valla, J.A. & Bollas, G.M. 2013. Characteristics and origin of char and coke from fast and slow, catalytic and thermal pyrolysis of biomass and relevant model compounds. *Green Chemistry*. 15(11):3214.
- Dutta, A., Sahir, A., Tan, E., Humbird, D., Snowden-swan, L.J., Meyer, P., Ross, J., Sexton, D., et al. 2015. Process Design and Economics for the Conversion of Lignocellulosic Biomass to Hydrocarbon Fuels: Thermochemical Research Pathways with In Situ and Ex Situ Upgrading of Fast Pyrolysis Vapors. *National Renewable Energy Laboratory*.
- van Dyk, S., Su, J., McMillan, J.D. & Saddler, J. 2019. Potential synergies of drop-in biofuel production with further co-processing at oil refineries. *Biofuels, Bioproducts and Biorefining*. 13(3):760–775.
- Eskom. 2019. *Integrated Report*. [Online], Available: <http://www.eskom.co.za/IR2018/Pages/default.aspx> [2019, August 30].

- Farzad, S., Mandegari, M.A., Guo, M., Haigh, K.F., Shah, N. & Görgens, J.F. 2017. Multi-product biorefineries from lignocelluloses: a pathway to revitalisation of the sugar industry? *Biotechnology for Biofuels*. 10(1):87.
- Farzad, S., Mandegari, M.A. & Görgens, J.F. 2017. Integrated techno-economic and environmental analysis of butadiene production from biomass. *Bioresource Technology*. 239:37–48.
- Federal Reserve Economic Data. 2019. *Producer Price Index by Commodity for Chemicals and Allied Products*. [Online], Available: <https://fred.stlouisfed.org/series/WPU06#0> [2019, July 02].
- Fogassy, G., Thegarid, N., Schuurman, Y. & Mirodatos, C. 2012. The fate of bio-carbon in FCC co-processing products. *Green Chemistry*. 14(5):1367–1371.
- Forestry Economics Services. 2017. *Commercial Timber Resources and Primary Roundwood Processing in South Africa 2015/2016*. Pretoria: Department of Agriculture, Forestry and Fisheries.
- Galadima, A. & Muraza, O. 2015. In situ fast pyrolysis of biomass with zeolite catalysts for bioaromatics/gasoline production: A review. *Energy Conversion and Management*. 105:338–354.
- García-Pérez, M., Chaala, A., Pakdel, H., Kretschmer, D. & Roy, C. 2007. Vacuum pyrolysis of softwood and hardwood biomass. Comparison between product yields and bio-oil properties. *Journal of Analytical and Applied Pyrolysis*. 78(1):104–116.
- Gollakota, A.R.K., Reddy, M., Subramanyam, M.D. & Kishore, N. 2016. A review on the upgradation techniques of pyrolysis oil. *Renewable and Sustainable Energy Reviews*. 58:1543–1568.
- Gonçalves, J.L.M., Wichert, M.C.P., Gava, J.L., Masetto, A.V., Junior, A.J.C., Serrano, M.I.P. & Mello, S.L.M. 2007. Soil Fertility and Growth of Eucalyptus grandis in Brazil under Different Residue Management Practices. *Southern Hemisphere Forestry Journal*. 69(2):95–102.
- Gorgens, J.F., Mandegari, M., Farzad, S., Daful, A. & Haigh, K. 2016. *A biorefinery approach to improve the sustainability of the South African sugar industry: Assessment of selected scenarios*. Department of Environmental Affairs.
- Grain SA. 2019. *Fertilizer/Agro-chemical Report - October 2018*. [Online], Available: <https://www.grainsa.co.za/> [2019, May 07].
- Han, J., Elgowainy, A., Dunn, J.B. & Wang, M.Q. 2013. Life cycle analysis of fuel production from fast pyrolysis of biomass. *Bioresource Technology*. 133:421–428.
- Hill, D. 2011. *North Dakota Refining Capacity Study*. United States Department of Energy.
- Hsu, D.D. 2012. Life cycle assessment of gasoline and diesel produced via fast pyrolysis and hydroprocessing. *Biomass and Bioenergy*. 45:41–47.
- Hugo, W. 2016. *Bioenergy Atlas for South Africa*. Department of Science and Technology.
- Humbird, D., Davis, R., Tao, L., Kinchin, C., Hsu, D., Aden, A., Schoen, P., Lukas, J., et al. 2011. *Process Design and Economics for Biochemical Conversion of Lignocellulosic Biomass to Ethanol*. National Renewable Energy Laboratory.

- Ibarra, Á., Veloso, A., Bilbao, J., Arandes, J.M. & Castaño, P. 2016. Dual coke deactivation pathways during the catalytic cracking of raw bio-oil and vacuum gasoil in FCC conditions. *Applied Catalysis B: Environmental*. 182:336–346.
- IEA Renewable Energy Division. 2010. *Sustainable production of second-generation biofuels: Potential and perspectives in major economies and developing countries*. Paris: International Energy Agency.
- IEA Renewable Energy Division. 2011. *Technology Roadmap: Biofuels for Transport*. Paris: International Energy Agency.
- Iribarren, D., Peters, J.F. & Dufour, J. 2012. Life cycle assessment of transportation fuels from biomass pyrolysis. *Fuel*. 97:812–821.
- Isahak, W.N.R.W., Hisham, M.W.M., Yarmo, M.A. & Yun Hin, T. 2012. A review on bio-oil production from biomass by using pyrolysis method. *Renewable and Sustainable Energy Reviews*. 16(8):5910–5923.
- Jacobson, J.J., Roni, M.S., Lamers, P. & Cafferty, K.G. 2014. *Biomass Feedstock Supply System Design and Analysis*. Idaho National Laboratory.
- Jechura, J. 2016. *Refinery Feedstocks & Products: Properties & Specifications*. Colorado School of Mines.
- Jindo, K., Mizumoto, H., Sawada, Y., Sanchez-Monedero, M.A. & Sonoki, T. 2014. Physical and chemical characterization of biochars derived from different agricultural residues. *Biogeosciences*. 11(23):6613–6621.
- Jones, S., Meyer, P., Snowden-Swan, L., Asanga, P., Eric, T., Abhijit, D., Jacob, J. & Cafferty, K. 2013. *Process design and economics for the conversion of lignocellulosic biomass to hydrocarbon fuels: Fast pyrolysis and hydrotreating bio-oil pathway*. Pacific Northwest National Laboratory.
- Kalkor. 2019. *Price List*. [Online], Available: <http://www.kalkor.co.za/site/content/id/price-list> [2019, May 26].
- De Kam, M.J., Morey, R.V. & Tiffany, D.G. 2009. Biomass Integrated Gasification Combined Cycle for heat and power at ethanol plants. *Energy Conversion and Management*. 50(7):1682–1690.
- Kan, T., Strezov, V. & Evans, T.J. 2016. Lignocellulosic biomass pyrolysis: A review of product properties and effects of pyrolysis parameters. *Renewable and Sustainable Energy Reviews*. 57:126–1140.
- Kauffman, N., Hayes, D. & Brown, R. 2011. A life cycle assessment of advanced biofuel production from a hectare of corn. *Fuel*. 90(11):3306–3314.
- Kim, K.H., Kim, T.S., Lee, S.M., Choi, D., Yeo, H., Choi, I.G. & Choi, J.W. 2013. Comparison of physicochemical features of biooils and biochars produced from various woody biomasses by fast pyrolysis. *Renewable Energy*. 50:188–195.
- Konz, J., Cohen, B. & van der Merwe, A. 2015. *Assessment of the potential to produce biochar and its application to South African soils as a mitigation measure*. Department of Environmental Affairs.

- Lappas, A.A., Kalogiannis, K.G., Iliopoulou, E.F., Triantafyllidis, K.S. & Stefanidis, S.D. 2012. Catalytic pyrolysis of biomass for transportation fuels. *Wiley Interdisciplinary Reviews: Energy and Environment*. 1(3):285–297.
- Lee, Y., Park, J., Ryu, C., Gang, K.S., Yang, W., Park, Y.K., Jung, J. & Hyun, S. 2013. Comparison of biochar properties from biomass residues produced by slow pyrolysis at 500°C. *Bioresource Technology*. 148:196–201.
- Li, B., Ou, L., Dang, Q., Meyer, P., Jones, S., Brown, R. & Wright, M. 2015. Techno-economic and uncertainty analysis of in situ and ex situ fast pyrolysis for biofuel production. *Bioresource Technology*. 196:49–56.
- Li, W., Fu, F., Ma, L., Liu, P., Li, Z. & Dai, Y. 2013. A process-based model for estimating the well-to-tank cost of gasoline and diesel in China. *Applied Energy*. 102:718–725.
- Lin, Y., Zhang, C., Zhang, M. & Zhang, J. 2010. Deoxygenation of bio-oil during pyrolysis of biomass in the presence of CaO in a fluidized-bed reactor. *Energy and Fuels*. 24(10):5686–5695.
- Lindfors, C., Paasikallio, V., Kuoppala, E., Reinikainen, M., Oasmaa, A. & Solantausta, Y. 2015. Co-processing of dry bio-oil, catalytic pyrolysis oil, and hydrotreated bio-oil in a micro activity test unit. *Energy and Fuels*. 29(6):3707–3714.
- Liu, C., Wang, H., Karim, A.M., Sun, J. & Wang, Y. 2014. Catalytic fast pyrolysis of lignocellulosic biomass. *Chemical Society Reviews*. 43(22):7594–7623.
- Lu, H.R. & El Hanandeh, A. 2019. Life cycle perspective of bio-oil and biochar production from hardwood biomass; what is the optimum mix and what to do with it? *Journal of Cleaner Production*. 212:173–189.
- Lu, H., Zhang, W., Yang, Y., Huang, X., Wang, S. & Qiu, R. 2012. Relative distribution of Pb²⁺ sorption mechanisms by sludge-derived biochar. *Water Research*. 46(3):854–862.
- Luo, G., Chandler, D.S., Anjos, L.C.A., Eng, R.J., Jia, P. & Resende, F.L.P. 2017. Pyrolysis of whole wood chips and rods in a novel ablative reactor. *Fuel*. 194:229–238.
- Macrotrends. 2019. *Brent Crude Oil Prices - 10 Year Daily Chart*. [Online], Available: <https://www.macrotrends.net/2480/brent-crude-oil-price> [2019, May 13].
- Mandegari, M.A., Farzad, S. & Gorgens, J.F. 2016. Process Design, Flowsheeting, and Simulation of Bioethanol Production from Lignocelluloses. In R.S. Singh, A. Pandey, & E. Gnansounou (eds.) *Biofuels: Production and Future Perspectives*. 255–277.
- Meier, D., Oasmaa, A. & Peacocke, G.V.C. 1997. Properties of Fast Pyrolysis Liquids: Status of Test Methods. In A.V. Bridgwater & D.G.B. Boocock (eds.). Dordrecht: Springer *Developments in Thermochemical Biomass Conversion*. 391–408.
- Melendez, J., LeBel, L. & Stuart, P.R. 2013. A Literature Review of Biomass Feedstocks for a Biorefinery. In M.M. El-Halwagi & P.R. Stuart (eds.) *Integrated Biorefineries: Design, Analysis, and Optimization*. 433–455.

- de Miguel Mercader, F., Groeneveld, M.J., Kersten, S.R.A., Way, N.W.J., Schaverien, C.J. & Hogendoorn, J.A. 2010. Production of advanced biofuels: Co-processing of upgraded pyrolysis oil in standard refinery units. *Applied Catalysis B: Environmental*. 96:57–66.
- Mirkouei, A., Haapala, K.R., Sessions, J. & Murthy, G.S. 2017. A review and future directions in techno-economic modeling and optimization of upstream forest biomass to bio-oil supply chains. *Renewable and Sustainable Energy Reviews*. 67:15–35.
- Mitchell, K.A., Parker, N.C., Sharma, B. & Kaffka, S. 2015. *Potential for Biofuel Production from Forest Woody Biomass*. California Biomass Collaborative.
- Mohan, D., Pittman, C.U. & Steele, P.H. 2006. Pyrolysis of wood/biomass for bio-oil: A critical review. *Energy and Fuels*. 20(3):848–889.
- Morris, M.A. 2011. Production of bio-oils via catalytic pyrolysis. In First ed. R. Luque, J. Campelo, & J.H. Clark (eds.). Oxford: Woodhead Publishing Limited *Handbook of biofuels production - processes and technologies*. 349–389.
- Motiang, M. & Nembahe, R. 2017. *South African Energy Price Report*. Pretoria: Department of Energy.
- Mullen, C.A., Strahan, G.D. & Boateng, A.A. 2009. Characterization of various fast-pyrolysis bio-oils by NMR spectroscopy. *Energy and Fuels*. 23(5):2707–2718.
- Mullen, C.A., Boateng, A.A., Goldberg, N.M., Lima, I.M., Laird, D.A. & Hicks, K.B. 2010. Bio-oil and bio-char production from corn cobs and stover by fast pyrolysis. *Biomass and Bioenergy*. 34:67–74.
- Nambiar, E.K.S. & Kallio, M.H. 2008. Increasing and Sustaining Productivity in Subtropical and Tropical Plantation forests: Making a Difference through Research Partnership. In *Site management and productivity in tropical plantation forests: Proceedings of Workshops in Piracicaba (Brazil) 22-26 November 2004 and Bogor (Indonesia) 6-9 November 2006*. 205–227.
- Neves, D., Thunman, H., Matos, A., Tarelho, L. & Gómez-Barea, A. 2011. Characterization and prediction of biomass pyrolysis products. *Progress in Energy and Combustion Science*. 37(5):611-630.
- Nieder-Heitmann, M., Haigh, K.F. & Görgens, J.F. 2018. Process design and economic analysis of a biorefinery co-producing itaconic acid and electricity from sugarcane bagasse and trash lignocelluloses. *Bioresource Technology*. 262:159–168.
- Nikolaidis, P. & Poullikkas, A. 2017. A comparative overview of hydrogen production processes. *Renewable and Sustainable Energy Reviews*. 67:597–611.
- Nolte, M.W. & Shanks, B.H. 2017. A Perspective on Catalytic Strategies for Deoxygenation in Biomass Pyrolysis. *Energy Technology*. 5(1):7–18.
- Nsafu, F., Görgens, J.F. & Knoetze, J.H. 2013. Comparison of combustion and pyrolysis for energy generation in a sugarcane mill. *Energy Conversion and Management*. 74:524–534.
- Oasmaa, A., Kuoppala, E., Gust, S. & Solantausta, Y. 2003. Fast Pyrolysis of Forestry Residue. 1. Effect of Extractives on Phase Separation of Pyrolysis Liquids. *Energy and Fuels*. 17(1):1–12.

- Oasmaa, A., Solantausta, Y., Arpiainen, V., Kuoppala, E. & Sipilä, K. 2010. Fast pyrolysis bio-oils from wood and agricultural residues. *Energy and Fuels*. 24(2):1380–1388.
- Onarheim, K., Solantausta, Y. & Lehto, J. 2015. Process Simulation Development of Fast Pyrolysis of Wood Using Aspen Plus. *Energy and Fuels*. 29(1):205–217.
- Paasikallio, V., Kalogiannis, K., Lappas, A., Lehto, J. & Lehtonen, J. 2017. Catalytic Fast Pyrolysis: Influencing Bio-Oil Quality with the Catalyst-to-Biomass Ratio. *Energy Technology*. 5(1):94–103.
- PAMSA. 2019. *Paper in Perspective - Industry Report 2016*. [Online], Available: <https://www.thepaperstory.co.za/brochures-and-publications/> [2019, May 24].
- Patel, M., Zhang, X. & Kumar, A. 2016. Techno-economic and life cycle assessment on lignocellulosic biomass thermochemical conversion technologies: A review. *Renewable and Sustainable Energy Reviews*. 53:1486–1489.
- Perry, R.H., Green, D.W. & Maloney, J.O. 1997. *Perry's Chemical Engineers' Handbook*. Seventh ed. New York: McGraw-Hill.
- Peters, J.F., Iribarren, D. & Dufour, J. 2015. Life cycle assessment of pyrolysis oil applications. *Biomass Conversion and Biorefinery*. 5:1–19.
- Pinho, A. de R., de Almeida, M.B.B., Mendes, F.L., Casavechia, L.C., Talmadge, M.S., Kinchin, C.M. & Chum, H.L. 2017. Fast pyrolysis oil from pinewood chips co-processing with vacuum gas oil in an FCC unit for second generation fuel production. *Fuel*. 188:462–473.
- Pinho, A.D.R., De Almeida, M.B.B., Mendes, F.L., Ximenes, V.L. & Casavechia, L.C. 2015. Co-processing raw bio-oil and gasoil in an FCC Unit. *Fuel Processing Technology*. 131:159–166.
- Pisupati, S. V & Tchabda, A.H. 2015. Thermochemical Processing of Biomass. In P. Ravindra (ed.). Cham: Springer *Advances in Bioprocess Technology*. 277–314.
- Polagye, B.L., Hodgson, K.T. & Malte, P.C. 2007. An economic analysis of bio-energy options using thinnings from overstocked forests. *Biomass and Bioenergy*. 31:105–125.
- Puy, N., Murillo, R., Navarro, M. V., López, J.M., Rieradevall, J., Fowler, G., Aranguren, I., García, T., et al. 2011. Valorisation of forestry waste by pyrolysis in an auger reactor. *Waste Management*. 31(6):1339–1349.
- Qambrani, N.A., Rahman, M.M., Won, S., Shim, S. & Ra, C. 2017. Biochar properties and eco-friendly applications for climate change mitigation, waste management, and wastewater treatment: A review. *Renewable and Sustainable Energy Reviews*. 79:255–273.
- Qu, T., Guo, W., Shen, L., Xiao, J. & Zhao, K. 2011. Experimental study of biomass pyrolysis based on three major components: Hemicellulose, cellulose, and lignin. *Industrial and Engineering Chemistry Research*. 50(18):10424–10433.
- Republic of South Africa. 2019. *Carbon Tax Act 15 of 2019*. Cape Town: Government Printer.

- Richardson, Y., Blin, J., Volle, G., Motuzas, J. & Julbe, A. 2010. In situ generation of Ni metal nanoparticles as catalyst for H₂-rich syngas production from biomass gasification. *Applied Catalysis A: General*. 382(2):220–230.
- Ringer, M., Putsche, V. & Scahill, J. 2006. *Large-Scale Pyrolysis Oil Production: A Technology Assessment and Economic Analysis*. National Renewable Energy Laboratory.
- Roberts, K.G., Gloy, B.A., Joseph, S., Scott, N.R. & Lehmann, J. 2010. Life Cycle Assessment of Biochar Systems: Estimating the Energetic, Economic, and Climate Change Potential. *Environmental Science & Technology*. 44(2):827–833.
- Röser, D. 2008. *Sustainable use of forest biomass for energy: a synthesis with focus on the Baltic and Nordic region*. D. Röser, A. Asikainen, K. Raulund-Rasmussen, & I. Stupak (eds.). Dordrecht: Springer.
- Rowell, R.M., Pettersen, R., Han, J.S., Rowell, J.S. & Tshabalala, M.A. 2005. Cell Wall Chemistry. In R.M. Rowell (ed.) *Handbook of Wood Chemistry and Wood Composites*.
- Roy, P. & Dias, G. 2017. Prospects for pyrolysis technologies in the bioenergy sector: A review. *Renewable and Sustainable Energy Reviews*. 77:59–69.
- Sandström, L., Johansson, A.C., Wiinikka, H., Öhrman, O.G.W. & Marklund, M. 2016. Pyrolysis of Nordic biomass types in a cyclone pilot plant — Mass balances and yields. *Fuel Processing Technology*. 152:274–284.
- Seal Water Tech. 2019. *Granular Activated Carbon (GAC) Media*. [Online], Available: <https://www.sealwatertech.co.za/granular-activated-carbon> [2019, May 14].
- Serrano-Ruiz, J.-C. & Dumesic, J.A. 2012. Catalytic production of liquid hydrocarbon transportation fuels. In L. Gucci & A. Erdohelyi (eds.) *Catalysis for Alternative Energy Generation*. 29–56.
- Shadangi, K.P. & Mohanty, K. 2014a. Comparison of yield and fuel properties of thermal and catalytic Mahua seed pyrolytic oil. *Fuel*. 117:372–380.
- Shadangi, K.P. & Mohanty, K. 2014b. Thermal and catalytic pyrolysis of Karanja seed to produce liquid fuel. *Fuel*. 115:434–442.
- Sharifzadeh, M., Sadeqzadeh, M., Guo, M., Borhani, T.N., Murthy, N.V.S.N., Cortada, M., Wang, L., Hallett, J., et al. 2019. The multi-scale challenges of biomass fast pyrolysis and bio-oil upgrading: Review of the state of art and future research directions. *Progress in Energy and Combustion Science*. 71:1–80.
- Shemfe, M., Gu, S. & Fidalgo, B. 2017. Techno-economic analysis of biofuel production via bio-oil zeolite upgrading: An evaluation of two catalyst regeneration systems. *Biomass and Bioenergy*. 98:182–193.
- South African Petroleum Industry Association. 2017. *South African fuel industry*. [Online], Available: <http://www.sapia.org.za/Overview/Old-fuel-prices> [2017, October 20].

- Statistics South Africa. 2019. *Producer Price Index - December 2017*. [Online], Available: www.statssa.gov.za [2018, October 29].
- Steele, P., Puettmann, M.E., Penmetsa, V.K. & Cooper, J.E. 2012. Life-Cycle Assessment of Pyrolysis Bio-Oil Production. *Forest Products Journal*. 62(4):326–334.
- Stefanidis, S.D., Kalogiannis, K.G., Iliopoulou, E.F., Lappas, A.A. & Pilavachi, P.A. 2011. In-situ upgrading of biomass pyrolysis vapors: Catalyst screening on a fixed bed reactor. *Bioresource Technology*. 102(17):8261–8267.
- Stefanidis, S.D., Karakoulia, S.A., Kalogiannis, K.G., Iliopoulou, E.F., Delimitis, A., Yiannoulakis, H., Zampetakis, T., Lappas, A.A., et al. 2016. Natural magnesium oxide (MgO) catalysts: A cost-effective sustainable alternative to acid zeolites for the in situ upgrading of biomass fast pyrolysis oil. *Applied Catalysis B: Environmental*. 196:155–173.
- Talmadge, M.S., Baldwin, R.M., Bidy, M.J., McCormick, R.L., Beckham, G.T., Ferguson, G.A., Czernik, S., Magrini-bair, K.A., et al. 2014. A perspective on oxygenated species in the refinery integration of pyrolysis oil. *Green Chemistry*. 16:407–453.
- Thegarid, N., Fogassy, G., Schuurman, Y., Mirodatos, C., Stefanidis, S., Iliopoulou, E.F., Kalogiannis, K. & Lappas, A.A. 2014. Second-generation biofuels by co-processing catalytic pyrolysis oil in FCC units. *Applied Catalysis B: Environmental*. 145:161–166.
- Thilakarathne, R., Brown, T., Li, Y., Hu, G. & Brown, R. 2014. Mild catalytic pyrolysis of biomass for production of transportation fuels: a techno-economic analysis. *Green Chemistry*. 16:627–636.
- Torri, I.D.V., Paasikallio, V., Faccini, C.S., Huff, R., Caramão, E.B., Sacon, V., Oasmaa, A. & Zini, C.A. 2016. Bio-oil production of softwood and hardwood forest industry residues through fast and intermediate pyrolysis and its chromatographic characterization. *Bioresource Technology*. 200:680–690.
- Tripathi, M., Sahu, J.N. & Ganesan, P. 2016. Effect of process parameters on production of biochar from biomass waste through pyrolysis: A review. *Renewable and Sustainable Energy Reviews*. 55:467–481.
- Turton, R., Bailie, R.C., Whiting, W.B. & Shaeiwitz, J.A. 2009. *Analysis, synthesis, and design of chemical processes*. Third ed. Boston: Pearson Education, Inc.
- U.S. Bureau of Labor Statistics. 2019. *Employment, Hours, and Earnings from the Current Employment Statistics survey (National)*. [Online], Available: <https://data.bls.gov/pdq/SurveyOutputServlet> [2019, July 02].
- Van de Velden, M., Baeyens, J., Brems, A., Janssens, B. & Dewil, R. 2010. Fundamentals, kinetics and endothermicity of the biomass pyrolysis reaction. *Renewable Energy*. 35:232–242.
- Veses, A., Aznar, M., Martinez, I., Martinez, J.D., Lopez, J.M., Navarro, M. V., Callen, M.S., Murillo, R., et al. 2014. Catalytic pyrolysis of wood biomass in an auger reactor using calcium-based catalysts. *Bioresource Technology*. 162:250–258.

- Veses, A., Aznar, M., López, J.M., Callén, M.S., Murillo, R. & García, T. 2015. Production of upgraded bio-oils by biomass catalytic pyrolysis in an auger reactor using low cost materials. *Fuel*. 141:17-22.
- Vlysidis, A., Binns, M., Webb, C. & Theodoropoulos, C. 2011. A techno-economic analysis of biodiesel biorefineries: Assessment of integrated designs for the co-production of fuels and chemicals. *Energy*. 36(8):4671–4683.
- Walas, S.M. 1990. *Chemical Process Equipment: Selection and Design*. First ed. Boston: Butterworth-Heinemann.
- Wang, W. & Jan, J. 2018. From laboratory to pilot: Design concept and techno-economic analyses of the fluidized bed fast pyrolysis of biomass. *Energy*. 155:139–151.
- Wang, C., Li, M. & Fang, Y. 2016. Coprocessing of Catalytic-Pyrolysis-Derived Bio-Oil with VGO in a Pilot-Scale FCC Riser. *Industrial and Engineering Chemistry Research*. 55(12):3525–3534.
- Wang, C., Venderbosch, R. & Fang, Y. 2018. Co-processing of crude and hydrotreated pyrolysis liquids and VGO in a pilot scale FCC riser setup. *Fuel Processing Technology*. 181:157–165.
- Wang, K., Dayton, D.C., Peters, J.E. & Mante, O.D. 2017. Reactive catalytic fast pyrolysis of biomass to produce high-quality bio-crude. *Green Chemistry*. 19(14):3243–3251.
- Wang, S., Dai, G., Yang, H. & Luo, Z. 2017. Lignocellulosic biomass pyrolysis mechanism: A state-of-the-art review. *Progress in Energy and Combustion Science*. 62:33–86.
- Wattle Wood Farm. 2019. *Firewood For Sale - Pricelist - Wattle Products*. [Online], Available: <http://www.wattlewood.co.za/wattlewood-firewood-prices-product-pole-prices.html> [2019, May 13].
- Woods, D.R. 2007. *Rules of Thumb in Engineering Practice*. Weinheim: John Wiley & Sons.
- Wright, L.L., Eaton, L.M., Perlack, R.D. & Stokes, B.J. 2012. Woody biomass. In A. Sayigh (ed.). Elsevier *Comprehensive Renewable Energy*. 263–291.
- Wright, M.M., Satrio, J. a., Brown, R.C., Daugaard, D.E. & Hsu, D.D. 2010. *Techno-economic analysis of biomass fast pyrolysis to transportation fuels*. National Renewable Energy Laboratory.
- Yang, C., Li, R. & Zhang, B. 2016. Biomass harvesting and collection. In J.B. Holm-Nielsen & E.A. Ehimen (eds.). Elsevier *Biomass Supply Chains for Bioenergy and Biorefining*. 103–125.
- Yang, H., Kudo, S., Kuo, H., Norinaga, K., Mori, A., Ondrej, M. & Hayashi, J. 2013. Estimation of Enthalpy of Bio-Oil Vapor and Heat Required for Pyrolysis of Biomass. *Energy and Fuels*. 27:2675–2686.
- Yang, Y., Heaven, S., Venetsaneas, N., Banks, C.J. & Bridgwater, A. V. 2018. Slow pyrolysis of organic fraction of municipal solid waste (OFMSW): Characterisation of products and screening of the aqueous liquid product for anaerobic digestion. *Applied Energy*. 213:158–168.
- Yildiz, G., Ronsse, F., Duren, R. Van & Prins, W. 2016. Challenges in the design and operation of processes for catalytic fast pyrolysis of woody biomass. *Renewable and Sustainable Energy Reviews*. 57:1596–1610.

- Zhang, M., Resende, F.L.P. & Moutsoglou, A. 2014. Catalytic fast pyrolysis of aspen lignin via Py-GC/MS. *Fuel*. 116:358–369.
- Zhang, S., Yan, Y., Li, T. & Ren, Z. 2005. Upgrading of liquid fuel from the pyrolysis of biomass. *Bioresource Technology*. 96(5):545–550.
- Zhao, B., Zhang, X., Chen, L., Sun, L., Si, H. & Chen, G. 2014. High quality fuel gas from biomass pyrolysis with calcium oxide. *Bioresource Technology*. 156:78–83.

8 Appendices

8.1 Appendix A

Table A1: Pilot plant results for non-catalytic pyrolysis

		Feed	Char	C1	C2A	C2O	C3	C4	Gas
Yield (wt. %)			28.71	8.34	19.96	4.92	4.13	2.42	20.62
Elemental Analysis (wt. %, db)	C	48.01	83.15	44.31	42.51	71.80	67.46	74.24	
	H	6.36	3.40	8.02	4.98	6.67	8.74	6.91	
	O	45.46	13.04	47.67	52.51	21.29	23.79	18.85	
	N	0.12	0.34	0.00	0.00	0.23	0.00	0.00	
	S	0.06	0.08	0.00	0.00	0.00	0.00	0.00	
Proximate analysis (wt. %)	Moisture	8.28	0.00	8.73	87.17	18.00	26.09	21.39	
	Fixed carbon	15.06	77.42						
	Volatile matter	75.70	19.27						
	Ash	0.95	3.32						
HHV (MJ/kg, db)		19.33		22.10		29.08	30.17	32.63	
Density (kg/m ³ , db)				1184	1288	1041	1117	1234	
Composition (wt. %)	CO ₂								50.34
	CO								33.98
	CH ₄								8.54
	H ₂								0.57
	C ₂ H ₆								3.74
	C ₂ H ₄								1.11
	C ₃ H ₈								1.11
C ₄ H ₆								0.61	

Table A2: Pilot plant results for catalytic pyrolysis

		Feed	Char	CO ₂ (CaCO ₃)	C1	C2A	C2O	C3	C4	Gas
Yield (wt. %)			16.48	20.85	10.00	15.70	3.73	2.77	1.90	17.63
Elemental Analysis (wt. %, db)	C	48.01	79.37		79.67	28.90	80.64	60.56	82.10	
	H	6.36	3.37		7.11	6.46	6.09	6.14	7.29	
	O	45.46	16.58		12.78	63.28	13.23	32.42	10.38	
	N	0.12	0.68		0.44	1.36	0.05	0.88	0.22	
	S	0.06	0.00		0.00	0.00	0.00	0.00	0.00	
Proximate analysis (wt. %)	Moisture	8.28	0.00		22.78	86.60	13.82	58.97	17.01	
	Fixed carbon	15.06	56.25							
	Volatile matter	75.70	37.98							
	Ash	0.95	5.77							
HHV (MJ/kg, db)		19.33		35.37		34.61	25.93	37.84		
Density (kg/m ³ , db)				1152	1198	1040	1031	1042		
Composition (wt. %)	CO ₂									22.11
	CO									40.45
	CH ₄									15.32
	H ₂									2.29
	C ₂ H ₆									13.57
	C ₂ H ₄									1.93
	C ₃ H ₈									3.41
	C ₄ H ₆									0.92

8.2 Appendix B

Table B1: Stream Table for Biorefinery Scenario NC-100

Stream		0001	0002	0003	0004	0005	0006	0007	0008	0009
Temperature	C	25	58	130	131	51	51	100	100	100
Pressure	BAR	1.01	1.01	1.29	1.3	1.01	1.01	1.01	1.01	1.01
Mass Flow	KG/H	9384.5	9384.5	28658.8	28658.8	29847	8196.3	8196.3	6926.2	1270.1
Component Mass Flow										
CO2	KG/H	0	0	7664.2	7664.2	7656.5	7.7	7.7	7.7	0
N2	KG/H	0	0	18924	18924	18918.9	5.2	5.2	5.1	0
O2	KG/H	0	0	957.5	957.5	957.1	0.4	0.4	0.4	0
H2O	KG/H	9384.5	9384.5	1113.1	1113.1	2314.5	8183.1	8183.1	6913.1	1270
Mass Enthalpy	MJ/KG	-15.9	-15.7	-2.8	-2.8	-3.3	-15.7	-13.6	-13.3	-15.5
Substream: NCPD										
Component Mass Flow										
EGRANDIS	KG/H	14076.7	14076.7	0	0	0	14076.7	14076.7	0	14076.7

Table B1: Stream Table for Biorefinery Scenario NC-100 (continued...)

Stream		1001	1002	1003	1004	1005	1006	1007	1008	1010
Temperature	C	0	25	25	25	25	25	25	100	100
Pressure	BAR	0	1.01	1.01	1.01	1.01	1.01	1.01	1.01	1.01
Mass Flow	KG/H	0	9384.5	9384.5	9384.5	9384.5	8113.4	1271	1271	1271
Component Mass Flow										
H2O	KG/H	0	9384.5	9384.5	9384.5	9384.5	8113.4	1271	1271	1271
Mass Enthalpy	MJ/KG	0	-15.9	-15.9	-15.9	-15.9	-15.9	-15.9	-15.5	-15.5
Substream: NCPD										
Component Mass Flow										
EGRANDIS	KG/H	14076.7	0	14076.7	14076.7	14076.7	0	14076.7	14076.7	14076.7

Table B1: Stream Table for Biorefinery Scenario NC-100 (continued...)

Stream		2001	2002	2003	2004	2005	2006	2007	2008	2009
Temperature	C	100	500	500	500	500	0	0	0	0
Pressure	BAR	1.01	1.01	1.01	1.01	1.01	0	0	0	0
Mass Flow	KG/H	1271	10904.3	10904.3	10904	10904	0	0	0	0
Component Mass Flow										
CO2	KG/H	0	2342.5	2342.5	2342.5	2343	0	0	0	0
CO	KG/H	0	1326.5	1326.5	1326.5	1327	0	0	0	0
H2	KG/H	0	206.9	206.9	206.9	206.9	0	0	0	0
CH4	KG/H	0	58.6	58.6	58.6	58.6	0	0	0	0
ETHYLENE	KG/H	0	31.6	31.6	31.6	31.6	0	0	0	0
ETHANE	KG/H	0	22.2	22.2	22.2	22.2	0	0	0	0
BUTANE	KG/H	0	5	5	5	5	0	0	0	0
PROPANE	KG/H	0	5	5	5	5	0	0	0	0
CROTONIC	KG/H	0	105.2	105.2	105.2	105.2	0	0	0	0
3-METHOX	KG/H	0	37	37	37	37	0	0	0	0
H2O	KG/H	1271	3594.7	3594.7	3594.7	3595	0	0	0	0
LIGNINA	KG/H	0	56.3	56.3	56.3	56.3	0	0	0	0
BENZDIOL	KG/H	0	155.3	155.3	155.3	155.3	0	0	0	0
ACETOL	KG/H	0	625.7	625.7	625.7	625.7	0	0	0	0
ISOEUGEN	KG/H	0	40.3	40.3	40.3	40.3	0	0	0	0
LEVOG-01	KG/H	0	214.8	214.8	214.8	214.8	0	0	0	0
FURAN	KG/H	0	250.5	250.5	250.5	250.5	0	0	0	0
CELLO-01	KG/H	0	399.8	399.8	399.8	399.8	0	0	0	0
DIMETHOX	KG/H	0	102.9	102.9	102.9	102.9	0	0	0	0
ABIETIC	KG/H	0	125.5	125.5	125.5	125.5	0	0	0	0
LIGNINB	KG/H	0	55.8	55.8	55.8	55.8	0	0	0	0
ACETIC	KG/H	0	529.1	529.1	529.1	529.1	0	0	0	0
GUAIA-01	KG/H	0	34.9	34.9	34.9	34.9	0	0	0	0
SYRIN-01	KG/H	0	40.3	40.3	40.3	40.3	0	0	0	0
FORMI-01	KG/H	0	175.6	175.6	175.6	175.6	0	0	0	0
N-PRO-01	KG/H	0	41.2	41.2	41.2	41.2	0	0	0	0
PHENO-01	KG/H	0	97.6	97.6	97.6	97.6	0	0	0	0
TOLUE-01	KG/H	0	33.8	33.8	33.8	33.8	0	0	0	0
FURFU-01	KG/H	0	80.4	80.4	80.4	80.4	0	0	0	0
BENZE-01	KG/H	0	109.1	109.1	109.1	109.1	0	0	0	0
Mass Enthalpy	MJ/KG	-15.5	-7.3	-7.3	-7.3	-7.3	0	0	0	0
Substream: NCPSD										
Component Mass Flow										
CHAR	KG/H	0	4412.9	4412.9	4412.9	0	4412.9	948.8	3464.1	3464.1
EGRANDIS	KG/H	14076.7	0	0	0	0	0	0	0	0
BALANCE	KG/H	0	30.6	30.6	30.6	0	30.6	6.6	24	24

Table B1: Stream Table for Biorefinery Scenario NC-100 (continued...)

Stream		3001	3002	3003	3004	3005	3006	3007	3008	3009	3010
Temperature	C	500	260	210	80	80	80	60	60	60	60
Pressure	BAR	1.01	1.01	1.01	1.01	1.01	1.01	1.01	1.01	1.01	1.01
Mass Flow	KG/H	10904.3	10904.3	10904	10904	1681.3	9223	9223	4189.6	765.8	3423.8
Component Mass Flow											
CO2	KG/H	2342.5	2342.5	2342.5	2342.5	0	2342.5	2343	0	0	0
CO	KG/H	1326.5	1326.5	1326.5	1326.5	0	1326.5	1327	0	0	0
H2	KG/H	206.9	206.9	206.9	206.9	0	206.9	206.9	0	0	0
CH4	KG/H	58.6	58.6	58.6	58.6	0	58.6	58.6	0	0	0
ETHYLENE	KG/H	31.6	31.6	31.6	31.6	0	31.6	31.6	0	0	0
ETHANE	KG/H	22.2	22.2	22.2	22.2	0	22.2	22.2	0	0	0
BUTANE	KG/H	5	5	5	5	0	5	5	0	0	0
PROPANE	KG/H	5	5	5	5	0	5	5	0	0	0
CROTONIC	KG/H	105.2	105.2	105.2	105.2	79.2	26.1	26.1	26.1	26.1	0
3-METHOX	KG/H	37	37	37	37	34.5	2.5	2.5	2.4	2.3	0.2
H2O	KG/H	3594.7	3594.7	3594.7	3594.7	127	3467.7	3468	3189.2	154.4	3034.7
LIGNINA	KG/H	56.3	56.3	56.3	56.3	0	56.3	56.3	56.3	56.3	0
BENZDIOL	KG/H	155.3	155.3	155.3	155.3	0	155.3	155.3	155.2	155.1	0.1
ACETOL	KG/H	625.7	625.7	625.7	625.7	527.5	98.3	98.3	2.3	2.3	0
ISOEUGEN	KG/H	40.3	40.3	40.3	40.3	0	40.3	40.3	40.2	40.2	0
LEVOG-01	KG/H	214.8	214.8	214.8	214.8	102.7	112.1	112.1	112	2.4	109.6
FURAN	KG/H	250.5	250.5	250.5	250.5	0	250.5	250.5	249.3	228.2	21.2
CELLO-01	KG/H	399.8	399.8	399.8	399.8	267.5	132.2	132.2	28.1	2.5	25.6
DIMETHOX	KG/H	102.9	102.9	102.9	102.9	0	102.9	102.9	10.8	10.6	0.3
ABIETIC	KG/H	125.5	125.5	125.5	125.5	0	125.5	125.5	1.5	1.3	0.3
LIGNINB	KG/H	55.8	55.8	55.8	55.8	0	55.8	55.8	1.9	1.9	0
ACETIC	KG/H	529.1	529.1	529.1	529.1	525.9	3.2	3.2	3.1	3.1	0
GUAIA-01	KG/H	34.9	34.9	34.9	34.9	0	34.9	34.9	2	2	0
SYRIN-01	KG/H	40.3	40.3	40.3	40.3	0	40.3	40.3	40.2	40.2	0
FORMI-01	KG/H	175.6	175.6	175.6	175.6	17	158.6	158.6	158.5	4.4	154.1
N-PRO-01	KG/H	41.2	41.2	41.2	41.2	0	41.2	41.2	21.1	21.1	0
PHENO-01	KG/H	97.6	97.6	97.6	97.6	0	97.6	97.6	1.7	1.7	0
TOLUE-01	KG/H	33.8	33.8	33.8	33.8	0	33.8	33.8	6.5	6.5	0
FURFU-01	KG/H	80.4	80.4	80.4	80.4	0	80.4	80.4	80	2.3	77.8
BENZE-01	KG/H	109.1	109.1	109.1	109.1	0	109.1	109.1	1.1	1.1	0
Mass Enthalpy	MJ/KG	-7.3	-7.8	-7.9	-8.4	-7.1	-8.5	-9.1	-12.8	-4.8	-14.6

Table B1: Stream Table for Biorefinery Scenario NC-100 (continued...)

Stream		3011	3012	3013	3014	3015	3016	3017	3018	3019	3020	3021
Temperature	C	60	40	40	40	20	20	45	20	65	65	65
Pressure	BAR	1.01	1.01	1.01	1.01	1.01	1.01	1.3	1.01	1.01	2	2
Mass Flow	KG/H	5034	5033.5	652.4	4381.1	4381.1	3998	3998.4	382.7	3482.1	3482	3482.1
Component Mass Flow												
CO2	KG/H	2343	2342.5	0	2342.5	2342.5	2343	2342.5	0	0	0	0
CO	KG/H	1327	1326.5	0	1326.5	1326.5	1327	1326.5	0	0	0	0
H2	KG/H	206.9	206.9	0	206.9	206.9	206.9	206.9	0	0	0	0
CH4	KG/H	58.6	58.6	0	58.6	58.6	58.6	58.6	0	0	0	0
ETHYLENE	KG/H	31.6	31.6	0	31.6	31.6	31.6	31.6	0	0	0	0
ETHANE	KG/H	22.2	22.2	0	22.2	22.2	22.2	22.2	0	0	0	0
BUTANE	KG/H	5	5	0	5	5	5	5	0	0	0	0
PROPANE	KG/H	5	5	0	5	5	5	5	0	0	0	0
CROTONIC	KG/H	0	0	0	0	0	0	0	0	105.2	105.2	105.2
3-METHOX	KG/H	0.1	0.1	0	0.1	0.1	0	0	0.1	36.8	36.8	36.8
H2O	KG/H	278.6	278.6	188.1	90.4	90.4	0	0	90.4	560	560	560
LIGNINA	KG/H	0	0	0	0	0	0	0	0	56.3	56.3	56.3
BENZDIOL	KG/H	0.2	0.2	0	0.2	0.2	0	0	0.2	155.2	155.2	155.2
ACETOL	KG/H	95.9	95.9	95.9	0	0	0	0	0	625.7	625.7	625.7
ISOEUGEN	KG/H	0.1	0.1	0	0.1	0.1	0	0	0.1	40.3	40.3	40.3
LEVOG-01	KG/H	0	0	0	0	0	0	0	0	105.2	105.2	105.2
FURAN	KG/H	1.1	1.1	0	1.1	1.1	0	0	1.1	229.3	229.3	229.3
CELLO-01	KG/H	104.1	104.1	48.1	56.1	56.1	0	0	56.1	374.2	374.2	374.2
DIMETHOX	KG/H	92	92	91.9	0.1	0.1	0	0	0.1	102.6	102.6	102.6
ABIETIC	KG/H	124	124	124	0.1	0.1	0	0	0.1	125.3	125.3	125.3
LIGNINB	KG/H	54	54	24.1	29.8	29.8	0	0	29.8	55.8	55.8	55.8
ACETIC	KG/H	0.1	0.1	0	0.1	0.1	0	0	0.1	529.1	529.1	529.1
GUAIA-01	KG/H	32.9	32.9	32.9	0	0	0	0	0	34.9	34.9	34.9
SYRIN-01	KG/H	0.1	0.1	0	0.1	0.1	0	0	0.1	40.3	40.3	40.3
FORMI-01	KG/H	0.1	0.1	0	0.1	0.1	0	0	0.1	21.5	21.5	21.5
N-PRO-01	KG/H	20.1	20.1	20.1	0	0	0	0	0	41.2	41.2	41.2
PHENO-01	KG/H	95.9	95.9	0	95.9	95.9	0	0	95.9	97.6	97.6	97.6
TOLUE-01	KG/H	27.2	27.2	27.2	0	0	0	0	0	33.8	33.8	33.8
FURFU-01	KG/H	0.4	0.4	0	0.4	0.4	0	0	0.4	2.7	2.7	2.7
BENZE-01	KG/H	108	108	0	108	108	0	0	108	109.1	109.1	109.1
Mass Enthalpy	MJ/KG	-6.3	-6.4	-6.6	-6.4	-6.5	-6.6	-6.6	-5.3	-6.3	-6.3	-6.3

Table B1: Stream Table for Biorefinery Scenario NC-100 (continued...)

Stream		4001	4002	4003	4004	4005	4006	4007	4008	4009	4010
Temperature	C	500	56	25	52	259	865	800	300	130	130
Pressure	BAR	1.01	1.3	1.01	1.3	1.3	1.3	1.3	1.29	1.29	1.29
Mass Flow	KG/H	824.3	3164.4	24670.1	24670.1	24670.1	28658.8	28658.8	28658.8	28658.8	28659
Component Mass Flow											
CO2	KG/H	0	1593.1	0	0	0	7664.2	7664.2	7664.2	7664	7664.2
CO	KG/H	0	1075.2	0	0	0	0	0	0	0	0
H2	KG/H	0	18	0	0	0	0	0	0	0	0
CH4	KG/H	0	270.2	0	0	0	0	0	0	0	0
ETHYLENE	KG/H	0	35.2	0	0	0	0	0	0	0	0
ETHANE	KG/H	0	118.4	0	0	0	0	0	0	0	0
BUTANE	KG/H	0	19.3	0	0	0	0	0	0	0	0
PROPANE	KG/H	0	35	0	0	0	0	0	0	0	0
N2	KG/H	0	0	18924	18924	18924	18924	18924	18924	18924	18924
O2	KG/H	0	0	5746.1	5746.1	5746.1	957.5	957.5	957.5	958	957.5
H2O	KG/H	0	0	0	0	0	1113.1	1113.1	1113.1	1113	1113.1
CARBON	KG/H	824.3	0	0	0	0	0	0	0	0	0
Mass Enthalpy	MJ/KG	0.6	-6.3	0	0	0.2	-2	-2	-2.6	-2.8	-2.8

Table B1: Stream Table for Biorefinery Scenario NC-100 (continued...)

Stream		5001	5002	5003	5004	5005	5006	5007	5008	5009
Temperature	C	100	102	128	228	234	35	234	234	361
Pressure	BAR	1.45	30	30	30	30	1.01	29.99	29.99	29.99
Mass Flow	KG/H	9482.7	9482.7	9482.7	9483	9483	284.5	284.5	9198.2	9198.2
Component Mass Flow										
H2O	KG/H	9482.7	9482.7	9482.7	9483	9483	284.5	284.5	9198.2	9198.2
Mass Enthalpy	MJ/KG	-15.5	-15.5	-15.4	-14.9	-13.1	-15.8	-14.8	-13	-12.8

Table B1: Stream Table for Biorefinery Scenario NC-100 (continued...)

Stream		5010	5011	5012	5013	5014	5015	5017	5018	5019	5020
Temperature	C	168	168	60	50	168	110	102	25	25	100
Pressure	BAR	4.5	4.5	0.2	0.2	4.5	1.43	1.45	1.01	2	1.45
Mass Flow	KG/H	9198.2	1230.9	1230.9	1230.9	7967	7967.3	9198	284.5	284.5	9482.7
Component Mass Flow											
H2O	KG/H	9198.2	1230.9	1230.9	1230.9	7967	7967.3	9198	284.5	284.5	9482.7
Mass Enthalpy	MJ/KG	-13.2	-13.2	-13.6	-15.8	-13	-15.5	-15.5	-15.9	-15.9	-15.5

Table B2: Stream Table for Biorefinery Scenario C-100

Stream		0001	0002	0003	0004	0005	0006	0007	0008	0009
Temperature	C	25	100	130	131	58	58	100	100	100
Pressure	BAR	1.01	1.01	1.29	1.3	1.01	1.01	1.01	1.01	1.01
Mass Flow	KG/H	9384.5	9384.5	40327.6	40327.6	42960.9	6751.1	6751.1	5480	1271.1
Component Mass Flow										
CO2	KG/H	0	0	5047.6	5047.6	5045.2	2.4	2.4	2.4	0
N2	KG/H	0	0	28859.1	28859.1	28855.2	4	4	4	0
O2	KG/H	0	0	4026	4026	4025.2	0.8	0.8	0.8	0
H2O	KG/H	9384.5	9384.5	2394.9	2394.9	5035.4	6744	6744	5472.9	1271.1
Mass Enthalpy	MJ/KG	-15.9	-15.5	-1.8	-1.8	-2.6	-15.7	-13.7	-13.3	-15.5
Substream: NCPSD										
Component Mass Flow										
EGRANDIS	KG/H	14076.7	14076.7	0	0	0	14076.7	14076.7	0	14076.7

Table B2: Stream Table for Biorefinery Scenario C-100 (continued...)

Stream		1001	1002	1003	1004	1005	1006	1007	1008	1009	1010
Temperature	C	0	25	25	25	25	25	25	100	0	89
Pressure	BAR	0	1.01	1.01	1.01	1.01	1.01	1.01	1.01	0	1.01
Mass Flow	KG/H	0	9384.5	9384.5	9384.5	9384.5	8113.4	1271	1271	0	1271
Component Mass Flow											
H2O	KG/H	0	9384.5	9384.5	9384.5	9384.5	8113.4	1271	1271	0	1271
Mass Enthalpy	MJ/KG	0	-15.9	-15.9	-15.9	-15.9	-15.9	-15.9	-15.5	0	-15.6
Substream: NCPSD											
Component Mass Flow											
EGRANDIS	KG/H	14076.7	0	14076.7	14076.7	14076.7	0	14076.7	14076.7	0	14076.7
Substream: CISOLID											
Component Mass Flow											
CAO	KG/H	0	0	0	0	0	0	0	0	6575	6575

Table B2: Stream Table for Biorefinery Scenario C-100 (continued...)

Stream		2001	2002	2003	2004	2005	2006	2007	2008	2009
Temperature	C	89	500	500	500	500	0	0	0	0
Pressure	BAR	1.01	1.01	1.01	1.01	1.01	0	0	0	0
Mass Flow	KG/H	1271	12791	9598.6	9598.6	9598.6	0	0	0	0
Component Mass Flow										
CO2	KG/H	0	4905.6	1713.2	1713.2	1713.2	0	0	0	0
CO	KG/H	0	79.2	79.2	79.2	79.2	0	0	0	0
H2	KG/H	0	35.9	35.9	35.9	35.9	0	0	0	0
CH4	KG/H	0	629.9	629.9	629.9	629.9	0	0	0	0
ETHYLENE	KG/H	0	124.1	124.1	124.1	124.1	0	0	0	0
ETHANE	KG/H	0	31.9	31.9	31.9	31.9	0	0	0	0
BUTANE	KG/H	0	43.5	43.5	43.5	43.5	0	0	0	0
PROPANE	KG/H	0	897.4	897.4	897.4	897.4	0	0	0	0
CROTONIC	KG/H	0	46.9	46.9	46.9	46.9	0	0	0	0
3-METHOX	KG/H	0	36.8	36.8	36.8	36.8	0	0	0	0
H2O	KG/H	1271	3267.9	3267.9	3267.9	3267.9	0	0	0	0
LIGNINA	KG/H	0	34.8	34.8	34.8	34.8	0	0	0	0
BENZDIOL	KG/H	0	34.7	34.7	34.7	34.7	0	0	0	0
ACETOL	KG/H	0	41	41	41	41	0	0	0	0
ISOEUGEN	KG/H	0	77	77	77	77	0	0	0	0
LEVOG-01	KG/H	0	80.2	80.2	80.2	80.2	0	0	0	0
FURAN	KG/H	0	482.4	482.4	482.4	482.4	0	0	0	0
CELLO-01	KG/H	0	49.5	49.5	49.5	49.5	0	0	0	0
DIMETHOX	KG/H	0	566	566	566	566	0	0	0	0
ABIETIC	KG/H	0	49.5	49.5	49.5	49.5	0	0	0	0
LIGNINB	KG/H	0	44.4	44.4	44.4	44.4	0	0	0	0
ACETIC	KG/H	0	42.6	42.6	42.6	42.6	0	0	0	0
GUAIA-01	KG/H	0	32.1	32.1	32.1	32.1	0	0	0	0
SYRIN-01	KG/H	0	35.5	35.5	35.5	35.5	0	0	0	0
FORMI-01	KG/H	0	276.6	276.6	276.6	276.6	0	0	0	0
N-PRO-01	KG/H	0	42.3	42.3	42.3	42.3	0	0	0	0
PHENO-01	KG/H	0	35.9	35.9	35.9	35.9	0	0	0	0
TOLUE-01	KG/H	0	541.7	541.7	541.7	541.7	0	0	0	0
FURFU-01	KG/H	0	36.9	36.9	36.9	36.9	0	0	0	0
BENZE-01	KG/H	0	188.6	188.6	188.6	188.6	0	0	0	0
Mass Enthalpy	MJ/KG	-15.6	-6.8	-6.2	-6.2	-6.2	0	0	0	0
Substream: NCPD										
Component Mass Flow										
CHAR	KG/H	0	2537.4	2537.4	2537.4	0	2537.4	0	2537.4	2537.4
EGRANDIS	KG/H	14076.7	0	0	0	0	0	0	0	0
BALANCE	KG/H	0	19.3	19.3	19.3	0	19.3	0	19.3	19.3
Substream: CISOLID										
Component Mass Flow										
CAO	KG/H	6575	6575	2507.3	2507.3	0	2507.3	0	2507.3	2507.3
CACO3	KG/H	0	0	7260.1	7260.1	0	7260.1	0	7260.1	7260.1

Table B2: Stream Table for Biorefinery Scenario C-100 (continued...)

Stream		3001	3002	3003	3004	3005	3006	3007	3008	3009	3010
Temperature	C	500	260	210	80	80	80	60	60	60	60
Pressure	BAR	1.01	1.01	1.01	1.01	1.01	1.01	1.01	1.01	1.01	1.01
Mass Flow	KG/H	9598.6	9598.6	9598.6	9598.6	1969.7	7628.9	7628.9	3314.4	580.2	2734.1
Component Mass Flow											
CO2	KG/H	1713.2	1713.2	1713.2	1713.2	0	1713.2	1713.2	0	0	0
CO	KG/H	79.2	79.2	79.2	79.2	0	79.2	79.2	0	0	0
H2	KG/H	35.9	35.9	35.9	35.9	0	35.9	35.9	0	0	0
CH4	KG/H	629.9	629.9	629.9	629.9	0	629.9	629.9	0	0	0
ETHYLENE	KG/H	124.1	124.1	124.1	124.1	0	124.1	124.1	0	0	0
ETHANE	KG/H	31.9	31.9	31.9	31.9	0	31.9	31.9	0	0	0
BUTANE	KG/H	43.5	43.5	43.5	43.5	0	43.5	43.5	0	0	0
PROPANE	KG/H	897.4	897.4	897.4	897.4	0	897.4	897.4	0	0	0
CROTONIC	KG/H	46.9	46.9	46.9	46.9	0.8	46.1	46.1	25.3	25.3	0
3-METHOX	KG/H	36.8	36.8	36.8	36.8	8.1	28.7	28.7	28.7	28.7	0
H2O	KG/H	3267.9	3267.9	3267.9	3267.9	405.9	2862.1	2862.1	2513.9	91.9	2422
LIGNINA	KG/H	34.8	34.8	34.8	34.8	34.8	0	0	0	0	0
BENZDIOL	KG/H	34.7	34.7	34.7	34.7	34.7	0	0	0	0	0
ACETOL	KG/H	41	41	41	41	6.8	34.2	34.2	34.2	25.7	8.5
ISOEUGEN	KG/H	77	77	77	77	32.2	44.8	44.8	9.3	9.3	0
LEVOG-01	KG/H	80.2	80.2	80.2	80.2	16.6	63.5	63.5	34.9	15.4	19.5
FURAN	KG/H	482.4	482.4	482.4	482.4	192.1	290.3	290.3	262.7	262.7	0
CELLO-01	KG/H	49.5	49.5	49.5	49.5	36.8	12.8	12.8	2.8	0	2.8
DIMETHOX	KG/H	566	566	566	566	546.6	19.4	19.4	19.4	9.9	9.5
ABIETIC	KG/H	49.5	49.5	49.5	49.5	49.5	0	0	0	0	0
LIGNINB	KG/H	44.4	44.4	44.4	44.4	44.4	0	0	0	0	0
ACETIC	KG/H	42.6	42.6	42.6	42.6	1.8	40.8	40.8	5.3	0	5.3
GUAIA-01	KG/H	32.1	32.1	32.1	32.1	32.1	0	0	0	0	0
SYRIN-01	KG/H	35.5	35.5	35.5	35.5	1.7	33.8	33.8	0	0	0
FORMI-01	KG/H	276.6	276.6	276.6	276.6	0.1	276.6	276.6	266.6	0	266.6
N-PRO-01	KG/H	42.3	42.3	42.3	42.3	42.3	0	0	0	0	0
PHENO-01	KG/H	35.9	35.9	35.9	35.9	35.9	0	0	0	0	0
TOLUE-01	KG/H	541.7	541.7	541.7	541.7	430.3	111.4	111.4	111.4	111.4	0
FURFU-01	KG/H	36.9	36.9	36.9	36.9	16.1	20.8	20.8	0	0	0
BENZE-01	KG/H	188.6	188.6	188.6	188.6	0	188.6	188.6	0	0	0
CARBON	KG/H	0	0	0	0	0	0	0	0	0	0
Mass Enthalpy	MJ/KG	-6.2	-6.8	-6.9	-7.4	-3.9	-8.4	-8.9	-12.8	-3.3	-14.9

Table B2: Stream Table for Biorefinery Scenario C-100 (continued...)

Stream		3011	3012	3013	3014	3015	3016	3017	3018	3019	3020	3021
Temperature	C	60	40	40	40	20	20	38	20	64	64	64
Pressure	BAR	1.01	1.01	1.01	1.01	1.01	1.01	1.3	1.01	1.01	2	2
Mass Flow	KG/H	4314.5	4314.5	461.5	3853	3853	3555.2	3555.2	297.8	3309.3	3309.3	3309.3
Component Mass Flow												
CO2	KG/H	1713.2	1713.2	0	1713.2	1713.2	1713.2	1713.2	0	0	0	0
CO	KG/H	79.2	79.2	0	79.2	79.2	79.2	79.2	0	0	0	0
H2	KG/H	35.9	35.9	0	35.9	35.9	35.9	35.9	0	0	0	0
CH4	KG/H	629.9	629.9	0	629.9	629.9	629.9	629.9	0	0	0	0
ETHYLENE	KG/H	124.1	124.1	0	124.1	124.1	124.1	124.1	0	0	0	0
ETHANE	KG/H	31.9	31.9	0	31.9	31.9	31.9	31.9	0	0	0	0
BUTANE	KG/H	43.5	43.5	0	43.5	43.5	43.5	43.5	0	0	0	0
PROPANE	KG/H	897.4	897.4	0	897.4	897.4	897.4	897.4	0	0	0	0
CROTONIC	KG/H	20.8	20.8	7.7	13.1	13.1	0	0	13.1	46.9	46.9	46.9
3-METHOX	KG/H	0	0	0	0	0	0	0	0	36.8	36.8	36.8
H2O	KG/H	348.2	348.2	290.6	57.6	57.6	0	0	57.6	846	846	846
LIGNINA	KG/H	0	0	0	0	0	0	0	0	34.8	34.8	34.8
BENZDIOL	KG/H	0	0	0	0	0	0	0	0	34.7	34.7	34.7
ACETOL	KG/H	0	0	0	0	0	0	0	0	32.5	32.5	32.5
ISOEUGEN	KG/H	35.5	35.5	35.5	0	0	0	0	0	77	77	77
LEVOG-01	KG/H	28.6	28.6	0	28.6	28.6	0	0	28.6	60.7	60.7	60.7
FURAN	KG/H	27.5	27.5	17	10.5	10.5	0	0	10.5	482.4	482.4	482.4
CELLO-01	KG/H	10	10	0	10	10	0	0	10	46.8	46.8	46.8
DIMETHOX	KG/H	0	0	0	0	0	0	0	0	556.5	556.5	556.5
ABIETIC	KG/H	0	0	0	0	0	0	0	0	49.5	49.5	49.5
LIGNINB	KG/H	0	0	0	0	0	0	0	0	44.4	44.4	44.4
ACETIC	KG/H	35.5	35.5	35.5	0	0	0	0	0	37.4	37.4	37.4
GUAIA-01	KG/H	0	0	0	0	0	0	0	0	32.1	32.1	32.1
SYRIN-01	KG/H	33.8	33.8	33.8	0	0	0	0	0	35.5	35.5	35.5
FORMI-01	KG/H	10	10	10	0	0	0	0	0	10.1	10.1	10.1
N-PRO-01	KG/H	0	0	0	0	0	0	0	0	42.3	42.3	42.3
PHENO-01	KG/H	0	0	0	0	0	0	0	0	35.9	35.9	35.9
TOLUE-01	KG/H	0	0	0	0	0	0	0	0	541.7	541.7	541.7
FURFU-01	KG/H	20.8	20.8	20.8	0	0	0	0	0	36.9	36.9	36.9
BENZE-01	KG/H	188.6	188.6	10.5	178	178	0	0	178	188.6	188.6	188.6
CARBON	KG/H	0	0	0	0	0	0	0	0	0	0	0
Mass Enthalpy	MJ/KG	-6	-6.1	-11.3	-5.6	-5.6	-5.8	-5.8	-3.8	-4.8	-4.8	-4.8

Table B2: Stream Table for Biorefinery Scenario C-100 (continued...)

Stream		4001	4002	4003	4004	4005	4006	4007	4008	4009	4010
Temperature	C	500	56	25	52	247	1048	975	300	130	130
Pressure	BAR	1.01	1.3	1.01	1.3	1.3	1.3	1.3	1.29	1.29	1.29
Mass Flow	KG/H	0	2705.7	37621.9	37621.9	37621.9	40327.6	40327.6	40327.6	40327.6	40327.6
Component Mass Flow											
CO2	KG/H	0	598.3	0	0	0	5047.6	5047.6	5047.6	5047.6	5047.6
CO	KG/H	0	1094.4	0	0	0	0	0	0	0	0
H2	KG/H	0	61.9	0	0	0	0	0	0	0	0
CH4	KG/H	0	414.4	0	0	0	0	0	0	0	0
ETHYLENE	KG/H	0	52.2	0	0	0	0	0	0	0	0
ETHANE	KG/H	0	367.1	0	0	0	0	0	0	0	0
BUTANE	KG/H	0	92.3	0	0	0	0	0	0	0	0
PROPANE	KG/H	0	25	0	0	0	0	0	0	0	0
N2	KG/H	0	0	28859.1	28859.1	28859.1	28859.1	28859.1	28859.1	28859.1	28859.1
O2	KG/H	0	0	8762.8	8762.8	8762.8	4026	4026	4026	4026	4026
H2O	KG/H	0	0	0	0	0	2394.9	2394.9	2394.9	2394.9	2394.9
Mass Enthalpy	MJ/KG	0.6	-4.7	0	0	0.2	-0.7	-0.8	-1.6	-1.8	-1.8

Table B2: Stream Table for Biorefinery Scenario C-100 (continued...)

Stream		5001	5002	5003	5004	5005	5006	5007	5008	5009	
Temperature	C	75	76	91	159	234	35	234	234	363	
Pressure	BAR	1.45	30	30	30	30	1.01	29.99	29.99	29.99	
Mass Flow	KG/H	15096.8	15096.8	15096.8	15096.8	15096.8	452.9	452.9	14643.9	14643.9	
Component Mass Flow											
H2O	KG/H	15096.8	15096.8	15096.8	15096.8	15096.8	452.9	452.9	14643.9	14643.9	
Mass Enthalpy	MJ/KG	-15.7	-15.6	-15.6	-15.3	-13.1	-15.8	-14.8	-13	-12.8	

Table B2: Stream Table for Biorefinery Scenario C-100 (continued...)

Stream		5010	5011	5012	5013	5014	5015	5017	5018	5019	5020
Temperature	C	170	170	60	50	170	110	76	25	25	75
Pressure	BAR	4.5	4.5	0.2	0.2	4.5	1.43	1.45	1.01	2	1.45
Mass Flow	KG/H	14643.9	8374.3	8374.3	8374.3	6269.6	6269.6	14643.9	452.9	452.9	15096.8
Component Mass Flow											
H2O	KG/H	14643.9	8374.3	8374.3	8374.3	6269.6	6269.6	14643.9	452.9	452.9	15096.8
Mass Enthalpy	MJ/KG	-13.1	-13.1	-13.6	-15.8	-13.1	-15.5	-15.6	-15.9	-15.9	-15.7

8.3 Appendix C

Table C1: Purchased equipment costs, installations factors and scaling factors

Equipment	Equipment ID	Base Scale	Unit	Base Purchased Equipment Cost	Base Year (CEPCI)	Scaling Factor	Installation Factor	Reference*
A000/A11000: Pre-treatment								
Hammer Grinder	MILL	2 857	MT/DAY	\$4 081 875	2015	0.8	1.7	[1]
Bale Transport Conveyor		2 857	MT/DAY	\$1 388 963	2015	0.8	1.7	[1]
Bale Unwrapping Conveyor		2 857	MT/DAY	\$521 187	2015	0.8	1.7	[1]
Discharge Conveyor		2 857	MT/DAY	\$87 299	2015	0.8	1.7	[1]
Truck Scales		2 857	MT/DAY	\$58 634	2015	0.8	1.7	[1]
Truck Unloading Forklift		2 857	MT/DAY	\$125 085	2015	0.8	1.7	[1]
Bale Moving Forklift		2 857	MT/DAY	\$125 085	2015	0.8	1.7	[1]
Concrete Storage Slab		2 857	MT/DAY	\$781 780	2015	0.8	1.7	[1]
Flue Gas Blower	FAN0001	204	HP	\$59 300	2013	0.78	1.94	[2]
Biomass Preheater	HX0001	10	SQM	\$132 000	(1000)	1.04	2.4	[4]
Direct Dryer	DR0001	7 600	KG/H	\$323 000	1984	0.88	1	[3]
Indirect Dryer	HX0002/DR0002	100	SQM	\$155 000	(1000)	0.75	3	[4]
Biomass/Catalyst Mixer	MIX1001	3	CUM	\$66 000	(1000)	0.6	2.25	[4]
A2000: Pyrolysis								
Biomass/Catalyst Feeding Bin		2 222	MT/DAY	\$395 054	2015	0.8	1.7	[1]
Pyrolysis Reactor (Incl. Piston Feeder and Furnace)	PYRO	24	MT/DAY	\$1 016 000	2017	0.7	3	Quote from supplier
Char Cyclone	CY2001	2 222	MT/DAY	\$3 944 673	2015	0.8	1	[1]
A3000: Product Recovery								
Process Heat Exchanger	HX3001	100	SQM	\$70 000	(1000)	0.71	5.6	[4]
	HX3002							
Condenser	CON3001	100	SQM	\$70 000	(1000)	0.71	5.6	[4]
	CON3002							
	CON3003							
	CON3004							
Vapour/Liquid Separator	S3001	20.0	CUM	\$100 000	(1000)	0.52	6.325	[4]
	S3002A							
	S3003							
	S3004							

Table C1: Purchased equipment costs, installations factors and scaling factors (continued...)

Equipment	Equipment ID	Base Scale	Unit	Base Purchased Equipment Cost	Base Year (CEPCI)	Scaling Factor	Installation Factor	Reference*
Decanter	S3002B	1 013 050	LB/H	\$294 700	2013	0.7	1.82	[2]
Aqueous Phase Filter		182	GPM	\$26 500	2013	0.8	1.77	[2]
Aqueous Filter Charge Pump		182	GPM	\$7 500	2013	0.8	4.2	[2]
Bio-oil Pump	P3001	23	KW	\$9 500	(1000)	0.79	2.793	[4]
Non-condensable Gas Blower	FAN3001	10	CUM/S	\$27 750	(1000)	0.93	1.7	[4]
A4000: Heat Recovery								
Char Feeding Bin		2 222	MT/DAY	\$395 054	2015	0.8	1	[1]
Air Blower	FAN4001	10	CUM/S	\$27 750	(1000)	0.93	1.7	[4]
Air Preheater	HX4002	100	SQM	\$70 000	(1000)	0.71	5.6	[4]
Process Heat Exchanger	HX4001	100	SQM	\$70 000	(1000)	0.71	5.6	[4]
	HX4003							
Flue Gas Cyclone	CY4001	10	CUM/S	\$35 000	(1000)	0.56	2.5	[4]
A5000: Steam and Power Production								
BFW Pump	P5001	494 622	LB/H	\$304 578	2007	0.3	1.35	[2]
Steam Drum	STEAM	494 622	LB/H	\$104 100	2007	0.65	2.28	[2]
Blowdown Cooler	CON5002	381 671	BTU/H	\$16 780	2007	0.65	4.32	[2]
Blowdown Flash Drum		9 892	LB/H	\$47 205	2007	0.65	3.41	[2]
Steam Turbine Generator	C5001	-40 418	HP	\$7 700 000	2010	0.7	1.8	[2]
	C5002							
Low Pressure Steam Condenser	CON5001	100	SQM	\$70 000	(1000)	0.71	2.8	[4]
Low Pressure Steam Condensate Tank		500 400	LB/H	\$28 505	2007	0.65	6.83	[2]
Low Pressure Steam Condensate Pump		247 010	LB/H	\$9 810	2007	0.3	4.61	[2]
Condensate Collection Pump		247 010	LB/H	\$9 810	2007	0.3	4.61	[2]
Condensate Collection Tank	S5002	500 400	LB/H	\$28 505	2007	0.65	6.83	[2]
BFW EDI and Polishing		300 000	LB/H	\$1 325 000	2010	0.6	2	[2]
EDI Pump		247 010	LB/H	\$9 810	2007	0.3	4.61	[2]
Condensate Surge Tank		500 400	LB/H	\$27 704	2007	0.65	6.51	[2]
Deaerator		494 619	LB/H	\$53 299	2007	0.65	5.07	[2]
Deaerator Packed Column		494 619	LB/H	\$18 405	2007	0.65	5.18	[2]
BFW Makeup Pump	P5002	80 411	LB/H	\$6 528	2007	0.3	4.72	[2]
Start-up Boiler		204 131	LB/H	\$275 500	2013	0.6	1.69	[2]

Table C1: Purchased equipment costs, installations factors and scaling factors (continued...)

Equipment	Equipment ID	Base Scale	Unit	Base Purchased Equipment Cost	Base Year (CEPCI)	Scaling Factor	Installation Factor	Reference*
A6000: Wastewater Treatment								
Aerobic Digestion System		1 000	MT/DAY	\$1 554 000	2004	0.65	3	[5]
A7000: Utilities								
Cooling Tower System		7 506 000	LB/H	\$260 852	2010	0.78	2.47	[2]
Chilled Water System		28 200 000	BTU/H	\$637 500	2011	0.6	1.8	[2]
Flue Gas Scrubber		489 600	LB/H	\$436 250	2010	0.65	2.47	[2]
Flue Gas Scrubber Circulation Pump		489 600	LB/H	\$12 510	2007	0.3	4.12	[2]
Flue Gas Stack		939 119	LB/H	\$169 187	2007	0.65	1.3	[2]
BFW Chemical Pump		262 454	LB/H	\$3 842	2007	0.3	5.21	[2]
BFW Chemical Storage Tank		262 454	LB/H	\$22 004	2007	0.65	6.7	[2]
Firewater Pump		262 454	LB/H	\$23 043	2007	0.3	3.7	[2]
Firewater Storage Tank		262 454	LB/H	\$229 900	2007	0.65	1.46	[2]
Cooling Water Pump		7 001 377	LB/H	\$239 375	2007	0.3	2.14	[2]
Plant Air Compressor		262 454	LB/H	\$87 922	2007	0.3	1.57	[2]
Plant Air Receiver		262 454	LB/H	\$21 005	2007	0.65	5.44	[2]
Instrument Air Dryer		262 454	LB/H	\$8 349	2002	0.6	2.47	[2]
Ammonia Pump		262 454	LB/H	\$3 842	2007	0.3	5.21	[2]
Ammonia Storage Tank		262 454	LB/H	\$15 704	2007	0.65	5.39	[2]
Caustic Pump		262 454	LB/H	\$4 906	2007	0.3	4.3	[2]
Caustic Storage Tank		262 454	LB/H	\$16 005	2007	0.65	3.01	[2]
Hydraulic Truck Dump With Scale		367 437	LB/H	\$80 000	1998	0.6	2.47	[2]
Product Loading Rack		262 454	LB/H	\$25 000	2011	1	2.47	[2]
Storage								
Bio-oil Storage Tank	T3001	50	GPM	\$442 700	2013	0.7	1.75	[2]
Char/Agri-lime Storage Bin		350	CUM	\$350 000	(1000)	0.65	2.5	[4]
Biomass Storage Bin		350	CUM	\$350 000	(1000)	0.65	2.5	[4]
Catalyst Storage Bin		350	CUM	\$350 000	(1000)	0.65	2.5	[4]

*[1] (Carrasco *et al.*, 2017)

[4] (Woods, 2007)

[2] (Dutta *et al.*, 2015)

[5] (Jones *et al.*, 2013)

[3] (Amos, 1998)

Table C2: Installed equipment costs, direct costs, indirect costs, FCI and TCI for each biorefinery scenario

Scenario			NC-100	NC-5	NC-200	NC-300	C-100	C-200	C-10	C-300
Installed Equipment Costs	A1000: Pre-treatment		\$8 843 217	\$18 154 051	\$32 634 788	\$46 689 452	\$9 923 272	\$38 498 702	\$39 591 973	\$55 972 836
	A2000: Pyrolysis		\$21 735 295	\$40 380 087	\$66 691 067	\$90 457 375	\$27 949 296	\$85 783 539	\$87 769 462	\$116 364 134
	A3000: Product Recovery		\$9 339 216	\$15 037 968	\$22 167 870	\$28 091 412	\$7 455 856	\$17 696 000	\$18 012 826	\$22 423 916
	A4000: Heat Recovery		\$1 149 868	\$2 150 398	\$3 574 696	\$4 870 134	\$1 442 124	\$4 475 224	\$4 580 111	\$6 093 991
	A5000: Steam and Power		\$3 085 883	\$5 307 565	\$8 312 771	\$10 954 591	\$5 089 947	\$14 221 583	\$14 527 393	\$18 895 397
	Production		\$2 943 191	\$5 208 439	\$8 267 751	\$10 945 789	\$2 943 191	\$8 267 751	\$8 443 764	\$10 945 789
	A6000: Wastewater Treatment		\$2 024 817	\$3 112 018	\$4 496 489	\$5 670 515	\$2 354 721	\$5 312 593	\$5 407 232	\$6 732 019
	A7000: Utilities		\$5 531 320	\$9 839 313	\$15 686 582	\$20 823 851	\$7 150 068	\$20 236 577	\$20 670 675	\$26 848 693
	A8000: Storage									
Total Inside-Battery-Limits (ISBL)			\$41 067 597	\$75 722 504	\$125 068 421	\$170 108 373	\$46 770 548	\$146 453 465	\$149 954 373	\$200 854 877
Total Installed Equipment Cost			\$54 652 808	\$99 189 839	\$161 832 014	\$218 503 120	\$64 308 476	\$194 491 970	\$199 003 436	\$264 276 776
Direct Costs	Warehouse	4% ISBL	\$1 642 704	\$3 028 900	\$5 002 737	\$6 804 335	\$1 870 822	\$5 858 139	\$5 998 175	\$8 034 195
	Site Development	9% ISBL	\$3 696 084	\$6 815 025	\$11 256 158	\$15 309 754	\$4 209 349	\$13 180 812	\$13 495 894	\$18 076 939
	Additional Piping	4.5% ISBL	\$1 848 042	\$3 407 513	\$5 628 079	\$7 654 877	\$2 104 675	\$6 590 406	\$6 747 947	\$9 038 469
Total Direct Cost (TDC)			\$61 839 637	\$112 441 277	\$183 718 987	\$248 272 085	\$72 493 322	\$220 121 326	\$225 245 451	\$299 426 380
Indirect Costs	Prorateable costs	10% TDC	\$6 183 964	\$11 244 128	\$18 371 899	\$24 827 209	\$7 249 332	\$22 012 133	\$22 524 545	\$29 942 638
	Field Expenses	10% TDC	\$6 183 964	\$11 244 128	\$18 371 899	\$24 827 209	\$7 249 332	\$22 012 133	\$22 524 545	\$29 942 638
	Home Office and Construction Fees	20% TDC	\$12 367 927	\$22 488 255	\$36 743 797	\$49 654 417	\$14 498 664	\$44 024 265	\$45 049 090	\$59 885 276
	Project Contingency	10% TDC	\$6 183 964	\$11 244 128	\$18 371 899	\$24 827 209	\$7 249 332	\$22 012 133	\$22 524 545	\$29 942 638
	Other Costs	10% TDC	\$6 183 964	\$11 244 128	\$18 371 899	\$24 827 209	\$7 249 332	\$22 012 133	\$22 524 545	\$29 942 638
Total Indirect Cost			\$37 103 782	\$67 464 766	\$110 231 392	\$148 963 251	\$43 495 993	\$132 072 796	\$135 147 271	\$179 655 828
Fixed Capital Investment (FCI)			\$98 943 420	\$179 906 043	\$293 950 380	\$397 235 337	\$115 989 315	\$352 194 122	\$360 392 722	\$479 082 208
Working Capital		5% FCI	\$4 947 171	\$8 995 302	\$14 697 519	\$19 861 767	\$5 799 466	\$17 609 706	\$18 019 636	\$23 954 110
Land			\$531 399	\$1 278 758	\$2 603 314	\$4 008 696	\$531 399	\$2 603 314	\$2 689 066	\$4 008 696
Total Capital Investment (TCI)			\$104 421 989	\$190 180 104	\$311 251 213	\$421 105 799	\$122 320 179	\$372 407 143	\$381 101 425	\$507 045 014

Table C3: Fixed operating costs, variable operating costs and total operating costs for each biorefinery scenario

Scenario			NC-100	NC-5	NC-200	NC-300	C-100	C-200	C-10	C-300
Fixed Operating Costs	Salaries		\$1 235 563	\$2 314 514	\$4 064 640	\$6 259 799	\$1 235 563	\$4 064 640	\$4 159 082	\$6 259 799
	Benefits and Overheads	90% Salaries	\$1 112 006	\$2 083 063	\$3 658 176	\$5 633 819	\$1 112 006	\$3 658 176	\$3 743 174	\$5 633 819
	Maintenance	3% FCI	\$2 968 303	\$5 397 181	\$8 818 511	\$11 917 060	\$3 479 679	\$10 565 824	\$10 811 782	\$14 372 466
	Insurance and Taxes	0.7% FCI	\$692 604	\$1 259 342	\$2 057 653	\$2 780 647	\$811 925	\$2 465 359	\$2 522 749	\$3 353 575
Total Fixed Operating Cost			\$6 008 476	\$11 054 101	\$18 598 980	\$26 591 326	\$6 639 174	\$20 753 998	\$21 236 787	\$29 619 660
Variable Operating Costs	Feedstock		\$3 092 034	\$8 570 117	\$19 471 953	\$33 793 904	\$3 092 034	\$19 471 953	\$20 818 036	\$33 793 904
	Catalyst	\$150/MT	\$0	\$0	\$0	\$0	\$7 929 501	\$38 846 496	\$40 126 080	\$59 817 507
	Cooling Tower Water Makeup	\$0.32/MT	\$63 796	\$153 049	\$311 466	\$479 480	\$118 727	\$581 208	\$600 405	\$894 957
	BFW Makeup	\$0.32/MT	\$931	\$2 239	\$4 556	\$7 015	\$1 482	\$7 256	\$7 495	\$11 172
	Cooling Tower Chemicals	\$7 583/year/MW	\$30 235	\$72 697	\$147 943	\$227 771	\$56 935	\$278 735	\$287 916	\$429 162
	BFW Chemicals	\$0.16/MT blowdown	\$378	\$909	\$1 850	\$2 849	\$602	\$2 947	\$3 044	\$4 537
	50 wt. % Caustic	\$0.18/kg	\$54 010	\$129 970	\$264 594	\$407 434	\$54 010	\$264 594	\$273 310	\$407 434
	Ash Disposal	\$28.30/MT	\$8 661	\$20 843	\$42 432	\$65 339	\$0	\$0	\$0	\$0
	Wastewater	\$0.71/CUM	\$97 934	\$235 111	\$478 509	\$736 675	\$159 729	\$781 994	\$807 814	\$1 204 131
Total Variable Operating Cost			\$3 347 979	\$9 184 935	\$20 723 303	\$35 720 467	\$11 413 020	\$60 235 181	\$62 924 099	\$96 562 804
Total Operating Cost			\$9 356 455	\$20 239 036	\$39 322 283	\$62 311 793	\$18 052 194	\$80 989 180	\$84 160 886	\$126 182 464

8.4 Appendix D

Table D1: LCI for non-catalytic pyrolysis of 1 kg of dry forest residues in Scenario 1

Product	Amount	Unit	Alloc.
Bio-oil	0.24737	kg	50.76%
Biochar	0.23792	kg	48.82%
Electricity	0.05862	MJ	0.41%
Input	Amount	Unit	
Air	1.75801	kg	
Water, unspecified natural origin, ZA	1.45042	L	
Transport, tractor and trailer, agricultural {GLO} market for APOS, S	1.00000	kgkm	
Wood chipping, chipper, mobile, diesel, at forest road {GLO} market for APOS, S	0.00008	hr	
Transport, freight, lorry >32 metric ton, EURO3 {GLO} market for APOS, S	596.67	kgkm	
Output	Amount	Unit	
Carbon dioxide, to soil or biomass stock	1.74071	kg	
Carbon dioxide	0.52813	kg	
Water	1.19139	kg	
Oxygen	0.06823	kg	
Nitrogen dioxide	0.00083	kg	
Nitrogen, atmospheric	1.34854	kg	
Sulphur dioxide	0.00025	kg	
Wood ash mixture, pure {RoW} market for wood ash mixture, pure APOS, S	0.01040	kg	
Wastewater, unpolluted {RoW} treatment of, capacity 5E9l/year APOS, S	1.18879	L	

Table D2: LCI for catalytic pyrolysis of 1 kg of dry forest residues in Scenario 1

Product	Amount	Unit	Alloc.
Bio-oil	0.23509	kg	21.13%
Biochar	0.18026	kg	15.25%
Agri-lime	0.69387	kg	62.31%
Electricity	0.34429	MJ	1.31%
Input	Amount	Unit	
Quicklime, milled, packed {GLO} market for APOS, S	0.46709	kg	
Air	2.67273	kg	
Water, unspecified natural origin, ZA	2.66133	L	
Transport, tractor and trailer, agricultural {GLO} market for APOS, S	1.00000	kgkm	
Wood chipping, chipper, mobile, diesel, at forest road {GLO} market for APOS, S	0.00008	hr	
Transport, freight, lorry >32 metric ton, EURO3 {GLO} market for APOS, S	596.67	kgkm	
Output	Amount	Unit	
Carbon dioxide, to soil or biomass stock	1.74071	kg	
Carbon dioxide	0.35859	kg	
Water	1.68902	kg	
Oxygen	0.28601	kg	
Nitrogen dioxide	0.00000	kg	
Nitrogen, atmospheric	2.05020	kg	
Sulphur dioxide	0.00000	kg	
Wood ash mixture, pure {RoW} market for wood ash mixture, pure APOS, S	0.01040	kg	
Wastewater, unpolluted {RoW} treatment of, capacity 5E9l/year APOS, S	1.92458	L	

Table D3: LCI for combustion of 1 kg of dry forest residues in Scenario 1

Input	Amount	Unit
Air	5.65926	kg
Output	Amount	Unit
Carbon dioxide, to soil or biomass stock	1.74071	kg
Carbon dioxide	1.74071	kg
Water	1.22869	kg
Oxygen	0.00000	kg
Nitrogen dioxide	0.00385	kg
Nitrogen, atmospheric	4.34112	kg
Sulphur dioxide	0.00115	kg
Wood ash mixture, pure {RoW} market for wood ash mixture, pure APOS, S	0.01040	kg

Table D4: LCI for producing 1 MJ of crude bio-oil in Scenario 2

Product	Amount	Unit	Alloc.
Bio-oil	0.0486	kg	49.93%
Biochar	0.04834	kg	49.67%
Electricity	0.0115	MJ	0.41%
Input	Amount	Unit	
Air	0.34535	kg	
Water, unspecified natural origin, ZA	0.28487	L	
Transport, tractor and trailer, agricultural {GLO} market for APOS, S	0.19645	kgkm	
Wood chipping, chipper, mobile, diesel, at forest road {GLO} market for APOS, S	0.00002	hr	
Transport, freight, lorry >32 metric ton, EURO3 {GLO} market for APOS, S	117.22	kgkm	
Output	Amount	Unit	
Carbon dioxide, to soil or biomass stock	0.34196	kg	
Carbon dioxide	0.10375	kg	
Water	0.23402	kg	
Oxygen	0.01340	kg	
Nitrogen dioxide	0.00016	kg	
Nitrogen, atmospheric	0.26491	kg	
Sulphur dioxide	0.00005	kg	
Wood ash mixture, pure {RoW} market for wood ash mixture, pure APOS, S	0.00204	kg	
Wastewater, unpolluted {RoW} treatment of, capacity 5E9l/year APOS, S	0.23350	L	

Table D5: LCI for transporting 1 MJ of crude bio-oil in Scenario 2

Input	Amount	Unit
Bio-oil	0.04860	kg
Transport, freight, lorry 16-32 metric ton, EURO3 {GLO} market for APOS, S	31.587	kgkm

Table D6: LCI for transporting and applying non-catalytic biochar in Scenario 2

Input	Amount	Unit
Biochar	0.04834	kg
Transport, freight, lorry >32 metric ton, EURO3 {GLO} market for APOS, S	29.007	kgkm
Output	Amount	Unit
Carbon dioxide	0.02843	kg
Fertiliser, applied (N component)	0.00018	kg
Carbon dioxide, to soil or biomass stock	0.11374	kg

Table D7: LCI for producing 1 MJ of upgraded bio-oil in Scenario 2

Product	Amount	Unit	Alloc.
Bio-oil	0.03870	kg	21.13%
Biochar	0.02967	kg	15.25%
Agri-lime	0.11421	kg	62.31%
Electricity	0.05677	MJ	1.31%
Input	Amount	Unit	
Quicklime, milled, packed {GLO} market for APOS, S	0.07688	kg	
Air	0.43921	kg	
Water, unspecified natural origin, ZA	0.43783	L	
Transport, tractor and trailer, agricultural {GLO} market for APOS, S	0.16460	kgkm	
Wood chipping, chipper, mobile, diesel, at forest road {GLO} market for APOS, S	0.00001	hr	
Transport, freight, lorry >32 metric ton, EURO3 {GLO} market for APOS, S	98.21	kgkm	
Output	Amount	Unit	
Carbon dioxide, to soil or biomass stock	0.28653	kg	
Carbon dioxide	0.05902	kg	
Water	0.27793	kg	
Oxygen	0.04691	kg	
Nitrogen dioxide	0.00000	kg	
Nitrogen, atmospheric	0.33691	kg	
Sulphur dioxide	0.00000	kg	
Wood ash mixture, pure {RoW} market for wood ash mixture, pure APOS, S	0.00171	kg	
Wastewater, unpolluted {RoW} treatment of, capacity 5E9l/year APOS, S	0.31664	L	

Table D8: LCI for transporting 1 MJ of upgraded bio-oil in Scenario 2

Input	Amount	Unit
Bio-oil	0.03870	kg
Transport, freight, lorry 16-32 metric ton, EURO3 {GLO} market for APOS, S	25.152	kgkm

Table D9: LCI for transporting and applying catalytic biochar in Scenario 2

Input	Amount	Unit
Biochar	0.02967	kg
Transport, freight, lorry >32 metric ton, EURO3 {GLO} market for APOS, S	17.805	kgkm
Output	Amount	Unit
Carbon dioxide	0.01620	kg
Fertiliser, applied (N component)	0.00019	kg
Carbon dioxide, to soil or biomass stock	0.06482	kg

Table D10: LCI for transporting and applying agri-lime in Scenario 2

Avoided Product	Amount	Unit
Soil pH raising agent, as CaCO ₃ {GLO} market for APOS, S	0.13738	kg
Input	Amount	Unit
Agri-lime	0.11421	kg
Transport, freight, lorry >32 metric ton, EURO3 {GLO} market for APOS, S	68.526	kgkm
Output	Amount	Unit
Carbon dioxide	0.03735	kg
Water	0.02471	kg
Calcium	0.05490	kg